

Longevity Risk Management: Models and Hedging Strategies

by

Kenneth Q. Zhou

A thesis
presented to the University of Waterloo
in fulfillment of the
thesis requirement for the degree of
Doctor of Philosophy
in
Actuarial Science

Waterloo, Ontario, Canada, 2019

© Kenneth Q. Zhou 2019

Examining Committee Membership

The following served on the Examining Committee for this thesis. The decision of the Examining Committee is by majority vote.

External Examiner: Jennifer So-Kuen Chan
Associate Professor, School of Mathematics and Statistics
University of Sydney

Supervisor(s): Johnny S.-H. Li
Professor, Department of Statistics and Actuarial Science
University of Waterloo

Departmental Member(s): Jun Cai
Professor, Department of Statistics and Actuarial Science
University of Waterloo
Mary Hardy
Professor, Department of Statistics and Actuarial Science
University of Waterloo

Internal-External Member: Justin W.L. Wan
Professor, David R. Cheriton School of Computer Science
University of Waterloo

I hereby declare that I am the sole author of this thesis. This is a true copy of the thesis, including any required final revisions, as accepted by my examiners.

I understand that my thesis may be made electronically available to the public.

Abstract

Longevity risk management is becoming increasingly important in the pension and life insurance industries. The unexpected mortality improvements observed in recent decades are posing serious concerns to the financial stability of defined-benefit pension plans and annuity portfolios. It has recently been argued that the overwhelming longevity risk exposures borne by the pension and life insurance industries may be transferred to capital markets through standardized longevity derivatives that are linked to broad-based mortality indexes. To achieve the transfer of risk, two technical issues need to be addressed first: (1) how to model the dynamics of mortality indexes, and (2) how to optimize a longevity hedge using standardized longevity derivatives. The objective of this thesis is to develop sensible solutions to these two questions.

In the first part of this thesis, we focus on incorporating stochastic volatility in mortality modeling, introducing the notion of longevity Greeks, and analysing the properties of longevity Greeks and their applications in index-based longevity hedging. In more detail, we derive three important longevity Greeks—delta, gamma and vega—on the basis of an extended version of the Lee-Carter model that incorporates stochastic volatility. We also study the properties of each longevity Greek, and estimate the levels of effectiveness that different longevity Greek hedges can possibly achieve. The results reveal several interesting facts. For example, we found and explained that, other things being equal, the magnitude of the longevity gamma of a q-forward increases with its reference age. As with what have been developed for equity options, these properties allow us to know more about standardized longevity derivatives as a risk mitigation tool. We also found that, in a delta-vega hedge formed by q-forwards, the choice of reference ages does not materially affect hedge effectiveness, but the choice of times-to-maturity does. These facts may aid insurers to better formulate their hedge portfolios, and issuers of mortality-linked securities to determine what security structures are more likely to attract liquidity.

We then move onto delta hedging the trend and cohort components of longevity risk under the M7-M5 model. In a recent project commissioned by the Institute and Faculty of Actuaries and the Life and Longevity Markets Association, a two-population mortality model called the M7-M5 model is developed and recommended as an industry standard

for the assessment of population basis risk. We develop a longevity delta hedging strategy for use with the M7-M5 model, taking into account of not only period effect uncertainty but also cohort effect uncertainty and population basis risk. To enhance practicality, the hedging strategy is formulated in both static and dynamic settings, and its effectiveness can be evaluated in terms of either variance or 1-year ahead Value-at-Risk (the latter is highly relevant to solvency capital requirements). Three real data illustrations are constructed to demonstrate (1) the impact of population basis risk and cohort effect uncertainty on hedge effectiveness, (3) the benefit of dynamically adjusting a delta longevity hedge, and (3) the relationship between risk premium and hedge effectiveness.

The last part of this thesis sets out to obtain a deeper understanding of mortality volatility and its implications on index-based longevity hedging. The volatility of mortality is crucially important to many aspects of index-based longevity hedging, including instrument pricing, hedge calibration, and hedge performance evaluation. We first study the potential asymmetry in mortality volatility by considering a wide range of GARCH-type models that permit the volatility of mortality improvement to respond differently to positive and negative mortality shocks. We then investigate how the asymmetry of mortality volatility may impact index-based longevity hedging solutions by developing an extended longevity Greeks framework, which encompasses longevity Greeks for a wider range of GARCH-type models, an improved version of longevity vega, and a new longevity Greek known as ‘dynamic delta’. Our theoretical work is complemented by two real-data illustrations, the results of which suggest that the effectiveness of an index-based longevity hedge could be significantly impaired if the asymmetry in mortality volatility is not taken into account when the hedge is calibrated.

Acknowledgements

I would like to express my deepest gratitude to my supervisor, Professor Johnny Li, who has inspired, guided and helped me through my graduate studies with his insightful ideas and unreserved support. I would also like to thank Professor Jun Cai, Professor Jennifer Chan, Professor Mary Hardy and Professor Justin Wan for their time and effort in examining this thesis. Special thanks to Professor Wai-Sum Chan and Professor Rui Zhou for their constructive suggestions on my PhD research. Lastly, many thanks to the faculty and staff in the Department of Statistics and Actuarial Science, especially to Ms. Mary Lou Dufton, who has given me countless support and made my graduate studies cheerful.

I would like to also acknowledge the financial support for my PhD studies from the Alexander Graham Bell Canada Graduate Scholarships of the Natural Sciences and Engineering Research Council of Canada, the James C. Hickman Scholar program of the Society of Actuaries, and the Department of Statistics and Actuarial Science.

Dedication

To my parents and wife for their limitless love, support and encouragement.

Table of Contents

List of Tables	xiii
List of Figures	xv
1 Introduction	1
1.1 Background	1
1.2 Objectives and Outline of the Thesis	5
2 Longevity Greeks: What Do Insurers and Capital Market Investors Need to Know?	7
2.1 Introduction	7
2.2 The Lee-Carter Model with Stochastic Volatility	12
2.3 The Longevity Greeks	16
2.3.1 Defining Survival Probabilities	16
2.3.2 The Longevity Greeks for $p_{x,t}(T, \kappa_0, \sigma_0^2)$	18
2.3.3 The Longevity Greeks of a Stylized Pension Plan	20
2.3.4 The Longevity Greeks of q-Forwards	21
2.4 Analyzing the Longevity Greeks of q-Forwards	22
2.4.1 Introducing the Curve of $\exp(-\exp(Y_{x,t}(1)))$ against $Y_{x,t}(1)$	22

2.4.2	Properties of the Longevity Delta	24
2.4.3	Properties of the Longevity Gamma	25
2.4.4	Properties of the Longevity Vega	27
2.5	Greek Hedging of Longevity Risk	30
2.5.1	Assumptions	30
2.5.2	The Evaluation Metric	31
2.5.3	Single Longevity Greek Hedging	32
2.5.4	Multiple Longevity Greek Hedging	36
2.6	Validation with a Model-Free Approach	41
2.6.1	The Non-parametric Bootstrap	41
2.6.2	Other Considerations	44
2.7	Concluding Remarks	46
3	Delta-Hedging Longevity Risk under the M7-M5 Model: The Impact of Cohort Effect Uncertainty and Population Basis Risk	51
3.1	Introduction	51
3.2	The M7-M5 Model	56
3.2.1	Model Specification	56
3.2.2	Model Estimation	58
3.2.3	The Processes for the Period and Cohort Effects	59
3.3	The Set-up	63
3.3.1	Survival Probabilities	63
3.3.2	The (u, \mathcal{F}_t) -Value of a Random Cash Flow Stream	64
3.3.3	The Liability Being Hedged	64
3.3.4	The Hedging Instruments	65

3.4	Evaluation of $E[S_{x,u}^{(i)}(T) \mathcal{F}_t]$	66
3.4.1	Computing $E[S_{x,u}^{(i)}(T) \mathcal{F}_t]$ for $t = t_b$	66
3.4.2	Approximating $E[S_{x,u}^{(i)}(T) \mathcal{F}_t]$ for $t > t_b$	67
3.4.3	Summary	74
3.5	Valuation of the Liability Being Hedged and the Hedging Instruments . . .	74
3.5.1	The Liability Being Hedged	74
3.5.2	The Hedging Instruments	77
3.6	Delta Hedging	79
3.6.1	Static Delta Hedging	79
3.6.2	Dynamic Delta Hedging	81
3.7	Hedge Evaluation	84
3.7.1	Evaluation with Variance	84
3.7.2	Evaluation with Value-at-Risk	86
3.8	Illustrations	88
3.8.1	Illustration 1: Population Basis Risk and Cohort Effect Uncertainty	88
3.8.2	Illustration 2: Static vs. Dynamic	94
3.8.3	Illustration 3: Cost of Hedging	96
3.9	Concluding Remarks	98
4	Asymmetry in Mortality Volatility and Its Implications on Index-based Longevity Hedging	101
4.1	Introduction	101
4.2	Modeling Mortality Volatility	105
4.2.1	Data	105
4.2.2	The Lee-Carter Structure	105

4.2.3	Conditional Heteroskedasticity	106
4.2.4	Asymmetry in Mortality Volatility	108
4.3	A Brief Review of Chapter 2	110
4.3.1	The Key Building Block	111
4.3.2	Longevity Greeks for $p_{x,t}(T, \kappa_0, \sigma_0^2)$	112
4.3.3	Longevity Greeks for the Values of Liabilities and Hedging Instruments	113
4.4	The Enhanced Framework of Longevity Greeks	114
4.4.1	Motivations	114
4.4.2	Redefining the Building Block	115
4.4.3	Longevity Vega for $p_{x,t}(T, \kappa_0, \sigma_1^2)$	115
4.4.4	Longevity Delta and Gamma for $p_{x,t}(T, \kappa_0, \sigma_1^2)$	116
4.4.5	Additional Remarks	117
4.5	A New Longevity Greek: Dynamic Delta	117
4.6	Illustrations	120
4.6.1	General Assumptions	120
4.6.2	Longevity Greeks for the Liability being Hedged	121
4.6.3	Longevity Greeks for the Hedging Instrument	122
4.6.4	Hedge Calibration	124
4.6.5	Illustration 1: Value Hedge	125
4.6.6	Illustration 2: Cash Flow Hedge	126
4.7	Concluding Remarks	127
5	Conclusion and Future Research	137
References		140

APPENDICES	149
A Derivation of the Longevity Greeks	150
B Proof of Theorem 1	152
C Proof of Theorem 2	154
D Proof of Theorem 3	156
E Deriving the Approximation Formula for Case B	160
F Evaluating the Accuracy of the Approximation Methods	162
G Deriving the Sensitivities of $\mathbf{E}[S_{x,u}^{(i)}(T) \mathcal{F}_t]$ for $t = t_b$	166
H Deriving the Sensitivities of $\mathbf{E}[S_{x,u}^{(i)}(T) \mathcal{F}_t]$ for $t > t_b$	168

List of Tables

2.1	The values of the test statistic for Engle's ARCH test and the Ljung-Box test on $(\kappa_t - \kappa_{t-1})^2$	15
2.2	The estimated values of μ , ω , α and β	15
2.3	The values of the test statistic for Engle's ARCH test and the Ljung-Box test on the squared standardized residuals	17
3.1	The estimated values of $\kappa_t^{(R)}$, $\kappa_t^{(\mathcal{B})}$ and γ_{t-x}	61
3.2	The values of HE of the static hedges for the annuity liabilities with $\tau = 0$ and $\tau = 9$	90
3.3	The values of HE for the eight static hedges produced under the baseline specification of $\Sigma^{(\mathcal{B})}$ and the four alternatives specifications of $\Sigma^{(\mathcal{B})}$	93
3.4	The values of HE for the static and dynamic hedges in Scenarios I and II	96
3.5	The values of HEVaR for the four assumed values of λ	98
4.1	A summary of the mortality data used in this chapter	105
4.2	The test statistic and p-value of the Engle's ARCH test applied to the series of $(\kappa_t - \kappa_{t-1})$ for each of the nine populations under consideration	107
4.3	The test statistic and p-value of the Engle's ARCH test applied to the squared standardized residuals for each of the nine populations under consideration	131

4.4	The BIC values resulting from the constant volatility assumption, the GARCH model and four GARCH-type models for the nine populations under consideration	132
4.5	Estimates of parameter γ in the best performing models for Finland, France, Italy, Spain, UK and Japan	132
4.6	Expression of σ_u^2 , $u = 2, 3, \dots$, in terms of σ_1^2 for all GARCH-type models under consideration	133
4.7	Expressions of $\frac{\partial \sigma_u^2}{\partial \sigma_1^2}$, $u = 2, 3, \dots$, for all GARCH-type models under consideration	133
4.8	Parameter estimates of the fitted E-GARCH model for the Italian female population	134

List of Figures

1.1	Mortality rates of the Canadian male population from year 1961 to 2011	2
2.1	The estimated values of a_x , b_x and κ_t	13
2.2	The sample autocorrelation functions for $(\kappa_t - \kappa_{t-1})^2$ and the squared standardized residuals	14
2.3	The retrieved values σ_t^2 over the sample period of 1921 to 2011	16
2.4	The curve $\exp(-\exp(Y_{x,t}(1)))$ against $Y_{x,t}(1)$	23
2.5	The longevity delta of q-forwards	25
2.6	The longevity gamma of q-forwards	27
2.7	The longevity vega of q-forwards	28
2.8	The simulated values of $\exp(-\exp(Y_{x,t}(1))) \mathcal{F}_0$	29
2.9	The values of HE for the delta hedges, vega hedges and optimal hedges	33
2.10	The notional amount of the delta hedge, vega hedge and optimal hedge	34
2.11	The values of HE for the delta-gamma hedges, delta-vega hedges and <i>ex post</i> optimal hedges with $t_1^f = 5$ and $t_2^f = 15$	38
2.12	The delta-gamma and delta-vega ratios for q-forwards with $t_1^f = 5$ and $t_2^f = 15$	40
2.13	The values of HE for the delta-gamma hedges, delta-vega hedges and <i>ex post</i> optimal hedges with $x_1^f = 80$ and $x_2^f = 89$	41

2.14	The delta-gamma and delta-vega ratios for q-forwards with $x_1^f = 80$ and $x_2^f = 89$	42
2.15	The values of HE produced by the delta, vega, delta-gamma, delta-vega and <i>ex post</i> optimal hedges using the non-parametric bootstrapping method	48
2.16	The explanation ratio $\text{ER}(x)$ for $x = 60, \dots, 89$	49
2.17	The values of HE produced by the delta, vega, delta-gamma, delta-vega and <i>ex post</i> optimal hedges using the CBD model	50
3.1	A Lexis diagram showing the first and last period/cohort effects by the data sample	59
3.2	The estimate values of $\kappa_t^{(1)}, \kappa_t^{(2)}, \kappa_t^{(3)}, \kappa_t^{(1,B)}, \kappa_t^{(2,B)}$ and $\gamma_{t-x}^{(R)}$	60
3.3	A Lexis diagram illustrating the distinctions between Case A, Case B and Case C	68
3.4	A Lexis diagram illustrating the distinction between Case C1, and Case C2	72
3.5	A road map summarizing the methods for calculating $E(S_{x,u}^{(i)}(T) \mathcal{F}_t)$	75
3.6	The empirical distributions of the $(t_{2005}, \mathcal{F}_{2006})$ -values of the unhedged position and the hedged position given \mathcal{F}_{2005}	99
4.1	The estimated series of $(\kappa_t - \kappa_{t-1})$ for each of the nine populations under consideration	129
4.2	The inferred values of σ_t^2 derived from the estimated GARCH(1,1) models for the nine populations under consideration	130
4.3	Effectiveness of the value hedges for S-forward with times-to-maturity ranging from 1 to 15 years.	135
4.4	Effectiveness of the cash flow hedges for S-forward with times-to-maturity ranging from 10 to 20 years.	136
F.1	Contour plots showing the percentage errors in approximating $E(S_{x,t}^{(R)}(10) \mathcal{F}_{2010})$ for $x = 65$ and $t = 2010$	164

F.2 Contour plots showing the percentage errors in approximating $E(S_{x,t}^{(i)}(1) \mathcal{F}_{2010})$ for $x = 70$ and $t = 2019$	165
--	-----

Chapter 1

Introduction

1.1 Background

In recent decades, rapid increases in human life expectancy have been observed in most countries. According to Statistics Canada (2018), the Canadian male and female life expectancy at birth increased respectively by an average of 2.9 and 1.8 months each year from 1981 to 2012. Figure 1.1 shows the mortality rates of the Canadian male population at ages 60, 70 and 80 from year 1961 to 2011. It is clear that the realized rates for all ages exhibit a downward/improvement trend over the period shown. More importantly, there is a certain level of uncertainty surrounding the improvement trend of mortality, which we refer to as *longevity risk*.

Longevity risk is borne by institutions that have financial obligations linked to how long an individual may live. Two typical examples of these institutions are defined-benefit pension plans and life insurance companies. For instance, the number of payments a pension plan has to make to a pensioner is proportional to how long the pensioner may live. If this pensioner lives longer than expected, then the pension plan may not have enough money reserved to fulfil its financial obligations to this pensioner.

The size of the longevity risk exposures borne by the pension and life insurance industries is enormous. According to Biffis and Blake (2014), the total amount of pension-related

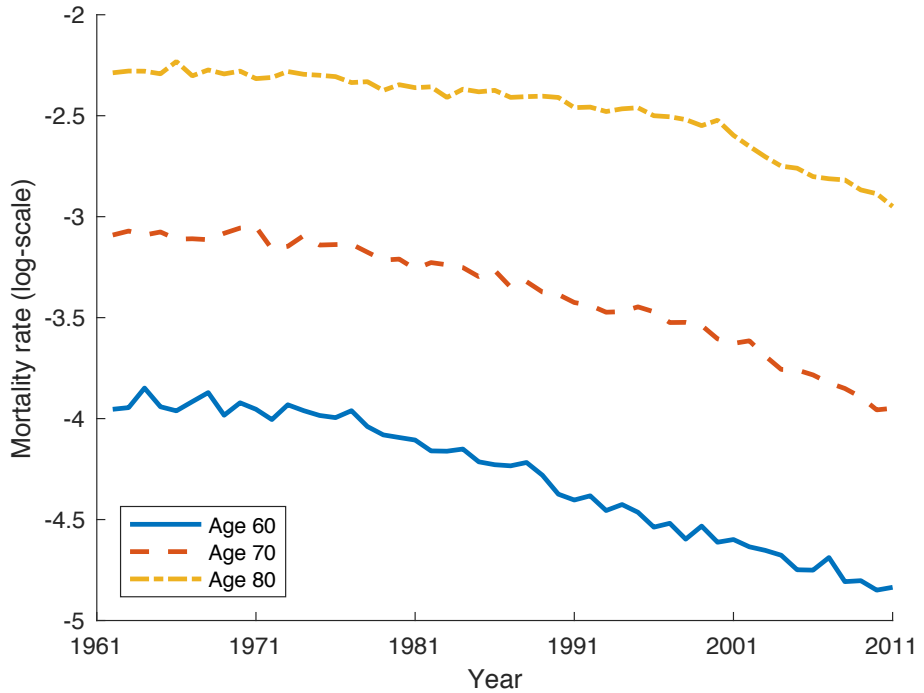


Figure 1.1: The realized mortality rates (log-scale) of the Canadian male population at ages 60, 70 and 80 from year 1961 to 2011.

longevity risk exposures is globally estimated at \$25 trillion (USD). More importantly, longevity risk is a systematic risk that cannot be managed internally through the Law of Large Numbers. That means, unlike a typical insurance risk, selling more insurance products or having more pensioners will not decrease the risk, but instead increase it.

In recent years, the overwhelming longevity risk exposure combined with its systematic nature have driven some pension plans to seek external de-risking solutions. For example, in 2012, General Motors engaged in a pension transfer agreement with Prudential Financial to reduce its pension obligations by approximately \$26 billion (USD). In 2015, the Bell Canada Pension Plan executed a \$5 billion (CAD) longevity swap with Sun Life Financial, SCOR SE, and Reinsurance Group of America. In the UK market, 48 longevity swaps with a total amount of £75 billion (GBP) were completed between 2007 and 2016, covering 13 insurance companies and 22 pension plans (Blake et al., 2018). These transactions have

fostered a new market, called the longevity risk transfer market.

Although we have seen many successful transactions in the past, the size of the current longevity risk transfer market is still small when compared to the total amount of global longevity risk exposures. Zhou and Li (2017) argued that the underdevelopment of the market may be attributed the marked imbalance between the demand and supply for acceptance of longevity risk. Most of the past transactions are insurance-based, which means that the longevity risk is being transferred from a pension plan to an (re-)insurance company, and hence is also kept within the insurance industry. While the insurance industry has the scope and financial stability to accept longevity risk, its capacity is not large enough to generate sufficient supply for acceptance. Using the global size of pension assets as a proxy for demand and the global insurance assets for non-life risks as a proxy for supply, Graziani (2014) concluded that the demand for acceptance of longevity risk is 10 times higher than the supply. A similar conclusion was reached by Michaelson and Mulholland (2014) using the total capital of the global insurance industry and the potential increase in pension liabilities due to unexpected mortality improvement.

To overcome the problem of shortage in supply, some recent studies have argued that the longevity risk exposures borne by pension plans and annuity providers can be transferred to capital markets (e.g., Biffis and Blake, 2014; Blake et al., 2013; Michaelson and Mulholland, 2014). In addition to a risk premium, capital market investors may enjoy diversification benefits from including longevity risk into their portfolio, as longevity risk exhibits no apparent correlations with typical market risk factors, such as equity, inflation and foreign exchange (Ribeiro and Di Pietro, 2009). To further draw interest from these investors, the transfer of risk has to be executed through standardized securities that are (1) linked to broad-based mortality indexes, such as the mortality of a national population, and (2) structured like typical capital market derivatives, such as bonds, swaps and forwards. The act of standardization is important because it fosters liquidity and transparency, both of which are highly demanded by capital market investors.

The act of standardization also poses two fundamental challenges to the end-users of standardized longevity securities. The first challenge concerns modeling the dynamics of broad-based mortality indexes. In particular, a statistical model is needed to explain the mortality behaviour of a national population and/or the population of a pension plan.

Furthermore, based on an established mortality model, one has to be able to accurately measure the level of uncertainty/risk underlying a population's future mortality.

Researchers have contributed significantly on the topic of mortality modeling. A large number of them worked along the lines of the Lee-Carter model, the seminal work of Lee and Carter (1992) (see, e.g., Brouhns et al., 2002; Currie et al., 2004; Czado et al., 2005; Kleinow, 2015; Koissi et al., 2006; Lee and Miller, 2001; Li and Hardy, 2011; Li and Lee, 2005; Li et al., 2009; Pedroza, 2006; Renshaw and Haberman, 2006; Villegas and Haberman, 2014; Zhou et al., 2014). The Cairns-Blake-Dowd model proposed by Cairns et al. (2006) along with its extensions (see, e.g., Cairns et al., 2009, 2011; Haberman et al., 2014; Li et al., 2015) created another large category of mortality modeling studies. Other than the above two groups, many other research projects, such as Ahmadi and Li (2014), Hatzopoulos and Haberman (2013), Jarner and Kryger (2011), Tsai and Yang (2015) and Yang et al. (2010), have also contributed various innovative approaches to modeling the dynamics of mortality.

The second challenge relates to developing a hedging strategy for longevity risk using standardized longevity derivatives. In particular, given a collection of standardized longevity derivatives, how should a hedger optimize a longevity hedge? To answer this question, a hedger needs to determine the types of standardized derivatives to purchase, the notional amounts and other specifications of the chosen derivatives, and also how to evaluate the effectiveness of an implemented hedge.

Over the past few years, there has been a wave of work on addressing the second challenge. Generally speaking, existing hedging strategies can be categorized as either a risk-minimizing approach or a sensitivity-matching approach. A risk-minimizing approach focuses on minimizing a certain risk measure that reflects the extent of the longevity risk exposure of the hedger. Studies that have adopted this approach include Coughlan et al. (2011), Cairns et al. (2014), Dahl and Møller (2006), Dahl et al. (2008), Dahl et al. (2011), Liu and Li (2016), Ngai and Sherris (2011) and Wong et al. (2014). A sensitivity-matching approach, on the other hand, equates the sensitivities of the liability being hedged and the standardized derivatives to changes in the underlying mortality. Examples of this approach include the work of Cairns (2011), Cairns (2013), Li and Hardy (2011), Li and Luo (2012), Lin and Tsai (2013), Lin and Tsai (2014), Luciano et al. (2012), Luciano et al. (2017), Tsai

et al. (2010), Tsai and Chung (2013) and Zhou and Li (2017).

1.2 Objectives and Outline of the Thesis

The objectives of this thesis are to (1) procure a deeper understanding of mortality modeling with a specific focus on the volatility of mortality (i.e., the level of uncertainty surrounding the improvement trend of mortality), and (2) further investigate the implementation and implications of index-based longevity hedging. On the modeling front, we propose several extensions of the Lee-Carter model to incorporate conditional heteroskedasticity and asymmetry in the volatility of mortality. We achieve this goal by applying different variations of the generalized autoregressive conditional heteroskedasticity (GARCH) model to the period effect of the Lee-Carter model. We also utilize the M7-M5 model, a two-population extension of the Cairns-Blake-Dowd model that is capable of capturing the period, cohort (year-of-birth-related) and population basis effects. On the hedging front, we focus on the sensitivity-matching approach of index-based longevity hedging, and work along lines of longevity Greeks (an analogous to option Greeks) and Greek hedging. In particular, we study the properties of longevity Greeks, propose several Greek hedging strategies for longevity risk, and use real data illustrations to explore the implications of the proposed hedging strategies.

In Chapter 2, we focus on incorporating stochastic volatility in the Lee-Carter model, introducing the notion of longevity Greeks, and analysing the properties of longevity Greeks and their applications in index-based longevity hedging. In more detail, we first derive three important longevity Greeks—delta, gamma and vega—on the basis of an extended version of the Lee-Carter model that incorporates stochastic volatility. We then study the properties of each longevity Greek, and estimate the levels of effectiveness that different longevity Greek hedges can possibly achieve. The results reveal several interesting facts. For example, we found and explained that, other things being equal, the magnitude of the longevity gamma of a q -forward increases with its reference age. As with what have been developed for equity options, these properties allow us to know more about standardized longevity derivatives as a risk mitigation tool. Our findings on hedge effectiveness may

also aid insurers to better formulate their hedge portfolios, and issuers of mortality-linked securities to determine what security structures are more likely to attract liquidity. Lastly, we investigate how much hedge effectiveness may be eroded if the mortality model from which the longevity Greeks are derived does not hold.

In Chapter 3, we move onto delta hedging the trend and cohort components of longevity risk under the M7-M5 model. The M7-M5 model is a two-population mortality model developed and recommended (as an industry standard for the assessment of population basis risk) by a recent project commissioned by the Institute and Faculty of Actuaries and the Life and Longevity Markets Association. We develop a longevity delta hedging strategy for use with the M7-M5 model, taking into account of not only period effect uncertainty but also cohort effect uncertainty and population basis risk. To enhance practicality, the hedging strategy is formulated in both static and dynamic settings, and its effectiveness can be evaluated in terms of either variance or 1-year ahead Value-at-Risk (the latter is highly relevant to solvency capital requirements). Three real data illustrations are constructed to demonstrate (1) the impact of population basis risk and cohort effect uncertainty on hedge effectiveness, (2) the benefit of dynamically adjusting a delta longevity hedge, and (3) the relationship between risk premium and hedge effectiveness.

In Chapter 4, we set out to study the potential asymmetry in mortality volatility and its implications on index-based longevity hedging. We first explore the potential asymmetry in mortality volatility by considering a wide range of GARCH-type models that permit the volatility of mortality improvement to respond differently to positive and negative mortality shocks. We then investigate how the asymmetry of mortality volatility may impact index-based longevity hedging solutions by developing an extended longevity Greeks framework, which encompasses longevity Greeks for a wider range of GARCH-type models, an improved version of longevity vega, and a new longevity Greek known as ‘dynamic delta’. Lastly, our theoretical work is complemented by two real-data illustrations. The empirical results suggest that the effectiveness of an index-based longevity hedge could be significantly impaired if the asymmetry in mortality volatility is not taken into account when the hedge is calibrated.

Finally, Chapter 5 concludes the thesis with some suggestions on future research work.

Chapter 2

Longevity Greeks: What Do Insurers and Capital Market Investors Need to Know?

2.1 Introduction

It has been argued that capital markets may share some of the overwhelming longevity risk exposures borne by the pension and life insurance industries (Blake et al., 2013; Biffis and Blake, 2014; Graziani, 2014; Michaelson and Mulholland, 2014). Capital market investors may be interested in taking longevity risk in exchange for a risk premium, because it has no apparent correlations with typical market risk factors such as equity, inflation and foreign exchange. The resulting diversification effect allows capital market investors to expand their efficient frontiers, achieving better risk and reward combinations.

Capital market investors demand liquidity and transparency. Therefore, to attract their participation in longevity risk transfers, there is a need to package longevity risk as standardized products which are structured like typical capital market derivatives such as swaps and forwards. Hedgers have to compromise, as standardized hedging instruments do not give a full elimination of risk (which bespoke de-risking solutions such as pension

buy-outs can offer). The act of standardization leads to a fundamental question: given a collection of standardized mortality derivatives, how should a hedger optimize a longevity hedge? Over the past few years, there has been a wave of work on this research question. The contributions can be divided into two broad categories: (1) risk minimization and (2) sensitivity matching.

A risk minimization strategy is one that aims to minimize a certain risk measure which reflects the hedger's exposure to longevity risk. The most commonly used risk measure is the variance of the present values of the unexpected cash flows arising from the liability being hedged and the hedging instruments used. Examples of such strategies include those proposed by Dahl and Møller (2006), Dahl et al. (2008), Coughlan et al. (2011), Dahl et al. (2011), Ngai and Sherris (2011), Cairns et al. (2014) and Wong et al. (2014). These strategies are very well suited for hedgers with a definite hedging objective (e.g., minimizing variance). However, a solution that is optimum with respect to one objective may require compromising other objectives. That being said, when a hedger cares about the overall longevity risk profile (based on a collection of risk measures), then a risk minimization strategy may not result in the most preferred hedge portfolio.

A sensitivity matching strategy is one that equates the sensitivities of the liability being hedged and the hedging instruments used to changes in the underlying mortality. Rather than focusing on a particular objective, it aims to find a ‘replicating portfolio’ that is a broadly similar to the liability being hedged in terms of its longevity risk exposure. Compared to risk minimization, sensitivity matching appears to be more flexible as measures of mortality sensitivity can be applied to, in principle, all types of life-contingent liabilities (e.g., life insurance and annuities) and mortality derivatives (e.g., mortality forwards and swaps). It is also more adaptable to the formation of a liability hedging platform (Coughlan et al., 2007), in which risks other than longevity (e.g., equity and inflation) are also hedged so that a synthetic pension buy-out can be created. This is because the other risks can be mitigated by matching additional sensitivity measures (e.g., the equity delta), without the need to re-derive the optimal solution.

Depending on how sensitivity is quantified, sensitivity matching strategies can be further classified into two types. The first type is based on the sensitivity to the changes in the (future) mortality rates themselves. For instance, the key q-duration proposed by

Li and Luo (2012) measures the sensitivity to changes in several representative mortality rates on the relevant mortality curve/surface. Other examples include those considered by Li and Hardy (2011), Plat (2011), Tsai et al. (2010), Tsai and Jiang (2011), Lin and Tsai (2013) and Tsai and Chung (2013). In addition to calibrating standardized longevity hedges, sensitivity matching techniques have also been used in the context of natural hedging, whereby the offsetting longevity exposures in life insurance and life annuity books are utilized (see, e.g., Wang et al., 2010; Lin and Tsai, 2014).

The second type, which is the focus of this chapter, is based on the sensitivity to changes in certain parameter(s) in the stochastic process driving the evolution of mortality. Such measures of sensitivity are sometimes known as ‘longevity Greeks’, as they are largely analogous to option Greeks that are utilized extensively to hedge equity-related risks. In a continuous-time setting, Luciano et al. (2012), Luciano and Regis (2014) and Luciano et al. (2017) use two longevity Greeks (delta and gamma) to develop their hedge portfolios. Their contributions have been extended by De Rosa et al. (2017), who incorporate an additional longevity Greek (theta) to measure the change in the value of a life-contingent liability with respect to the passage of time. In a discrete-time setting, delta hedging has been considered by Cairns (2011) and Zhou and Li (2017), and extended by Cairns (2013) to delta-nuga hedging which incorporates additionally the sensitivity to the drift vector of the random walk embedded in the author’s assumed stochastic mortality model.

The continuous-time setting has many mathematical appeals, including analytical solutions that require no simulation to evaluate. However, it often relies on rather restrictive mortality processes, which inevitably compromise its applicability in practice. As an example, the result of Luciano et al. (2012) is developed from an Ornstein-Uhlenbeck process which captures the mortality intensity of one birth cohort only, and hence it does not facilitate the comparison between hedging instruments that are associated with different years of birth. In this chapter we choose to consider the discrete-time setting, which is more practical at the expense of more computationally involved calculations. We work along the lines of Cairns (2011) with an objective to develop a better understanding of (discrete-time) longevity Greek hedging. As described below, the contributions are quadrifold.

First, we propose to use two additional longevity Greeks: gamma and vega. Considered previously in the continuous-time setting, longevity gamma measures the second-order sen-

sitivity to changes in the period (time-related) effect in the assumed mortality model, complementing the corresponding first-order sensitivity captured by longevity delta. Longevity vega, on the other hand, quantifies the sensitivity to changes in the volatility of the period effects. Despite not being considered in previous studies, we believe that it is important to consider longevity vega, as there exists profound evidence that the evolution of mortality over time is subject to (stochastically) varying volatility (see, e.g., Lee and Miller, 2001; Gao and Hu, 2009; Chai et al., 2013). In the context of equity risk, the importance of vega in a stochastic volatility environment is highlighted by Engle and Rosenberg (1995, 2000), Lehar et al. (2002), Javaheri et al. (2004) and Cr  pey (2004). Several researchers including Gao and Hu (2009), Giacometti et al. (2012), Chai et al. (2013), Chen et al. (2015) and Wang and Li (2016) have used different variants of the generalized autoregressive conditional heteroskedasticity (GARCH) model to capture the stochastic volatility of mortality over time. However, they have made no attempt to relate their GARCH models to longevity hedging.

The longevity Greeks are derived from the Lee-Carter model (Lee and Carter, 1992), which is augmented to incorporate stochastic volatility. In particular, the evolution of its period effect is modeled by a random walk (with drift), of which the innovations are assumed to follow a GARCH(1,1) process. We focus on static hedges, so all longevity Greeks are calculated at time 0 when the hedge is established. The longevity vega of a liability/instrument is defined as the first derivative of its value with respect to the conditional volatility of the innovations at time 0. Likewise, longevity delta and gamma are calculated as the first and second derivatives with respect to the time-0 value of the period effect, respectively. Compared to those of Cairns (2011), our longevity Greeks are different in that they are expressed in a semi-analytical form. For this reason, the computation of our longevity Greeks does not require finite differencing and is therefore somewhat less computationally intensive.

Second, we derive and explain the properties of the three longevity Greeks for q-forwards with different specifications. Simply speaking, a q-forward is a zero-coupon swap with its floating leg proportional to the realized death rate at a certain age (the reference age) in a certain year (the reference year) and its fixed leg proportional to the corresponding pre-determined forward mortality rate. We focus on q-forwards, in part because they

form basic building blocks from which other more complex mortality derivatives can be constructed (Coughlan, 2009), and in part because they have been considered extensively in the literature (e.g., Cairns, 2011, 2013; Cairns et al., 2014; Li and Hardy, 2011; Li and Luo, 2012). We found and explained that, for example, other things equal, the magnitude of the longevity gamma of a q-forward increases with its reference age. As with what have been developed for equity options (see, e.g., McDonald, 2012), these properties allow us to know more about q-forwards as a risk mitigation tool. Also, in practice when a perfect Greek neutralization is not always possible, these properties can guide the hedger to choose an appropriate q-forward which can offset his/her longevity risk exposure in a particular dimension. For instance, if the hedger has an annuity liability with a large longevity gamma, then based on our results he/she should contemplate acquiring a q-forward with a high reference age.

Third, using the properties of longevity Greeks, we identify and explain several relationships between hedge effectiveness and q-forward specification. The results reveal several interesting facts; for example, in a delta-vega hedge formed by q-forwards, the choice of reference ages does not materially affect hedge effectiveness, but the choice of times-to-maturity does. What we found may aid insurers to better formulate their hedge portfolios, in terms of choosing what q-forwards to use and what longevity Greek(s) to match. The relationships we identified also allow us to go beyond the classical problem of longevity hedge optimization, shedding light on questions like “what q-forward specification is likely to be the most useful to typical hedgers?” The answers to such questions may help issuers of mortality derivatives determine what security specifications are more likely to attract demand and hence liquidity.

Fourth and finally, we investigate how much hedge effectiveness may be eroded if the mortality model from which the longevity Greeks are derived does not hold. We also examine if the identified patterns of hedge effectiveness relative to q-forward specifications are still preserved if the evolution of mortality does not follow the assumed model. To this end, we employ the non-parametric bootstrapping method considered by Li and Ng (2011), in which scenarios of future mortality are simulated by drawing pseudo samples of mortality improvement rates from the historical data. This bootstrapping method is chosen for our analyses, because among all available mortality bootstrapping methods (Brouhns

et al., 2005; Koissi et al., 2006; Renshaw and Haberman, 2008; Liu and Braun, 2010; Li, 2014; Yang et al., 2015), it appears to be the only one that entails no assumed model. So far as we aware, this study represents the first attempt to validate longevity hedging results with a non-parametric, model-free approach.

The rest of this chapter is organized as follows. Section 2.2 introduces the extension of the Lee-Carter model that incorporates stochastic volatility. Section 2.3 defines the three longevity Greeks considered, and derives these Greeks for annuity liabilities and q-forwards. Section 2.4 studies the properties of the three longevity Greeks for q-forwards with different specifications. Section 2.5 considers several longevity Greek hedging strategies and estimate the levels of hedge effectiveness that these strategies can possibly achieve. Section 2.6 validates the results in the previous section using the non-parametric bootstrapping method. Finally, Section 2.7 concludes with a discussion of the limitations of this study.

2.2 The Lee-Carter Model with Stochastic Volatility

The model we consider is developed from the Lee-Carter structure, which assumes that

$$\ln(m_{x,t}) = a_x + b_x \kappa_t, \quad (2.1)$$

where $m_{x,t}$ represents the *underlying* central death rate at age x and in year t , a_x is a parameter capturing the average level of mortality at age x , κ_t is a time-varying index (the period effect) reflecting the overall level of mortality in year t , and b_x is a parameter measuring the sensitivity of the mortality at age x to changes in κ_t .

As in many studies of the Lee-Carter model including the original work of Lee and Carter (1992), we assume that κ_t follows a random walk with drift. However, to capture the potential stochastic volatility of mortality, we permit the innovations of the random walk to follow a GARCH(1,1) process. Overall, the dynamics of κ_t are governed by the following set of equations:

$$\begin{cases} \kappa_t &= \kappa_{t-1} + \mu + \epsilon_t \\ \epsilon_t &= \sigma_t \eta_t \\ \sigma_t^2 &= \omega + \alpha \epsilon_{t-1}^2 + \beta \sigma_{t-1}^2 \end{cases}, \quad (2.2)$$

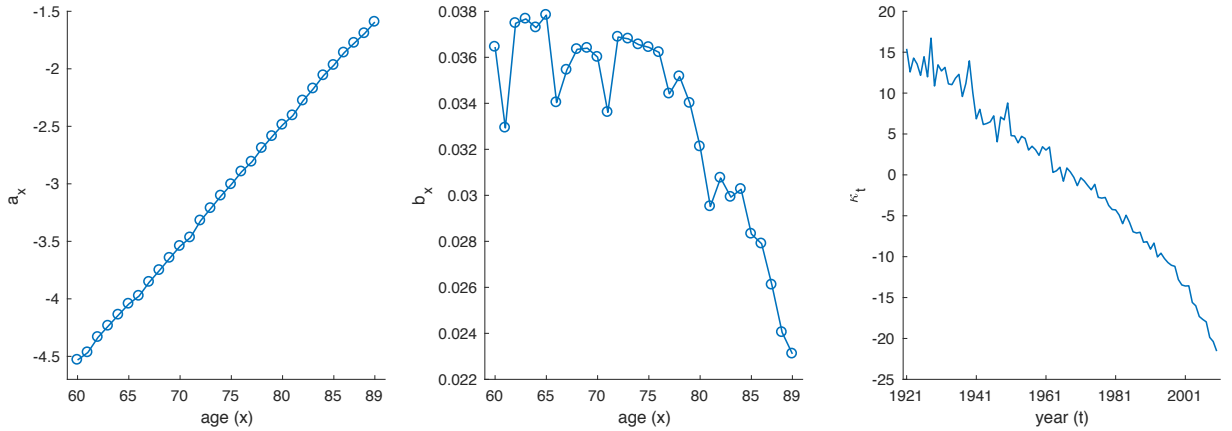


Figure 2.1: The estimated values of a_x , b_x and κ_t .

where μ is the drift term representing the expected rate of change in κ_t , ϵ_t is the innovation at time t , σ_t^2 is the conditional variance of ϵ_t , η_t is a standard normal random variable which possesses no serial correlation, and ω , α , β are parameters in the GARCH process that determines the evolution of σ_t^2 . Parameters α and β , which respectively measures the dependence of σ_t^2 on ϵ_{t-1}^2 and σ_{t-1}^2 , play the most crucial role in modeling stochastic volatility. In the extreme case when $\alpha = \beta = 0$, the volatility of ϵ_t becomes constant over time and equation (2.2) degenerates to an ordinary random walk with drift.

We illustrate the proposed model using data from the female population of England and Wales (EW), over an age range of 60 to 89 and a sample period of 1921 to 2011. This data set and the estimated model are used throughout the rest of this chapter.

We first use Poisson maximum likelihood (Brouhns et al., 2002) to estimate the parameters in equation (2.1). The estimated values of a_x , b_x and κ_t are shown in Figure 2.1. Of our particular interest is the pattern of κ_t . As expected, κ_t possesses a downward trend, which reflects the historical improvement in mortality. The augmented Dickey-Fuller test confirms that this trend is removed after first differencing; that is, the series of $\kappa_t - \kappa_{t-1}$ is stationary. More importantly, we observe signs of varying volatility from the pattern of κ_t , particularly during 1921-1961.

We use Engle's ARCH test and the Ljung-Box test to verify the existence of conditional heteroskedasticity. Reported in Table 2.1, the test results reject the null hypothesis

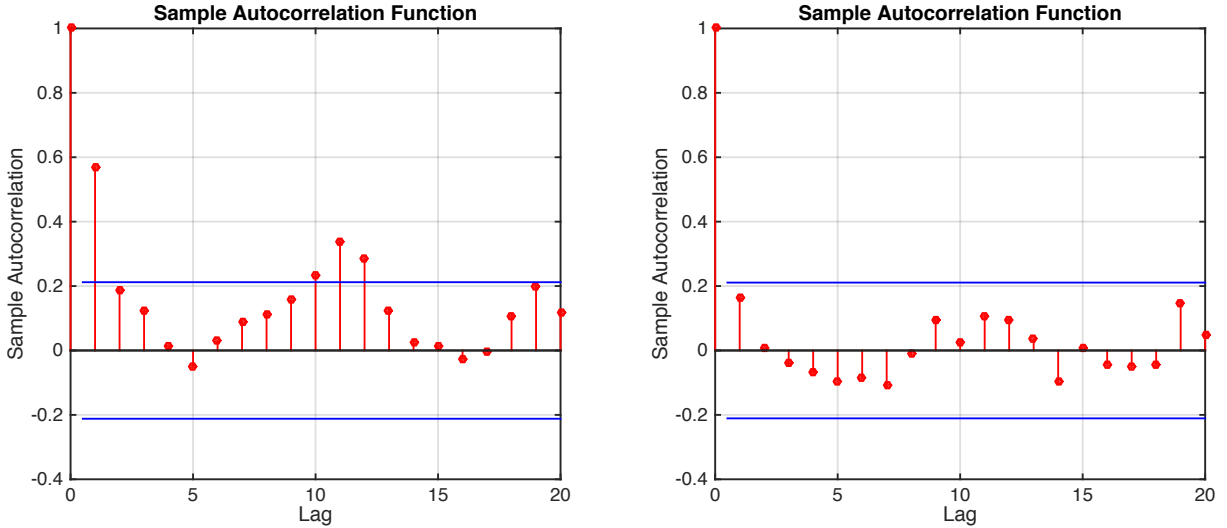


Figure 2.2: The sample autocorrelation functions for $(\kappa_t - \kappa_{t-1})^2$ (the left panel) and the squared standardized residuals $(\epsilon_t^2 / \sigma_t^2)$ in equation (2.2) (the right panel), lags 1 to 20.

that $(\kappa_t - \kappa_{t-1})^2$ possesses no serial correlation, confirming the existence of conditional heteroskedasticity. The test results are echoed in the sample autocorrelation function for $(\kappa_t - \kappa_{t-1})^2$ (Figure 2.2, left panel), from which we observe that the sample autocorrelation for $(\kappa_t - \kappa_{t-1})^2$ at lags 1, 10, 11 and 12 are significant. There is hence a strong ground for using a GARCH process for ϵ_t instead of assuming a constant volatility.

We then fit equation (2.2) to the estimates of κ_t over the sample period. The retrieved values of σ_t^2 are displayed in Figure 2.3, while the estimates of μ , ω , α and β are reported in Table 2.2. The existence of conditional heteroskedasticity is further supported by the empirical facts that σ_t^2 is not constant over time and that the estimates of α and β are significantly different from zero.

Finally, we evaluate the adequacy of the assumed stochastic process by applying Engle's ARCH test and the Ljung-Box test to the squared standardized residuals $(\epsilon_t^2 / \sigma_t^2)$. For both tests, the null hypothesis that $\epsilon_t^2 / \sigma_t^2$ is free of serial correlation is not rejected (see Table 2.3), suggesting that conditional heteroskedasticity is adequately captured by the assumed stochastic process. The same conclusion can be drawn from the right panel of Figure 2.2, where we plot the sample autocorrelation function for the squared standardized residuals.

Lag	1	2	3	4	5
Engle's ARCH test	19.9426 (<0.0001)	21.7042 (<0.0001)	22.8088 (<0.0001)	22.7850 (0.0001)	23.1499 (0.0003)
The Ljung-Box test	20.5841 (<0.0001)	21.5166 (<0.0001)	22.2887 (<0.0001)	22.5414 (0.0002)	23.0843 (0.0003)

Table 2.1: The values of the test statistic for Engle's ARCH test and the Ljung-Box test on $(\kappa_t - \kappa_{t-1})^2$, lags 1 to 5. The p-Values are reported in parentheses.

Parameter	Estimate	Standard error	t-value
μ	-0.49476	0.109296	-4.52677
ω	0.03297	0.046127	0.71482
α	0.13450	0.062155	2.16393
β	0.83494	0.071398	11.6941

Table 2.2: The estimates of μ , ω , α and β in equation (2.2).

We conclude this section with two remarks. First, admittedly, the existence of conditional heteroskedasticity is data dependent. Nevertheless, it has been detected in the historical mortality experiences of quite a few other populations; see Gao and Hu (2009) for Iceland, Giacometti et al. (2012) for Italy, Chai et al. (2013) for the UK (including the part of UK outside England and Wales), Chen et al. (2015) and Wang and Li (2016) for Canada, France, Germany, Japan and the USA. Second, to keep the mathematics in the derivation of longevity Greeks modest, we consider only the simplest possible GARCH process and do not impose an autoregressive moving average (ARMA) structure for the conditional mean of $\kappa_t - \kappa_{t-1}$. In principle, a more general GARCH($P \geq 1, Q \geq 1$) process can be assumed, but, as Tsay (2005, Ch.3) mentioned, in most applications only lower order GARCH processes such as GARCH(1,1) are used.

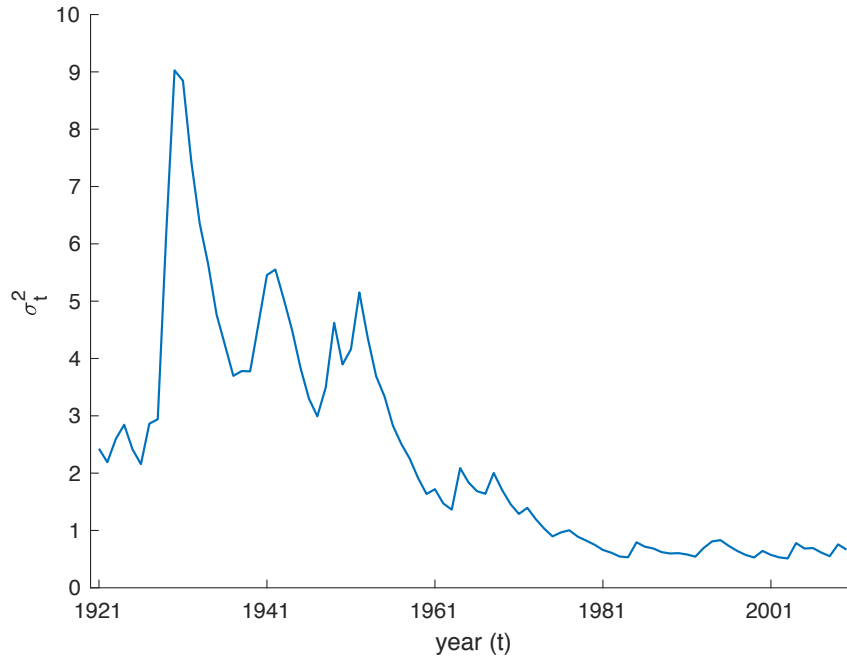


Figure 2.3: The retrieved values σ_t^2 over the sample period of 1921 to 2011.

2.3 The Longevity Greeks

2.3.1 Defining Survival Probabilities

Let

$$S_{x,t}(T) = \prod_{s=1}^T (1 - q_{x+s-1, t+s})$$

be the *ex post* probability that an individual aged x at time t would have survived to time $t + T$, where $q_{x,t}$ represents the probability that an individual aged x at time $t - 1$ dies between time $t - 1$ and t (during year t). Using the approximation that $q_{x,t} \approx 1 - \exp(-m_{x,t})$, which holds exact if the force of mortality between two integer ages is

Lag	1	2	3	4	5
Engle's ARCH test	2.3773 (0.1231)	2.5549 (0.2787)	2.5148 (0.4726)	2.8920 (0.5761)	3.2689 (0.6586)
The Ljung-Box test	2.4791 (0.1154)	2.4819 (0.2891)	2.6298 (0.4523)	3.0612 (0.5476)	3.9322 (0.5592)

Table 2.3: The values of the test statistic for Engle's ARCH test and the Ljung-Box test on the squared standardized residuals (ϵ_t^2/σ_t^2) in equation (2.2), lags 1 to 5. The p-Values are reported in parentheses.

constant, we can express $S_{x,t}(T)$ in terms of the Lee-Carter parameters as

$$\begin{aligned} S_{x,t}(T) &\approx \exp\left(-\sum_{s=1}^T \exp(a_{x+s-1} + b_{x+s-1}\kappa_{t+s})\right) \\ &= \exp\left(-\sum_{s=1}^T \exp(Y_{x,t}(s))\right) \\ &= \exp(-W_{x,t}(T)), \end{aligned}$$

where $Y_{x,t}(s) = a_{x+s-1} + b_{x+s-1}\kappa_{t+s}$ and $W_{x,t}(T) = \sum_{s=1}^T \exp(Y_{x,t}(s))$ are defined for simplicity.

For ease of exposition, from now on time $t = 0$ represents the time at which the (static) longevity hedge is established. In the illustrations, we set time 0 to the end of 2011, the year in which the data sample ends. We let \mathcal{F}_t be the information about mortality up to and including time t . It is clear that for $t \geq 0$, $S_{x,t}(T)|\mathcal{F}_0$ is a random variable which depends on the random realizations of κ_s for $s = t+1, \dots, t+T$.

According to equation (2.2), we have the following expression for κ_t given \mathcal{F}_0 :

$$\kappa_t = \kappa_0 + t\mu + \sum_{s=1}^t \epsilon_s = \kappa_0 + t\mu + \sum_{s=1}^t \sigma_s \eta_s,$$

where

$$\sigma_t^2 = \begin{cases} \omega \left(1 + \sum_{s=1}^{t-1} \prod_{u=1}^s (\alpha \eta_{t-u}^2 + \beta)\right) + (\alpha \epsilon_0^2 + \beta \sigma_0^2) \prod_{u=1}^{t-1} (\alpha \eta_{t-u}^2 + \beta) & \text{if } t \geq 2 \\ \omega + \alpha \epsilon_0^2 + \beta \sigma_0^2 & \text{if } t = 1 \end{cases}.$$

It follows that $S_{x,t}(T)$ depends on κ_0 (the time-0 value of the period effect), σ_0^2 (the time-0 value of the conditional volatility) and the sequence of i.i.d. standard normal random variables $\{\eta_s; s = 1, \dots, t + T\}$.

Finally, we let

$$p_{x,t}(T, \kappa_0, \sigma_0^2) := \mathbb{E}[S_{x,t}(T) \mid \mathcal{F}_0],$$

which represents the expected probability that an individual aged x at time t survives to time $t + T$, given the information about mortality up to and including time 0. Revealed later in this section, $p_{x,t}(T, \kappa_0, \sigma_0^2)$ is the key building block for the expected present values of the liability being hedged and the hedging instruments at the time when the hedge is established. We can compute $p_{x,t}(T, \kappa_0, \sigma_0^2)$ by simulations. Specifically, we can simulate a large number, say N , of sample paths of $\{\eta_s; s = 1, \dots, t + T\}$, from which N realizations of $S_{x,t}(T)|\mathcal{F}_0$ can be obtained; the value of $p_{x,t}(T, \kappa_0, \sigma_0^2)$ can be evaluated by averaging the N realizations of $S_{x,t}(T)|\mathcal{F}_0$.

2.3.2 The Longevity Greeks for $p_{x,t}(T, \kappa_0, \sigma_0^2)$

In this section, we define the three longevity Greeks for $p_{x,t}(T, \kappa_0, \sigma_0^2)$. The full derivation of each Greek is presented in Appendix A.

The longevity delta for $p_{x,t}(T, \kappa_0, \sigma_0^2)$ is defined as

$$\Delta_{x,t}(T) := \frac{\partial p_{x,t}(T, \kappa_0, \sigma_0^2)}{\partial \kappa_0} = - \sum_{s=1}^T b_{x+s-1} \mathbb{E}[\exp(Y_{x,t}(s) - W_{x,t}(T)) \mid \mathcal{F}_0], \quad (2.3)$$

which measures the first-order sensitivity of $p_{x,t}(T, \kappa_0, \sigma_0^2)$ to κ_0 (the time-0 value of the period effect). For most mortality data sets (including the one we consider), the estimates of b_x are all positive. In this case, according to the above formula, $\Delta_{x,t}(T)$ is always negative, which means that $p_{x,t}(T, \kappa_0, \sigma_0^2)$ is negatively related to κ_0 .

The longevity gamma for $p_{x,t}(T, \kappa_0, \sigma_0^2)$ is defined as

$$\begin{aligned} & \Gamma_{x,t}(T) \\ &:= \frac{\partial^2 p_{x,t}(T, \kappa_0, \sigma_0^2)}{\partial \kappa_0^2} \end{aligned} \tag{2.4}$$

$$= \mathbb{E} \left[\exp(-W_{x,t}(T)) \left(\left(\sum_{s=1}^T b_{x+s-1} \exp(Y_{x,t}(s)) \right)^2 - \sum_{s=1}^T b_{x+s-1}^2 \exp(Y_{x,t}(s)) \right) \middle| \mathcal{F}_0 \right], \tag{2.5}$$

which represents the second-order sensitivity of $p_{x,t}(T, \kappa_0, \sigma_0^2)$ to κ_0 and, equivalently, the first-order sensitivity of the longevity delta $\Delta_{x,t}(T)$ to κ_0 . If $\Gamma_{x,t}(T)$ is negative, then $p_{x,t}(T, \kappa_0, \sigma_0^2)$ is a concave function of κ_0 . The implications of the sign of $\Gamma_{x,t}(T)$ is further discussed later in section 2.4.

The longevity vega for $p_{x,t}(T, \kappa_0, \sigma_0^2)$ is defined as

$$\begin{aligned} V_{x,t}(T) &:= \frac{\partial p_{x,t}(T, \kappa_0, \sigma_0^2)}{\partial \sigma_0^2} \\ &= - \sum_{s=1}^T b_{x+s-1} \mathbb{E} \left[\exp(Y_{x,t}(s) - W_{x,t}(T)) \left(\frac{\partial \kappa_{t+s}}{\partial \sigma_0^2} \right) \middle| \mathcal{F}_0 \right], \end{aligned} \tag{2.6}$$

where

$$\frac{\partial \kappa_{t+s}}{\partial \sigma_0^2} = \sum_{u=1}^{t+s} \frac{\eta_u}{2\sigma_u} \frac{\partial \sigma_u^2}{\partial \sigma_0^2}$$

and

$$\frac{\partial \sigma_u^2}{\partial \sigma_0^2} = \begin{cases} \beta \prod_{v=1}^{u-1} (\alpha \eta_{u-v}^2 + \beta) & \text{if } u \geq 2 \\ \beta & \text{if } u = 1 \end{cases}.$$

It measures the first-order sensitivity of $p_{x,t}(T, \kappa_0, \sigma_0^2)$ to changes in σ_0^2 (the time-0 value of the conditional volatility). Compared to $\Delta_{x,t}(T)$, $V_{x,t}(T)$ contains additionally $\partial \kappa_{t+s} / \partial \sigma_0^2$, which measures the sensitivity of the period effect at time $t+s$ to σ_0^2 . It is also noteworthy that the longevity vega depends critically on parameter β , which measures the extent of GARCH effect (i.e., the serial dependence in the conditional variance). If β equals zero,

then the longevity vega is always zero, which means that $p_{x,t}(T, \kappa_0, \sigma_0^2)$ is no longer sensitive to the time-0 value of the conditional volatility.

The value of $\Delta_{x,t}(T)$, $\Gamma_{x,t}(T)$ and $V_{x,t}(T)$ can be obtained numerically. In particular, using N simulated paths of $\{\eta_s; s = 1, \dots, t + T\}$ (which should be the same as those used for calculating $p_{x,t}(T, \kappa_0, \sigma_0^2)$), we can readily obtain N realizations of $Y_{x,t}(s)|\mathcal{F}_0$ and $W_{x,t}(T)|\mathcal{F}_0$, with which the expectations in expressions (2.3), (2.4) and (2.6) can be evaluated.

2.3.3 The Longevity Greeks of a Stylized Pension Plan

We consider a pension plan for a single cohort of pensioners, who are aged x_0 at time 0. The plan pays each pensioner \$1 at the end of each year until death or time τ , whichever is the earliest. Let r be the constant interest rate at which future cash flows are discounted. When viewed at time 0, the present value of the pension plan's future cash flows is

$$\mathcal{L}(x_0, \tau) = \sum_{s=1}^{\tau} (1+r)^{-s} S_{x_0,0}(s),$$

which is a random variable that depends on the random realizations of κ_t for $t = 1, \dots, \tau$.

At time 0, the expected present value of the pension plan's future cash flows is given by

$$L(x_0, \tau) = \mathbb{E}[\mathcal{L} | \mathcal{F}_0] = \sum_{s=1}^{\tau} (1+r)^{-s} p_{x_0,0}(s, \kappa_0, \sigma_0^2),$$

which is just a linear combination of various expected survival probabilities. It follows that the longevity delta, gamma and vega for the pension plan are

$$\Delta^{(L)}(x_0, \tau) = \sum_{s=1}^{\tau} (1+r)^{-s} \Delta_{x_0,0}(s),$$

$$\Gamma^{(L)}(x_0, \tau) = \sum_{s=1}^{\tau} (1+r)^{-s} \Gamma_{x_0,0}(s)$$

and

$$V^{(L)}(x_0, \tau) = \sum_{s=1}^{\tau} (1+r)^{-s} V_{x_0,0}(s),$$

respectively. These longevity Greeks respectively measure the first-order sensitivity of $L(x_0, \tau)$ to κ_0 , the second-order sensitivity of $L(x_0, \tau)$ to κ_0 , and the first-order sensitivity of $L(x_0, \tau)$ to σ_0^2 .

2.3.4 The Longevity Greeks of q-Forwards

A q-forward is characterized by three parameters: the reference age x^f , the time-to-maturity (also known as the reference year) t^f , and the forward mortality rate q^f . For a q-forward issued at time 0, the payoff to the fixed rate receiver, payable at time t^f , is $q^f - q_{x^f, t^f}$ per \$1 notional. At an interest rate of r , its (random) discounted value at time 0 is given by

$$\begin{aligned}\mathcal{Q}(x^f, t^f) &= (1+r)^{-t^f} (q^f - q_{x^f, t^f}) \\ &= (1+r)^{-t^f} (q^f - (1 - S_{x^f, t^f-1}(1))) \\ &= (1+r)^{-t^f} (S_{x^f, t^f-1}(1) - (1 - q^f)).\end{aligned}$$

Hence, at time 0, the expected present value of the q-forward's payoff from the perspective of the fixed rate receiver is

$$Q(x^f, t^f) = E[\mathcal{Q} | \mathcal{F}_0] = (1+r)^{-t^f} (p_{x^f, t^f-1}(1, \kappa_0, \sigma_0^2) - (1 - q^f)) \quad (2.7)$$

per \$1 notional. As $Q(x^f, t^f)$ is linearly related to $p_{x^f, t^f-1}(1, \kappa_0, \sigma_0^2)$, we can easily calculate the longevity Greeks of the q-forward using what we have developed in Section 2.3.2. It turns out that the longevity delta, gamma and vega of the q-forward (per \$1 notional and from the fixed receiver's perspective) are

$$\begin{aligned}\Delta^{(Q)}(x^f, t^f) &= (1+r)^{-t^f} \Delta_{x^f, t^f-1}(1), \\ \Gamma^{(Q)}(x^f, t^f) &= (1+r)^{-t^f} \Gamma_{x^f, t^f-1}(1),\end{aligned}$$

and

$$V^{(Q)}(x^f, t^f) = (1+r)^{-t^f} V_{x^f, t^f-1}(1),$$

respectively. These longevity Greeks respectively represent the first-order sensitivity of $Q(x^f, t^f)$ to κ_0 , the second-order sensitivity of $Q(x^f, t^f)$ to κ_0 , and the first-order sensitivity

of $Q(x^f, t^f)$ to σ_0^2 . Of course, they are functions of the reference age x^f and time-to-maturity t^f . However, they do not depend on the forward mortality rate q^f , which appears in $Q(x^f, t^f)$ as a constant term and thus becomes irrelevant when derivative is taken.

2.4 Analyzing the Longevity Greeks of q-Forwards

In this section, we study the properties of the three longevity Greeks of q-forwards. All empirical illustrations are based on the data and model described in Section 2.2 and a constant interest rate of $r = 5\%$ per annum.

2.4.1 Introducing the Curve of $\exp(-\exp(Y_{x,t}(1)))$ against $Y_{x,t}(1)$

It follows from equation (2.7) that the expected present value of the payoff to the fixed-rate receiver of a q-forward (with reference age x^f and time-to-maturity t^f) can be expressed as

$$\begin{aligned} Q(x^f, t^f) &= (1+r)^{-t^f} (p_{x^f, t^f-1}(1, \kappa_0, \sigma_0^2) - (1-q^f)) \\ &= (1+r)^{-t^f} (\mathbb{E}[S_{x^f, t^f-1}(1) \mid \mathcal{F}_0] - (1-q^f)) \\ &= (1+r)^{-t^f} (\mathbb{E}[\exp(-\exp(Y_{x^f, t^f-1}(1))) \mid \mathcal{F}_0] - (1-q^f)), \end{aligned}$$

which is linearly related to $\mathbb{E}[\exp(-\exp(Y_{x^f, t^f-1}(1))) \mid \mathcal{F}_0]$.

It is clear that the curve of $\exp(-\exp(Y_{x,t}(1)))$ against $Y_{x,t}(1)$ is very influential to the expected present value and hence the longevity Greeks of a q-forward. It can be verified easily that the curve possesses the following properties.

1. For all real values of $Y_{x,t}(1)$, the curve is downward sloping.
2. For all $Y_{x,t}(1) < 0$ (equivalently speaking, for all $m_{x,t} = \exp(Y_{x,t}(1)) < 1$), the curve is concave.
3. For $Y_{x,t}(1) < -1$ (equivalently speaking, for all $m_{x,t} < \exp(-1) \approx 0.3679$), the curve becomes increasingly concave as $Y_{x,t}$ increases.

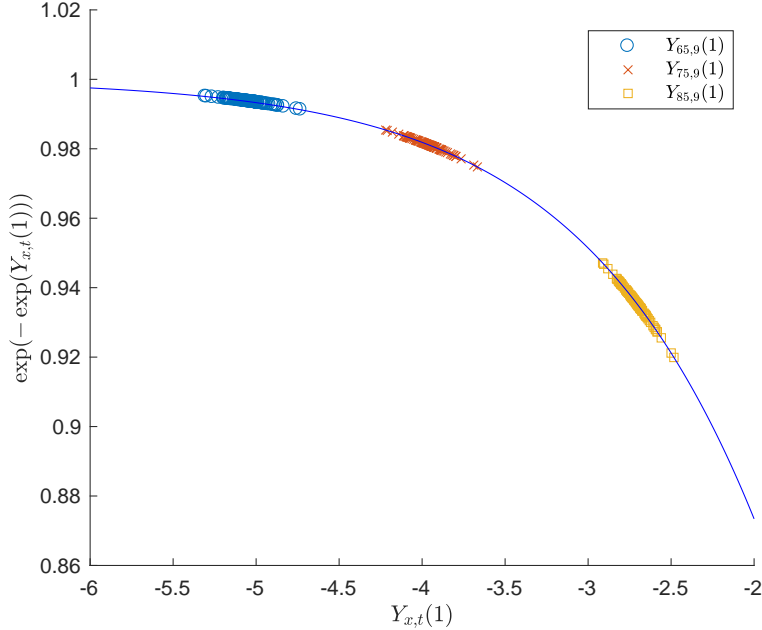


Figure 2.4: The curve $\exp(-\exp(Y_{x,t}(1)))$ against $Y_{x,t}(1)$, for $-6 < Y_{x,t}(1) < -2$, and 100 simulated values of $Y_{65,9}(1)$ (circles), $Y_{75,9}(1)$ (crosses) and $Y_{85,9}(1)$ (squares).

The value of $m_{x,t}$ is typically less than the threshold of 0.3679, except for very high ages. For instance, this threshold is not exceeded until age 97 (100) for English and Welsh males (females) in 2011. In practice, it is unlikely that a q-forward with such an extremely high reference age will be available in the market. Therefore, the portion of the curve of $\exp(-\exp(Y_{x,t}(1)))$ that is of our interest is concave, with a concavity that increases with $Y_{x,t}(1)$. Figure 2.4 shows the curve of $\exp(-\exp(Y_{x,t}(1)))$ for $-6 < Y_{x,t}(1) < -2$, a range that encompasses all values of $Y_{x,t}(1)|\mathcal{F}_0$ for $x = 60, \dots, 89$ and $t = 1, \dots, 30$, calculated from 10,000 simulated sample paths of $\{\kappa_t|\mathcal{F}_0; t = 1, \dots, 30\}$.

Also shown in Figure 2.4 are 100 simulated values of $Y_{x,9}(1)|\mathcal{F}_0$, for $x = 65, 75, 85$. As x increases, the cloud of simulated values moves to the right. This outcome is not surprising, because $Y_{x,t}$, which represents the log central death rate at age x in year t , should be monotonically increasing with x when t is fixed. Consequently, for a given t , the simulated values of $Y_{x,t}(1)|\mathcal{F}_0 = (a_x + b_x \kappa_{t+1})|\mathcal{F}_0$ tend to be larger as x increases. Similarly, because

of the downward trend in κ_t , we can deduce that for a given x , the simulated values of $Y_{x,t}(1)|\mathcal{F}_0$ tend to be smaller as t increases.

The following analyses draw heavily from the facts concerning the curve of $\exp(-\exp(Y_{x,t}(1)))$ against $Y_{x,t}(1)$ and the simulated values of $Y_{x,t}(1)|\mathcal{F}_0$.

2.4.2 Properties of the Longevity Delta

The longevity delta of a q-forward (with reference age x^f and time-to-maturity t^f) is defined as the first partial derivative of $Q(x^f, t^f)$ with respect to κ_0 . Assuming the expectation and differential operator can be interchanged, it can be expressed as

$$\begin{aligned}\Delta^{(Q)}(x^f, t^f) &= (1+r)^{-t^f} \Delta_{x^f, t^f-1}(1) \\ &= (1+r)^{-t^f} \frac{\partial}{\partial \kappa_0} \mathbb{E}[\exp(-\exp(Y_{x^f, t^f-1}(1))) \mid \mathcal{F}_0] \\ &= (1+r)^{-t^f} \mathbb{E}\left[\left(\frac{\partial \exp(-\exp(Y_{x^f, t^f-1}(1)))}{\partial Y_{x^f, t^f-1}(1)}\right) \left(\frac{\partial Y_{x^f, t^f-1}(1)}{\partial \kappa_0}\right) \mid \mathcal{F}_0\right] \\ &= (1+r)^{-t^f} b_{x^f} \mathbb{E}\left[\frac{\partial \exp(-\exp(Y_{x^f, t^f-1}(1)))}{\partial Y_{x^f, t^f-1}(1)} \mid \mathcal{F}_0\right].\end{aligned}\quad (2.8)$$

Figure 2.5 shows the longevity deltas of q-forwards with reference ages $x^f = 60, \dots, 89$ and times-to-maturity $t^f = 1, \dots, 30$. All of the longevity deltas are negative, which is expected because the curve of $\exp(-\exp(Y_{x,t}(1)))$ against $Y_{x,t}(1)$ is always downward sloping (so that the expectation of the partial derivative is negative) and the values of b_x for all $x \in [60, 89]$ are positive.

We also observe that the longevity delta of a q-forward increases (becomes less negative) when its time-to-maturity t^f lengthens, but decreases (becomes more negative) when its reference age x^f rises. These trends can be explained by considering equation (2.8), which suggests that the estimate of $\Delta^{(Q)}(x^f, t^f)$ is proportional to the gradient of the curve of $\exp(-\exp(Y_{x^f, t^f-1}(1)))$ against $Y_{x^f, t^f-1}(1)$ over the region of $Y_{x^f, t^f-1}(1)$ that the simulated values of $Y_{x^f, t^f-1}(1)|\mathcal{F}_0$ span.

As argued in Section 2.4.1, for a fixed x^f , the cloud of the simulated values of $Y_{x^f, t^f-1}(1)|\mathcal{F}_0$ tends to move leftwards as t^f increases, lining up along the flatter portion

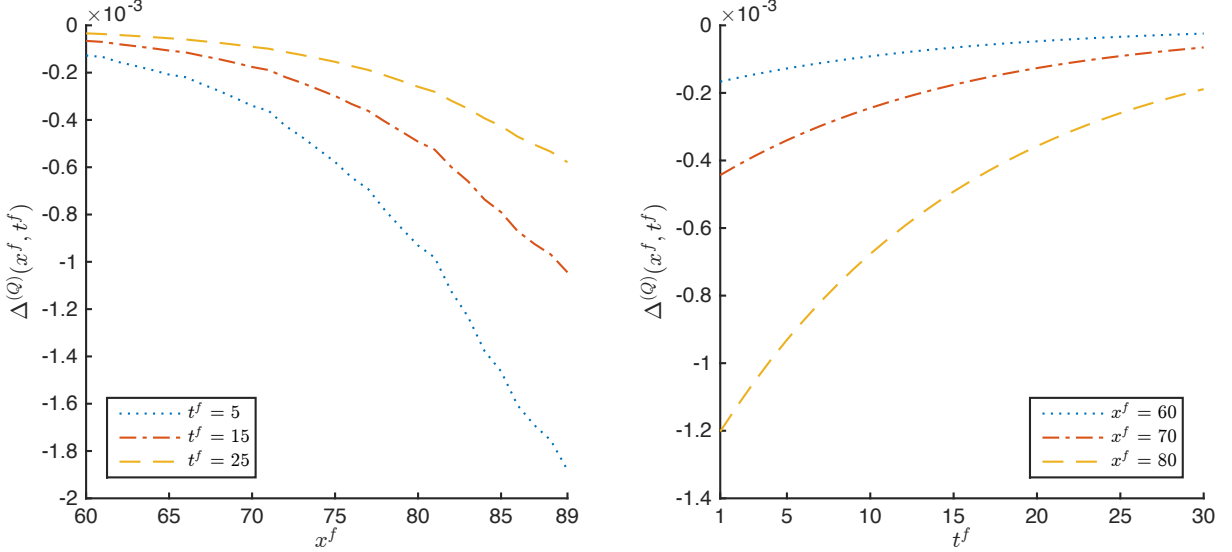


Figure 2.5: The longevity delta of q-forwards with reference ages $x^f = 60, \dots, 89$ and times-to-maturity $1, \dots, 30$.

of the curve of $\exp(-\exp(Y_{x^f, t^f-1}(1)))$ against $Y_{x^f, t^f-1}(1)$. Moreover, the discount factor in $\Delta^{(Q)}(x^f, t^f)$ approaches zero as t^f increases. As such, the magnitude of the longevity delta is smaller as the time-to-maturity t^f becomes longer.

The relationship between $\Delta^{(Q)}(x^f, t^f)$ and x^f is more complicated. On one hand, the magnitude of the expectation in equation (2.8) increases with x^f , as the cloud of the simulated values of $Y_{x^f, t^f-1}(1)|\mathcal{F}_0$ tends to move rightwards when x^f increases. On the other hand, the magnitude of b_{x^f} reduces as x^f increases (see Figure 2.1). However, in this illustration, the former effect outweighs the latter, and consequently the magnitude of the longevity delta becomes larger as the reference age x^f becomes higher.

2.4.3 Properties of the Longevity Gamma

The longevity gamma of a q-forward (with reference age x^f and time-to-maturity t^f) is defined as the second partial derivative of $Q(x^f, t^f)$ with respect to κ_0 . Assuming the

expectation and differential operator are interchangeable, it can be expressed as

$$\begin{aligned}
\Gamma^{(Q)}(x^f, t^f) &= (1+r)^{-t^f} \Gamma_{x^f, t^f-1}(1), \\
&= (1+r)^{-t^f} \frac{\partial^2}{\partial \kappa_0^2} \mathbb{E}[\exp(-\exp(Y_{x^f, t^f-1}(1))) \mid \mathcal{F}_0] \\
&= (1+r)^{-t^f} b_{x^f}^2 \mathbb{E}\left[\frac{\partial^2 \exp(-\exp(Y_{x^f, t^f-1}(1)))}{\partial (Y_{x^f, t^f-1}(1))^2} \mid \mathcal{F}_0\right]. \tag{2.9}
\end{aligned}$$

Figure 2.6 shows the longevity gamma of q-forwards with reference ages $x^f = 60, \dots, 89$ and times-to-maturity $t^f = 1, \dots, 30$. The following observations can be made:

- As the curve of $\exp(-\exp(Y_{x^f, t^f-1}(1)))$ against $Y_{x^f, t^f-1}(1)$ is concave, the expectation of the second partial derivative in equation (2.9) is negative and so is $\Gamma^{(Q)}(x^f, t^f)$.
- As t^f increases, the cloud of the simulated values of $Y_{x^f, t^f-1}(1) \mid \mathcal{F}_0$ tends to move leftwards where the curve of $\exp(-\exp(Y_{x^f, t^f-1}(1)))$ against $Y_{x^f, t^f-1}(1)$ is less concave, so the expectation of the second partial derivative in equation (2.9) becomes less negative. Compounded by the fact that the discount factor diminishes with t^f , the value of $\Gamma^{(Q)}(x^f, t^f)$ becomes less negative as t^f increases.
- The relationship between $\Gamma^{(Q)}(x^f, t^f)$ and x^f depends on two offsetting effects. As x^f increases, the cloud of the simulated values of $Y_{x^f, t^f-1}(1) \mid \mathcal{F}_0$ tends to move rightwards where the curve of $\exp(-\exp(Y_{x^f, t^f-1}(1)))$ against $Y_{x^f, t^f-1}(1)$ is more concave, which in turn means that the expectation of the second partial derivative in equation (2.9) becomes larger in magnitude. On the other hand, as x^f increases, the magnitude of b_{x^f} reduces (see Figure 2.1). For $x^f < 85$, b_{x^f} reduces rather gently with x^f , so the former effect dominates and the magnitude of $\Gamma^{(Q)}(x^f, t^f)$ increases with x^f . However, the opposite is true for $x^f > 85$ when b_{x^f} reduces rapidly with x^f .
- The relationship between $\Gamma^{(Q)}(x^f, t^f)$ and x^f is somewhat jagged. The jaggedness arises because the estimates of b_x are not perfectly smooth across ages (see Figure 2.1).

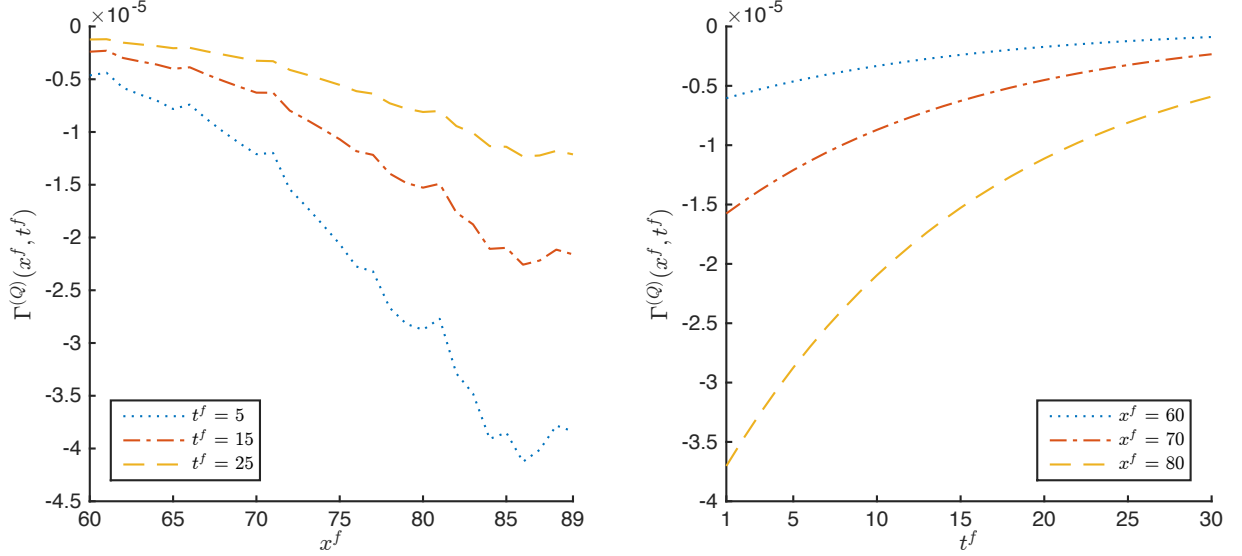


Figure 2.6: The longevity gamma of q-forwards with reference ages $x^f = 60, \dots, 89$ and times-to-maturity $t^f = 1, \dots, 30$.

2.4.4 Properties of the Longevity Vega

In terms of $Y_{x^f, t^f-1}(1)$, the longevity vega of a q-forward (with reference age x^f and time-to-maturity t^f) can be expressed as

$$\begin{aligned} V^{(Q)}(x^f, t^f) &= (1+r)^{-t^f} V_{x^f, t^f-1}(1), \\ &= (1+r)^{-t^f} \frac{\partial}{\partial \sigma_0^2} \mathbb{E}[\exp(-\exp(Y_{x^f, t^f-1}(1))) \mid \mathcal{F}_0], \end{aligned} \quad (2.10)$$

which suggests that from a numerical perspective, $V^{(Q)}(x^f, t^f)$ measures how the average of the simulated values of $\exp(-\exp(Y_{x^f, t^f-1}(1)))$ will change when the time-0 conditional volatility σ_0^2 increases by an arbitrarily small amount.

Figure 2.7 shows the longevity vega of q-forwards with reference ages $x^f = 60, \dots, 89$ and times-to-maturity $t^f = 1, \dots, 30$. As with the longevity delta and gamma, the longevity vega is negative for all reference ages and times-to-maturity considered. A negative longevity vega means that the expected present value of a q-forward decreases as the conditional volatility (σ_0^2) of the current period effect increases. The negativeness

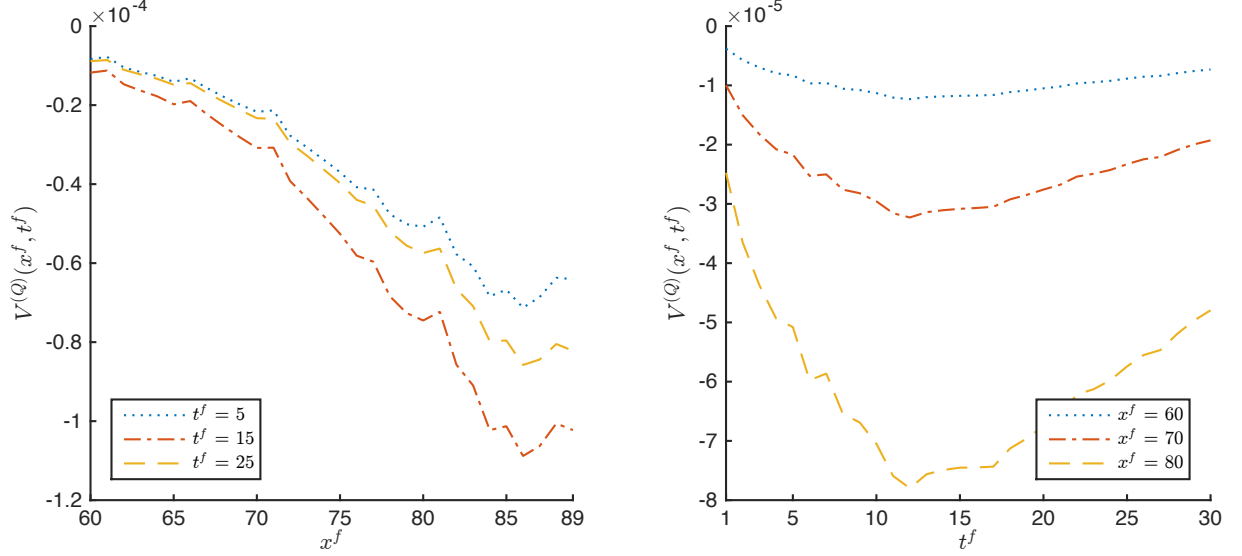


Figure 2.7: The longevity vega of q-forwards with reference ages $x^f = 60, \dots, 89$ and times-to-maturity $1, \dots, 30$.

of the longevity vega is related to the concavity of the curve of $\exp(-\exp(Y_{x^f, t^f-1}(1)))$ against $Y_{x^f, t^f-1}(1)$, which means that the sensitivity of $\exp(-\exp(Y_{x^f, t^f-1}(1)))$ to changes in $Y_{x^f, t^f-1}(1)$ is asymmetric. When σ_0^2 increases, the range of the simulated values of $Y_{x^f, t^f-1}(1)|\mathcal{F}_0$ widens symmetrically around $E[Y_{x^f, t^f-1}(1) | \mathcal{F}_0]$; however, because of the asymmetric sensitivity, the average of the simulated values of $\exp(-\exp(Y_{x^f, t^f-1}(1)))|\mathcal{F}_0$ reduces, thereby resulting in a negative longevity vega.¹ This phenomenon is demonstrated in Figure 2.8, which compares the simulated values of $\exp(-\exp(Y_{x^f, t^f-1}(1)))|\mathcal{F}_0$ that are based on two different assumed values of σ_0^2 .

The relationship between the longevity vega and the reference age (x^f) is a result of the tradeoff between two offsetting effects:

- When x^f increases, the cloud of the simulated values of $Y_{x^f, t^f-1}(1)|\mathcal{F}_0$ tends to move rightwards where the curve of $\exp(-\exp(Y_{x^f, t^f-1}(1)))$ against $Y_{x^f, t^f-1}(1)$ is more

¹According to Theorem 2 in Section 2.5.3, the third moment of $\kappa_{t^f}|\mathcal{F}_0$ about its mean is zero. It follows that the distribution of $Y_{x^f, t^f-1}(1) = a_{x^f} + b_{x^f} \kappa_{t^f}$ given \mathcal{F}_0 is symmetric.

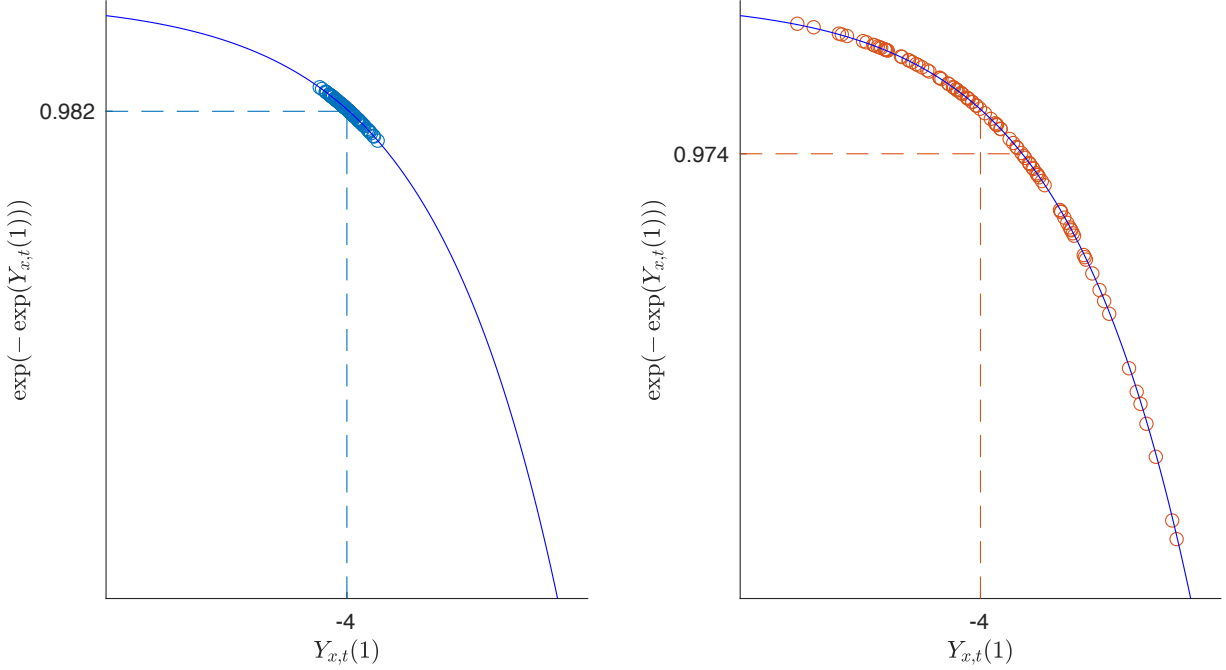


Figure 2.8: The simulated values of $\exp(-\exp(Y_{x,t}(1)))|\mathcal{F}_0$ based on a smaller value of σ_0^2 (the left panel) and a larger value of σ_0^2 (the right panel). The values of x and t used are arbitrary.

concave. The effect of asymmetric sensitivity becomes more severe, thereby pushing the longevity vega more negative.

2. When x^f increases, b_{x^f} reduces and so does the variance of $Y_{x^f,t^f-1}(1)|\mathcal{F}_0$ (which is proportional to the square of b_{x^f}). As the simulated values of $Y_{x^f,t^f-1}(1)|\mathcal{F}_0$ span a smaller range, the effect of asymmetric sensitivity becomes less significant, and hence the longevity vega tends to be less negative.

As seen in the left panel of Figure 2.7, in this illustration the first effect dominates for $x^f < 85$ but the opposite happens when $x^f > 85$.

The relationship between the longevity vega and the time-to-maturity (t^f) depends on the following three factors:

1. Given the assumed stochastic process for κ_t , the volatility of $\kappa_{t^f}|\mathcal{F}_0$ increases with

t^f . As such, when t^f increases, the volatility of $Y_{x^f, t^f-1}(1)|\mathcal{F}_0 = (a_{x^f} + b_{x^f} \kappa_{t^f})|\mathcal{F}_0$ increases and thus the simulated values of $Y_{x^f, t^f-1}(1)|\mathcal{F}_0$ span a wider range. Consequently, the effect of asymmetric sensitivity becomes more significant, thereby pushing the longevity vega more negative.

2. As t^f increases, the cloud of the simulated values of $Y_{x^f, t^f-1}(1)|\mathcal{F}_0$ tends to move leftwards where the curve of $\exp(-\exp(Y_{x^f, t^f-1}(1)))$ against $Y_{x^f, t^f-1}(1)$ is less concave. The effect of asymmetric sensitivity becomes less significant, and thus the longevity vega tends to be less negative.
3. As t^f increases, the discount factor in equation (2.10) reduces and hence the longevity vega tends to be less negative.

The first factor dominates when t^f is small, but the second and third factors become more influential when t^f is high. In this illustration, the turning point is at $t^f = 12$ (see the right panel of Figure 2.7).

2.5 Greek Hedging of Longevity Risk

In this section, we consider different static longevity Greek hedging strategies, and investigate the how much hedge effectiveness can be obtained using different combinations of longevity Greeks and q-forwards.

2.5.1 Assumptions

The following assumptions are used in the rest of this section:

1. The liability being hedged is a pension plan for a single cohort of individuals aged $x_0 = 60$ at time 0. The pension plan pays each pensioner \$1 at the end of each year until age 89 or death, whichever is the earliest (i.e. $\tau = 30$).
2. At time 0, a static longevity hedge for the pension plan is constructed using one or two q-forwards.

3. At time 0, q-forwards with reference ages $x^f = 60, \dots, 89$ and times-to-maturity $t^f = 1, \dots, 30$ years are available. The q-forwards' reference population is the EW female population.
4. The mortality experience of the plan members is identical to that of the EW female population, so that there is no population basis risk.
5. The interest rate for all durations is $r = 5\%$ per annum.
6. The longevity Greeks are numerically calculated based on 10,000 mortality scenarios that are generated from the model described in Section 2.2.

Under these assumptions, the longevity Greeks of the liability being hedged are fixed regardless of how many q-forwards are used and what the reference age(s) and time(s)-to-maturity are. It turns out that the liability being hedged has an expected present value of $L(60, 30) = 13.4403$, a longevity delta $\Delta^{(L)}(60, 30) = -0.0562$, a longevity gamma of $\Gamma^{(L)}(60, 30) = -0.0014$, and a longevity vega of $V^{(L)}(60, 30) = -0.0053$.

2.5.2 The Evaluation Metric

We measure hedge effectiveness with the following metric:

$$HE = 1 - \frac{\text{Var}(\mathcal{L}(60, 30) - \sum_{i=1}^{\mathcal{J}} u(x_i^f, t_i^f) \mathcal{Q}(x_i^f, t_i^f) | \mathcal{F}_0)}{\text{Var}(\mathcal{L}(60, 30) | \mathcal{F}_0)}, \quad (2.11)$$

where

- \mathcal{J} denotes the number of q-forwards used,
- $u(x_i^f, t_i^f)$ represents the notional amount of the i th q-forward used, and
- x_i^f and t_i^f are the reference age and time-to-maturity for the i th q-forward used, respectively.

In the fraction, the numerator is the hedged position's variance whereas the denominator is the unhedged position's variance. It follows that a value of HE that is close to one indicates a good hedge effectiveness.

We simulate 10,000 mortality scenarios on top of those used for calculating the longevity Greeks. The additional 10,000 simulated mortality scenarios enable us to calculate realizations of $\mathcal{L}(60, 30)|\mathcal{F}_0$ and $\mathcal{Q}(x^f, t^f)|\mathcal{F}_0$, with which the value of HE can be estimated.

2.5.3 Single Longevity Greek Hedging

When using $\mathcal{J} = 1$ q-forward to match one longevity Greek, we find the required notional amount by setting

$$\mathcal{G}^{(L)}(60, 30) - u^{(\mathcal{G})}(x^f, t^f)\mathcal{G}^{(Q)}(x^f, t^f) = 0,$$

which gives

$$u^{(\mathcal{G})}(x^f, t^f) = \frac{\mathcal{G}^{(L)}(60, 30)}{\mathcal{G}^{(Q)}(x^f, t^f)},$$

where $\mathcal{G} = \Delta, V$ represents the longevity Greek being matched. We do not consider gamma hedges here, as it does not seem legitimate to match the second-order sensitivity to κ_0 without matching the first-order sensitivity.

It is clear that the notional amount and hence the hedge effectiveness depend on \mathcal{G} , x^f and t^f . Figure 2.9 (left and middle panels) shows the values of HE for $\mathcal{G} = \Delta, V$, $x^f = 60, \dots, 89$ and $t^f = 1, \dots, 30$.

We also benchmark the Greek hedges against the corresponding *ex post* ‘optimal’ hedges, which are obtained by searching for the notional amount that minimizes the hedged position’s variance. Following the results of Cairns et al. (2014), for a hedge with $\mathcal{J} = 1$ q-forward, the *ex post* optimal notional amount is

$$u^{(\text{opt})}(x^f, t^f) = \sqrt{\frac{\text{Var}(\mathcal{L}(60, 30)|\mathcal{F}_0)}{\text{Var}(\mathcal{Q}(x^f, t^f)|\mathcal{F}_0)}} \times \text{Corr}(\mathcal{L}(60, 30), \mathcal{Q}(x^f, t^f)|\mathcal{F}_0), \quad (2.12)$$

which gives a hedge effectiveness equal to the square of $\text{Corr}(\mathcal{L}(60, 30), \mathcal{Q}(x^f, t^f)|\mathcal{F}_0)$. The variances and correlation in equation (2.12) are estimated using the 10,000 mortality sce-

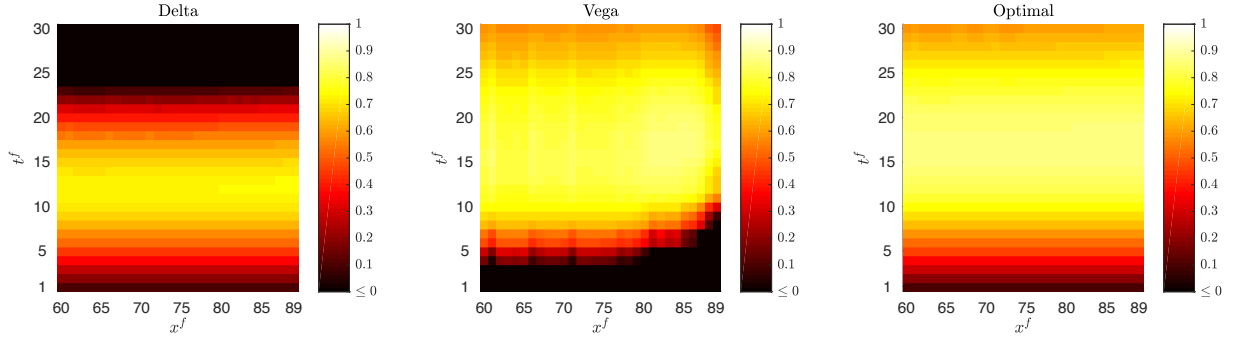


Figure 2.9: The values of HE for the delta hedges (left panel), vega hedges (middle panel) and *ex post* optimal hedges (right panel) with $\mathcal{J} = 1$ q-forward, $x^f = 60, \dots, 89$ and $t^f = 1, \dots, 30$.

narios which we use to evaluate the Greek hedges. The right panel of Figure 2.9 shows the *ex post* optimal hedge effectiveness for different combinations of x^f and t^f .

Several interesting relationships are observed in Figure 2.9. First, for a given time-to-maturity, the hedge effectiveness is insensitive to the choice of the reference age. This outcome is not overly surprising, because the assumed Lee-Carter structure implies that $\ln(m_{x,t})$ and $\ln(m_{y,t})$ are perfectly correlated even if $x \neq y$. As such, q-forwards with the same time-to-maturity but different reference ages should result in similar levels of hedge effectiveness.

Second, a delta hedge is almost equally effective as the *ex post* optimal hedge when the q-forward's time-to-maturity is short (less than 15 years), but is very ineffective when the q-forward's time-to-maturity is long. This outcome can be attributed to the pattern of $\Delta^{(Q)}(x^f, t^f)$ against t^f (Figure 2.5, right panel), which implies that in a delta hedge the notional amount $u^{(\Delta)}(x^f, t^f) = \Delta^{(L)}(60, 30)/\Delta^{(Q)}(x^f, t^f)$ of the q-forward increases rapidly as t^f increases. However, the optimal notional amount $u^{(\text{opt})}(x^f, t^f)$ does not increase rapidly with t^f . In effect, as t^f increases, $u^{(\Delta)}(x^f, t^f)$ moves away from $u^{(\text{opt})}(x^f, t^f)$, leading to a highly sub-optimal hedge effectiveness. See Figure 2.10 for an illustration.

Third, in contrast, the effectiveness of a vega hedge approaches that of the *ex post* optimal hedge when the q-forward's time-to-maturity becomes longer. This relationship is associated with the moments of κ_{tf} (about its mean) under the assumed GARCH process. In more detail, recall that $Q(x^f, t^f)$ (the expected present value of the payoff from a q-

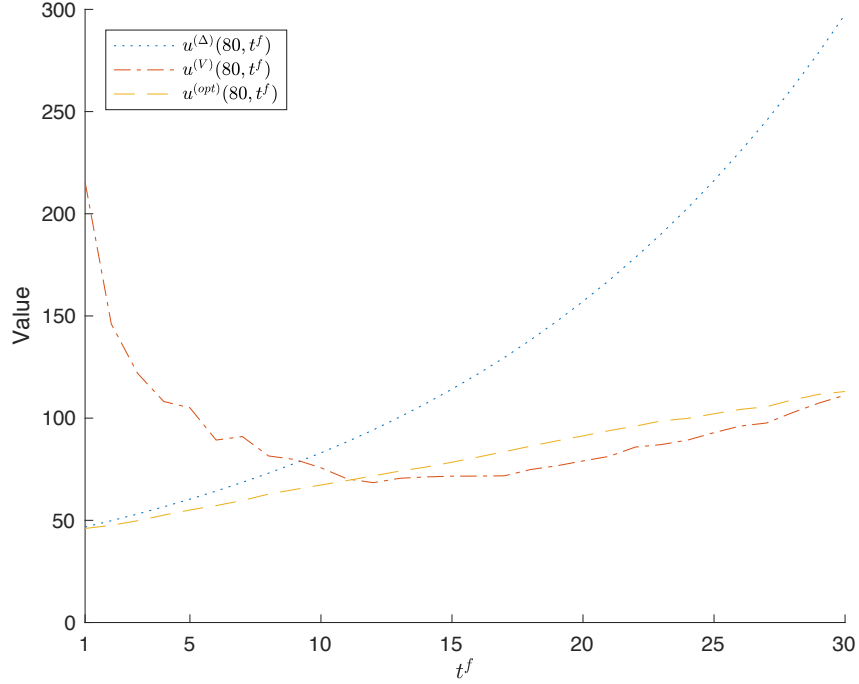


Figure 2.10: The notional amount of the delta hedge, vega hedge and optimal hedge that are built using a q-forward with reference age $x^f = 80$ and times-to-maturity $t^f = 1, \dots, 30$.

forward with reference age x^f and time-to-maturity t^f) is linearly related to

$$p_{x^f, t^f-1}(1, \kappa_0, \sigma_0^2) = \mathbb{E}[\exp(-\exp(a_{x^f} + b_{x^f} \kappa_{t^f})) \mid \mathcal{F}_0] = \mathbb{E}[f(\kappa_{t^f}) \mid \mathcal{F}_0],$$

where

$$f(\kappa_{t^f}) := \exp(-\exp(a_{x^f} + b_{x^f} \kappa_{t^f}))$$

is defined for convenience. Using a fourth order Taylor's expansion, we have

$$\begin{aligned} p_{x^f, t^f-1}(1, \kappa_0, \sigma_0^2) &\approx f(\kappa_0 + t^f \mu) + \frac{1}{2!} \frac{\partial^2 f}{\partial \kappa_{t^f}^2} \mathbb{E} \left[\left(\sum_{s=1}^{t^f} \sigma_s \eta_s \right)^2 \middle| \mathcal{F}_0 \right] \\ &\quad + \frac{1}{3!} \frac{\partial^3 f}{\partial \kappa_{t^f}^3} \mathbb{E} \left[\left(\sum_{s=1}^{t^f} \sigma_s \eta_s \right)^3 \middle| \mathcal{F}_0 \right] + \frac{1}{4!} \frac{\partial^4 f}{\partial \kappa_{t^f}^4} \mathbb{E} \left[\left(\sum_{s=1}^{t^f} \sigma_s \eta_s \right)^4 \middle| \mathcal{F}_0 \right], \end{aligned}$$

where partial derivatives are evaluated at $E[\kappa_{tf} \mid \mathcal{F}_0] = \kappa_0 + t^f \mu$, which is free of σ_0^2 . The moments of $\sum_{s=1}^{t^f} \sigma_s \eta_s$ (i.e., the moments of κ_{tf} about its mean) satisfy the following results.

Theorem 1. *For $t^f \geq 1$,*

$$E\left[\left(\sum_{s=1}^{t^f} \sigma_s \eta_s\right)^2 \mid \mathcal{F}_0\right] = z_{tf,0} + z_{tf,1} \sigma_0^2, \quad (2.13)$$

where $z_{tf,0}$ and $z_{tf,1}$ do not depend on σ_0^2 .

Proof. See Appendix B. \square

Theorem 2. *For $t^f \geq 1$,*

$$E\left[\left(\sum_{s=1}^{t^f} \sigma_s \eta_s\right)^3 \mid \mathcal{F}_0\right] = 0. \quad (2.14)$$

Proof. See Appendix C. \square

Theorem 3. *For $t^f \geq 1$,*

$$E\left[\left(\sum_{s=1}^{t^f} \sigma_s \eta_s\right)^4 \mid \mathcal{F}_0\right] = c_{tf,0} + c_{tf,1} \sigma_0^2 + c_{tf,2} \sigma_0^4, \quad (2.15)$$

where $c_{tf,0}$, $c_{tf,1}$ and $c_{tf,2}$ do not depend on σ_0^2 . Furthermore, $c_{tf,1}$ tends to ∞ as $t^f \rightarrow \infty$, and if $3\alpha^2 + 2\alpha\beta + \beta^2 < 1$ then $c_{tf,2}$ tends to a constant as $t^f \rightarrow \infty$.

Proof. See Appendix D. \square

Our estimated GARCH(1,1) model satisfies the condition that $3\alpha^2 + 2\alpha\beta + \beta^2 < 1$ (see Table 2.2).² It follows from the results above that $Q(x^f, t^f)$ is approximately a quadratic function of σ_0^2 , with a curvature that diminishes as t^f tends to infinity. In other words, the longevity vega $V^{(Q)}(x^f, t^f) = \partial Q(x^f, t^f) / \partial \sigma_0^2$ tends to be a more accurate measure of the sensitivity of $Q(x^f, t^f)$ to σ_0^2 as t^f increases, and thus the effectiveness of a vega hedge tends to be closer to that of the *ex post* optimal hedge for higher values of t^f .

²All stationary ARCH(1) models (in which $\alpha = 0$ and $\beta < 1$) meet this condition. However, admittedly, not all GARCH(1,1) models satisfy this condition, even if they are stationary with $\alpha + \beta < 1$.

2.5.4 Multiple Longevity Greek Hedging

Calculating the Notional Amounts

We now consider matching two longevity Greeks with $\mathcal{J} = 2$ q-forwards. We let \mathcal{G}_1 and \mathcal{G}_2 be the two longevity Greeks being matched, and $u^{(\mathcal{G}_1, \mathcal{G}_2)}(x_1^f, t_1^f)$ and $u^{(\mathcal{G}_1, \mathcal{G}_2)}(x_2^f, t_2^f)$ be the notional amounts of the two q-forwards in the resulting hedge portfolio. We have

$$\begin{pmatrix} \mathcal{G}_1^{(Q)}(x_1^f, t_1^f) & \mathcal{G}_1^{(Q)}(x_2^f, t_2^f) \\ \mathcal{G}_2^{(Q)}(x_1^f, t_1^f) & \mathcal{G}_2^{(Q)}(x_2^f, t_2^f) \end{pmatrix} \begin{pmatrix} u^{(\mathcal{G}_1, \mathcal{G}_2)}(x_1^f, t_1^f) \\ u^{(\mathcal{G}_1, \mathcal{G}_2)}(x_2^f, t_2^f) \end{pmatrix} = \begin{pmatrix} \mathcal{G}_1^{(L)}(60, 30) \\ \mathcal{G}_2^{(L)}(60, 30) \end{pmatrix}, \quad (2.16)$$

which gives

$$u^{(\mathcal{G}_1, \mathcal{G}_2)}(x_1^f, t_1^f) = \frac{\mathcal{G}_1^{(L)}(60, 30)\mathcal{G}_2^{(Q)}(x_2^f, t_2^f) - \mathcal{G}_1^{(Q)}(x_2^f, t_2^f)\mathcal{G}_2^{(L)}(60, 30)}{\mathcal{G}_1^{(Q)}(x_1^f, t_1^f)\mathcal{G}_2^{(Q)}(x_2^f, t_2^f) - \mathcal{G}_1^{(Q)}(x_2^f, t_2^f)\mathcal{G}_2^{(Q)}(x_1^f, t_1^f)} \quad (2.17)$$

and

$$u^{(\mathcal{G}_1, \mathcal{G}_2)}(x_2^f, t_2^f) = \frac{\mathcal{G}_2^{(L)}(60, 30)\mathcal{G}_1^{(Q)}(x_1^f, t_1^f) - \mathcal{G}_2^{(Q)}(x_1^f, t_1^f)\mathcal{G}_1^{(L)}(60, 30)}{\mathcal{G}_1^{(Q)}(x_1^f, t_1^f)\mathcal{G}_2^{(Q)}(x_2^f, t_2^f) - \mathcal{G}_1^{(Q)}(x_2^f, t_2^f)\mathcal{G}_2^{(Q)}(x_1^f, t_1^f)}. \quad (2.18)$$

It is clear that $u^{(\mathcal{G}_1, \mathcal{G}_2)}(x_1^f, t_1^f)$ and $u^{(\mathcal{G}_1, \mathcal{G}_2)}(x_2^f, t_2^f)$ depend on the two q-forwards' specifications as well as the two matched longevity Greeks $(\mathcal{G}_1, \mathcal{G}_2)$, which can be either (Δ, Γ) or (Δ, V) . We do not consider (Γ, V) , because it does not seem appropriate to match Γ without matching Δ .

A necessary (but not sufficient) condition for two q-forwards with *different* times-to-maturity to provide risk reduction is that the notional amounts of both q-forwards must be positive; that is, the hedger must be the fixed leg receiver in both q-forwards. This condition can explained as follows.

- When both notional amounts are negative, the present values of the q-forward portfolio and the pension liability change in the same direction for any departure from the expected mortality trajectory. The pension plan provider will be subject to even more longevity risk compared to the naked position.

- If one notional amount is negative and the other is positive, then the hedged position will be very vulnerable to ‘non-linear’ mortality scenarios. To illustrate, let us suppose that the notional amount of the shorter-dated q-forward is negative while that of the longer-dated is positive. Suppose further that on the earlier maturity date the realized mortality is lower than expected, so that the hedger suffers a loss (arising from both the unexpected increase in the pension liability and the net payment to the q-forward’s counterparty). If the realized mortality on the later maturity date is also lower than expected, then the payoff from the longer-dated q-forward may defray the earlier hedge loss (provided that the notional amount of the longer-dated q-forward is sufficiently large). However, if it turns out to be higher than expected (i.e., a ‘non-linear’ scenario), then the earlier hedge loss can never be recovered.

We remark that this condition does not apply when the q-forwards have the same time-to-maturity, because in this case the payoffs from both q-forwards are made at the same time.

Using equations (2.17) and (2.18), it can be shown straightforwardly that to have both $u^{(G_1, G_2)}(x_1^f, t_1^f)$ and $u^{(G_1, G_2)}(x_2^f, t_2^f)$ being positive, we require

$$\frac{\mathcal{G}_1^{(Q)}(x_1^f, t_1^f)}{\mathcal{G}_2^{(Q)}(x_1^f, t_1^f)} > \frac{\mathcal{G}_1^{(L)}(60, 30)}{\mathcal{G}_2^{(L)}(60, 30)} > \frac{\mathcal{G}_1^{(Q)}(x_2^f, t_2^f)}{\mathcal{G}_2^{(Q)}(x_2^f, t_2^f)}, \quad (2.19)$$

that is, the ratio of the two matched longevity Greeks for the liability being hedged must be strictly in between those of the two q-forwards. This necessary condition explains many of the hedging results we are about to present.

The Impact of the Reference Age Combinations

We now examine the effectiveness of the delta-gamma and delta-vega hedges for different reference ages when the times-to-maturity are fixed to 5 and 15 years, respectively. As in the previous sub-section, we benchmark the Greek hedges against their corresponding *ex post* optimal hedges, which are obtained by minimizing the hedged position’s variance on the basis of the 10,000 mortality scenarios used for evaluating the Greek hedges. The

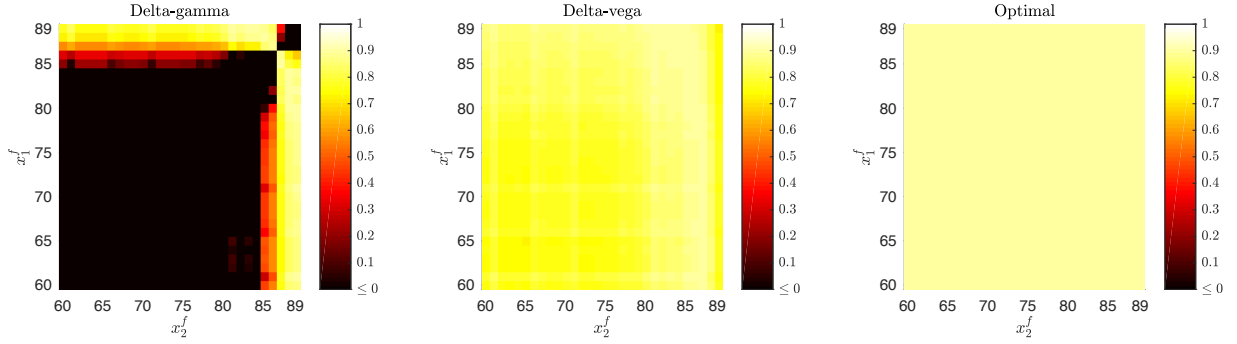


Figure 2.11: The values of HE for the delta-gamma hedges (left panel), delta-vega hedges (middle panel) and *ex post* optimal hedges (right panel) with $\mathcal{J} = 2$ q-forwards, $t_1^f = 5$, $t_2^f = 15$, $x_1^f, x_2^f = 60, \dots, 89$.

hedging results are displayed in Figure 2.11. For delta-gamma hedges, most reference age combinations yield low or even negative hedge effectiveness; a meaningful reduction in risk only happens when one reference age is greater than 86 but the other is not. In contrast, for delta-vega hedges, the hedge effectiveness is much more robust relative to the choice of reference ages, and is much closer to that produced by the corresponding *ex post* optimal hedges.

To explain the hedging results, let us study Figure 2.12 which demonstrates how the delta/gamma and delta/vega ratios of a q-forward may vary with its reference age when its time-to-maturity is fixed. Also shown in Figure 2.12 are the corresponding delta/gamma and delta/vega ratios for the liability being hedged (the solid horizontal lines).

Let us first focus on the delta/gamma ratios (the left panel of Figure 2.12). The delta/gamma ratio of a q-forward depends quite heavily on its reference age. The sensitivity to x^f can be understood from the following formula:

$$\frac{\Delta^{(Q)}(x^f, t^f)}{\Gamma^{(Q)}(x^f, t^f)} = \frac{\mathbb{E}[\exp(Y_{x^f, t^f-1}(1) - W_{x^f, t^f-1}(1)) \mid \mathcal{F}_0]}{b_{x^f} \mathbb{E}[\exp(Y_{x^f, t^f-1}(1) - W_{x^f, t^f-1}(1))(1 - \exp(Y_{x^f, t^f-1}(1))) \mid \mathcal{F}_0]}, \quad (2.20)$$

which says that the delta/gamma ratio is inversely related to b_{x^f} . Indeed, the pattern of the delta/gamma ratios against x^f is reminiscent of the pattern of b_x against x (Figure 2.1). However, the trends for $t^f = 5$ and $t^f = 15$ almost overlap each other, indicating that

the delta/gamma ratio is very insensitive to its reference age. From the graph, it is quite clear that in order to satisfy the necessary condition specified by (2.19), one q-forward in the portfolio must have a reference age less than or equal to 86 and the other must have a reference age greater than 86.

Next, we turn to the delta/vega ratios (the right panel of Figure 2.12). In stark contrast, the delta/vega ratio of a q-forward are rather sensitive to its time-to-maturity (the trends for $t^f = 5$ and $t^f = 15$ are far apart), but are relatively less sensitive to its reference age. The following formula casts some light on the observed sensitivity to t^f and insensitivity to x^f :

$$\frac{\Delta^{(Q)}(x^f, t^f)}{V^{(Q)}(x^f, t^f)} = \frac{\mathbb{E}[\exp(Y_{x^f, t^f-1}(1) - W_{x^f, t^f-1}(1)) \mid \mathcal{F}_0]}{\mathbb{E}[\exp(Y_{x^f, t^f-1}(1) - W_{x^f, t^f-1}(1)) \left(\frac{\partial \kappa_{t^f}}{\partial \sigma_0^2}\right) \mid \mathcal{F}_0]},$$

In the above, the only difference between the denominator and numerator is $\partial \kappa_{t^f} / \partial \sigma_0^2$, which of course depends heavily on t^f . Compared to equation (2.20), b_{x^f} no longer appears as a coefficient of the expectation in the denominator, offering an explanation to why the delta/vega ratio is relatively less sensitive to x^f . As a consequence, for the chosen times-to-maturity (5 and 15 years), all reference age combinations meet the necessary condition specified by (2.19), offering a reason as to why the effectiveness of a delta-vega hedge is fairly robust relative to the q-forwards' reference ages.

The Impact of the Time-to-Maturity Combinations

We now fix the reference ages to $x_1^f = 80$ and $x_2^f = 89$, and examine how the hedge effectiveness may vary with the q-forwards' times-to-maturity.³ The hedging results are presented in Figure 2.13.

Except when both times-to-maturity are high, the delta-gamma hedges are almost as effective as their corresponding *ex post* optimal hedges for all time-to-maturity combinations. We can attribute this outcome to the property that the delta/gamma ratio of a q-forward is sensitive to its reference age but not to its time-to-maturity. The implication

³When considering delta-gamma hedges with $t_1^f = 5$ and $t_2^f = 15$, these two reference ages result in the highest level of hedge effectiveness. Other reference ages may also be used in this analysis, provided that one of them is less than or equal to 86 and the other is greater than 86.

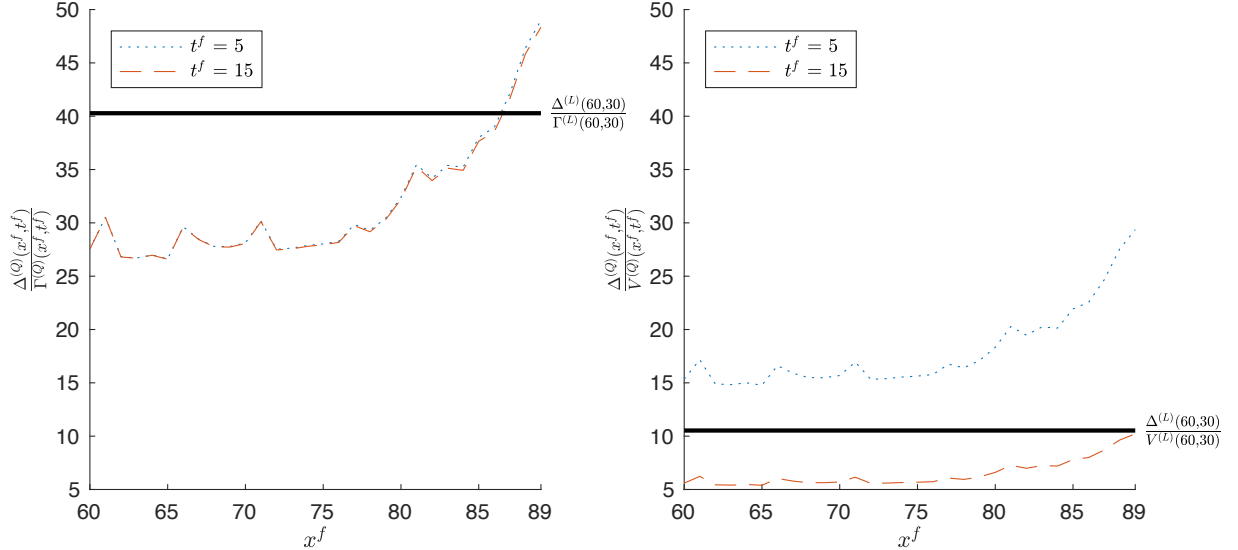


Figure 2.12: The delta-gamma (left penal) and delta-vega (right penal) ratios for q-forwards with $t^f = 5, 15$ and $x^f = 60, \dots, 89$. The solid horizontal line in the left (right) panel represents the delta-gamma (delta-vega) ratio for the liability being hedged.

of this property can be observed from the left panel of Figure 2.14, which shows that when the reference ages are fixed to 80 and 89 the necessary condition specified by (2.19) is met no matter what times-to-maturity are chosen. The delta-gamma hedges do not perform well when both times-to-maturity are high, because in this case the deltas and gammas of both q-forwards are very small (see Figures 2.5 and 2.6) so that the matrix on the left-hand-side of equation (2.16) is close to singular.

On the other hand, the delta-vega hedges perform well for only some time-to-maturity combinations. This outcome can be explained by considering the property that the delta/vega ratio of a q-forward is sensitive to its time-to-maturity but not so much to its reference age. Because of this property, from Figure 2.14 we observe that in order to satisfy the necessary condition specified by (2.19), when the q-forward with $x^f = 80$ has a time-to-maturity of less than 10 years, the other q-forward (with $x^f = 89$) must have a time-to-maturity of greater than 15 years; likewise, when the q-forward with $x^f = 89$ has a time-to-maturity of less than 15 years, the other q-forward (with $x^f = 80$) must have a

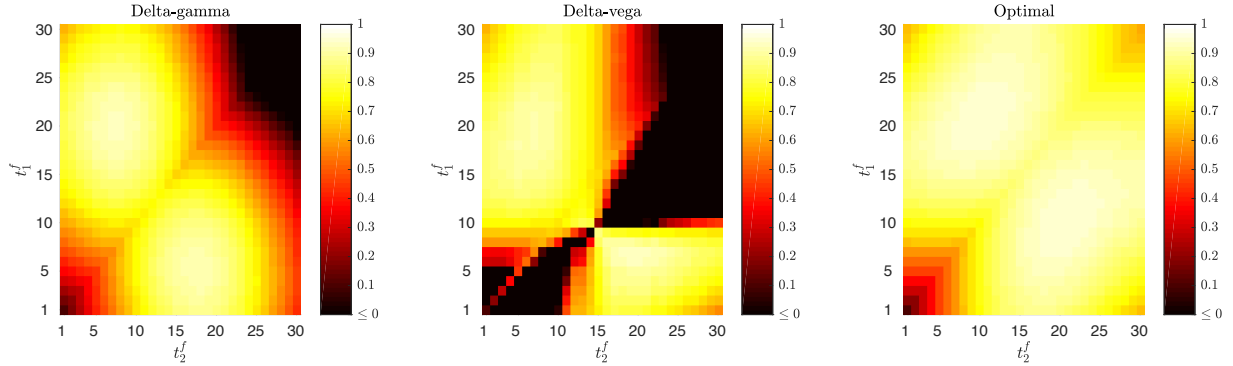


Figure 2.13: The values of HE for the delta-gamma hedges (left panel), delta-vega hedges (middle panel) and *ex post* optimal hedges (right panel) with $\mathcal{J} = 2$ q-forwards, $x_1^f = 80$, $x_2^f = 89$, $t_1^f, t_2^f = 1, \dots, 30$.

time-to-maturity of greater than 10 years. It is noteworthy that part of the diagonal in the middle panel of Figure 2.13 is fairly bright. This result is because, as previously mentioned, the necessary condition specified by (2.19) does not apply when the two q-forwards have identical time-to-maturity.

2.6 Validation with a Model-Free Approach

2.6.1 The Non-parametric Bootstrap

In Section 2.5, the model used to generate the evaluation scenarios is identical to the model from which the longevity Greeks are derived. We now examine how the hedging results may change when the model assumptions are waived in the evaluation work. To this end, we employ the non-parametric (model-free) bootstrapping method that was considered by Li and Ng (2011). The method is implemented as follows:

1. Calculate the historical mortality reduction rates, defined as

$$r_{x,t} = \frac{m_{x,t+1}}{m_{x,t}}.$$

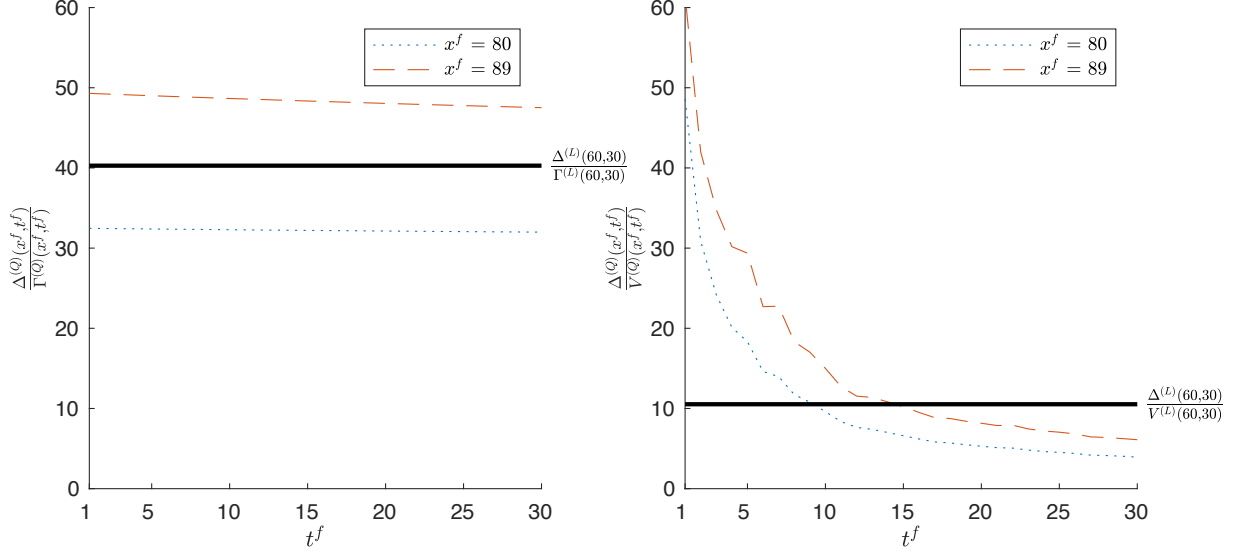


Figure 2.14: The delta-gamma (left panel) and delta-vega (right panel) ratios for q-forwards with $x^f = 80, 89$ and $t^f = 1, \dots, 30$. The solid horizontal line in the left (right) panel represents the delta-gamma (delta-vega) ratio for the liability being hedged.

Since we have 91 years of data, 90 values of $r_{x,t}$ are obtained for each age. The augmented Dickey-Fuller test is performed to confirm that the trend of $r_{x,t}$ over time at every age is weakly stationary.

2. Construct vectors of historical mortality improvement rates, i.e.,

$$\mathbf{r}_t = (r_{60,t}, \dots, r_{89,t})'$$

for $t = 1921, \dots, 2010$. The vectorization is performed to preserve any potential correlation across the age dimension.

3. To retain the potential serial dependence, \mathbf{r}_t for $t = 1921, \dots, 2010$ are grouped into overlapping blocks of size 2. The following 89 blocks are obtained:

$$(\mathbf{r}_{1921}, \mathbf{r}_{1922}), (\mathbf{r}_{1922}, \mathbf{r}_{1923}), \dots, (\mathbf{r}_{2008}, \mathbf{r}_{2009}), (\mathbf{r}_{2009}, \mathbf{r}_{2010}).$$

The same block size was also used by Li and Ng (2011). We have considered other block sizes, which lead to similar conclusions.

4. A pseudo sample of reduction rates is obtained by drawing randomly from the 89 blocks in the previous step with replacement and pasting the blocks drawn end to end. The pseudo sample of reduction rates is multiplied by the most recent central death rates ($m_{x,2011}; x = 60, \dots, 89$) to form a simulated mortality scenario.
5. Repeat the previous step 10,000 times to obtain 10,000 simulated mortality scenarios, which give 10,000 realizations of $\mathcal{L}(60, 30)|\mathcal{F}_0$ and $\mathcal{Q}(x^f, t^f)|\mathcal{F}_0$ for $x^f = 60, \dots, 89$ and $t^f = 1, \dots, 30$. The realizations of $\mathcal{L}(60, 30)|\mathcal{F}_0$ and $\mathcal{Q}(x^f, t^f)|\mathcal{F}_0$ allow us to estimate the effectiveness of the Greek hedges using equation (2.11). They also permit us to derive the *ex post* optimal (variance-minimizing) hedges. Note that the longevity Greeks (and hence the notional amounts in the Greek hedges) are still calculated from the Lee-Carter model with GARCH effects.

Figure 2.15 shows the effectiveness of various hedges, estimated using the non-parametric bootstrapping method. As expected, the effectiveness of all hedges is reduced as the model assumptions are waived.

Let us first focus on the top row, where the effectiveness of the single Greek hedges is presented. Still, the delta and vega hedges can still perform comparably to the *ex post* optimal hedges, provided that the q-forward's time-to-maturity is appropriately selected. The vega hedges are almost as effective as the *ex post* optimal hedges if the q-forward's time-to-maturity is longer than 10 years, whereas the delta hedges perform similarly to the *ex post* optimal hedges only if a short-dated q-forward is used. These observations are in line with those made in Section 2.5.3.

When both the evaluation scenarios and the longevity Greeks are obtained from our assumed model, which implies that the log mortality rates at a given time point are perfectly correlated across ages, the effectiveness of the single Greek hedges is robust relative to the q-forward's reference age (see Figure 2.9). When the evaluation scenarios are obtained from the non-parametric bootstrap, the assumption of perfect age correlation no longer holds and thus we observe that the robustness with respect to the choice of reference ages is weakened. For both delta and vega hedges, the non-parametrically estimated hedge effectiveness increases and then decreases with the q-forward's reference age. This

pattern may be explained by considering the age-specific goodness-of-fit produced by the Lee-Carter model, which can be measured by the following explanation ratio:

$$\text{ER}(x) = 1 - \frac{\sum_t (\ln(m_{x,t}) - a_x - b_x \kappa_t)^2}{\sum_t (\ln(m_{x,t}) - a_x)^2},$$

where the summations are taken over the entire sample period.⁴ The model gives a better fit to age x than age y if $\text{ER}(x)$ is greater than $\text{ER}(y)$. As shown in Figure 2.16, the estimated values of $\text{ER}(x)$ suggest that the Lee-Carter model gives a poorer fit at the ends of the age range. As a consequence, the sensitivity measures for a q-forward tend to be more inaccurate when its reference age is too high or low. The inaccuracy in turn leads to a low hedge effectiveness.

Next, we turn to the middle row of Figure 2.15, which displays the non-parametrically calculated HE values for the hedges with two q-forwards, of which the times-to-maturity are fixed to 5 and 15 years and the reference ages are allowed to vary from 60 to 89. The major conclusions drawn in Section 2.5.4 are still preserved even when the evaluation scenarios are generated using a model-free approach: (i) the delta-gamma hedges do not give a satisfactory performance for most combination of reference ages (that lead to one negative and one positive notional amounts); (ii) compared to a delta-gamma hedges, a delta-vega hedge is much more robust with respect to the choice of reference ages.

Finally, we study the bottom row of Figure 2.15, which displays the non-parametrically calculated HE values for the hedges with two q-forwards, of which the reference ages are fixed to 80 and 89 and the times-to-maturity are allowed to vary from 1 to 30 years. The key conclusions drawn in Section 2.5.4 can still be observed: (i) the delta-vega hedges perform satisfactorily only for some time-to-maturity combinations; (ii) delta-gamma hedges do not work well when the q-forwards' times-to-maturity are long.

2.6.2 Other Considerations

With modest adaptations, the procedure presented in the previous sub-section can be used to examine what may happen to the hedge effectiveness if the true model is different from

⁴This metric is adopted from the (non-age-specific) explanation ratio considered by Li and Lee (2005).

the assumed model with which the longevity Greeks are derived.

We now study the changes in hedge effectiveness if the true model is the Cairns-Blake-Dowd (CBD) model (Cairns et al., 2006), which is different from the assumed model in two aspects: (1) there is one additional period effect; (2) the age effect that interacts with a period effect is perfectly linear. The study is accomplished by replacing Steps 1 to 4 in the procedure presented in the previous sub-section with the following:

- Obtain one set of simulated central death rates ($m_{x,2011}; x = 60, \dots, 89$) from the CBD model that is fitted to the data set described in Section 2.2.

Step 5 in the procedure remains unchanged.

The results are displayed graphically in Figure 2.17, which has exactly the same layout as that of Figure 2.15. The heat maps in Figure 2.17 are generally brighter than those in Figure 2.15, suggesting that the Greek hedges perform better when the actual mortality dynamics follow a certain model (which is not necessarily the same as the model assumed in the calculation of Greeks) than when the actual mortality dynamics follow no specific model. More importantly, we observe that the following relationships (identified in Section 2.5) are still valid when the true model is the CBD model instead of the one on which the calculation of Greeks is based:

1. The delta and vega hedges can still perform comparably to the ex post optimal hedges, provided that the q-forward's time-to-maturity is appropriately selected.
2. The delta-gamma hedges do not give a satisfactory performance for most combination of reference ages.
3. Compared to a delta-gamma hedges, a delta-vega hedge is much more robust with respect to the choice of reference ages.
4. The delta-vega hedges perform satisfactorily only for some time-to-maturity combinations.
5. Delta-gamma hedges do not work well only when the q-forwards' times-to-maturity are long.

2.7 Concluding Remarks

In this chapter, we consider three longevity Greeks which enable us to calibrate an index-based longevity hedge. Most notably, we propose the longevity vega to address the empirical fact that for many populations the volatility of mortality improvement rates changes stochastically over time. Semi-analytical formulas for the longevity Greeks of a q-forward and a stylized pension plans are provided.

The properties of the three longevity Greeks for q-forwards are studied. It is found that, for example, while the magnitudes of the longevity delta and gamma reduce with the time-to-maturity, the magnitude of the longevity vega increases and then decreases with the time-to-maturity. All of these properties can be explained by considering (i) the gradient and concavity of the curve of $\exp(-\exp(Y_{x,t}(1)))$ against $Y_{x,t}(1)$, (ii) the magnitude and variability of $Y_{x,t}(1)$, (iii) the pattern of b_x across age, and (iv) the time-value of money.

We construct static hedges by matching one or two longevity Greeks, and examine how the performance of the Greek hedges may vary with the reference age(s) and time(s)-to-maturity of the q-forward(s) used. For instance, when matching one longevity Greek (with one q-forward), the hedge effectiveness is highly sensitive to the q-forward's time-to-maturity but not so to the q-forward's reference age. Specifically, a delta hedge performs satisfactory only when the time-to-maturity is short, whereas a vega hedge behaves in the opposite way. This finding may help hedgers decide which longevity Greek to use when a q-forward with a certain specification is available to them.

We fully acknowledge that the longevity Greeks are model dependent. Under another stochastic mortality model, the expressions for the longevity Greeks would become quite different. To address this problem, we validate our Greek hedges using the non-parametric bootstrapping method which does not depend on any model. As expected, the hedge effectiveness estimated using the model-free approach is not as good as that estimated using the model from which the longevity Greeks are derived. Nevertheless, many of the points we made concerning the relationship between hedge effectiveness and q-forward specifications are still observed even when the evaluation scenarios are generated by a model-free approach.

We conclude this chapter with a discussion of its caveats. First, the existence of

stochastic volatility (and hence the necessity of the longevity vega) is data dependent. For some populations, particularly those with little historical mortality data, conditional heteroskedasticity may not be statistically significant. We will revisit this issue in Chapter 4. Second, we focus on q-forwards only and paid no attention to other mortality-linked securities such as S-forwards and longevity bonds. While the longevity Greeks for these more complex securities can be derived, their properties may not be easily explained using simple arguments. In Chapter 4, we will use S-forwards as the hedging instrument. Finally, we disregard small sample risk and population basis risk. Small sample risk can be easily taken into account by using a death count process in future research. The impact of population basis risk on an index-based longevity hedge is investigated in Chapter 3 using a multi-population mortality model.

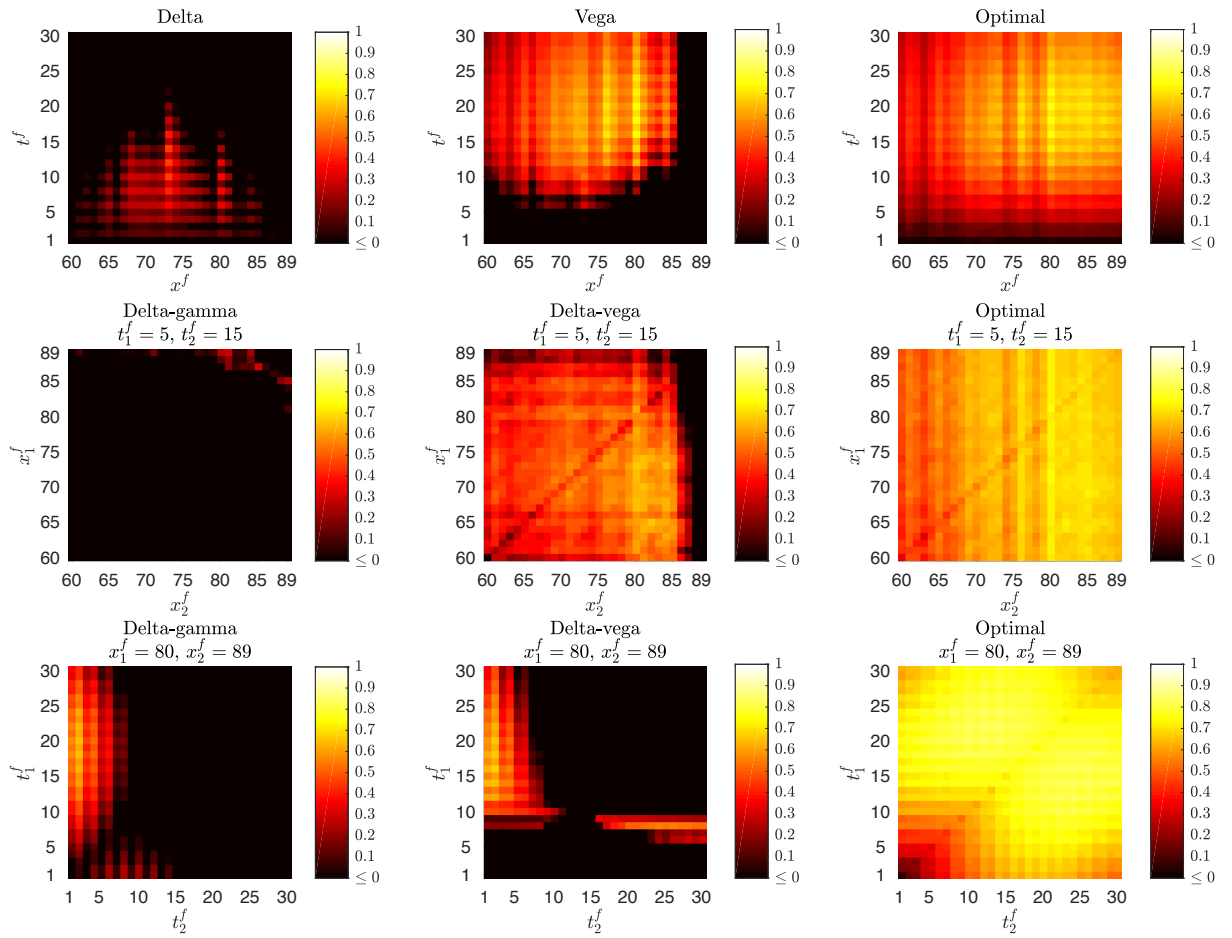


Figure 2.15: The values of HE produced by the delta, vega, delta-gamma, delta-vega and *ex post* optimal hedges for different choices of reference age(s) and time(s)-to-maturity. All HE values are calculated using the non-parametric bootstrapping method with a block size of 2.

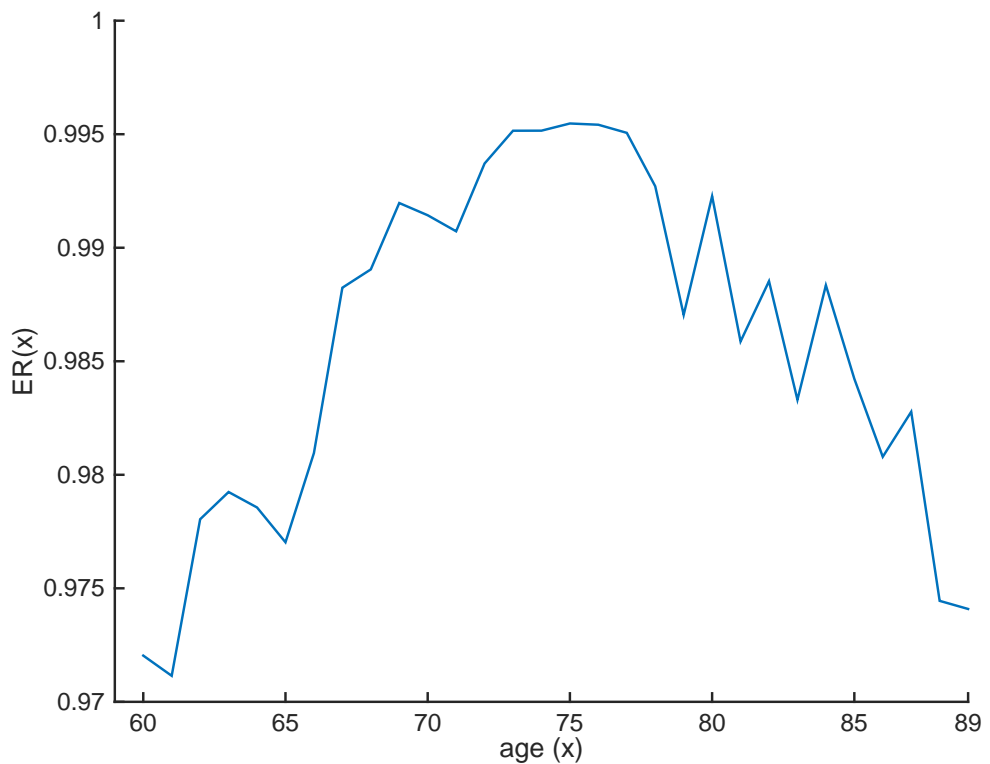


Figure 2.16: The explanation ratio $ER(x)$ for $x = 60, \dots, 89$.

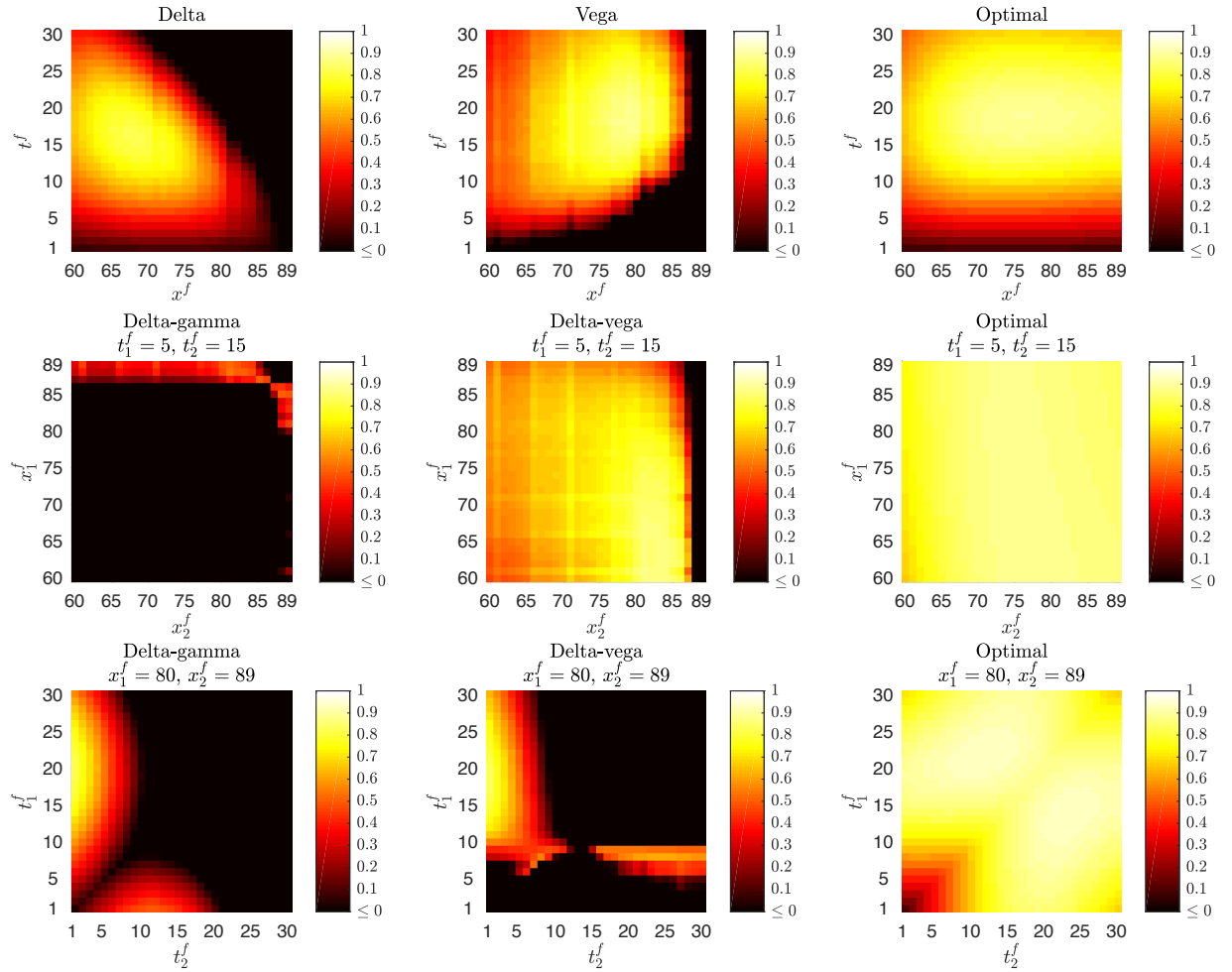


Figure 2.17: The values of HE produced by the delta, vega, delta-gamma, delta-vega and *ex post* optimal hedges for different choices of reference age(s) and time(s)-to-maturity. All HE values are calculated using the CBD model that is fitted to the data set described in Section 2.2.

Chapter 3

Delta-Hedging Longevity Risk under the M7-M5 Model: The Impact of Cohort Effect Uncertainty and Population Basis Risk

3.1 Introduction

The Life and Longevity Markets Association (LLMA) is a non-profit organization funded by AVIVA, AXA, Deutsche Bank, J.P. Morgan, Morgan Stanley, Prudential PLC and Swiss Re to advance the development of a liquid longevity market. In 2012, the LLMA acquired ownership of the LifeMetrics Index (originally created by J.P. Morgan), on which standardized mortality-linked derivatives such as q-forwards can be written. The LLMA has also invested heavily on researching on population basis risk, the risk which arises from the fact that future mortality improvements of two different populations (the hedger's portfolio of individuals and the reference population of the hedging instrument) are unlikely to be identical. It is believed by many that the lack of understanding of population basis risk is a major obstacle to market development.

In 2013, the LLMA and the Institute and Faculty of Actuaries (IFoA) jointly commissioned a project with an objective to develop a well-established methodology for assessing population basis risk. Phase I of the project was undertaken by a team of researchers from Cass Business School and practitioners from Hymans Robertson, who performed a systematic assessment of over 20 existing mortality models, aiming to identify the most suitable two-population mortality model for measuring population basis risk. Through a ‘best of breed’ selection process, the project team recommended the M7-M5 model, which can be regarded as a two-population extension of the Cairns-Blake-Dowd (CBD) family of models (Cairns et al., 2006, 2009). The selection process and estimation results can be found in the project report (Haberman et al., 2014).

Although the project team’s recommendation does not preclude the consideration of alternative models in future work, the M7-M5 model is likely to be regarded by market participants as an industry standard for assessing population basis risk. The M7-M5 model captures the most important drivers of the mortality dynamics of two related populations, including (1) the period (time-related) effect that applies to both populations, (2) the cohort (year-of-birth-related) effect that applies to both populations, (3) the period effect that applies to the mortality differential between the two populations, and (4) the interaction between age and period effects.

As discussed in Chapter 2, users of index-based longevity hedges are challenged by the question of how to best use a collection of mortality-linked derivatives. In this chapter, we attempt to seek an answer to this question, on the basis of the assumption that the true underlying mortality dynamics of the populations involved follow the M7-M5 model. Given the expected popularity of the M7-M5 model, the research problem we consider is important and practically relevant, but to our knowledge it has not been investigated seriously. Some related work has been performed by Villegas et al. (2017), who estimated hedge effectiveness under the M7-M5 model assumption using a hedge ratio of $h^* = \text{cov}(L, H)/\text{var}(H)$, where L and H represent the random present values of the unhedged liability and hedging instrument, respectively. It can be shown that the hedge ratio of $h = h^*$ minimizes the variance of the hedged position $L - hH$. However, this simple one-instrument hedging strategy is far from being adequate, and is not even valid when the hedger’s objective is not minimizing variance. It is also unclear as to how this strategy can be applied in a

dynamic-setting with manageable computational efforts.

Similar to Chapter 2, we again propose to take a sensitivity-matching approach, in which the optimal hedging strategy is formulated by matching the longevity Greeks (derived specifically under the M7-M5 model assumption) of the liability being hedged and the portfolio of hedging instruments. Longevity Greeks, defined as partial derivatives with respect to the key model parameters, can be seen as a functional equivalent of the option Greeks that are used extensively in managing equity risk, so that practitioners should find them easy to interpret and understand. The approach we take is highly dissimilar from risk-minimization approaches (see, e.g., Coughlan et al., 2011; Cairns et al., 2014; Dahl and Møller, 2006; Dahl et al., 2008, 2011; Liu and Li, 2016; Ngai and Sherris, 2011; Wong et al., 2014), in which one particular risk metric such as variance is minimized (but other risk metrics may have to be compromised). It is also different from duration-matching approaches (see, e.g., Tsai et al., 2010; Li and Hardy, 2011; Li and Luo, 2012; Lin and Tsai, 2013, 2014; Tsai and Jiang, 2011; Tsai and Chung, 2013), in which the sensitivities to the mortality rates themselves (rather than those to the parameters in the assumed model) are being matched.

Longevity Greeks have been studied previously by Luciano et al. (2012), Luciano and Regis (2014), Luciano et al. (2017) and De Rosa et al. (2017) in continuous-time settings and Cairns (2011), Cairns (2013), Liu and Li (2017) and Zhou and Li (2017) in discrete-time settings. We choose to draw on the recent contributions of Cairns (2013) and Zhou and Li (2017), because they fit the fact that the M7-M5 model is defined in discrete-time and our ambition to develop not only static but also dynamic hedging strategies. As in the original work of Cairns (2013) and Zhou and Li (2017), we use q-forwards as hedging instruments and assume that the liability being hedged is a life annuity. However, to enhance flexibility, we permit the annuity liability to have a non-zero deferment period. Furthermore, unlike Cairns (2013) and Zhou and Li (2017) who focused on period effects only, we consider both period and cohort effects, incorporating the circumstances when the q-forwards and/or the annuity liability are subject to cohort effect uncertainty. Of course, we allow the annuity liability and q-forwards to be linked to different populations, leveraging the ability of the M7-M5 model to capture population basis risk.

We first introduce a static hedging strategy by deriving the semi-analytical expressions

for the longevity deltas (i.e., the first partial derivatives with respect to the most recently realized period and cohort effects) of the annuity liability and q-forwards. The expressions are semi-analytical in the sense that a large part of the calculations are accomplished using the structural and statistical properties of the assumed stochastic processes for the period and cohort effects.

We then extend the hedging strategy to a dynamic setting, in which the hedger is allowed to rebalance the portfolio of q-forwards periodically. To this end, we utilize the ‘approximation of survival functions’ method, considered previously by Cairns (2013) and Zhou and Li (2017), to avoid the nested simulations that would otherwise be required in the calculation of the following:

1. the values of the q-forwards at each time point when the hedge portfolio is adjusted, for each simulated sample path of future mortality;
2. the deltas of the q-forwards and annuity liability at each time point when the hedge portfolio is adjusted, for each simulated sample path of future mortality.

The application of the ‘approximation of survival functions’ method under the M7-M5 model assumption is significantly more complicated than that in the previous studies, due primarily to the fact that the M7-M5 model incorporates both period and cohort effects. To overcome this technical challenge, we systematically divide all possibly encountered survival functions into five cases, according to the duration, the starting age, the starting time and the given information (filtration), and tailor a specific approximation (or calculation) method for each of the five cases.

In addition to aforementioned contributions, this chapter adds value to the literature on longevity Greeks on the following aspects:

- Unlike Cairns (2011) and Zhou and Li (2017) who assume that the hedging instruments are costless to the hedger, we better mimic reality by allowing the counterparty of the q-forwards to charge a non-zero risk premium. Although the cost of hedging has no impact on hedge effectiveness measured in terms of variance reduction, its effect on asymmetric risk measures such as Value-at-Risk can be significant. Such an effect is examined in this chapter.

- We consider not only cash flow hedges (of which the focus is the variability of cash flows) but also value hedges (of which the focus is the variability of the portfolio values at a certain future time point), in contrast to the existing work on discrete-time longevity Greek hedging which considers only the former. In line with Solvency II capital requirements, we measure the effectiveness of value hedges in terms of the reduction in the Value-at-Risk over a one-year horizon at a confidence level of 99.5%.
- We study the benefit of a dynamically adjusted hedge over a hedge that is left unadjusted over time. Cairns et al. (2008) has also investigated this issue, but their study takes no account of population basis risk and cohort effect uncertainty.

Our theoretical work is supplemented by three real data illustrations, which respectively demonstrate (1) the impact of cohort effect uncertainty and population basis risk on hedge effectiveness, (2) the benefit of dynamically adjusting a hedge portfolio in different market conditions, and (3) how the risk premium demanded by the counterparty may affect hedge effectiveness. The empirical work leads to several conclusions that may inform future studies of index-based longevity hedging. For example, it is found that if the liability being hedged is free of cohort effect uncertainty, then the effectiveness of a longevity hedge reduces as the extent of the cohort effect uncertainty surrounding the hedging instruments increases.

The rest of this chapter is structured as follows. In Section 3.2, we specify the M7-M5 model and estimate it to real data. In Section 3.3, we define the *ex post* survival probability, from which most of the theoretical work in this chapter is developed. In Section 3.4, we explain how survival probabilities can be approximated in different circumstances. The approximation methods are then applied in Section 3.5 where the valuation of the annuity liability and q-forwards is discussed, and in Section 3.6 where the longevity deltas of the annuity liability and q-forwards are derived. In Section 3.7, we define the metrics for evaluating hedge effectiveness, which are then used in Section 3.8 where the three real data illustrations are presented. Finally, Section 3.9 concludes the chapter.

3.2 The M7-M5 Model

3.2.1 Model Specification

Proposed by Haberman et al. (2014), the M7-M5 model is a two-population stochastic mortality model that is formed by amalgamating the M5 model (the original Cairns-Blake-Dowd) model and the M7 model (the Cairns-Blake-Dowd model with quadratic age and cohort effects). In the M7-M5 model, one of the two populations being modelled is regarded as the dominant population (also referred to as the reference population), driving the mortality dynamics of both populations being modelled. The mortality dynamics of the reference population is assumed to follow an M7 model; that is,

$$\ln \left(\frac{q_{x,t}^{(R)}}{1 - q_{x,t}^{(R)}} \right) = \kappa_t^{(1)} + (x - \bar{x})\kappa_t^{(2)} + ((x - \bar{x})^2 - \sigma_x^2)\kappa_t^{(3)} + \gamma_{t-x}, \quad (3.1)$$

where

- x and t are integers representing age and time, respectively,
- $q_{x,t}^{(R)}$ denotes the probability that an individual from the reference population (R) dies in calendar year t (between time $t - 1$ and time t), given that he/she has survived to age x at the beginning of year t ,
- $\kappa_t^{(1)}$, $\kappa_t^{(2)}$ and $\kappa_t^{(3)}$ are the first, second and third period effects for calendar year t , respectively,
- γ_{t-x} is the cohort effect for year-of-birth $t - x$,
- \bar{x} is the mid-point of the age range to which the model is fitted, and
- σ_x^2 is the average value of $(x - \bar{x})^2$ over the age range to which the model is fitted.

The other population is called the book population. The mortality differential between the book and reference populations is assumed to follow an M5 model; that is,

$$\ln \left(\frac{q_{x,t}^{(B)}}{1 - q_{x,t}^{(B)}} \right) - \ln \left(\frac{q_{x,t}^{(R)}}{1 - q_{x,t}^{(R)}} \right) = \kappa_t^{(1,B)} + (x - \bar{x})\kappa_t^{(2,B)}, \quad (3.2)$$

where

- $q_{x,t}^{(B)}$ denotes the probability that an individual from the book population (B) dies in calendar year t (between time $t - 1$ and time t), given that he/she has survived to age x at the beginning of year t , and
- $\kappa_t^{(1,B)}$ and $\kappa_t^{(2,B)}$ are the period effects that determine the mortality differential in year t .

Using equations (3.1) and (3.2), we have

$$\ln \left(\frac{q_{x,t}^{(B)}}{1 - q_{x,t}^{(B)}} \right) = (\kappa_t^{(1)} + \kappa_t^{(1,B)}) + (x - \bar{x})(\kappa_t^{(2)} + \kappa_t^{(2,B)}) + ((x - \bar{x})^2 - \sigma_x^2)\kappa_t^{(3)} + \gamma_{t-x},$$

which in turn means that the mortality dynamics of the book population also follow an M7 model, whose third period effect and cohort effect are identical to those in the M7 model for the reference population.

For ease of reading, we define $y_{x,t}^{(i)} := \ln(q_{x,t}^{(i)} / (1 - q_{x,t}^{(i)}))$, and express the M7-M5 model in a vector form as

$$y_{x,t}^{(i)} = \boldsymbol{\beta}_x^{(i)} \boldsymbol{\kappa}_t^{(i)} + \gamma_{t-x}, \quad i = R, B, \quad (3.3)$$

where

- $\boldsymbol{\beta}_x^{(R)} = (1, x - \bar{x}, (x - \bar{x})^2 - \sigma_x^2)$,
- $\boldsymbol{\beta}_x^{(B)} = (1, x - \bar{x}, (x - \bar{x})^2 - \sigma_x^2, 1, x - \bar{x})$,
- $\boldsymbol{\kappa}_t^{(R)} = (\kappa_t^{(1)}, \kappa_t^{(2)}, \kappa_t^{(3)})'$ is the vector of period effects that are relevant to the reference population, and
- $\boldsymbol{\kappa}_t^{(B)} = (\kappa_t^{(1,B)}, \kappa_t^{(2,B)}, \kappa_t^{(3)}, \kappa_t^{(1,B)}, \kappa_t^{(2,B)})'$ is the vector of period effects that are relevant to the book population.

We also define $\boldsymbol{\kappa}_t^{(B)} := (\kappa_t^{(1,B)}, \kappa_t^{(2,B)})'$ as the vector of period effects that determine the mortality differential.

3.2.2 Model Estimation

Let $[x_a, x_b]$ be the sample age range and $[t_a, t_b]$ be the sample period of the data set under consideration. Fitting the M7-M5 model to such a data set yields estimates of $\kappa_t^{(1)}$, $\kappa_t^{(2)}$, $\kappa_t^{(3)}$, $\kappa_t^{(1,B)}$ and $\kappa_t^{(2,B)}$ for $t = t_a, \dots, t_b$, and estimates of γ_{t-x} for $t - x = t_a - x_b$ (the earliest cohort covered by the data set) to $t - x = t_b - x_a$ (the latest cohort covered by the data set). That being said, the period effects beyond calendar year $t = t_b$ and the cohort effects beyond year-of-birth $t_b - x_a$ have to be obtained by extrapolations. Also, for ages $x = x_b + 1, \dots, \omega$, where ω is the highest attainable age, the values of $q_{x,t}^{(R)}$ and $q_{x,t}^{(B)}$ are obtained by extrapolations with the built-in age functions in the M7-M5 model. We assume that $\omega = 100$ in our illustrations. The set-up is illustrated in Figure 3.1.

It is well known that the M7 model is subject to an identifiability problem. Following Haberman et al. (2014), we impose the following constraints to ensure parameter uniqueness in the M7 component:

$$\sum_{c=t_a-x_b}^{t_b-x_a} \gamma_c = 0; \quad \sum_{c=t_a-x_b}^{t_b-x_a} c\gamma_c = 0; \quad \sum_{c=t_a-x_b}^{t_b-x_a} c^2\gamma_c = 0.$$

With these constraints, the resulting values of $\gamma_{t_a-x_b}, \dots, \gamma_{t_b-x_a}$ would fluctuate around zero and exhibit no linear or quadratic trend. Note that the chosen constraints are also used in the paper by Cairns et al. (2009) where the M7 model is first introduced. We acknowledge that there exist other ways to formulate the identifiability constraints, but we choose to preserve the original setting specified by Haberman et al. (2014).

The illustrations in this chapter are based on an M7-M5 model that is fitted to the historical mortality experience of the English and Welsh male population (the reference population) and U.K. male insured lives (the book population). The former population's data are obtained from the Human Mortality Database, whereas that for the latter population's data are obtained from the Institute and Faculty of Actuaries. The sample age range and sample period used are $[x_a, x_b] = [60, 89]$ and $[t_a, t_b] = [1961, 2005]$, respectively.

We estimate the M7 component using the method of binomial maximum likelihood, implemented with the R package StMoMo (Villegas et al., 2016), and estimate the M5 component using the method of least squares as in the original work of Cairns et al.

(2006). Figure 3.2 shows the estimates of the period effects for calendar years $t_a = 1961$ to $t_b = 2005$, and the estimates of the cohort effects for years-of-birth $t_a - x_b = 1961 - 89 = 1872$ to $t_b - x_a = 2005 - 60 = 1945$.

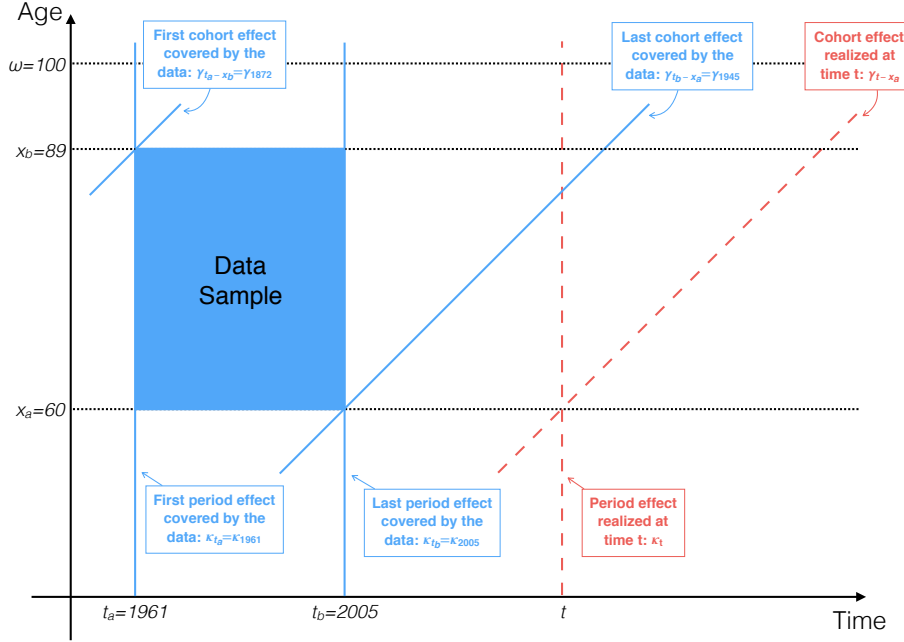


Figure 3.1: A Lexis diagram showing the first and last period/cohort effects covered by the data sample, and an example of the period and cohort effects that have to be obtained by extrapolations.

3.2.3 The Processes for the Period and Cohort Effects

Following Haberman et al. (2014), we assume that $\kappa_t^{(R)}$ follows a tri-variate random walk,

$$\kappa_t^{(R)} = \mu + \kappa_{t-1}^{(R)} + z_t^{(R)},$$

where μ is the drift vector, and $z_t^{(R)}$ is the innovation vector which follows a tri-variate normal distribution with a zero mean vector and a constant covariance matrix of $\Sigma^{(R)}$, and assume that $\kappa_t^{(B)}$ follows a first-order vector-autoregressive process,

$$\kappa_t^{(B)} = \theta_0 + \Theta_1 \kappa_{t-1}^{(B)} + z_t^{(B)},$$

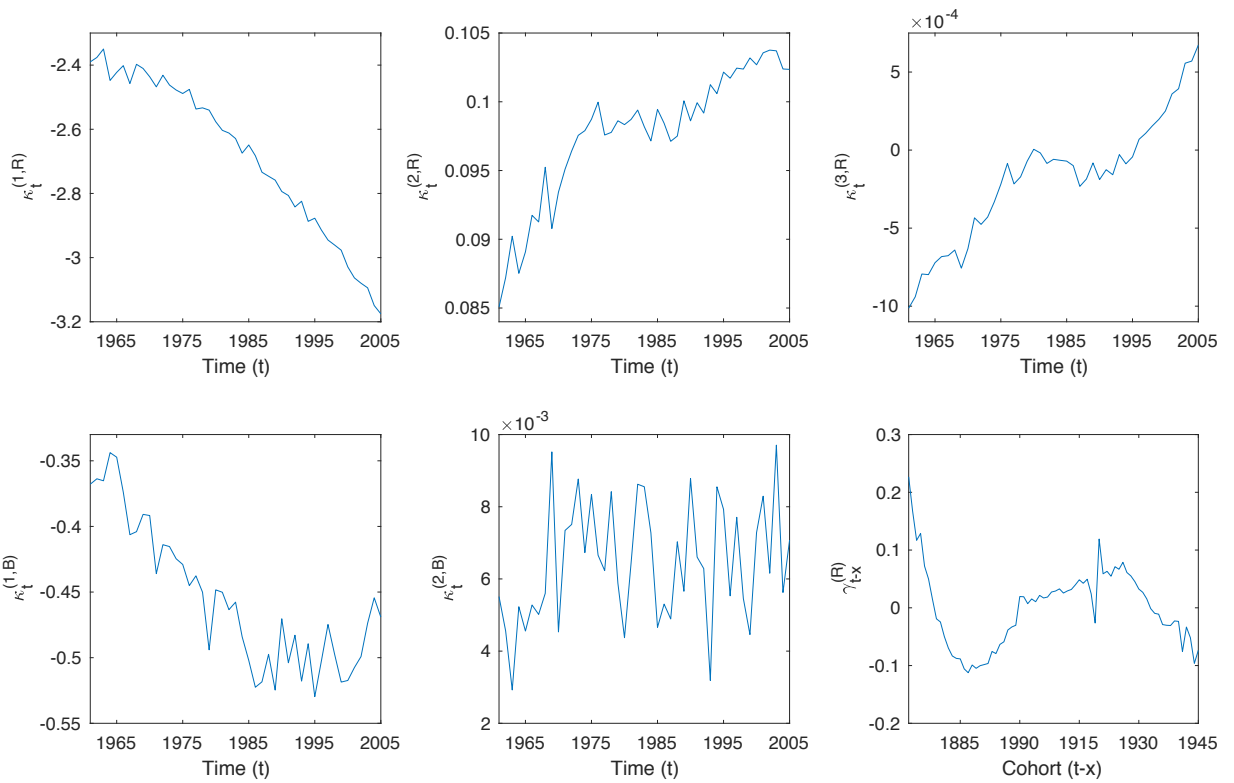


Figure 3.2: The estimates of $\kappa_t^{(1)}$, $\kappa_t^{(2)}$, $\kappa_t^{(3)}$, $\kappa_t^{(1,B)}$, $\kappa_t^{(2,B)}$ for $t = 1961, \dots, 2005$, and the estimates of $\gamma_{t-x}^{(R)}$ for $t - x = 1872, \dots, 1945$

where $\boldsymbol{\theta}_0$ is the offset vector, $\boldsymbol{\Theta}_1$ is the 2-by-2 matrix of AR coefficients, and $\mathbf{z}_t^{(\mathcal{B})}$ is the innovation vector which follows a bivariate normal distribution with a zero mean vector and a constant covariance matrix of $\boldsymbol{\Sigma}^{(\mathcal{B})}$.

Haberman et al. (2014) do not assume any process for γ_{t-x} , because their case study does not involve any unknown cohort effect. On the grounds that the estimated values of γ_{t-x} fluctuate around zero and exhibit no trend, we choose to assume a first-order autoregression for γ_{t-x} :

$$\gamma_{t-x}^{(R)} = \psi_0 + \psi_1 \gamma_{t-x-1}^{(R)} + z_{t-x},$$

where ψ_0 and ψ_1 are the constant term and the autoregressive coefficient, respectively, and z_{t-x} is the innovation which follows a univariate normal distribution with a mean of zero and a constant variance of σ_γ^2 . It is further assumed that $\mathbf{z}_t^{(R)}$, $\mathbf{z}_t^{(\mathcal{B})}$ and z_{t-x} are independently distributed and possess no serial correlation. The estimates of the parameters in the three processes are shown in Table 3.1.

Parameters in the process for $\kappa_t^{(R)}$
$\boldsymbol{\mu} = \begin{pmatrix} -1.7847 \times 10^{-2} \\ 3.9294 \times 10^{-4} \\ 3.8309 \times 10^{-5} \end{pmatrix}, \quad \boldsymbol{\Sigma}^{(R)} = \begin{pmatrix} 9.0330 \times 10^{-4} & 3.4619 \times 10^{-5} & 6.9415 \times 10^{-7} \\ 3.4619 \times 10^{-5} & 2.6108 \times 10^{-6} & 7.3790 \times 10^{-8} \\ 6.9415 \times 10^{-7} & 7.3790 \times 10^{-8} & 6.0241 \times 10^{-9} \end{pmatrix}$
Parameters in the process for $\kappa_t^{(\mathcal{B})}$
$\boldsymbol{\theta}_0 = \begin{pmatrix} -2.5406 \times 10^{-1} \\ 4.5888 \times 10^{-3} \end{pmatrix}, \quad \boldsymbol{\Theta}_1 = \begin{pmatrix} 4.6170 \times 10^{-1} & 6.8288 \times 10^{-1} \\ -3.9184 \times 10^{-3} & 1.8264 \times 10^{-2} \end{pmatrix}$
$\boldsymbol{\Sigma}^{(\mathcal{B})} = \begin{pmatrix} 1.2758 \times 10^{-3} & 2.9297 \times 10^{-9} \\ 2.9297 \times 10^{-9} & 2.5984 \times 10^{-6} \end{pmatrix}$
Parameters in the process for γ_{t-x}
$\psi_0 = -2.8093 \times 10^{-3}, \quad \psi_1 = 9.0507 \times 10^{-1}, \quad \sigma_\gamma^2 = 6.8077 \times 10^{-4}$

Table 3.1: Estimated values of the parameters in the assumed processes of $\kappa_t^{(R)}$, $\kappa_t^{(\mathcal{B})}$ and γ_{t-x} .

Let \mathcal{F}_t be the information concerning the evolution of mortality up to and including time t (the end of year t) for $t = t_b, t_b + 1, \dots$. For $t = t_b$,

$$\mathcal{F}_{t_b} = \{\kappa_{t_a}^{(R)}, \dots, \kappa_{t_b}^{(R)}, \kappa_{t_a}^{(\mathcal{B})}, \dots, \kappa_{t_b}^{(\mathcal{B})}, \gamma_{t_a-x_b}, \dots, \gamma_{t_b-x_a}\}$$

contains the values of the period and cohort effects that are estimated from the historical data, whereas for $t = t_b + 1, t_b + 2, \dots$,

$$\mathcal{F}_t = \{\kappa_{t_a}^{(R)}, \dots, \kappa_{t_b}^{(R)}, \dots, \kappa_t^{(R)}, \kappa_{t_a}^{(\mathcal{B})}, \dots, \kappa_{t_b}^{(\mathcal{B})}, \dots, \kappa_t^{(\mathcal{B})}, \gamma_{t_a-x_b}, \dots, \gamma_{t_b-x_a}, \dots, \gamma_{t-x_a}\}$$

contains additionally the realized values of the period effects for calendar years $t_b + 1$ to t and the realized values of the cohort effects for years-of-birth $t_b + 1 - x_a$ to $t - x_a$.

Given \mathcal{F}_t , $\kappa_{t+s}^{(R)}$, $\kappa_{t+s}^{(\mathcal{B})}$ and γ_{t-x_a+s} for $s = 1, 2, \dots$ can be expressed as

$$\kappa_{t+s}^{(R)} = s\mu + \kappa_t^{(R)} + \sum_{v=0}^{s-1} z_{t+s-v}^{(R)}, \quad (3.4)$$

$$\kappa_{t+s}^{(\mathcal{B})} = \sum_{v=0}^{s-1} \Theta_1^v \phi_0 + \Theta_1^s \kappa_t^{(\mathcal{B})} + \sum_{v=0}^{s-1} \Theta_1^v z_{t+s-v}^{(\mathcal{B})}, \quad (3.5)$$

and

$$\gamma_{t-x_a+s} = \sum_{v=0}^{s-1} \psi_1^v \psi_0 + \psi_1^s \gamma_{t-x_a} + \sum_{v=0}^{s-1} \psi_1^v z_{t-x_a+s-v}, \quad (3.6)$$

respectively. It follows that

$$E[\kappa_{t+s}^{(R)} | \mathcal{F}_t] = s\mu + \kappa_t^{(R)}, \quad (3.7)$$

$$\text{Var}[\kappa_{t+s}^{(R)} | \mathcal{F}_t] = s\Sigma^{(R)}, \quad (3.8)$$

$$E[\kappa_{t+s}^{(\mathcal{B})} | \mathcal{F}_t] = (\mathbf{I} - \Theta_1)^{-1} (\mathbf{I} - \Theta_1^s) \theta_0 + \Theta_1^s \kappa_t^{(\mathcal{B})}, \quad (3.9)$$

$$\text{Var}[\kappa_{t+s}^{(\mathcal{B})} | \mathcal{F}_t] = (\mathbf{I} - \Theta_1^2)^{-1} (\mathbf{I} - \Theta_1^{2s}) \Sigma^{(\mathcal{B})}, \quad (3.10)$$

$$E[\gamma_{t-x_a+s} | \mathcal{F}_t] = (1 - \psi_1)^{-1} (1 - \psi_1^s) \psi_0 + \psi_1^s \gamma_{t-x_a}, \quad (3.11)$$

$$\text{Var}[\gamma_{t-x_a+s} | \mathcal{F}_t] = (1 - \psi_1^2)^{-1} (1 - \psi_1^{2s}) \sigma_\gamma^2. \quad (3.12)$$

where \mathbf{I} is a 2-by-2 identity matrix. Finally, as $\kappa_{t+s}^{(R)} | \mathcal{F}_t$ is independent of $\kappa_{t+s}^{(\mathcal{B})} | \mathcal{F}_t$, we have

$$E[\kappa_{t+s}^{(\mathcal{B})} | \mathcal{F}_t] = \begin{pmatrix} E[\kappa_{t+s}^{(R)} | \mathcal{F}_t] \\ E[\kappa_{t+s}^{(\mathcal{B})} | \mathcal{F}_t] \end{pmatrix}$$

and

$$\text{Var}[\boldsymbol{\kappa}_{t+s}^{(B)}|\mathcal{F}_t] = \begin{pmatrix} \text{Var}[\boldsymbol{\kappa}_{t+s}^{(R)}|\mathcal{F}_t] & \mathbf{O}_{3 \times 3} \\ \mathbf{O}_{2 \times 2} & \text{Var}[\boldsymbol{\kappa}_{t+s}^{(B)}|\mathcal{F}_t] \end{pmatrix},$$

where $\mathbf{O}_{k \times k}$ is a k -by- k zero matrix. The results above are used extensively in later sections.

3.3 The Set-up

3.3.1 Survival Probabilities

We let

$$\begin{aligned} S_{x,u}^{(i)}(T) &= \prod_{s=1}^T (1 - q_{x+s-1,u+s}^{(i)}) \\ &= \prod_{s=1}^T \left(1 + \exp(\boldsymbol{\beta}_{x+s-1}^{(i)} \boldsymbol{\kappa}_{u+s}^{(i)} + \gamma_{u-x+1}) \right)^{-1}, \end{aligned}$$

for integer-valued x , u and T , and $i = R, B$, be the *ex post* probability that an individual (born in year $u - x + 1$) from population i , aged x at time u (the beginning of year $u + 1$) would have survived to the end of year $u + T$. It is clear from the above expression that $S_{x,u}^{(i)}(T)$ is a function of $\boldsymbol{\kappa}_{u+1}^{(i)}, \dots, \boldsymbol{\kappa}_{u+T}^{(i)}$ and γ_{u-x+1} .

Using the definitions of \mathcal{F}_t and $S_{x,u}^{(i)}(T)$, the following statements concerning the randomness surrounding $S_{x,u}^{(i)}(T)|\mathcal{F}_t$ can be deduced.

- If $t \leq u$, then none of the period effects in $S_{x,u}^{(i)}(T)$ has been realized at time t , and hence $S_{x,u}^{(i)}(T)|\mathcal{F}_t$ depends on the unknown random values of $\boldsymbol{\kappa}_{u+1}^{(i)}|\mathcal{F}_t, \dots, \boldsymbol{\kappa}_{u+T}^{(i)}|\mathcal{F}_t$.
- If $u < t < u+T$, then $S_{x,u}^{(i)}(T)|\mathcal{F}_t$ depends on the realized values of $\boldsymbol{\kappa}_{u+1}^{(i)}|\mathcal{F}_t, \dots, \boldsymbol{\kappa}_t^{(i)}|\mathcal{F}_t$ and also the unknown random values of $\boldsymbol{\kappa}_{t+1}^{(i)}|\mathcal{F}_t, \dots, \boldsymbol{\kappa}_{u+T}^{(i)}|\mathcal{F}_t$.
- If $t \geq u + T$, then all of the period effects in $S_{x,u}^{(i)}(T)$ have been realized at time t , and hence $S_{x,u}^{(i)}(T)|\mathcal{F}_t$ is not subject to any period effect uncertainty.

- If $t - x_a < u - x + 1$, $S_{x,u}^{(i)}(T)|\mathcal{F}_t$ depends on the unknown random value of $\gamma_{u-x+1}|\mathcal{F}_t$, since \mathcal{F}_t contains cohort effects only up to and including γ_{t-x_a} .
- If $t - x_a \geq u - x + 1$, then the cohort effect in $S_{x,u}^{(i)}(T)$ has already been realized at time t , and thus $S_{x,u}^{(i)}(T)|\mathcal{F}_t$ is not subject to any cohort effect uncertainty.

It follows that $S_{x,u}^{(i)}(T)|\mathcal{F}_t$ is a random variable if $t < u + T \vee u - x + 1 + x_a$, and a known constant otherwise.

The expected value of $S_{x,u}^{(i)}(T)$ given \mathcal{F}_t ,

$$\mathbb{E}[S_{x,u}^{(i)}(T)|\mathcal{F}_t],$$

is crucially important in this study. In Sections 3.3.3 and 3.3.4, we explain how this conditional expectation is involved in the valuation of the liability being hedged and the hedging instruments. In Section 3.4, we discuss how this conditional expectation can be computed in different circumstances.

3.3.2 The (u, \mathcal{F}_t) -Value of a Random Cash Flow Stream

The following definition is used throughout the rest of this chapter.

Definition 1. *The (u, \mathcal{F}_t) -value of a cash flow stream is the conditional expectation of the discounted value of all of the cash flows beyond time u , with u being the time point to which the cash flows are discounted and \mathcal{F}_t being the condition on which the expectation is taken.*

3.3.3 The Liability Being Hedged

Suppose that the hedger wishes to establish a longevity hedge at an integer time point t_b (at the end of the last year of the sample period to which the M7-M5 model is fitted). The liability being hedged is a τ -year deferred whole life annuity, payable to an individual from the book population B , who has survived to age $x_0 - \tau$ at time t_b (the beginning of year $t_b + 1$). The annuity makes no payment in years $t_b + 1, \dots, t_b + \tau$, and pays \$1 at the end

of each year until death starting in year $t_b + \tau + 1$. Note that x_0 is the age of the annuitant at the beginning of the year in which the annuity begins to pay, and that the annuitant was born in year $t_b - x_0 + \tau + 1$.

Let r be the constant interest rate at which future payments are discounted. Discounting the liability cash flows to time t_b when the longevity hedge is established, we have

$$\mathcal{L}^{(B)}(\tau) = \sum_{s=1}^{\omega-x_0} (1+r)^{-(\tau+s)} S_{x_0-\tau,t_b}^{(B)}(\tau+s).$$

It follows from Definition 1 that the (t_b, \mathcal{F}_t) -value of the liability being hedged is

$$\begin{aligned} L_t^{(B)}(\tau) &:= \mathbb{E}[\mathcal{L}^{(B)}(\tau) | \mathcal{F}_t] \\ &= \sum_{s=1}^{\omega-x_0} (1+r)^{-(\tau+s)} \mathbb{E}[S_{x_0-\tau,t_b}^{(B)}(\tau+s) | \mathcal{F}_t], \end{aligned}$$

for $t = t_b, t_b + 1, \dots$

3.3.4 The Hedging Instruments

Suppose that the hedging instruments used are q-forwards that are linked to the reference population R . As the hedging instruments are not linked to the book population B , the hedge is subject to population basis risk.

Consider a q-forward whose date-of-issue is t^* , reference population is R , reference age is x^f and time-to-maturity is t^f , where t^* , x^f and t^f are both integers. From the perspective of the fixed rate receiver, the payoff of this q-forward per \$1 notional at maturity is $q^f - q_{x^f, t^*+t^f}^{(R)}$, where q^f is the forward mortality rate which is a constant fixed at time t^* . We assume that all q-forwards used are issued on or after the day when the hedge is first established (i.e., $t^* \geq t_b$).

Discounting the q-forward's payoff to time t^* at a constant interest rate r , we have

$$\begin{aligned} Q^{(R)}(t^*, x^f, t^f) &= (1+r)^{-t^f} (q^f - q_{x^f, t^*+t^f}^{(R)}) \\ &= (1+r)^{-t^f} (S_{x^f, t^*+t^f-1}^{(R)}(1) - (1 - q^f)). \end{aligned}$$

It then follows from Definition 1 that the (t^*, \mathcal{F}_t) -value of the q-forward is given by

$$\begin{aligned} Q_t^{(R)}(t^*, x^f, t^f) &:= \mathbb{E}[\mathcal{Q}^{(R)}(t^*, x^f, t^f) | \mathcal{F}_t] \\ &= (1+r)^{-t^f} (\mathbb{E}[S_{x^f, t^*+t^f-1}^{(R)}(1) | \mathcal{F}_t] - (1-q^f)), \end{aligned}$$

for $t = t^*, t^* + 1, \dots$

Following Coughlan et al. (2007) and Li and Hardy (2011), we determine the forward mortality rate q^f (fixed at time t^* when the q-forward is launched) as a fraction of $\mathbb{E}[q_{x^f, t^*+t^f}^{(R)} | \mathcal{F}_{t^*}]$; that is

$$q^f = (1-\lambda)(1 - \mathbb{E}[S_{x^f, t^*+t^f-1}^{(R)}(1) | \mathcal{F}_{t^*}]), \quad (3.13)$$

where λ is a parameter that reflects the risk premium demanded by the counterparty.

3.4 Evaluation of $\mathbb{E}[S_{x,u}^{(i)}(T) | \mathcal{F}_t]$

This section discusses the evaluation of $\mathbb{E}[S_{x,u}^{(i)}(T) | \mathcal{F}_t]$. The evaluation method depends on the value of t relative to the values of u and t_b .

3.4.1 Computing $\mathbb{E}[S_{x,u}^{(i)}(T) | \mathcal{F}_t]$ for $t = t_b$

This sub-section explains how $\mathbb{E}[S_{x,u}^{(i)}(T) | \mathcal{F}_{t_b}]$ can be computed. We focus only on the situation when $u \geq t_b$, because the otherwise situation is never encountered in our set-up. For $u \geq t_b$, $S_{x,u}^{(i)}(T) | \mathcal{F}_{t_b}$ is a random variable with the following properties.

- All of the period effects in $S_{x,u}^{(i)}(T)$ are not contained in \mathcal{F}_{t_b} , so they are random as of $t = t_b$, depending on the value of $\kappa_{t_b}^{(i)}$ (by the Markov property of the period effect processes).
- If $t_b - x_a \geq u - x + 1$, then the cohort effect γ_{u-x+1} in $S_{x,u}^{(i)}(T)$ is covered by \mathcal{F}_{t_b} and is thus a known constant.

- If $t_b - x_a < u - x + 1$, then the cohort effect in $S_{x,u}^{(i)}(T)$ is not covered by \mathcal{F}_{t_b} , and is hence random as of $t = t_b$. Using the Markov property of the cohort effect process, it depends on the value of $\gamma_{t_b-x_a}$ (the latest cohort effect contained in \mathcal{F}_{t_b}).

These properties imply that

$$\mathbb{E}[S_{x,u}^{(i)}(T)|\mathcal{F}_{t_b}] = \begin{cases} \mathbb{E}[S_{x,u}^{(i)}(T)|\kappa_{t_b}^{(i)}, \gamma_{t_b-x_a}] & \text{if } t_b - x_a < u - x + 1 \\ \mathbb{E}[S_{x,u}^{(i)}(T)|\kappa_{t_b}^{(i)}, \gamma_{u-x+1}] & \text{if } t_b - x_a \geq u - x + 1 \end{cases},$$

which is equivalent to

$$\mathbb{E}[S_{x,u}^{(i)}(T)|\mathcal{F}_{t_b}] = \mathbb{E}[S_{x,u}^{(i)}(T)|\kappa_{t_b}^{(i)}, \gamma_{t_b-x_a \wedge u-x+1}]. \quad (3.14)$$

This expectation is calculated by simulating sample paths of the period and/or cohort effects involved in $S_{x,u}^{(i)}(T)$, given the values of $\kappa_{t_b}^{(i)}$ and/or $\gamma_{t_b-x_a}$.

3.4.2 Approximating $\mathbb{E}[S_{x,u}^{(i)}(T)|\mathcal{F}_t]$ for $t > t_b$

At time t_b when the hedge is established (and when hedge effectiveness is evaluated), $\mathbb{E}[S_{x,u}^{(i)}(T)|\mathcal{F}_t]$ for $t > t_b$ is a random variable. The (empirical) distribution of $\mathbb{E}[S_{x,u}^{(i)}(T)|\mathcal{F}_t]$ given \mathcal{F}_{t_b} may be obtained using nested simulations.

The nested simulations involve a generation of N realizations of \mathcal{F}_t (i.e., N realizations of $\kappa_u^{(i)}|\mathcal{F}_{t_b}$ and $\gamma_{u-x_a}|\mathcal{F}_{t_b}$ for $u = t_b + 1, \dots, t$). Also, for each of the N realizations of \mathcal{F}_t , another M simulations are needed to obtain the value of $\mathbb{E}[S_{x,u}^{(i)}(T)|\mathcal{F}_t]$. In total, $N \times M$ simulations are required to obtain an empirical distribution of N realizations of $\mathbb{E}[S_{x,u}^{(i)}(T)|\mathcal{F}_t]$ given \mathcal{F}_{t_b} . As both N and M are typically large, the procedure is computationally demanding.

Drawing from the work of Cairns (2011), we develop methods to approximate $\mathbb{E}[S_{x,u}^{(i)}(T)|\mathcal{F}_t]$ for any given realization of \mathcal{F}_t , so that the second set of simulations is no longer required. The approximation method used depends on which one of the following three cases u and t fall into.

- Case A: $\mathbb{E}[S_{x,u}^{(i)}(T)|\mathcal{F}_t]$ for $t = u$

- Case B: $E[S_{x,u}^{(i)}(T)|\mathcal{F}_t]$ for $t < u$
- Case C: $E[S_{x,u}^{(i)}(T)|\mathcal{F}_t]$ for $t > u$

The distinction between these three cases is illustrated in Figure 3.3. In the rest of this section, we explain how $E[S_{x,u}^{(i)}(T)|\mathcal{F}_t]$ is approximated in each case. The accuracy of the approximation methods is demonstrated in Appendix F.

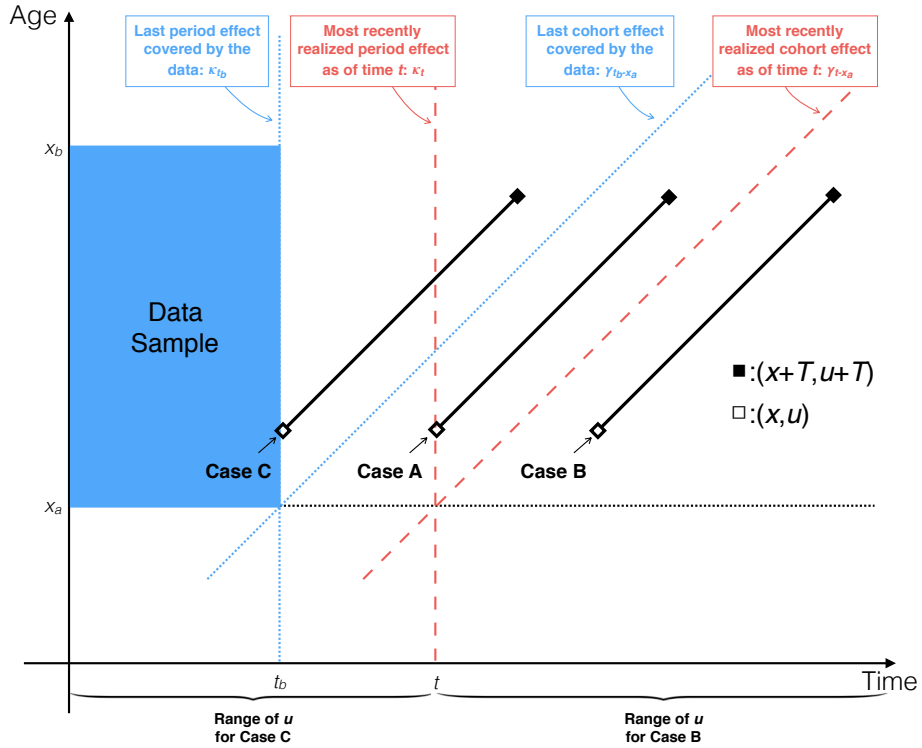


Figure 3.3: A Lexis diagram illustrating the distinctions between Case A ($t = u$), Case B ($t < u$) and Case C ($t > u$).

Case A: $E[S_{x,u}^{(i)}(T)|\mathcal{F}_t]$ for $t = u$

Using arguments similar to those made in Section 3.4.1, we obtain

$$E[S_{x,u}^{(i)}(T)|\mathcal{F}_t] = E[S_{x,u}^{(i)}(T)|\kappa_u^{(i)}, \gamma_{u-x_a \wedge u-x+1}]. \quad (3.15)$$

The approximation is set around $\hat{\kappa}_u^{(i)} := \text{E}[\kappa_u^{(i)} | \mathcal{F}_{t_b}]$ and $\hat{\gamma}_{u-x_a \wedge u-x+1} := \text{E}[\gamma_{u-x_a \wedge u-x+1} | \mathcal{F}_{t_b}]$, and is applied to the probit transform of $\text{E}[S_{x,u}^{(i)}(T) | \kappa_u^{(i)}, \gamma_{u-x_a \wedge u-x+1}]$; that is,

$$\begin{aligned} & \Phi^{-1}(\text{E}[S_{x,u}^{(i)}(T) | \kappa_u^{(i)}, \gamma_{u-x_a \wedge u-x+1}]) \\ & \approx d_{x,u,0}^{(i)}(T) + \mathbf{d}_{x,u}^{(i)}(T)'(\kappa_u^{(i)} - \hat{\kappa}_u^{(i)}) + d_{x,u,\gamma}^{(i)}(T)(\gamma_{u-x_a \wedge u-x+1} - \hat{\gamma}_{u-x_a \wedge u-x+1}), \end{aligned} \quad (3.16)$$

where Φ is the standard normal distribution function,

$$d_{x,u,0}^{(i)}(T) = \Phi^{-1}(\text{E}[S_{x,u}^{(i)}(T) | \hat{\kappa}_u^{(i)}, \hat{\gamma}_{u-x_a \wedge u-x+1}]),$$

$$\mathbf{d}_{x,u}^{(R)}(T) = (d_{x,u,1}^{(R)}(T), d_{x,u,2}^{(R)}(T), d_{x,u,3}^{(R)}(T))'$$

and

$$\mathbf{d}_{x,u}^{(B)}(T) = (d_{x,u,1}^{(B)}(T), d_{x,u,2}^{(B)}(T), d_{x,u,3}^{(B)}(T), d_{x,u,4}^{(B)}(T), d_{x,u,5}^{(B)}(T))',$$

with

$$\left\{ \begin{array}{lcl} d_{x,u,j}^{(i)}(T) & = & \frac{\partial}{\partial \kappa_u^{(j)}} \Phi^{-1}(\text{E}[S_{x,u}^{(i)}(T) | \kappa_u^{(i)}, \gamma_{u-x_a \wedge u-x+1}]) \\ d_{x,u,3+k}^{(B)}(T) & = & \frac{\partial}{\partial \kappa_u^{(k,B)}} \Phi^{-1}(\text{E}[S_{x,u}^{(B)}(T) | \kappa_u^{(B)}, \gamma_{u-x_a \wedge u-x+1}]) \\ d_{x,u,\gamma}^{(i)}(T) & = & \frac{\partial}{\partial \gamma_{u-x_a \wedge u-x+1}} \Phi^{-1}(\text{E}[S_{x,u}^{(i)}(T) | \kappa_u^{(i)}, \gamma_{u-x_a \wedge u-x+1}]) \end{array} \right.$$

for $i = R, B$, $j = 1, 2, 3$ and $k = 1, 2$. Since the approximation is set around $\hat{\kappa}_u^{(i)}$ and $\hat{\gamma}_{u-x_a \wedge u-x+1}$, we evaluate $d_{x,u,j}^{(i)}(T)$, $d_{x,u,3+k}^{(B)}(T)$ and $d_{x,u,\gamma}^{(i)}(T)$ at $\kappa_u^{(i)} = \hat{\kappa}_u^{(i)}$ and $\gamma_{u-x_a \wedge u-x+1} = \hat{\gamma}_{u-x_a \wedge u-x+1}$.

To derive $d_{x,u,j}^{(i)}(T)$, $d_{x,u,3+k}^{(B)}(T)$ and $d_{x,u,\gamma}^{(i)}(T)$, we use the fact that

$$\frac{\partial \Phi^{-1}(f(x))}{\partial x} = \frac{1}{\phi(\Phi^{-1}(f(x)))} \frac{\partial f(x)}{\partial x},$$

where ϕ is the standard normal probability density function. First, we have

$$\begin{aligned} d_{x,u,j}^{(i)}(T) & = \frac{1}{\phi(\Phi^{-1}(\text{E}[S_{x,u}^{(i)}(T) | \kappa_u^{(i)}, \gamma_{u-x_a \wedge u-x+1}]))} \left(\frac{\partial}{\partial \kappa_u^{(j)}} \text{E}[S_{x,u}^{(i)}(T) | \kappa_u^{(i)}, \gamma_{u-x_a \wedge u-x+1}] \right) \\ & = \frac{1}{\phi(\Phi^{-1}(\text{E}[S_{x,u}^{(i)}(T) | \mathcal{F}_u]))} \left(\frac{\partial}{\partial \kappa_u^{(j)}} \text{E} \left[\prod_{s=1}^T \left(1 + \exp(y_{x+s-1, u+s}^{(i)}) \right)^{-1} \middle| \mathcal{F}_u \right] \right) \\ & = \frac{-1}{\phi(\Phi^{-1}(\text{E}[S_{x,u}^{(i)}(T) | \mathcal{F}_u]))} \text{E} \left[\left(S_{x,u}^{(i)}(T) \right)^2 \frac{\partial}{\partial \kappa_u^{(j)}} \prod_{s=1}^T \left(1 + \exp(y_{x+s-1, u+s}^{(i)}) \right) \middle| \mathcal{F}_u \right]. \end{aligned} \quad (3.17)$$

In the above, $\frac{\partial}{\partial \kappa_u^{(j)}} \prod_{s=1}^T \left(1 + \exp(y_{x+s-1, u+s}^{(i)})\right)$ can be calculated recursively as

$$\begin{aligned} & \frac{\partial}{\partial \kappa_u^{(j)}} \prod_{s=1}^T \left(1 + \exp(y_{x+s-1, u+s}^{(i)})\right) \\ &= \begin{cases} \frac{\partial y_{x, u+1}^{(i)}}{\partial \kappa_u^{(j)}} \exp(y_{x, u+1}^{(i)}) & \text{if } T = 1 \\ \frac{\partial y_{x+T-1, u+T}^{(i)}}{\partial \kappa_u^{(j)}} \exp(y_{x+T-1, u+T}^{(i)}) \prod_{s=1}^{T-1} \left(1 + \exp(y_{x+s-1, u+s}^{(i)})\right) \\ + \left(1 + \exp(y_{x+T-1, u+T}^{(i)})\right) \frac{\partial}{\partial \kappa_u^{(j)}} \prod_{s=1}^{T-1} \left(1 + \exp(y_{x+s-1, u+s}^{(i)})\right) & \text{if } T > 1 \end{cases}, \quad (3.18) \end{aligned}$$

where

$$\frac{\partial y_{x+T-1, u+T}^{(i)}}{\partial \kappa_u^{(j)}} = \begin{cases} \frac{\partial y_{x+T-1, u+T}^{(i)}}{\partial \kappa_{u+T}^{(1)}} \frac{\partial \kappa_{u+T}^{(1)}}{\partial \kappa_u^{(1)}} = 1 & \text{if } j = 1 \\ \frac{\partial y_{x+T-1, u+T}^{(i)}}{\partial \kappa_{u+T}^{(2)}} \frac{\partial \kappa_{u+T}^{(2)}}{\partial \kappa_u^{(2)}} = x + T - 1 - \bar{x} & \text{if } j = 2 \\ \frac{\partial y_{x+T-1, u+T}^{(i)}}{\partial \kappa_{u+T}^{(3)}} \frac{\partial \kappa_{u+T}^{(3)}}{\partial \kappa_u^{(3)}} = (x + T - 1 - \bar{x})^2 - \sigma_x^2 & \text{if } j = 3 \end{cases}$$

for $T \geq 1$ is obtained by using the chain rule and equations (3.3) and (3.4).

Second, $d_{x, u, 3+k}^{(B)}(T)$ is obtained by replacing $\kappa_u^{(j)}$ in equations (3.17) and (3.18) with $\kappa_u^{(k, \mathcal{B})}$. The result depends on the partial derivatives of $y_{x+T-1, u+T}^{(B)}$ with respect to $\kappa_u^{(1, \mathcal{B})}$ and $\kappa_u^{(1, \mathcal{B})}$, which can be obtained by using the chain rule and equation (3.3) and (3.5):

$$\frac{\partial y_{x+T-1, u+T}^{(B)}}{\partial \kappa_u^{(k, \mathcal{B})}} = \frac{\partial y_{x+T-1, u+T}^{(B)}}{\partial \kappa_u^{(1, \mathcal{B})}} \frac{\partial \kappa_u^{(1, \mathcal{B})}}{\partial \kappa_u^{(k, \mathcal{B})}} + \frac{\partial y_{x+T-1, u+T}^{(B)}}{\partial \kappa_u^{(2, \mathcal{B})}} \frac{\partial \kappa_u^{(2, \mathcal{B})}}{\partial \kappa_u^{(k, \mathcal{B})}} = [\Theta_1^T]_{1, k} + (x + T - 1 - \bar{x})[\Theta_1^T]_{2, k},$$

$k = 1, 2$, where $[\Theta_1^T]_{i, j}$ is the (i, j) th element in Θ_1^T .

Finally, $d_{x, u, \gamma}^{(i)}(T)$ is obtained by replacing $\kappa_u^{(j)}$ in equations (3.17) and (3.18) with $\gamma_{u-x_a \wedge u-x+1}$. The result depends on the partial derivative of $y_{x+T-1, u+T}^{(i)}$ with respect to $\gamma_{u-x_a \wedge u-x+1}$, which can be derived using the chain rule and equations (3.3) and (3.6):

$$\frac{\partial y_{x+T-1, u+T}^{(i)}}{\partial \gamma_{u-x_a \wedge u-x+1}} = \begin{cases} \frac{\partial y_{x+T-1, u+T}^{(i)}}{\partial \gamma_{u-x+1}} \frac{\partial \gamma_{u-x+1}}{\partial \gamma_{u-x_a}} = \psi_1^{x_a - x + 1} & \text{if } u - x_a < u - x + 1 \\ \frac{\partial y_{x+T-1, u+T}^{(i)}}{\partial \gamma_{u-x+1}} = 1 & \text{if } u - x_a \geq u - x + 1 \end{cases},$$

We can analytically calculate $\hat{\kappa}_u^{(i)}$ and $\hat{\gamma}_{u-x_a \wedge u-x+1}$ using equations (3.7), (3.9) and (3.11). Given the values of $\hat{\kappa}_u^{(i)}$ and $\hat{\gamma}_{u-x_a \wedge u-x+1}$, we can compute $d_{x,u,0}^{(i)}(T)$, $d_{x,u,j}^{(i)}(T)$, $d_{x,u,3+k}^{(B)}(T)$ and $d_{x,u,\gamma}^{(i)}(T)$ with a single set of (say M) simulations. Therefore, using the approximation method, the number of simulations required to obtain an empirical distribution of N values of $E[S_{x,u}^{(i)}(T)|\mathcal{F}_t]$ for $t = u$ is reduced from $N \times M$ to $N + M$ (N simulations are used to obtain realizations of \mathcal{F}_t).

Case B: $E[S_{x,u}^{(i)}(T)|\mathcal{F}_t]$ for $t < u$

As in Section 3.4.1 and 3.4.2, we use the Markov property of the assumed processes to obtain

$$E[S_{x,u}^{(i)}(T)|\mathcal{F}_t] = E[S_{x,u}^{(i)}(T)|\kappa_t^{(i)}, \gamma_{t-x_a \wedge u-x+1}]. \quad (3.19)$$

In Case B, t and u take different values. Therefore, if the approximation method for Case A is used, then a specific approximation formula is needed for each $u = t+1, t+2, \dots$, thereby demanding significant computational effort. As such, for Case B, we employ a variant of Case A's method, which yields the following approximation formula:

$$E[S_{x,u}^{(i)}(T)|\kappa_t^{(i)}, \gamma_{t-x_a \wedge u-x+1}] \approx \Phi \left(\frac{-E[V_u^{(i)}|\mathcal{F}_t]}{\sqrt{\text{Var}[V_u^{(i)}|\mathcal{F}_t]}} \right), \quad i = R, B, \quad (3.20)$$

where

$$\begin{aligned} & E[V_u^{(i)}|\mathcal{F}_t] \\ &= -d_{x,u,0}^{(i)}(T) - \mathbf{d}_{x,u}^{(i)}(T)'(E[\kappa_u^{(i)}|\mathcal{F}_t] - \hat{\kappa}_u^{(i)}) - d_{x,u,\gamma}^{(i)}(T)(E[\gamma_{u-x_a \wedge u-x+1}|\mathcal{F}_t] - \hat{\gamma}_{u-x_a \wedge u-x+1}) \end{aligned}$$

and

$$\text{Var}[V_u^{(i)}|\mathcal{F}_t] = 1 + \mathbf{d}_{x,u}^{(i)}(T)' \text{Var}[\kappa_u^{(i)}|\mathcal{F}_t] \mathbf{d}_{x,u}^{(i)}(T) + (d_{x,u,\gamma}^{(i)}(T))^2 \text{Var}[\gamma_{u-x_a \wedge u-x+1}|\mathcal{F}_t].$$

The full derivation is presented in Appendix E.

Using equations (3.7) to (3.12), we can analytically calculate $E[\kappa_u^{(i)}|\mathcal{F}_t]$, $\text{Var}[\kappa_u^{(i)}|\mathcal{F}_t]$, $E[\gamma_{u-x_a \wedge u-x+1}|\mathcal{F}_t]$ and $\text{Var}[\gamma_{u-x_a \wedge u-x+1}|\mathcal{F}_t]$ for a given realization of \mathcal{F}_t . Therefore, as in Case A, with approximation formula (3.20), the number of simulations required to obtain an empirical distribution of N values of $E[S_{x,u}^{(i)}(T)|\mathcal{F}_t]$ for $t > u$ is $N + M$.

Case C: $E[S_{x,u}^{(i)}(T)|\mathcal{F}_t]$ for $t > u$

We further divide Case C into Cases C1 and C2 as follows:

- Case C1: $E[S_{x,u}^{(i)}(T)|\mathcal{F}_t]$ for $t > u$ and $t - x_a \geq u - x + 1$;
- Case C2: $E[S_{x,u}^{(i)}(T)|\mathcal{F}_t]$ for $t > u$ and $t - x_a < u - x + 1$.

In Case C1, the cohort effect in $S_{x,u}^{(i)}(T)$ has already been realized at time t , but in Case C2, $S_{x,u}^{(i)}(T)|\mathcal{F}_t$ still depends on the unknown random value of $\gamma_{u-x+1}|\mathcal{F}_t$. Figure 3.4 illustrates the distinction between Cases C1 and C2. The shaded area in the diagram represents the combinations of u and x that fall into Case C2.

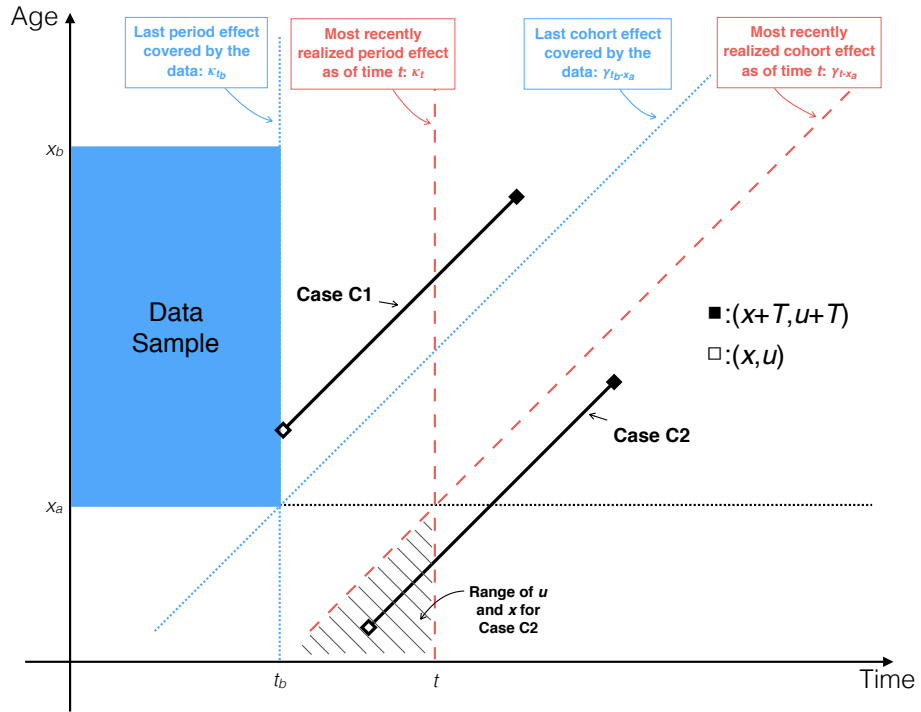


Figure 3.4: A Lexis diagram illustrating the distinction between Case C1 ($t > u$ and $t - x_a \geq u - x + 1$) and Case C2 ($t > u$ and $t - x_a < u - x + 1$). The shaded area represents the combinations of u and x that fall into Case C2.

Case C1

Let us first focus on Case C1. For $u < t < u + T$, we have

$$S_{x,u}^{(i)}(T) = S_{x,u}^{(i)}(t-u)S_{x+t-u,t}^{(i)}(T-t+u).$$

As the relevant cohort effect has already been realized at time t , $S_{x,u}^{(i)}(t-u)$ given \mathcal{F}_t is free of cohort effect uncertainty. Moreover, as \mathcal{F}_t contains all of the period effects to which $S_{x,u}^{(i)}(t-u)$ is linked, $S_{x,u}^{(i)}(t-u)$ given \mathcal{F}_t is also free of period effect uncertainty. Thus, $S_{x,u}^{(i)}(t-u)$ given \mathcal{F}_t is non-random, and we have

$$\begin{aligned} \mathbb{E}[S_{x,u}^{(i)}(T)|\mathcal{F}_t] &= \mathbb{E}[S_{x,u}^{(i)}(t-u)S_{x+t-u,t}^{(i)}(T-t+u)|\mathcal{F}_t] \\ &= S_{x,u}^{(i)}(t-u)\mathbb{E}[S_{x+t-u,t}^{(i)}(T-t+u)|\mathcal{F}_t] \\ &= S_{x,u}^{(i)}(t-u)\mathbb{E}[S_{x+t-u,t}^{(i)}(T-t+u)|\kappa_t^{(i)}, \gamma_{u-x+1}] \end{aligned} \quad (3.21)$$

The last step in the above follows from equation (3.15) and Case C1's condition that $t - x_a \geq u - x + 1$. The value of $S_{x,u}^{(i)}(t-u)$ can be calculated using the period and cohort effects contained in \mathcal{F}_t , whereas the value of $\mathbb{E}[S_{x+t-u,t}^{(i)}(T-t+u)|\kappa_t^{(i)}, \gamma_{u-x+1}]$ can be approximated using the method introduced in Section 3.4.2. For $t \geq u + T$, we have $\mathbb{E}[S_{x,u}^{(i)}(T)|\mathcal{F}_t] = S_{x,u}^{(i)}(T)$, as all of the relevant period and cohort effects are contained in \mathcal{F}_t ,

Case C2

Next, we turn to Case C2. Given \mathcal{F}_t , γ_{u-x+1} is still unknown and random; hence, given \mathcal{F}_t , $S_{x,u}^{(i)}(t-u)$ for $u < t < u + T$ and $S_{x,u}^{(i)}(T)$ for $t \geq u + T$ are still random variables, even though all of the relevant period effects are contained in \mathcal{F}_t . As a consequence, for $u < t < u + T$, $S_{x,u}^{(i)}(t-u)$ cannot be taken out from $\mathbb{E}[S_{x,u}^{(i)}(t-u)S_{x+t-u,t}^{(i)}(T-t+u)|\mathcal{F}_t]$, and for $t \geq u + T$, $S_{x,u}^{(i)}(T)$ cannot be taken out from $\mathbb{E}[S_{x,u}^{(i)}(T)|\mathcal{F}_t]$. Thus, we have

$$\mathbb{E}[S_{x,u}^{(i)}(T)|\mathcal{F}_t] = \begin{cases} \mathbb{E}[S_{x,u}^{(i)}(T)|\kappa_{u+1}^{(i)}, \dots, \kappa_t^{(i)}, \gamma_{t-x_a}] & \text{if } u < t < u + T \\ \mathbb{E}[S_{x,u}^{(i)}(T)|\kappa_{u+1}^{(i)}, \dots, \kappa_{u+T}^{(i)}, \gamma_{t-x_a}] & \text{if } t \geq u + T \end{cases}.$$

An approximation formula for the above may be obtained by applying a first order Taylor's expansion around $(\kappa_{u+1}^{(i)}, \dots, \kappa_t^{(i)}, \gamma_{t-x_a})$ for $u < t < u + T$ or $(\kappa_{u+1}^{(i)}, \dots, \kappa_{u+T}^{(i)}, \gamma_{t-x_a})$ for $t \geq u + T$. The approximation formula for Case C2 is inevitably much more tedious compared to those for the other cases. Fortunately, Case C2 is not encountered in our hedging set-up, given the assumptions made in the later sections.

3.4.3 Summary

Figure 3.5 summarizes the methods for calculating $E[S_{x,u}^{(i)}(T)|\mathcal{F}_t]$ in all possible circumstances. When $t = t_b$, we use non-nested simulations. When $t > t_b$, we use an approximation and the applicable approximation formula depends on the values of t and u . In Case A ($t = u$), we use approximation formula (3.16). In Case B ($t < u$), we use approximation formula (3.20). In Case C1 ($t > u$ and $t - x_a \geq u - x + 1$), we decompose the expression using equation (3.21) and apply approximation formula (3.16). In Case C2 (which is not encountered in the rest of this chapter), the approximation formula is significantly more involved.

3.5 Valuation of the Liability Being Hedged and the Hedging Instruments

3.5.1 The Liability Being Hedged

Let us revisit the annuity liability described in Section 3.3.3. Recall that the (t_b, \mathcal{F}_t) -value of the annuity liability is

$$L_t^{(B)}(\tau) = \sum_{s=1}^{\omega-x_0} (1+r)^{-(\tau+s)} E[S_{x_0-\tau, t_b}^{(B)}(\tau+s)|\mathcal{F}_t], \quad t = t_b, t_b + 1, \dots$$

We calculate, for any given realization of \mathcal{F}_t , the value of $E[S_{x_0-\tau, t_b}^{(B)}(\tau+s)|\mathcal{F}_t]$ for each $s = 1, \dots, \omega - x_0$ using the methods developed in Section 3.4.

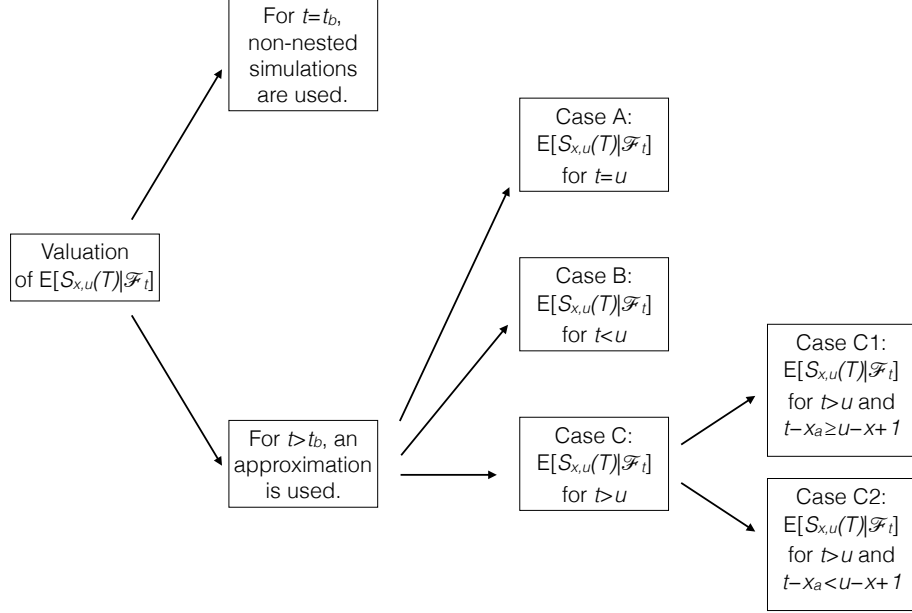


Figure 3.5: A road map summarizing the methods for calculating $E[S_{x,u}^{(i)}(T)|\mathcal{F}_t]$.

$$L_t^{(B)}(\tau) \text{ for } t = t_b$$

For $t = t_b$, we use equation (3.14) to get

$$L_{t_b}^{(B)}(\tau) = \sum_{s=1}^{\omega-x_0} (1+r)^{-(\tau+s)} E[S_{x_0-\tau,t_b}^{(B)}(\tau+s) | \kappa_{t_b}^{(B)}, \gamma_{t_b-x_a \wedge t_b-x_0+\tau+1}], \quad (3.22)$$

where, as described in Section 3.4.1, the value of $E[S_{x_0-\tau,t_b}^{(B)}(\tau+s) | \kappa_{t_b}^{(B)}, \gamma_{t_b-x_a \wedge t_b-x_0+\tau+1}]$ for each $s = 1, \dots, \omega - x_0$ is obtained by non-nested simulations.

$$L_t^{(B)}(\tau) \text{ for } t > t_b$$

When $t > t_b$, $E[S_{x_0-\tau,t_b}^{(B)}(\tau+s) | \mathcal{F}_t]$ falls into Case C, so its value is approximated by the methods presented in Section 3.4.2. In what follows, we assume that $x_0 - \tau \geq x_a$, which equivalently means that the annuitant is aged at least x_a at time t_b (the beginning of year $t_b + 1$). This working assumption is generally satisfied in practice, because the user may

fit the M7-M5 model to an age range $[x_a, x_b]$ that covers the age of the youngest annuitant in his/her portfolio.

As $t > t_b$ (the condition applicable to this sub-section) implies $t - x_a \geq t_b - x_a + 1$ and $x_0 - \tau \geq x_a$ (the assumption made) implies $t_b - x_a + 1 \geq t_b - x_0 + \tau + 1$, we have $t - x_a \geq t_b - x_0 + \tau + 1$. In this condition, $\mathbb{E}[S_{x_0-\tau,t_b}^{(B)}(\tau+s)|\mathcal{F}_t]$ always belongs to Case C1, and hence we can use the method for Case C1 to calculate the value of $\mathbb{E}[S_{x_0-\tau,t_b}^{(B)}(\tau+s)|\mathcal{F}_t]$ for each $s = 1, \dots, \omega - x_0$.

Using equation (3.21) and approximation formula (3.16), $L_t^{(B)}(\tau)$ for $t_b < t \leq t_b + \tau$ can be calculated as follows:

$$L_t^{(B)}(\tau) = \sum_{s=1}^{\omega-x_0} (1+r)^{-(\tau+s)} S_{x_0-\tau,t_b}^{(B)}(t-t_b) \mathbb{E}[S_{x_0-\tau+t-t_b,t}^{(B)}(\tau+s-t+t_b)|\kappa_t^{(B)}, \gamma_{t_b-x_0+\tau+1}], \quad (3.23)$$

where

$$\begin{aligned} & \mathbb{E}[S_{x_0-\tau+t-t_b,t}^{(B)}(\tau+s-t+t_b)|\kappa_t^{(B)}, \gamma_{t_b-x_0+\tau+1}] \\ & \approx \Phi \left(d_{x_0-\tau+t-t_b,t,0}^{(B)}(\tau+s-t+t_b) + \mathbf{d}_{x_0-\tau+t-t_b,t}^{(B)}(\tau+s-t+t_b)'(\kappa_t^{(B)} - \hat{\kappa}_t^{(B)}) \right. \\ & \quad \left. + d_{x_0-\tau+t-t_b,t,\gamma}^{(B)}(\tau+s-t+t_b)(\gamma_{t_b-x_0+\tau+1} - \hat{\gamma}_{t_b-x_0+\tau+1}) \right) \end{aligned}$$

for $s = 1, \dots, \omega - x_0$. Similarly, for $t_b + \tau < t < t_b + \tau + \omega - x_0$, we get

$$\begin{aligned} L_t^{(B)}(\tau) &= \sum_{s=1}^{t-t_b-\tau} (1+r)^{-(\tau+s)} \mathbb{E}[S_{x_0-\tau,t_b}^{(B)}(\tau+s)|\mathcal{F}_t] \\ &+ \sum_{s=t-t_b-\tau+1}^{\omega-x_0} (1+r)^{-(\tau+s)} \mathbb{E}[S_{x_0-\tau,t_b}^{(B)}(\tau+s)|\mathcal{F}_t] \\ &= \sum_{s=1}^{t-t_b-\tau} (1+r)^{-(\tau+s)} S_{x_0-\tau,t_b}^{(B)}(\tau+s) \\ &+ \sum_{s=1}^{\omega-x_0-t+t_b+\tau} (1+r)^{-(t-t_b+s)} S_{x_0-\tau,t_b}^{(B)}(t-t_b) \mathbb{E}[S_{x_0-\tau+t-t_b,t}^{(B)}(s)|\kappa_t^{(B)}, \gamma_{t_b-x_0+\tau+1}], \end{aligned} \quad (3.24)$$

where

$$\begin{aligned} \mathbb{E}[S_{x_0-\tau+t-t_b,t}^{(B)}(s)|\kappa_t^{(B)}, \gamma_{t_b-x_0+\tau+1}^{(R)}] &\approx \Phi\left(d_{x_0-\tau+t-t_b,t,0}^{(B)}(s) + \mathbf{d}_{x_0-\tau+t-t_b,t}^{(B)}(s)'(\kappa_t^{(B)} - \hat{\kappa}_t^{(B)})\right. \\ &\quad \left.+ d_{x_0-\tau+t-t_b,t,\gamma}^{(B)}(s)(\gamma_{t_b-x_0+\tau+1} - \hat{\gamma}_{t_b-x_0+\tau+1})\right) \end{aligned}$$

for $s = 1, \dots, \omega - x_0 - t + t_b + \tau$. Lastly, for $t \geq t_b + \tau + \omega - x_0$, we have

$$L_t^{(B)}(\tau) = \sum_{s=1}^{\omega-x_0} (1+r)^{-(\tau+s)} S_{x_0-\tau,t_b}^{(B)}(\tau+s),$$

since $\mathbb{E}[S_{x_0-\tau,t_b}^{(B)}(\tau+s)|\mathcal{F}_t] = S_{x_0-\tau,t_b}^{(B)}(\tau+s)$ for $s = 1, \dots, \omega - x_0$.

3.5.2 The Hedging Instruments

As mentioned in Section 3.3.4, the hedging instruments used are q-forwards that are linked to the reference population R . Recall that the (t^*, \mathcal{F}_t) -value of a q-forward linked to the reference population R can be expressed as

$$Q_t^{(R)}(t^*, x^f, t^f) = (1+r)^{-t^f} (\mathbb{E}[S_{x^f, t^*+t^f-1}^{(R)}(1)|\mathcal{F}_t] - (1-q^f)), \quad t = t^*, t^*+1, \dots,$$

where t^* is the date-of-issue, t^f is the time-to-maturity, x^f is the reference age, and q^f is the forward mortality rate. Again, the values of $\mathbb{E}[S_{x^f, t^*+t^f-1}^{(R)}(1)|\mathcal{F}_t]$ for $t = t^*, t^*+1, \dots$ (including $\mathbb{E}[S_{x^f, t^*+t^f-1}^{(R)}(1)|\mathcal{F}_{t^*}]$ in q^f) in the expression above are calculated with the methods developed in Section 3.4.

$Q_t^{(R)}(t^*, x^f, t^f)$ for $t = t_b$

As $t^* \geq t_b$ (an assumption made in Section 3.3.4), $t = t_b$ (the condition applicable to this sub-section) and $t \geq t^*$ (we only need to value a q-forward on or after its issue date), we have $t^* = t_b$. Thus, we may use equation (3.14) to obtain

$$Q_{t_b}^{(R)}(t^*, x^f, t^f) = (1+r)^{-t^f} (\mathbb{E}[S_{x^f, t_b+t^f-1}^{(R)}(1)|\kappa_{t_b}^{(R)}, \gamma_{t_b-x_a \wedge t_b+t^f-x^f}] - (1-q^f)), \quad (3.25)$$

and compute the value of $\mathbb{E}[S_{x^f, t_b+t^f-1}^{(R)}(1)|\kappa_{t_b}^{(R)}, \gamma_{t_b-x_a \wedge t_b+t^f-x^f}]$ using non-nested simulations (Case A, Section 3.4.1). When $t^* = t_b$, the conditional expectation in q^f (specified by equation (3.13)) can also be calculated with non-nested simulations.

$$Q_t^{(R)}(t^*, x^f, t^f) \text{ for } t > t_b$$

For $t > t_b$, the approximation methods introduced in Section 3.4.2 are used. When $t^* \leq t < t^* + t^f - 1$, $E[S_{x^f, t^* + t^f - 1}^{(R)}(1) | \mathcal{F}_t]$ falls into Case B, and hence we use approximation formula (3.20) to get

$$\begin{aligned} Q_t^{(R)}(t^*, x^f, t^f) &= (1+r)^{-t^f} (E[S_{x^f, t^* + t^f - 1}^{(R)}(1) | \kappa_t^{(R)}, \gamma_{t-x_a \wedge t^* + t^f - x^f}] - (1-q^f)) \\ &\approx (1+r)^{-t^f} \left(\Phi \left(\frac{-E[V_{t^* + t^f - 1}^{(R)} | \mathcal{F}_t]}{\sqrt{\text{Var}[V_{t^* + t^f - 1}^{(R)} | \mathcal{F}_t]}} \right) - (1-q^f) \right), \end{aligned} \quad (3.26)$$

where

$$\begin{aligned} E[V_{t^* + t^f - 1}^{(R)} | \mathcal{F}_t] &= -d_{x^f, t^* + t^f - 1, 0}^{(R)}(1) - \mathbf{d}_{x^f, t^* + t^f - 1}^{(R)}(1)' (E[\kappa_{t^* + t^f - 1}^{(R)} | \mathcal{F}_t] - \hat{\kappa}_{t^* + t^f - 1}^{(R)}) \\ &\quad - d_{x^f, t^* + t^f - 1, \gamma}^{(R)}(1) (E[\gamma_{t^* + t^f - 1 - x_a \wedge t^* + t^f - x^f} | \mathcal{F}_t] - \hat{\gamma}_{t^* + t^f - 1 - x_a \wedge t^* + t^f - x^f}) \end{aligned}$$

and

$$\begin{aligned} \text{Var}[V_{t^* + t^f - 1}^{(R)} | \mathcal{F}_t] &= 1 + \mathbf{d}_{x^f, t^* + t^f - 1}^{(R)}(1)' \text{Var}[\kappa_{t^* + t^f - 1}^{(R)} | \mathcal{F}_t] \mathbf{d}_{x^f, t^* + t^f - 1}^{(R)}(1) \\ &\quad + (d_{x^f, t^* + t^f - 1, \gamma}^{(R)}(1))^2 \text{Var}[\gamma_{t^* + t^f - 1 - x_a \wedge t^* + t^f - x^f} | \mathcal{F}_t]. \end{aligned}$$

As mentioned previously in Section 3.4.2, $E[\kappa_{t^* + t^f - 1}^{(R)} | \mathcal{F}_t]$, $E[\gamma_{t^* + t^f - 1 - x_a \wedge t^* + t^f - x^f} | \mathcal{F}_t]$, $\text{Var}[\kappa_{t^* + t^f - 1}^{(R)} | \mathcal{F}_t]$ and $\text{Var}[\gamma_{t^* + t^f - 1 - x_a \wedge t^* + t^f - x^f} | \mathcal{F}_t]$ in the above can be calculated analytically.

When $t = t^* + t^f - 1$, $E[S_{x^f, t^* + t^f - 1}^{(R)}(1) | \mathcal{F}_t]$ falls into Case A. Hence, we can apply approximation formula (3.16) to obtain

$$\begin{aligned} Q_t^{(R)}(t^*, x^f, t^f) &\approx (1+r)^{-t^f} \left(\Phi(d_{x^f, t^* + t^f - 1, 0}^{(R)}(1) + \mathbf{d}_{x^f, t^* + t^f - 1}^{(R)}(1)' (\kappa_{t^* + t^f - 1}^{(R)} - \hat{\kappa}_{t^* + t^f - 1}^{(R)}) \right. \\ &\quad \left. + d_{x^f, t^* + t^f - 1, \gamma}^{(R)}(1) (\gamma_{t^* + t^f - 1 - x_a \wedge t^* + t^f - x^f} - \hat{\gamma}_{t^* + t^f - 1 - x_a \wedge t^* + t^f - x^f}) \right) - (1-q^f). \end{aligned}$$

When $t > t^* + t^f - 1$, $E[S_{x^f, t^* + t^f - 1}^{(R)}(1) | \mathcal{F}_t]$ falls into Case C. In what follows, we assume that $x^f \geq x_a$, which equivalently means that the q-forward's reference age is no smaller

than x_a . This working assumption is generally satisfied in practice, as the reference age of a q-forward is typically a pensionable age, which should be encompassed in the age range $[x_a, x_b]$ to which the M7-M5 model is fitted. As $t > t^* + t^f - 1$ implies $t - x_a \geq t^* + t^f - x_a$ and $x^f \geq x_a$ (the assumption made) implies $t^* + t^f - x_a \geq t^* + t^f - x^f$, we have $t - x_a \geq t^* + t^f - x^f$. In this condition, $E[S_{x^f, t^* + t^f - 1}^{(R)}(1)|\mathcal{F}_t]$ always belongs to Case C1. Specifically, we have

$$Q_t^{(R)}(t^*, x^f, t^f) = (1+r)^{-t^f} (S_{x^f, t^* + t^f - 1}^{(R)}(1) - (1-q^f))$$

as $E[S_{x^f, t^* + t^f - 1}^{(R)}(1)|\mathcal{F}_t] = S_{x^f, t^* + t^f - 1}^{(R)}(1)$ for $t > t^* + t^f - 1$.

Lastly, the value of q^f in equation (3.26) can be calculated as follows: if $t^* = t_b$, use non-nested simulations; if $t^* > t_b$ and $t^f = 1$, use approximation formula (3.16); if $t^* > t_b$ and $t^f > 1$, use approximation formula (3.20).

3.6 Delta Hedging

In this section, we use the set-up and calculation methods developed previously to derive static and dynamic delta hedging strategies. The hedging strategies incorporate not only period effect uncertainty, but also cohort effect uncertainty and population basis risk.

3.6.1 Static Delta Hedging

A static delta hedge established at time t_b is calibrated by matching the first-order partial derivatives of the (t_b, \mathcal{F}_{t_b}) -values of the annuity liability and the q-forward portfolio with respect to the most recently realized period and cohort effects that are relevant to both the book and reference populations (i.e., $\kappa_{t_b}^{(1)}$, $\kappa_{t_b}^{(2)}$, $\kappa_{t_b}^{(3)}$ and $\gamma_{t_b-x_a}$). No adjustment is made to the q-forward portfolio after time t_b .

Sensitivities of the Hedging Instruments

In a static hedge, all of the q-forwards used are launched at time t_b . The partial derivatives of the (t_b, \mathcal{F}_{t_b}) -value of a q-forward with an issue date of t_b , a reference age of x^f and a

time-to-maturity of t^f with respect to $\kappa_{t_b}^{(1)}$, $\kappa_{t_b}^{(2)}$ and $\kappa_{t_b}^{(3)}$ are calculated as

$$\frac{\partial Q_{t_b}^{(R)}(t_b, x^f, t^f)}{\partial \kappa_{t_b}^{(j)}} = (1+r)^{-t^f} \frac{\partial}{\partial \kappa_{t_b}^{(j)}} \mathbb{E}[S_{x^f, t_b+t^f-1}^{(R)}(1) | \mathcal{F}_{t_b}], \quad j = 1, 2, 3,$$

Also, if the q-forward is subject to cohort effect uncertainty (i.e., $t_b - x_a < t_b + t^f - x^f$), we calculate the partial derivative of $Q_{t_b}^{(R)}(t_b, x^f, t^f)$ with respect to $\gamma_{t_b-x_a}$ as

$$\frac{\partial Q_{t_b}^{(R)}(t_b, x^f, t^f)}{\partial \gamma_{t_b-x_a}} = (1+r)^{-t^f} \frac{\partial}{\partial \gamma_{t_b-x_a}} \mathbb{E}[S_{x^f, t_b+t^f-1}^{(R)}(1) | \mathcal{F}_{t_b}].$$

Otherwise, $\partial Q_{t_b}^{(R)}(t_b, x^f, t^f)/\partial \gamma_{t_b-x_a}$ is simply zero. The partial derivatives of the expectations in the expressions above are derived in Appendix G.

Sensitivities of Liability Being Hedged

The partial derivatives of the (t_b, \mathcal{F}_{t_b}) -value of the annuity liability with respect to $\kappa_{t_b}^{(1)}$, $\kappa_{t_b}^{(2)}$ and $\kappa_{t_b}^{(3)}$ are calculated as

$$\frac{\partial L_{t_b}^{(B)}(\tau)}{\partial \kappa_{t_b}^{(j)}} = \sum_{s=1}^{\omega-x_0} (1+r)^{-(\tau+s)} \frac{\partial}{\partial \kappa_{t_b}^{(j)}} \mathbb{E}[S_{x_0-\tau, t_b}^{(B)}(\tau+s) | \mathcal{F}_{t_b}], \quad j = 1, 2, 3.$$

Also, if the annuity liability is subject to cohort effect uncertainty (i.e., $t_b - x_a < t_b - x_0 + \tau + 1$), we calculate the partial derivative of $L_{t_b}^{(B)}(\tau)$ with respect to $\gamma_{t_b-x_a}$ as

$$\frac{\partial L_{t_b}^{(B)}(\tau)}{\partial \gamma_{t_b-x_a}} = \sum_{s=1}^{\omega-x_0} (1+r)^{-(\tau+s)} \frac{\partial}{\partial \gamma_{t_b-x_a}} \mathbb{E}[S_{x_0-\tau, t_b}^{(B)}(\tau+s) | \mathcal{F}_{t_b}].$$

Otherwise, $\partial L_{t_b}^{(B)}(\tau)/\partial \gamma_{t_b-x_a}$ is simply zero. The partial derivatives of the expectations in the expressions above are presented in Appendix G.

Calculating the Notional Amounts

We let J be the number of q-forwards in the hedge portfolio, h_j be the notional amount of the j -th q-forward, and $Q_{t_b}^{(R)}(t_b, x_j^f, t_j^f)$ be the (t_b, \mathcal{F}_{t_b}) -value of the j -th q-forward with

a reference age of x_j^f and a time-to-maturity of t_j^f . Assuming that $J = 4$ q-forwards are used and that the sensitivities with respect to $\kappa_{t_b}^{(j)}$ for $j = 1, 2, 3$, and $\gamma_{t_b-x_a}$ are being matched, the values of h_j for $j = 1, \dots, 4$ are obtained by solving the following system of linear equations:

$$\begin{pmatrix} \frac{\partial Q_{t_b}^{(R)}(t_b, x_1^f, t_1^f)}{\partial \kappa_{t_b}^{(1)}} & \frac{\partial Q_{t_b}^{(R)}(t_b, x_2^f, t_2^f)}{\partial \kappa_{t_b}^{(1)}} & \frac{\partial Q_{t_b}^{(R)}(t_b, x_3^f, t_3^f)}{\partial \kappa_{t_b}^{(1)}} & \frac{\partial Q_{t_b}^{(R)}(t_b, x_4^f, t_4^f)}{\partial \kappa_{t_b}^{(1)}} \\ \frac{\partial Q_{t_b}^{(R)}(t_b, x_1^f, t_1^f)}{\partial \kappa_{t_b}^{(2)}} & \frac{\partial Q_{t_b}^{(R)}(t_b, x_2^f, t_2^f)}{\partial \kappa_{t_b}^{(2)}} & \frac{\partial Q_{t_b}^{(R)}(t_b, x_3^f, t_3^f)}{\partial \kappa_{t_b}^{(2)}} & \frac{\partial Q_{t_b}^{(R)}(t_b, x_4^f, t_4^f)}{\partial \kappa_{t_b}^{(2)}} \\ \frac{\partial Q_{t_b}^{(R)}(t_b, x_1^f, t_1^f)}{\partial \kappa_{t_b}^{(3)}} & \frac{\partial Q_{t_b}^{(R)}(t_b, x_2^f, t_2^f)}{\partial \kappa_{t_b}^{(3)}} & \frac{\partial Q_{t_b}^{(R)}(t_b, x_3^f, t_3^f)}{\partial \kappa_{t_b}^{(3)}} & \frac{\partial Q_{t_b}^{(R)}(t_b, x_4^f, t_4^f)}{\partial \kappa_{t_b}^{(3)}} \\ \frac{\partial Q_{t_b}^{(R)}(t_b, x_1^f, t_1^f)}{\partial \gamma_{t_b-x_a}} & \frac{\partial Q_{t_b}^{(R)}(t_b, x_2^f, t_2^f)}{\partial \gamma_{t_b-x_a}} & \frac{\partial Q_{t_b}^{(R)}(t_b, x_3^f, t_3^f)}{\partial \gamma_{t_b-x_a}} & \frac{\partial Q_{t_b}^{(R)}(t_b, x_4^f, t_4^f)}{\partial \gamma_{t_b-x_a}} \end{pmatrix} \begin{pmatrix} h_1 \\ h_2 \\ h_3 \\ h_4 \end{pmatrix} = \begin{pmatrix} \frac{\partial L_{t_b}^{(B)}(\tau)}{\partial \kappa_{t_b}^{(1)}} \\ \frac{\partial L_{t_b}^{(B)}(\tau)}{\partial \kappa_{t_b}^{(2)}} \\ \frac{\partial L_{t_b}^{(B)}(\tau)}{\partial \kappa_{t_b}^{(3)}} \\ \frac{\partial L_{t_b}^{(B)}(\tau)}{\partial \gamma_{t_b-x_a}} \end{pmatrix}.$$

All of the partial derivatives in the system of equations are evaluated at $\kappa_{t_b}^{(R)} = \hat{\kappa}_{t_b}^{(R)}$, $\kappa_{t_b}^{(B)} = \hat{\kappa}_{t_b}^{(B)}$ and $\gamma_{t_b-x_a} = \hat{\gamma}_{t_b-x_a}$.

If both the annuity liability and the q-forwards are not subject to cohort effect uncertainty at time t_b (all partial derivatives with respect to $\gamma_{t_b-x_a}$ are zero), then the above reduces to a system of three linear equations and only $J = 3$ q-forwards are needed.

3.6.2 Dynamic Delta Hedging

In a dynamic hedge, the q-forward portfolio is adjusted at the end of each year after time t_b (when the hedge is first established). We assume that at each time step $t = t_b + 1, t_b + 2, \dots$, the existing q-forwards (purchased at time $t - 1$) in the portfolio are closed out, and new q-forwards (freshly launched at time t) are purchased. The process continues until the annuity liability completely runs off.

For $t = t_b, t_b + 1, \dots$, the hedge is (re-)calibrated by matching the first-order partial derivatives of the (t, \mathcal{F}_t) -values of the annuity liability and the q-forward portfolio with respect to the most recently realized period and cohort effects that are relevant to both the book and reference populations (i.e., $\kappa_t^{(1)}, \kappa_t^{(2)}, \kappa_t^{(3)}$ and γ_{t-x_a}).

Sensitivities of the Hedging Instruments

By assumption, all q-forwards purchased at time t have an issue date of $t^* = t$. Let J_t be the number of q-forwards purchased at time t . We use $x_{t,j}^f$ and $t_{t,j}^f$ to denote the reference age and time-to-maturity of the j -th q-forward purchased at time t . Note that the (t, \mathcal{F}_t) -value of j -th q-forward purchased at time t is $Q_t^{(R)}(t, x_{t,j}^f, t_{t,j}^f)$.

To (re-)calibrate the hedge at time $t = t_b, t_b + 1, \dots$, we need the partial derivatives of $Q_t^{(R)}(t, x_{t,j}^f, t_{t,j}^f)$ with respect to the most recently realized period and cohort effects as of time t . We calculate the partial derivatives of $Q_t^{(R)}(t, x_{t,j}^f, t_{t,j}^f)$ with respect to $\kappa_t^{(1)}$, $\kappa_t^{(2)}$ and $\kappa_t^{(3)}$ as

$$\frac{\partial Q_t^{(R)}(t, x_{t,j}^f, t_{t,j}^f)}{\partial \kappa_t^{(j)}} = (1+r)^{-t^f} \frac{\partial}{\partial \kappa_t^{(j)}} \mathbb{E}[S_{x_{t,j}^f, t+t_{t,j}^f-1}^{(R)}(1) | \mathcal{F}_t], \quad j = 1, 2, 3.$$

Also, if the j -th q-forward purchased at time t is subject to cohort effect uncertainty (i.e., $t - x_a < t + t_{t,j}^f - x_{t,j}^f$), then we calculate the partial derivative of $Q_t^{(R)}(t, x_{t,j}^f, t_{t,j}^f)$ with respect to γ_{t-x_a} as follows:

$$\frac{\partial Q_t^{(R)}(t, x_{t,j}^f, t_{t,j}^f)}{\partial \gamma_{t-x_a}} = (1+r)^{-t^f} \frac{\partial}{\partial \gamma_{t-x_a}} \mathbb{E}[S_{x_{t,j}^f, t+t_{t,j}^f-1}^{(R)}(1) | \mathcal{F}_t].$$

Otherwise, the partial derivative of $Q_t^{(R)}(t, x_{t,j}^f, t_{t,j}^f)$ with respect to γ_{t-x_a} is simply zero. The partial derivatives of the expectations in the above expressions are presented in Appendix G (for $t = t_b$) and Appendix H (for $t > t_b$).

Sensitivities of Liability Being Hedged

Using equations (3.22) to (3.24), we can rewrite the (t_b, \mathcal{F}_t) -value of the annuity liability as

$$L_t^{(B)}(\tau) = \begin{cases} FL_t^{(B)}(\tau), & \text{if } t = t_b \\ (1+r)^{-(t-t_b)} S_{x_0-\tau, t_b}^{(B)}(t-t_b) FL_t^{(B)}(\tau), & \text{if } t_b < t \leq t_b + \tau \\ \sum_{s=1}^{t-t_b-\tau} (1+r)^{-(\tau+s)} S_{x_0-\tau, t_b}^{(B)}(\tau+s) \\ + (1+r)^{-(t-t_b)} S_{x_0-\tau, t_b}^{(B)}(t-t_b) FL_t^{(B)}(\tau), & \text{if } t_b + \tau < t < t_b + \tau + \omega - x_0 \end{cases},$$

where

$$FL_t^{(B)}(\tau) = \begin{cases} \sum_{s=1}^{\omega-x_0} (1+r)^{-(\tau+s)} \mathbb{E}[S_{x_0-\tau,t}^{(B)}(\tau+s)|\mathcal{F}_t], & \text{if } t = t_b \\ \sum_{s=1}^{\omega-x_0} (1+r)^{-(\tau+s-t+t_b)} \mathbb{E}[S_{x_0-\tau+t-t_b,t}^{(B)}(\tau+s-t+t_b)|\mathcal{F}_t], & \text{if } t_b < t \leq t_b + \tau \\ \sum_{s=1}^{\omega-x_0-t+t_b+\tau} (1+r)^{-s} \mathbb{E}[S_{x_0-\tau+t-t_b,t}^{(B)}(s)|\mathcal{F}_t], & \text{if } t_b + \tau < t < t_b + \tau + \omega - x_0 \end{cases}$$

for $t = t_b, t_b + 1, \dots$ is the (t, \mathcal{F}_t) -value of the annuity liability.

To (re-)calibrate the hedge at time $t = t_b, t_b + 1, \dots$, we need the partial derivatives of $FL_t^{(B)}(\tau)$ with respect to the most recently realized period and cohort effects as of time t . Using the information presented in Appendices G and H, we can easily compute the partial derivatives of $FL_t^{(B)}(\tau)$ with respect to $\kappa_t^{(1)}$, $\kappa_t^{(2)}$ and $\kappa_t^{(3)}$ for each $t = t_b, t_b + 1, \dots$, and the partial derivative of $FL_t^{(B)}(\tau)$ with respect to γ_{t-x_a} for each $t = t_b, t_b + 1, \dots$ if $FL_t^{(B)}(\tau)$ is still subject to cohort effect uncertainty (i.e., $t - x_a < t_b - x_0 + \tau + 1$). If $FL_t^{(B)}(\tau)$ is no longer subject to cohort effect uncertainty, its partial derivative with respect to γ_{t-x_a} is simply zero.

Calculating the Notional Amounts

Similar to a static hedge, the notional amounts of the q-forwards purchased at time $t = t_b, t_b + 1, \dots$ are determined by solving the following system of linear equations:

$$\begin{pmatrix} \frac{\partial Q_t^{(R)}(t, x_{t,1}^f, t_{t,1}^f)}{\partial \kappa_t^{(1)}} & \frac{\partial Q_t^{(R)}(t, x_{t,2}^f, t_{t,2}^f)}{\partial \kappa_t^{(1)}} & \frac{\partial Q_t^{(R)}(t, x_{t,3}^f, t_{t,3}^f)}{\partial \kappa_t^{(1)}} & \frac{\partial Q_t^{(R)}(t, x_{t,4}^f, t_{t,4}^f)}{\partial \kappa_t^{(1)}} \\ \frac{\partial Q_t^{(R)}(t, x_{t,1}^f, t_{t,1}^f)}{\partial \kappa_t^{(2)}} & \frac{\partial Q_t^{(R)}(t, x_{t,2}^f, t_{t,2}^f)}{\partial \kappa_t^{(2)}} & \frac{\partial Q_t^{(R)}(t, x_{t,3}^f, t_{t,3}^f)}{\partial \kappa_t^{(2)}} & \frac{\partial Q_t^{(R)}(t, x_{t,4}^f, t_{t,4}^f)}{\partial \kappa_t^{(2)}} \\ \frac{\partial Q_t^{(R)}(t, x_{t,1}^f, t_{t,1}^f)}{\partial \kappa_t^{(3)}} & \frac{\partial Q_t^{(R)}(t, x_{t,2}^f, t_{t,2}^f)}{\partial \kappa_t^{(3)}} & \frac{\partial Q_t^{(R)}(t, x_{t,3}^f, t_{t,3}^f)}{\partial \kappa_t^{(3)}} & \frac{\partial Q_t^{(R)}(t, x_{t,4}^f, t_{t,4}^f)}{\partial \kappa_t^{(3)}} \\ \frac{\partial Q_t^{(R)}(t, x_{t,1}^f, t_{t,1}^f)}{\partial \gamma_{t-x_a}} & \frac{\partial Q_t^{(R)}(t, x_{t,2}^f, t_{t,2}^f)}{\partial \gamma_{t-x_a}} & \frac{\partial Q_t^{(R)}(t, x_{t,3}^f, t_{t,3}^f)}{\partial \gamma_{t-x_a}} & \frac{\partial Q_t^{(R)}(t, x_{t,4}^f, t_{t,4}^f)}{\partial \gamma_{t-x_a}} \end{pmatrix} \begin{pmatrix} h_{t,1} \\ h_{t,2} \\ h_{t,3} \\ h_{t,4} \end{pmatrix} = \begin{pmatrix} \frac{\partial FL_t^{(B)}(\tau)}{\partial \kappa_t^{(1)}} \\ \frac{\partial FL_t^{(B)}(\tau)}{\partial \kappa_t^{(2)}} \\ \frac{\partial FL_t^{(B)}(\tau)}{\partial \kappa_t^{(3)}} \\ \frac{\partial FL_t^{(B)}(\tau)}{\partial \gamma_{t-x_a}} \end{pmatrix}. \quad (3.27)$$

where $h_{t,j}$, $j = 1, \dots, J_t$, denotes the notional amount of the j -th q-forward purchased at time t . All of the partial derivatives in the system of equations are evaluated at $\kappa_t^{(R)} = \hat{\kappa}_t^{(R)}$, $\kappa_t^{(B)} = \hat{\kappa}_t^{(B)}$ and $\gamma_{t-x_a} = \hat{\gamma}_{t-x_a}$.

If both the annuity liability and the q-forwards are not subject to cohort effect uncertainty at time t (all partial derivatives with respect to γ_{t-x_a} are zero), then the above reduces to a system of three linear equations and only $J_t = 3$ q-forwards are needed.

3.7 Hedge Evaluation

In this section, we define two metrics for evaluating the effectiveness of the delta longevity hedges. The first metric, which is based on the reduction in variance, is suited for evaluating cash flow hedges of which the focus is the variability of (the discounted values of) the cash flows involved in the portfolio. The second metric, which is based on the reduction in Value-at-Risk, is developed for evaluating value hedges of which the focus is the variability of the values of the portfolio at a certain future time point.

3.7.1 Evaluation with Variance

Static Hedging

Let us first consider on a static hedge. Suppose that the hedge is evaluated at time t_b , i.e., the time when the hedge is established. Discounted to time t_b , the net cash outflows arising from the hedged and unhedged positions sum to

$$\mathcal{L}^{(B)}(\tau) - \sum_{j=1}^J h_j \mathcal{Q}_{t_b+t_j^f}^{(R)}(t_b, x_j^f, t_j^f) \quad \text{and} \quad \mathcal{L}^{(B)}(\tau),$$

respectively. Therefore, the following metric quantifies the extent to which the static hedge reduces the variability of cash flows:

$$HE = 1 - \frac{\text{Var}[\mathcal{L}^{(B)}(\tau) - \sum_{j=1}^J h_j \mathcal{Q}_{t_b+t_j^f}^{(R)}(t_b, x_j^f, t_j^f) | \mathcal{F}_{t_b}]}{\text{Var}[\mathcal{L}^{(B)}(\tau) | \mathcal{F}_{t_b}]}.$$

The closer to 1 the value of HE is, the better the hedge effectiveness is. The variances in the expression for HE can be calculated easily using non-nested simulations.

Dynamic Hedging

As with static hedging, $\mathcal{L}^{(B)}(\tau)$ still represents the annuity liability's cash flows discounted to time t_b when the hedge is established and evaluated.

However, the cash flows from the hedge (the portfolio of q-forwards) are very different if it is dynamically adjusted instead of being kept unchanged. For a dynamic hedge, the following events occur for each $t = t_b, \dots, t_b + \tau + \omega - x_0 - 1$:

- At time t , write J_t freshly launched q-forwards. The notional amount for the j th q-forward (with a reference age of $x_{t,j}^f$ and a time-to-maturity of $t_{t,j}^f$) is $h_{t,j}$. Since all q-forwards written are freshly launched, this event does not incur any cash flow.
- At time $t + 1$, the J_t q-forwards written at time t are closed out. Per unit notional, the value of the j th q-forward at time $t + 1$ is $Q_{t+1}^{(R)}(t, x_{t,j}^f, t_{t,j}^f)$. Therefore, this event generates a cash inflow of $\sum_{j=1}^{J_t} h_{t,j} Q_{t+1}^{(R)}(t, x_{t,j}^f, t_{t,j}^f)$.

Discounted to time t_b , the cash inflows generated from the dynamically adjusted hedge sum to

$$\sum_{t=t_b}^{t_b+\tau+\omega-x_0-1} \sum_{j=1}^{J_t} (1+r)^{-(t-t_b)} h_{t,j} Q_{t+1}^{(R)}(t, x_{t,j}^f, t_{t,j}^f)$$

and hence the net cash outflows arising from the hedged position sum to

$$\mathcal{L}^{(B)}(\tau) - \sum_{t=t_b}^{t_b+\tau+\omega-x_0-1} \sum_{j=1}^{J_t} (1+r)^{-(t-t_b)} h_{t,j} Q_{t+1}^{(R)}(t, x_{t,j}^f, t_{t,j}^f). \quad (3.28)$$

It follows that the following metric quantifies the extent to which the dynamic hedge reduces the variability of cash flows:

$$HE = 1 - \frac{\text{Var}[\mathcal{L}^{(B)}(\tau) - \sum_{t=t_b}^{t_b+\tau+\omega-x_0-1} \sum_{j=1}^{J_t} (1+r)^{-(t-t_b)} h_{t,j} Q_{t+1}^{(R)}(t, x_{t,j}^f, t_{t,j}^f) | \mathcal{F}_{t_b}]}{\text{Var}[\mathcal{L}^{(B)}(\tau) | \mathcal{F}_{t_b}]}.$$

A value of HE that is close to 1 indicates the hedge is effective.

To estimate HE, we simulate a large number of mortality scenarios (i.e., sample paths of $\kappa_t^{(R)} | \mathcal{F}_{t_b}$, $\kappa_t^{(B)} | \mathcal{F}_{t_b}$ and $\gamma_{t-t_a} | \mathcal{F}_{t_b}$, for $t = t_b + 1, \dots, t_b + \tau + \omega - x_0$). For each mortality scenario, we obtain the following:

1. A realization of $\mathcal{L}^{(B)}(\tau)$
2. A realization of $h_{t,j}$ for $t = t_b, \dots, t_b + \tau + \omega - x_0 - 1$ and $j = 1, \dots, J_t$

In particular, for each $t = t_b, \dots, t_b + \tau + \omega - x_0 - 1$, we calculate

$$\frac{\partial Q_t^{(R)}(t, x_{t,j}^f, t_{t,j}^f)}{\partial \kappa_t^{(i)}}, \frac{\partial Q_t^{(R)}(t, x_{t,j}^f, t_{t,j}^f)}{\partial \gamma_{t-x_a}}, \frac{\partial FL_t^{(B)}(\tau)}{\partial \kappa_t^{(i)}}, \text{ and } \frac{\partial FL_t^{(B)}(\tau)}{\partial \gamma_{t-x_a}}$$

for $j = 1, \dots, J_t$ and $i = 1, 2, 3$, using the procedures outlined in Appendices G and H. Note that the procedure in Appendix H utilizes the approximation methods presented in Section 3.4.2. With the calculated partial derivatives, we then compute $h_{t,j}$ for $j = 1, \dots, J_t$ using equation (3.27).

3. A realization of $Q_{t+1}^{(R)}(t, x_{t,j}^f, t_{t,j}^f)$ for $t = t_b, \dots, t_b + \tau + \omega - x_0 - 1$ and $j = 1, \dots, J_t$

Specifically, for $t = t_b, \dots, t_b + \tau + \omega - x_0 - 1$, we calculate $Q_{t+1}^{(R)}(t, x_{t,j}^f, t_{t,j}^f)$ with the approximation methods described in Section 3.5.2.

The algorithm above generates empirical distributions of $\mathcal{L}^{(B)}(\tau)$ and (3.28), from which the variances in the expression for HE can be estimated.

The importance of the previously discussed approximation methods can now be clearly seen. Without the approximation methods, items 2 and 3 in the algorithm have to be calculated with simulations, thereby creating the situation of computationally demanding “simulations on simulations”.

3.7.2 Evaluation with Value-at-Risk

We now define a metric for measuring the effectiveness of a value hedge in terms of reduction in VaR. To avoid additional notation, we focus on a horizon of 1 year and a confidence level of 99.5% (consistent with Solvency II). With straightforward adaptations, other horizons and confidence levels can be considered.

First, note the following:

- The $(t_b, \mathcal{F}_{t_b+1})$ -value of the unhedged position is $L_{t_b+1}^{(B)}(\tau)$.

- The $(t_b, \mathcal{F}_{t_b+1})$ -value of the hedged position is $L_{t_b+1}^{(B)}(\tau) - \sum_{j=1}^J h_j Q_{t_b+1}^{(R)}(t_b, x_j^f, t_j^f)$.

Given \mathcal{F}_{t_b} , $L_{t_b+1}^{(B)}(\tau)$ and $Q_{t_b+1}^{(R)}(t_b, x_j^f, t_j^f)$ are random variables, depending on the period and/or cohort effects realized at time $t_b + 1$. Note also that when viewed at time t_b , the expected value of the annuity liability is $E[L_{t_b+1}^{(B)}(\tau) | \mathcal{F}_{t_b}] = L_{t_b}^{(B)}(\tau)$, which can be calculated easily with non-nested simulations.

It follows that the reduction in VaR (over the expected value of the annuity liability) produced by the delta hedge can be calculated as

$$\text{HEVaR} = 1 - \frac{\text{VaR}_{99.5\%}[L_{t_b+1}^{(B)}(\tau) - \sum_{j=1}^J h_j Q_{t_b+1}^{(R)}(t_b, x_j^f, t_j^f) | \mathcal{F}_{t_b}] - L_{t_b}^{(B)}(\tau)}{\text{VaR}_{99.5\%}[L_{t_b+1}^{(B)}(\tau) | \mathcal{F}_{t_b}] - L_{t_b}^{(B)}(\tau)}.$$

A value of HEVaR that is close to 1 indicates that the hedge is effective in mitigating the variability (in terms of VaR) of the values of the portfolio one year from the time when the hedge is established.

The following procedure is used to calculate the two values of $\text{VaR}_{99.5\%}$ in HEVaR:

- Simulate realizations of $\kappa_t^{(R)} | \mathcal{F}_{t_b}$, $\kappa_t^{(B)} | \mathcal{F}_{t_b}$ and $\gamma_{t-t_b} | \mathcal{F}_{t_b}$ for $t = t_b + 1$.
- For each realization of the period and cohort effects, calculate the realized values of $L_{t_b+1}^{(B)}(\tau)$ and $Q_{t_b+1}^{(R)}(t_b, x_j^f, t_j^f)$ for $j = 1, \dots, J$, using the approximation methods described in Sections 3.5.1 and 3.5.2.
- Using the result from the previous step, obtain empirical distributions of $L_{t_b+1}^{(B)}(\tau)$ and $L_{t_b+1}^{(B)}(\tau) - \sum_{j=1}^J h_j Q_{t_b+1}^{(R)}(t_b, x_j^f, t_j^f)$, of which the 99.5th percentile yield the values of $\text{VaR}_{99.5\%}$ in the denominator and numerator in the expression for HEVaR, respectively.

Note that the approximations methods we developed also play a crucial role in the calculation of HEVaR (Step (ii) in the procedure above).

3.8 Illustrations

In this section, we provide three illustrations of the longevity hedging strategies developed in Section 3.6.

3.8.1 Illustration 1: Population Basis Risk and Cohort Effect Uncertainty

The first illustration provides the baseline results. It also analyzes the impact of cohort effect uncertainty and population basis risk on hedge effectiveness.

Assumptions

The following assumptions are used for Illustration 1:

- The hedge is a static hedge, which is established and evaluated at time $t_b = 2005$. Recall that the data sample used ends in year 2005.
- The liability being hedged is a deferred annuity-immediate sold at time t_b . It has a deferment period of τ years, and begins payment at the end of the year in which the annuitant attains age 65. The mortality experience of the annuitant is identical to that of the UK male insured lives.

Two different values of τ are considered:

$$-\tau = 0$$

This value of τ implies that the annuitant was born in 1941. As this year-of-birth is covered by the data sample, the annuity is not subject to any cohort effect uncertainty.

$$-\tau = 9$$

This value of τ implies that the annuitant was born in 1950. This year-of-birth is beyond the data sample, and thus the annuity is subject to cohort effect uncertainty.

- The q-forwards used are issued at the end of year 2005 (i.e., $t^* = 2005$). We consider q-forwards with references ages 65, 69, 75 and 85, and times-to-maturity 5, 10 and 15 years. The table below shows the years-of-birth to which the q-forwards are linked. The number of asterisks (displayed next to the year-of-birth) indicates the relative level of cohort effect uncertainty.

$x^f \backslash t^f$	65	69	75	85
5	1945	1941	1935	1925
10	1950 (**)	1946 (*)	1940	1930
15	1955 (***)	1951 (**)	1945	1935

The q-forwards' reference population is the English and Welsh population. As the q-forwards and the annuity liability are associated with different populations, population basis risk exists.

To focus on the goals of this illustration, we set λ to 0. This assumption is relaxed in Section 3.8.3 when the relationship between the cost of hedging and hedge effectiveness is studied.

- Three or four q-forwards are used in each hedge, depending on whether or not the sensitivity to $\gamma_{t_b-x_a}$ is matched.
- The interest rate is at 5% per annum for all durations.

Baseline Results

The baseline results are displayed in Table 3.2. Hedges #1 to #3 are for the annuity liability with $\tau = 0$, whereas Hedges #4 to #8 are for the annuity liability with $\tau = 9$.

Hedge	q-forward 1	q-forward 2	q-forward 3	q-forward 4	HE
$\tau = 0$					
#1	(65,5,1945)	(75,10,1940)	(85,15,1935)	-	0.83
#2	(75,5,1935)	(65,10,1950) (**)	(85,15,1935)	-	0.78
#3	(75,5,1935)	(85,10,1930)	(65,15,1955) (***)	-	0.68
$\tau = 9$					
#4	(65,5,1945)	(75,10,1940)	(85,15,1935)	-	0.57
#5	(75,5,1935)	(65,10,1950) (**)	(85,15,1935)	-	0.60
#6	(75,5,1935)	(85,10,1930)	(65,15,1955) (***)	-	0.55
#7	(65,5,1945)	(75,10,1940)	(85,15,1935)	(65,10,1950) (**)	0.67
#8	(65,5,1945)	(75,10,1940)	(85,15,1935)	(69,10,1946) (*)	0.60

Table 3.2: The effectiveness of the static hedges for the annuity liabilities with $\tau = 0$ and $\tau = 9$. The specification of each q-forward used is presented by a triplet (x^f, t^f, c^f) , where $c^f = t_b + t^f - x^f$ is the cohort to which the q-forward is linked. The number of asterisks next to the triplet indicates the level of cohort effect uncertainty to which the q-forward is subject.

Annuity with $\tau = 0$

We first focus on the annuity liability with $\tau = 0$. Since it is not subject to any cohort effect uncertainty, the sensitivity to $\gamma_{t_b-x_a}$ is not matched and three q-forwards are used.

Even though the sensitivity to $\gamma_{t_b-x_a}$ is not matched, the hedger may still use q-forwards that are subject to cohort effect uncertainty. In Hedge #1, all of the q-forwards are free of cohort effect uncertainty, but in Hedges #2 and #3, one of the q-forwards used is subject to cohort effect uncertainty.

The following findings are observed:

- Even when population basis risk exists, a static hedge with only three q-forwards can still achieve an reasonably high level of hedge effectiveness (up to 83% reduction in variance).
- Among the three hedges constructed, Hedge #1 (the only one that is free of cohort effect uncertainty), is the most effective. This outcome is not overly surprising, because using a q-forward that is exposed to cohort effect uncertainty (Hedges #2 and #3) would introduce cohort effect uncertainty to the hedger's portfolio (which is originally free of such uncertainty). A similar reasoning can also explain why Hedge #2 yields a higher value of HE compared to Hedge #3.

Annuity with $\tau = 9$

We now turn to the annuity liability with $\tau = 9$. Since it is subject to cohort effect uncertainty, we can match the sensitivity to $\gamma_{t_b-x_a}$, provided that at least one of the q-forwards used is also subject to cohort effect uncertainty. The following observations are made:

- By comparing Hedges #4, #5 and #6 with Hedges #1, #2 and #3, we can deduce that hedge effectiveness is significantly reduced if the annuity liability is subject to cohort effect uncertainty but the sensitivity to $\gamma_{t_b-x_a}$ is not matched.

- While both Hedges #5 and #6 contains a q-forward that is exposed to cohort effect uncertainty, Hedge #5 is more effective than Hedge #6. This outcome can be attributed to the fact that the second q-forward in Hedge #5 and the annuity liability are linked to the same cohort (year-of-birth 1950).
- Hedges #4 and #7 are identical, except that Hedge #7 contains an additional q-forward that is subject to cohort effect uncertainty and is linked to the same cohort (year-of-birth 1950) as the annuity liability. It can be seen that by matching $\gamma_{t_b-x_a}$ using an additional q-forward that is also associated with year-of-birth 1950, the hedge effectiveness is significantly increased.
- Hedge #8 also contains an additional q-forward that is subject to cohort effect uncertainty. However, the additional q-forward is not associated with year-of-birth 1950. As the cohorts to which the annuity liability and the additional q-forward are linked do not coincide, Hedge #8 is not as effective as Hedge #7. However, Hedge #8 is still more effective than Hedge #4, in which the sensitivity to $\gamma_{t_b-x_a}$ is not matched at all.

From these observations, we can conclude that when the liability being hedged is subject to cohort effect uncertainty, it is important to match the sensitivity to $\gamma_{t_b-x_a}$. Furthermore, whenever possible, the hedger should include in his/her portfolio a q-forward that is linked to the same cohort as the liability being hedged.

The Impact of Population Basis Risk

In the M7-M5 model, the extent of population basis risk is determined exclusively by the covariance matrix $\Sigma^{(\mathcal{B})}$ in the process for $\kappa_t^{(\mathcal{B})}$. To examine the impact of population basis risk, we now consider four hypothetical scenarios for which the specifications of $\Sigma^{(\mathcal{B})}$ are different. In Scenario 1, $\Sigma^{(\mathcal{B})} = 0$ so that the hedge is not subject to any population basis risk. In Scenarios 2 to 4, the diagonal elements in $\Sigma^{(\mathcal{B})}$ are increased to 2, 5 and 10 times their estimated values, respectively.

In Table 3.3, we compare, for each of eight hedges constructed, the values of HE in the four hypothetical scenarios with the baseline HE value. The following observations are made:

- Compared to the baseline HE value, the value of HE when population basis risk is completely absent (Scenario 1) is only slightly higher.
- Across Scenarios 1 to 4, the extent of population basis risk increases rapidly, but the hedge effectiveness decreases very slowly. Even if population basis risk is 10 times that in the baseline scenario, the hedges still perform reasonably well.
- The conclusions made in the previous sub-section are still valid under all of the scenarios.

	Hedge	Baseline	Scenario 1	Scenario 2	Scenario 3	Scenario 4
$\tau = 0$	#1	0.83	0.84	0.82	0.79	0.75
	#2	0.78	0.79	0.77	0.75	0.71
	#3	0.68	0.69	0.68	0.66	0.62
$\tau = 9$	#4	0.57	0.57	0.56	0.55	0.54
	#5	0.60	0.60	0.60	0.58	0.57
	#6	0.55	0.55	0.54	0.53	0.52
	#7	0.67	0.67	0.67	0.65	0.63
	#8	0.60	0.61	0.60	0.59	0.57

Table 3.3: The values of HE for the eight static hedges produced under the baseline specification of $\Sigma^{(\mathcal{B})}$ and the four alternatives specifications of $\Sigma^{(\mathcal{B})}$.

From these observations, we can conclude that if a longevity hedge is properly calibrated (using the strategies developed earlier in this chapter), then the resulting hedge effectiveness is reasonably robust with respect to the level of population basis risk. In particular, with a proper calibration, the hedge effectiveness when there is a normal level of population basis risk is almost identical to that when population basis risk is completely absent.

3.8.2 Illustration 2: Static vs. Dynamic

In this illustration, we focus on the difference in hedge effectiveness between a static hedge and a dynamic hedge.

Assumptions

The following assumptions are made for Illustration 2:

- Both hedges (static and dynamic) are established and evaluated at time $t_b = 2005$. The dynamic hedge is rebalanced annually until one year before the liability completely runs off (i.e., from time $t_b + 1 = 2006$ to $t_b + \tau + \omega - x_0 - 1 = 2044$).
- The liability being hedged is a deferred annuity-immediate sold at time $t_b = 2005$. It has a deferment period of 5 years, and begins payment at the end of the year in which the annuitant attains age 65. The mortality experience of the annuitant is identical to that of the UK male insured lives.

These assumptions imply that the annuitant was born in 1946. This year-of-birth is not covered by the data sample, so at time t_b the annuity is subject to cohort effect uncertainty. However, as the cohort effect for year-of-birth 1946 will be realized at time $t_b + 1$, the annuity liability will be free of cohort effect uncertainty one year after the hedges are established.

- The reference population of the q-forwards used is English and Welsh males. To focus on the goals of this illustration, λ is again set to 0. All q-forwards used are freshly launched at the time when they are written.
- Two scenarios are considered. They differ in the specifications of the q-forwards used.

- Scenario I

For the static hedge, we use four q-forwards with $(x^f, t^f) = (65, 5), (69, 10), (75, 10), (85, 15)$. The q-forward with $(x^f, t^f) = (69, 10)$ is associated with the

same year-of-birth (1946) as the annuity liability, and is subject to cohort effect uncertainty. The other three q-forwards are not subject to cohort effect uncertainty.

For the dynamic hedge, we use four q-forwards with $(x^f, t^f) = (65, 5), (69, 10), (75, 10), (85, 15)$ when the hedge is first established at time $t_b = 2005$. As the annuity liability is free of cohort effect uncertainty after time $t_b + 1$, only three q-forwards, with $(x^f, t^f) = (65, 5), (75, 10), (85, 15)$, are used when the hedge is rebalanced. These three q-forwards are not subject to cohort effect uncertainty.

– Scenario II

For the static hedge, we use four q-forwards with $(x^f, t^f) = (69, 10), (70, 10), (75, 10), (80, 10)$. Note that they have the same time-to-maturity. The q-forward with $(x^f, t^f) = (69, 10)$ is associated with the same year-of-birth (1946) as the annuity liability, and is subject to cohort effect uncertainty. The other three q-forwards are not subject to cohort effect uncertainty.

For the dynamic hedge, we use four q-forwards with $(x^f, t^f) = (69, 10), (70, 10), (75, 10), (80, 10)$ when the hedge is first established at time $t_b = 2005$. As the annuity liability is free of cohort effect uncertainty after time $t_b + 1$, only three q-forwards, with $(x^f, t^f) = (70, 10), (75, 10), (80, 10)$, are used when the hedge is rebalanced. These three q-forwards are not subject to cohort effect uncertainty.

Empirical Results

The resulting values of HE are tabulated in Table 3.4. The following observations and conclusions are made:

- In both scenarios, the dynamic hedge yields a significantly higher value of HE compared to the static hedge. This finding highlights the benefit from dynamically adjusting a longevity hedge over time.
- The static hedge in Scenario II (whereby all q-forwards have the same time-to-maturity) is substantially less effective than that in Scenario I. However, the dynamic

hedges in both scenarios are similarly effective. This finding echoes that of Zhou and Li (2017), who identified and explained the empirical that the performance of a dynamically adjusted longevity hedge is robust with respect to the times-to-maturity of the q-forwards used.

This finding suggests that when the range of times-to-maturity in the q-forward market is limited, rebalancing a longevity hedge periodically is particularly beneficial. What is found in this illustration is practically relevant, because from the lessons learnt from the BNP/EIB longevity bond (see, e.g., Blake et al., 2006), we anticipate that it is unlikely that q-forwards with ultra-long times-to-maturity will become available in the market.

	Static Hedge	Dynamic Hedge
Scenario I	0.74	0.97
Scenario II	0.57	0.93

Table 3.4: The values of HE for the static and dynamic hedges in Scenarios I and II.

3.8.3 Illustration 3: Cost of Hedging

The third illustration investigates the impact of the cost of hedging. To this end, we now allow λ (which reflects the risk premium demanded by the counterparty) to deviate from zero. Recall from Section 3.3.4 that the cost of a q-forward is related to its forward mortality rate q^f , which is determined as a function of λ :

$$q^f = (1 - \lambda)(1 - E[S_{x^f, t^* + t^f - 1}^{(R)}(1) | \mathcal{F}_{t^*}]).$$

A higher value of λ means that a larger amount of risk premium is demanded by the counterparty.

We now also measure hedge effectiveness with HEVaR instead of HE, because the former takes the cost of hedging into account while the latter (which only measures the dispersion around the expected value) does not.

Assumptions

Other than the above assumptions regarding hedge evaluation and λ , the following assumptions are used in this illustration:

- The hedge is a static hedge, established and evaluated at time $t_b = 2005$.
- The liability being hedged is identical to that in Illustration 2.
- The q-forwards used are the same as those for the static hedge in Scenario 2 of Illustration 2.
- Four values of λ , namely 0, 0.005, 0.01 and 0.05, are considered.

Empirical Results

Table 3.5 shows the values of HEVaR for the four assumed values of λ . Figure 3.6 compares, for each of the four assumed values of λ , the empirical distributions of the $(t_{2005}, \mathcal{F}_{2006})$ -values of the hedged position (i.e., $L_{2006}^{(B)} - \sum_{j=1}^4 h_j Q_{2006}^{(R)}$) and unhedged positions (i.e., $L_{2006}^{(B)}$) given \mathcal{F}_{2005} . The following observations and conclusions can be made from Table 3.5 and Figure 3.6:

- When the q-forwards are costless (i.e., $\lambda = 0$), the value of HEVaR is 0.95, which means equivalently means that the longevity hedge reduces the 1-year ahead 99.5% VaR (over the expected value of the annuity liability) by 95%.
- For all of the four assumed values of λ , the hedged positions are equally less dispersed than the unhedged position. This phenomenon confirms the fact that the cost of hedging does not affect the mitigation of the dispersion surrounding the expected value.
- However, as λ increases, the distribution of $L_{2006}^{(B)} - \sum_{j=1}^4 h_j Q_{2006}^{(R)}$ given \mathcal{F}_{2005} shifts rightwards, and hence has a higher 99.5th percentile. Consequently, the value of HEVaR decreases with λ . It can be deduced that beyond a certain threshold value

of λ , the value of HEVaR would become negative, which in turn means that the longevity hedge would no longer be economically viable.

λ	0	0.005	0.01	0.05
HEVaR	0.95	0.90	0.85	0.45

Table 3.5: The values of HEVaR for the four assumed values of λ .

3.9 Concluding Remarks

In this chapter, we have contributed a discrete-time delta hedging strategy (constructed in both static and dynamic settings) for use with the M7-M5 model, a two-population mortality model that is recommended by the research team in charge of the population basis risk project (phase I) commissioned by the LLMA and IFoA. The hedging strategy takes into account of both cohort effect uncertainty and population basis risk, in contrast to those in previous work which ignore at least one of these two sources of randomness.

Under the M7-M5 model assumption, a survival function may involve both unrealized period effects and an unrealized cohort effect. As a consequence, the ‘approximation of survival function’ method, which is essential for keeping the computational effort entailed in a dynamic delta hedge manageable, is not straightforward to implement. We have overcome this technical challenge by systematically dividing all possibly encountered survival functions into five cases, and tailoring a specific approximation (or calculation) method for each.

We have defined several metrics for quantifying the effectiveness of cash flow hedges (of which the focus is the variability of cash flows) and value hedges (of which the focus is the variability of the portfolio values at a future time point). The metric based on the reduction in Value-at-Risk over a one-year horizon at a confidence level of 99.5% is particularly relevant to Solvency II capital requirements. Typically, the evaluation of such a metric requires simulations on simulations, but this need is waived by the approximation methods we consider.

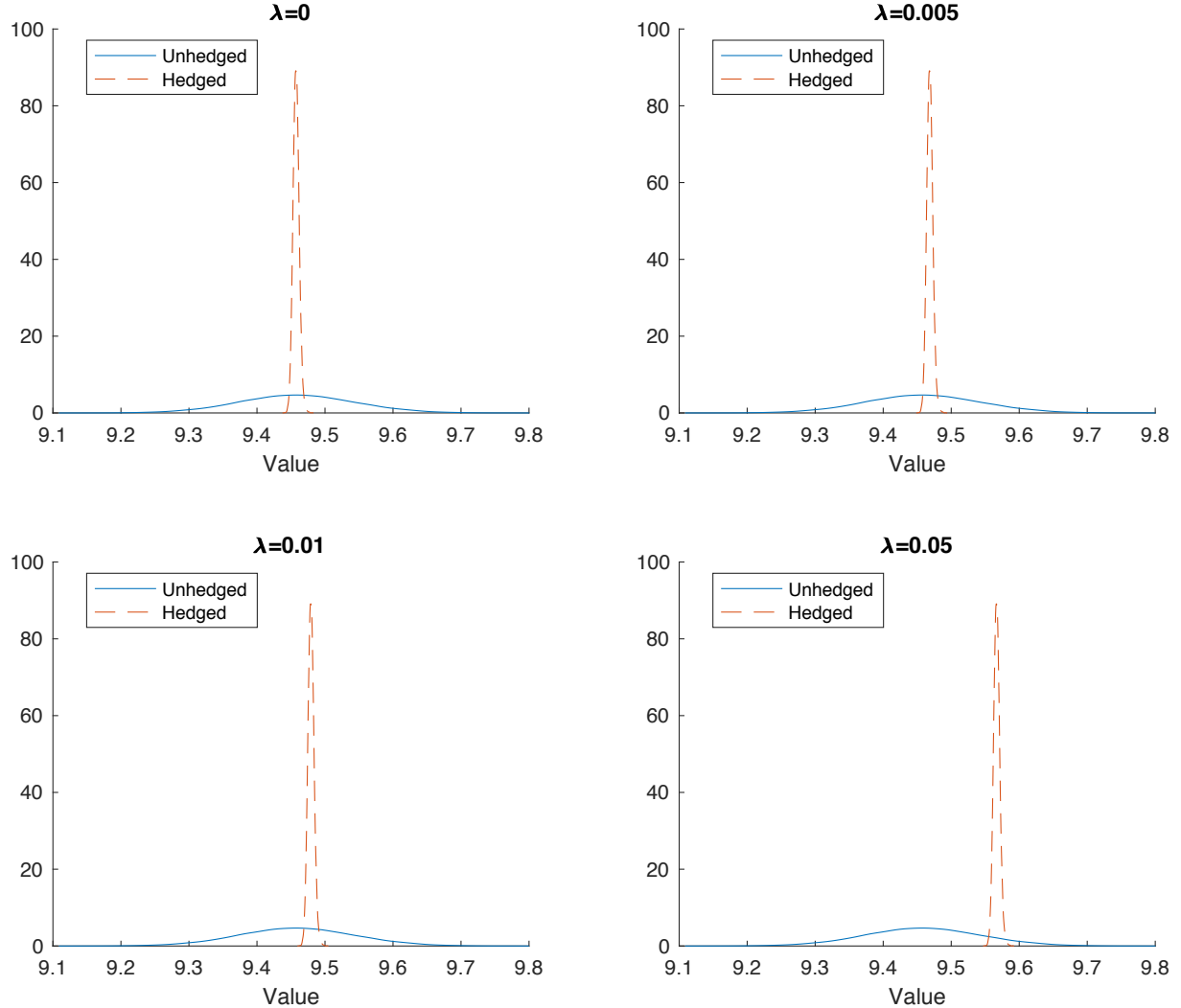


Figure 3.6: The empirical distributions of the $(t_{2005}, \mathcal{F}_{2006})$ -values of the unhedged position (i.e., $L_{2006}^{(B)}$) and the hedged position (i.e., $L_{2006}^{(B)} - \sum_{j=1}^4 h_j Q_{2006}^{(R)}$) given \mathcal{F}_{2005} , obtained using the four assumed values of λ .

We have provided three real data illustrations to supplement our theoretical work. The empirical work suggests the following points concerning index-based longevity hedging:

- If the liability being hedged is subject to cohort effect uncertainty, a delta hedge

that matches the sensitivity to the most recently realized cohort effect significantly outperforms one that does not.

- Whether possible, the hedger should include in his/her hedge portfolio a q-forward that is linked to the same cohort as his/her annuity liability.
- If a longevity hedge is properly calibrated (with the strategies developed in this chapter), then the resulting hedge effectiveness is reasonably robust with respect to the level of population basis risk.
- When the range of times-to-maturity of the q-forward market is limited, rebalancing a longevity hedge periodically is particularly beneficial.
- The hedge effectiveness measured in terms of Value-at-Risk reduces as the risk premium demanded by the counterparty of the q-forwards increases. When the risk premium becomes sufficiently high, a negative hedge effectiveness may be resulted.

Generally speaking, an index-based longevity hedge is subject to three sources of basis risk, namely (i) population basis risk (which arises from demographic or socioeconomic differences), (ii) sampling basis risk (which arises from the finite sample variation surrounding a fixed mortality trajectory), and (iii) structural basis risk (which arises from the differences in the payoff structures of the liability being hedged and the hedging instruments). In this chapter, we have focused on (i) and addressed (iii) by deriving longevity deltas that are specific to the payoff structures of the annuity liability and q-forwards, but have paid no attention to (ii). Future research warrants a study that incorporates (ii), using the M7-M5 model in conjunction with a suitable death count process. Note that (ii) has no impact on the calculation of deltas, but may reduce hedge effectiveness depending on the size of the hedger's portfolio.

Chapter 4

Asymmetry in Mortality Volatility and Its Implications on Index-based Longevity Hedging

4.1 Introduction

Mortality volatility, that is, the level of uncertainty surrounding the trend of mortality improvement, is crucially important to many aspects of index-based longevity hedging, including instrument pricing, hedge calibration, and hedge performance evaluation. Methods for pricing mortality-linked instruments often involve an estimate of mortality volatility. For example, the q -forward pricing formula considered by Coughlan et al. (2007) and Li and Hardy (2011) determines the forward mortality rate as the corresponding expected mortality rate (under the real-world probability measure) less the product of the assumed Sharpe ratio and an estimate of mortality volatility. When adjusting the real-world Cairns-Blake-Dowd model for pricing purposes, the adjustment amounts to the product of a vector of Sharpe ratios and an estimate of the volatility of the period (time-related) effects driving the evolution of mortality (Cairns et al., 2006). Mortality volatility is also heavily involved in many methods for calibrating longevity hedges. One example is the variance-minimizing method considered by Cairns et al. (2014) (and used in Chapter 2 as a benchmark), which

leads to an optimal hedge ratio of which both the numerator and denominator depend on an estimate of mortality volatility. Lastly, when evaluating a longevity hedge using typical metrics such as reduction in variance and reduction in Value-at-Risk (both of which are used in Chapter 3), an estimate of mortality volatility is needed.

While most studies in stochastic mortality modeling treat mortality volatility as a constant over time, there exists profound empirical evidence supporting the time-varying nature of mortality volatility (Lee and Miller, 2001; Gao and Hu, 2009; Giacometti et al., 2012; Lin et al., 2015). As discussed in Chapter 2, there has been a growing awareness of this empirical fact, and attempts have been made to extend existing stochastic mortality models to incorporate time-varying mortality volatility. One approach is to borrow methodologies used in the context of interest rate modeling; for instance, Fung et al. (2017) employed a discrete version of the Cox-Ingersoll-Ross model to capture the dynamics of mortality volatility. A more common approach is to utilize the family of generalized autoregressive conditional heteroskedasticity (GARCH) models, as seen in the recent contributions by Chai et al. (2013), Chen et al. (2015) Gao and Hu (2009), Giacometti et al. (2012), Lin et al. (2015), Wang and Li (2016), and also in Chapter 2 of this thesis.

This chapter sets out to obtain a deeper understanding of mortality volatility and its implications on index-based longevity hedging. The first objective is to investigate, from a global perspective, the potential asymmetry in mortality volatility, which arises when mortality volatility is more (or less) responsive to positive mortality shocks (due to, for example, wars and pandemics) than negative mortality shocks (due to, for example, medical breakthroughs). To this end, we apply a range of GARCH-type models that permit asymmetric volatility, including the E-GARCH model (Nelson, 1991), the GJR-GARCH model (Glosten et al., 1993), the N-GARCH model (Engle and Ng, 1993) and the T-GARCH model (Zakoian, 1994), to mortality data from nine countries that span four continents. While some of these models have previously been used to capture the dynamics of mortality volatility, this study represents the first attempt to compare these models with their symmetric counterpart (the GARCH model with symmetric volatility) with a goal to identify the need to incorporate asymmetric mortality volatility in modeling and applications.

In the context of equity risk, the financial impact of asymmetry in volatility (of equity

returns) has been demonstrated by many researchers including Campbell and Hentschel (1992), Koutmos and Booth (1995) and Bekaert and Wu (2000). It is therefore reasonable to conjecture that asymmetry in mortality volatility, if exists, has a financial impact on participants in the market of longevity risk transfers, and that failing to take such volatility asymmetry into account may result in erroneous index-based longevity hedges.

The second objective is to study how asymmetric mortality volatility may affect index-based longevity hedges through longevity Greeks. As introduced in Chapter 2, a longevity Greek measures the sensitivity to changes in a certain parameter in the stochastic process driving the evolution of mortality over time. Longevity Greeks have been proven to be an effective tool for calibrating index-based longevity hedges (Cairns, 2011, 2013; De Rosa et al., 2017; Liu and Li, 2017; Luciano et al., 2012, 2017; Luciano and Regis, 2014; Zhou and Li, 2017). Studies such as Cairns (2011) and Zhou and Li (2017), and also Chapter 3 have shown that longevity Greeks are useful in approximating the values of mortality-linked instruments and liabilities, and in assessing different dimensions of longevity risk inherent in pension plans or annuity portfolios.

In more detail, we make three technical contributions which enable us to link mortality volatility to index-based longevity hedging. First, we extend the work of Chapter 2 to the mentioned collection of GARCH-type models that permit asymmetric mortality volatility. Semi-analytical expressions, similar to those derived in Chapters 2 and 3, for three key longevity Greeks – delta, gamma, and vega – are derived for each of the models.

Second, we improve the framework introduced in Chapter 2 to enable a more robust estimate of longevity vega. As demonstrated in this chapter, the longevity vega defined in Chapter 2 may erroneously take a value of zero, even when volatility is actually time-varying and is influential to the value of the liability or instrument under consideration. This problem in turn leads to difficulties in establishing a vega hedge (a hedge that neutralizes the longevity vega of the hedger's position). Drawing on the ideas of Engle and Rosenberg (1995) and Badescu et al. (2014), in the improved longevity Greeks framework we treat the liability or instrument under consideration as a function of the conditional volatility at time 1 instead of that at time 0, and take partial derivatives accordingly. We show theoretically that the improved framework can mitigate the ‘zero problem’ found in the original framework.

Third, inspired by the work of Duan (2009), we contribute a new longevity Greek known as ‘dynamic delta’. When the period effect of mortality dynamics is modeled in a stochastic volatility framework, a shock to the period effect has the following two impacts: (1) a direct impact on the level of mortality, and (2) an indirect impact on the level of mortality as other parameters in the model are changed due to the shock to the period effect. The original longevity delta can only capture the former impact, because it is defined as the first *partial* derivative with respect to the time-0 period effect, and when the derivative is taken all parameters except the time-0 period effect are held constant. In contrast, defined as the *total* derivative with respect to the time-0 the period effect, dynamic delta can capture both direct and indirect impacts. The expression for dynamic delta turns out to be highly intuitive: it is the sum of the original longevity delta (which captures the direct impact) and the product of longevity vega and an adjustment term (which jointly reflect the indirect impact).

Our theoretical contributions are complemented by two real-data illustrations, one of which is based on a value hedge that focuses on the variability of the values of the hedged position at a certain future time point, the other of which is based on a cash flow hedge that focuses on the variability of all cash flows arising from the liability being hedged and the hedging instruments. In line with Solvency II capital requirements, we measure hedge effectiveness in terms of the reduction in the Value-at-Risk at a confidence level of 99.5%. Our empirical results point to the conclusion that if mortality volatility is in fact asymmetric but the asymmetry in mortality volatility is not taken into account when a longevity hedge is calibrated, then the resulting hedge effectiveness could be significantly impaired.

The remainder of the chapter is organized as follows. Section 4.2 describes the GARCH-type models we consider, and demonstrates the need of incorporating asymmetric mortality volatility. For ease of reading, Section 4.3 reviews the longevity Greeks defined in Chapter 2. Section 4.4 presents the improved longevity Greeks framework, which encompasses the enhanced version of longevity vega, and the longevity Greeks for a wider class of GARCH models that permit asymmetric mortality volatility. Section 4.5 introduces the new longevity Greek called dynamic delta. The two real-data illustrations are presented in Section 4.6. Finally, Section 4.7 concludes the chapter.

4.2 Modeling Mortality Volatility

4.2.1 Data

We consider mortality data from the female populations of nine countries which span four continents. All of the required data are obtained from the Human Mortality Database. The age range we use is 40 to 89, which covers typical ages of annuitants/pensioners and excludes the extreme ages for which the data are extrapolated values instead of raw counts. To better satisfy the data requirements of GARCH-type model and discern the potential asymmetry in mortality volatility, we use all available data (over the chosen age range) from 1900.¹ A summary of the mortality data used is summarized in Table 4.1.

Continent	Country	Calibration window	Age range	Gender
North America	Canada	1921-2011	40-89	Female
	US	1933-2016	40-89	Female
Europe	Finland	1900-2015	40-89	Female
	France	1900-2015	40-89	Female
	Italy	1900-2014	40-89	Female
	Spain	1908-2014	40-89	Female
	UK	1900-2016	40-89	Female
Oceania	Australia	1921-2014	40-89	Female
Asia	Japan	1947-2016	40-89	Female

Table 4.1: A summary of the mortality data used in this chapter.

4.2.2 The Lee-Carter Structure

Following Chapter 2, we assume that mortality follows the Lee-Carter structure:

$$\ln m_{x,t} = a_x + b_x \kappa_t, \quad (4.1)$$

¹For some populations, the available data series begins after 1900, and in this situation the beginning point of the calibration window is set to the earliest year for which data is available.

where $m_{x,t}$ is the central death rate at age x and in year t , a_x is an age-specific parameter measuring the average level of mortality at age x , κ_t is the time-varying index (also known as the period effect) capturing the overall level of mortality in year t , and b_x is an age-specific parameter reflecting the sensitivity of $m_{x,t}$ to changes in κ_t .

The dynamics of κ_t is specified as

$$\kappa_t = \kappa_{t-1} + \mu + \epsilon_t, \quad (4.2)$$

where μ is the drift term representing the expected rate of change in κ_t , and ϵ_t is the time- t innovation which has a zero mean.² While most previous studies in stochastic mortality modeling assume that the variance of ϵ_t is time-invariant, we permit the (conditional) variance of ϵ_t to vary over time.³ We use σ_t^2 to represent the conditional variance of ϵ_t .

In the rest of this section, we first identify any possible conditional heteroskedasticity, that is, the phenomenon that σ_t^2 is time-varying, for each of the nine populations. We then move to our first research objective to investigate the possibility that σ_t^2 responds asymmetrically to positive and negative shocks (innovations) prior to time t .

4.2.3 Conditional Heteroskedasticity

Using the Poisson maximum likelihood method (Brouhns et al., 2002), we obtain estimates of parameters in equation (4.1). Figure 4.1 shows the estimated series of $(\kappa_t - \kappa_{t-1})$ for each of the nine populations under consideration. For all populations except Australia and the US, the variation in $(\kappa_t - \kappa_{t-1})$ clearly varies over time. In particular, the variation seems more pronounced during certain periods such as 1910s and 1930s. Such a pattern suggests that conditional heteroskedasticity exists.

To verify the existence of conditional heteroskedasticity, we apply Engle's ARCH test to the series of $(\kappa_t - \kappa_{t-1})^2$ for each population. The test results are reported in Table 4.2. Except for US and Australia, the test results suggest a rejection of the null hypothesis

²It is assumed that $\{\epsilon_t\}$ and hence $\{\kappa_t - \kappa_{t-1}\}$ possess no serial correlation. Despite this assumption, $\{\epsilon_t^2\}$ and $\{(\kappa_t - \kappa_{t-1})^2\}$ are both serially correlated if conditional heteroskedasticity exists.

³The condition is the information up to and including time $t - 1$.

that $(\kappa_t - \kappa_{t-1})^2$ possesses no serial correlation, confirming the existence of conditional heteroskedasticity. We also apply the Ljung-Box test to the series of $(\kappa_t - \kappa_{t-1})^2$ for each population. The test results (not shown for the sake of space) point to the same conclusion.

Lag	1	2	3	4	5
Canada	3.9186 (0.0478)	34.6104 (<0.0001)	38.2005 (<0.0001)	41.9446 (<0.0001)	39.9087 (<0.0001)
US	0.6037 (0.4372)	1.8717 (0.3923)	3.5025 (0.3204)	4.8071 (0.3077)	10.5270 (0.0616)
Finland	11.9455 (0.0005)	11.7071 (0.0029)	12.7023 (0.0053)	18.3154 (0.0011)	27.5272 (<0.0001)
France	17.9267 (<0.0001)	18.7987 (0.0001)	19.1268 (0.0003)	28.9292 (<0.0001)	30.6836 (<0.0001)
Italy	25.0178 (<0.0001)	33.2536 (<0.0001)	38.0725 (<0.0001)	39.3564 (<0.0001)	39.6428 (<0.0001)
Spain	24.3091 (<0.0001)	27.2442 (<0.0001)	28.3534 (<0.0001)	28.2829 (<0.0001)	28.0881 (<0.0001)
UK	24.4022 (<0.0001)	25.0509 (<0.0001)	24.8998 (<0.0001)	24.8032 (0.0001)	24.8135 (0.0002)
Australia	0.0976 (0.7547)	0.7170 (0.6987)	0.7759 (0.8552)	6.3877 (0.1720)	7.5213 (0.1847)
Japan	0.6633 (0.4154)	8.1174 (0.0173)	10.0398 (0.0182)	10.6085 (0.0313)	15.1785 (0.0096)

Table 4.2: The test statistic and p-value (in parentheses) of the Engle's ARCH test (at lag 1 to 5) applied to the series of $(\kappa_t - \kappa_{t-1})$ for each of the nine populations under consideration.

In our preliminary modeling work, we estimate a GARCH(1,1) model, the model considered in Chapter 2, to the series of ϵ_t (i.e., the mean corrected series of $(\kappa_t - \kappa_{t-1})$) for each

of the nine populations under consideration. The GARCH(1,1) model can be expressed as

$$\epsilon_t = \sigma_t \eta_t, \quad (4.3)$$

$$\sigma_t^2 = \omega + \alpha \epsilon_{t-1}^2 + \beta \sigma_{t-1}^2, \quad (4.4)$$

where σ_t^2 is the conditional variance of ϵ_t , η_t -s are independent and identically distributed (i.i.d.) standard normal random variables, and ω , α and β are constant parameters. In particular, parameters α and β govern the dependence of the time- t conditional variance on the time- $(t - 1)$ squared innovation and the time- $(t - 1)$ conditional variance, respectively.

Having fitted the GARCH(1,1) model, the inferred values of σ_t^2 over the calibration window are extracted and are reported in Figure 4.2. The existence of conditional heteroskedasticity is further supported by the fact that the patterns of the inferred values of σ_t^2 over the calibration window are far from being flat for all of the populations considered, except US and Australia. We then apply Engle's ARCH test to the series of squared standardized residuals⁴ for each population. Reported in Table 4.3, the test results indicate no significant serial correlations in the squared standardized residuals, suggesting that conditional heteroskedasticity is adequately captured by the GARCH(1,1) models. We also apply the Ljung-Box test to the series of squared standardized residuals for each population. The test results (not shown for the sake of space) point to the same conclusion.

While the GARCH(1,1) model appears to have captured conditional heteroskedasticity adequately, it does not capture any asymmetry in volatility. It is clear from equation (4.4) that a positive shock (innovation) at time $t - 1$, say $|\epsilon_{t-1}^*|$, and a negative shock of the same magnitude, that is, $-|\epsilon_{t-1}^*|$, have exactly the same impact on the time- t conditional variance.

4.2.4 Asymmetry in Mortality Volatility

To investigate the potential asymmetry in mortality volatility, a wider range of GARCH-type models are considered. The additional models include the E-GARCH model, the

⁴The standardized residual at time t is defined as the ratio of the residual at time- t to the inferred value of σ_t .

GJR-GARCH model, the N-GARCH model, and the T-GARCH model. These models differ from the GARCH model in the way in which the dynamics of the conditional variance σ_t^2 is specified. We consider an order of (1,1) for all of the additional models, because the results in the previous sub-section suggest that this order can adequately capture the serial correlation in the conditional variances.

Below we describe, for each of the additional GARCH-type models, the specification of the dynamics of σ_t^2 and the way in which the asymmetry in volatility is captured. In all of the models, ω , α , β and γ are constant parameters, and γ is the parameter controlling the asymmetry in volatility.

- **E-GARCH**

The E-GARCH(1,1) model assumes that

$$\ln(\sigma_t^2) = \omega + \gamma\eta_{t-1} + \alpha \left(|\eta_{t-1}| - \sqrt{\frac{2}{\pi}} \right) + \beta \ln \sigma_{t-1}^2, \quad (4.5)$$

where $\eta_{t-1} = \epsilon_{t-1}/\sigma_{t-1}$. A positive time- $(t-1)$ innovation with a magnitude of $|\epsilon_{t-1}^*|$ affects $\ln(\sigma_t^2)$ by $\gamma|\epsilon_{t-1}^*|/\sigma_{t-1} + \alpha(|\epsilon_{t-1}^*|/\sigma_{t-1} - \sqrt{2/\pi})$, whereas an otherwise identical negative innovation affects $\ln(\sigma_t^2)$ by $-\gamma|\epsilon_{t-1}^*|/\sigma_{t-1} + \alpha(|\epsilon_{t-1}^*|/\sigma_{t-1} - \sqrt{2/\pi})$.

- **GJR-GARCH**

The GJR-GARCH(1,1) model assumes that

$$\sigma_t^2 = \omega + \alpha\epsilon_{t-1}^2 + \gamma\epsilon_{t-1}^2 \mathcal{I}_{\{\epsilon_{t-1}<0\}} + \beta\sigma_{t-1}^2, \quad (4.6)$$

where \mathcal{I}_A is an indicator function which equals 1 if event A holds true and 0 otherwise. A positive time- $(t-1)$ innovation with a magnitude of $|\epsilon_{t-1}^*|$ affects σ_t^2 by $\alpha(\epsilon_{t-1}^*)^2$, whereas an otherwise identical negative innovation affects σ_t^2 by $(\alpha + \gamma)(\epsilon_{t-1}^*)^2$.

- **N-GARCH**

The N-GARCH(1,1) model assumes that

$$\sigma_t^2 = \omega + \alpha\sigma_{t-1}^2(\eta_{t-1} - \gamma)^2 + \beta\sigma_{t-1}^2. \quad (4.7)$$

A positive time- $(t-1)$ innovation with a magnitude of $|\epsilon_{t-1}^*|$ affects σ_t^2 by $\alpha\sigma_{t-1}^2(|\epsilon_{t-1}^*|/\sigma_{t-1} - \gamma)^2$, whereas an otherwise identical negative innovation affects σ_t^2 by $\alpha\sigma_{t-1}^2(-|\epsilon_{t-1}^*|/\sigma_{t-1} - \gamma)^2$.

- **T-GARCH**

The T-GARCH(1,1) model assumes that

$$\sigma_t = \omega + \alpha(|\epsilon_{t-1}| - \gamma\epsilon_{t-1}) + \beta\sigma_{t-1}. \quad (4.8)$$

A positive time- $(t-1)$ innovation with a magnitude of $|\epsilon_{t-1}^*|$ affects σ_t by $\alpha(1-\gamma)|\epsilon_{t-1}^*|$, whereas an otherwise identical negative innovation affects σ_t by $\alpha(1+\gamma)|\epsilon_{t-1}^*|$.

We apply the above mentioned models to all of the nine populations under consideration. To compare the performances of these models as well as the GARCH model and the constant volatility assumption, we consider the Bayesian information criterion (BIC), which is defined such that a lower BIC value indicates a better goodness-of-fit with the number of model parameters being taken into account.

In line with the results in Section 4.2.3, the constant volatility assumption produces the lowest BIC values for US and Australia. For all but one of the remaining populations, the best performing model is either the E-GARCH, GJR-GARCH or T-GARCH model, suggesting that there exists asymmetry in mortality volatility. We further examine the estimates of parameter γ for these populations (Table 4.5). It is found that all of the six estimates of γ are significant at any reasonable level of significance, further confirming the existence of asymmetry in mortality volatility and the need for capturing it.

4.3 A Brief Review of Chapter 2

We study the impact of asymmetry in mortality volatility on index-based longevity hedging through various extensions of existing longevity Greeks. These extensions draw on the work

of Chapter 2, which we summarize in this section for ease of reading.

4.3.1 The Key Building Block

Denote by $q_{x,t}$ the probability that an individual who has survived to age x at time $t - 1$ dies between time $t - 1$ and t . We have

$$S_{x,t}(T) = \prod_{s=1}^T (1 - q_{x+s-1,t+s})$$

being the *ex post* probability that an individual who has survived to age x at time t would have survived to time $t + T$ for $T = 1, 2, \dots$. Assuming a constant force of mortality between consecutive integer ages, which in turn implies that $q_{x,t} = 1 - \exp(-m_{x,t})$, we can express $S_{x,t}(T)$ as follows:

$$\begin{aligned} S_{x,t}(T) &= \prod_{s=1}^T \exp(-m_{x+s-1,t+s}) \\ &= \exp\left(-\sum_{s=1}^T \exp(a_{x+s-1} + b_{x+s-1}\kappa_{t+s})\right) \end{aligned} \tag{4.9}$$

$$\begin{aligned} &= \exp\left(-\sum_{s=1}^T \exp(Y_{x,t}(s))\right) \\ &= \exp(-W_{x,t}(T)), \end{aligned} \tag{4.10}$$

where

$$Y_{x,t}(s) = a_{x+s-1} + b_{x+s-1}\kappa_{t+s} \tag{4.11}$$

and

$$W_{x,t}(T) = \sum_{s=1}^T \exp(Y_{x,t}(s)) \tag{4.12}$$

are defined to make the expressions of longevity Greeks more compact.

We set time 0 to the end point of the calibration window to which the model is fitted. Using equations (4.2) and (4.3), we obtain

$$\kappa_t = \kappa_0 + t\mu + \sum_{s=1}^t \sigma_s \eta_s, \quad t \geq 1, \tag{4.13}$$

so that

$$S_{x,t}(T) = \exp \left(- \sum_{s=1}^T \exp \left(a_{x+s-1} + b_{x+s-1} \left(\kappa_0 + (t+s)\mu + \sum_{u=1}^{t+s} \sigma_u \eta_u \right) \right) \right). \quad (4.14)$$

A GARCH(1,1) model is assumed in Chapter 2, which implies that

$$\sigma_s^2 = \begin{cases} \omega \left(1 + \sum_{u=1}^{s-1} \prod_{v=1}^u (\alpha \eta_{s-v}^2 + \beta) \right) + (\alpha \epsilon_0^2 + \beta \sigma_0^2) \prod_{v=1}^{s-1} (\alpha \eta_{s-v}^2 + \beta) & \text{if } s \geq 2 \\ \omega + \alpha \epsilon_0^2 + \beta \sigma_0^2 & \text{if } s = 1 \end{cases}. \quad (4.15)$$

Let \mathcal{F}_t be the information about the evolution of mortality up to and including time t . It follows from equations (4.14) and (4.15) that given \mathcal{F}_0 , $S_{x,t}(T)$ depends on κ_0 (the time-0 value of the period effect), σ_0^2 (the time-0 value of the conditional volatility) and a sequence of i.i.d. standard normal random variables $\{\eta_s; s = 1, \dots, t+T\}$. It is clear that $S_{x,t}(T)$ given \mathcal{F}_0 is a random variable due to its dependence on $\{\eta_s; s = 1, \dots, t+T\}$.

Finally, we arrive at the following key building block of the longevity Greeks framework:

$$p_{x,t}(T, \kappa_0, \sigma_0^2) := \mathbb{E}[S_{x,t}(T) \mid \mathcal{F}_0],$$

which can be interpreted to mean the probability for an individual aged x at time t to survive to time $t+T$, given the information about the evolution of mortality up to and including time 0.

4.3.2 Longevity Greeks for $p_{x,t}(T, \kappa_0, \sigma_0^2)$

The longevity Greeks for $p_{x,t}(T, \kappa_0, \sigma_0^2)$ are obtained by taking the partial derivatives of $p_{x,t}(T, \kappa_0, \sigma_0^2)$ with respect to either κ_0 or σ_0^2 .

The longevity delta for $p_{x,t}(T, \kappa_0, \sigma_0^2)$ is

$$\frac{\partial p_{x,t}(T, \kappa_0, \sigma_0^2)}{\partial \kappa_0} = - \sum_{s=1}^T b_{x+s-1} \mathbb{E}[\exp(Y_{x,t}(s) - W_{x,t}(T)) \mid \mathcal{F}_0],$$

a quantity which measures the first-order sensitivity of $p_{x,t}(T, \kappa_0, \sigma_0^2)$ to changes in κ_0 .

The longevity gamma for $p_{x,t}(T, \kappa_0, \sigma_0^2)$ is

$$\begin{aligned} & \frac{\partial^2 p_{x,t}(T, \kappa_0, \sigma_0^2)}{\partial \kappa_0^2} \\ &= E \left[\exp(-W_{x,t}(T)) \left(\left(\sum_{s=1}^T b_{x+s-1} \exp(Y_{x,t}(s)) \right)^2 - \sum_{s=1}^T b_{x+s-1}^2 \exp(Y_{x,t}(s)) \right) \middle| \mathcal{F}_0 \right], \end{aligned}$$

a quantity which represents the second-order sensitivity of $p_{x,t}(T, \kappa_0, \sigma_0^2)$ to changes in κ_0 .

Finally, the longevity vega for $p_{x,t}(T, \kappa_0, \sigma_0^2)$ is defined as

$$\frac{\partial p_{x,t}(T, \kappa_0, \sigma_0^2)}{\partial \sigma_0^2} = - \sum_{s=1}^T b_{x+s-1} E \left[\exp(Y_{x,t}(s) - W_{x,t}(T)) \left(\frac{\partial \kappa_{t+s}}{\partial \sigma_0^2} \right) \middle| \mathcal{F}_0 \right], \quad (4.16)$$

where

$$\frac{\partial \kappa_{t+s}}{\partial \sigma_0^2} = \sum_{u=1}^{t+s} \frac{\eta_u}{2\sigma_u} \frac{\partial \sigma_u^2}{\partial \sigma_0^2} \quad (4.17)$$

and

$$\frac{\partial \sigma_u^2}{\partial \sigma_0^2} = \begin{cases} \beta \prod_{v=1}^{u-1} (\alpha \eta_{u-v}^2 + \beta) & \text{if } u \geq 2 \\ \beta & \text{if } u = 1 \end{cases}. \quad (4.18)$$

This longevity Greek measures the first-order sensitivity of $p_{x,t}(T, \kappa_0, \sigma_0^2)$ to changes in σ_0^2 . A full derivation of the above formulas can be found in Appendix A.

4.3.3 Longevity Greeks for the Values of Liabilities and Hedging Instruments

The values of annuity/liabilities and hedging instruments such as q-forwards and S-forwards can be expressed as a linear combination of $p_{x,t}(T, \kappa_0, \sigma_0^2)$ for different values of x, t and T . As such, the longevity Greeks for the values of annuity/liabilities and hedging instruments can be computed easily as a linear combination of the longevity Greeks of $p_{x,t}(T, \kappa_0, \sigma_0^2)$ for different values of x, t and T .

4.4 The Enhanced Framework of Longevity Greeks

In this section, we improve the framework of Chapter 2 to avoid a technical problem that may happen in practice. We also expand the framework to incorporate the GARCH-type models that permit asymmetry in volatility.

4.4.1 Motivations

One problem of the previous framework is that it produces a longevity vega that is highly sensitive to parameter β in the GARCH(1,1) model, a parameter that measures the extent of serial dependence in $\{\sigma_t^2\}$. It can be seen from equation (4.18) that the longevity vega of the value of a liability/instrument must be zero if parameter β equals zero (which happens when the fitted model is an ARCH(1) model), even when volatility is not constant (parameter α is not zero) and the value of the liability/instrument is in fact sensitive to changes in volatility. This zero longevity vega not only leads to a misleading conclusion concerning the liability/instrument's exposure to mortality volatility risk, but also causes difficulties when establishing a vega hedge (i.e., a hedge that neutralizes the longevity vega of the hedge's portfolio) due to a division-by-zero problem.

One possible way to circumvent this problem is to create a new Greek that measures the sensitivity to ϵ_0^2 (the squared innovation at time 0). Calculated as a partial derivative of $E[S_{x,t}(T) | \mathcal{F}_0]$ with respect to ϵ_0^2 , this new longevity Greek can be expressed as

$$-\sum_{s=1}^T b_{x+s-1} E \left[\exp(Y_{x,t}(s) - W_{x,t}(T)) \left(\frac{\partial \kappa_{t+s}}{\partial \epsilon_0^2} \right) \middle| \mathcal{F}_0 \right],$$

where

$$\frac{\partial \sigma_u^2}{\partial \epsilon_0^2} = \begin{cases} \alpha \prod_{v=1}^{u-1} (\alpha \eta_{u-v}^2 + \beta) & \text{if } u \geq 2 \\ \alpha & \text{if } u = 1 \end{cases}. \quad (4.19)$$

However, this solution opens up another problem. As implied by equation (4.19), this new longevity Greek is spuriously zero whenever parameter α (which measures the serial dependence in $\{\epsilon_t^2\}$) in the GARCH(1,1) model is zero even if volatility is in fact not constant (parameter β is non-zero).

Instead of introducing another longevity Greek, we propose to adapt the previous framework by considering $E[S_{x,t}(T) | \mathcal{F}_0]$ as a function of κ_0 and σ_1 rather than κ_0 and σ_0 , and redefining longevity vega accordingly.

4.4.2 Redefining the Building Block

In developing the improved framework, the first step is to obtain recursive expressions of σ_u^2 , $u = 2, 3, \dots$, in terms of σ_1^2 , using equations (4.4) to (4.8). The expressions of σ_u^2 , $u = 2, 3, \dots$, in terms of σ_1^2 for the GARCH model as well as the four GARCH-type models that permit asymmetry in volatility are summarized in Table 4.6.

Then, using the expressions in Table 4.6 and equation (4.14), we can express $S_{x,t}(T)$ in terms of κ_0 and σ_1 for each of the GARCH-type models we consider. Finally, noting that σ_1^2 is non-random given \mathcal{F}_0 , we obtain

$$p_{x,t}(T, \kappa_0, \sigma_1^2) := E[S_{x,t}(T) | \mathcal{F}_0] \quad (4.20)$$

as the key building block of the improved longevity Greeks framework.

4.4.3 Longevity Vega for $p_{x,t}(T, \kappa_0, \sigma_1^2)$

In the improved longevity Greeks framework, the longevity vega for $p_{x,t}(T, \kappa_0, \sigma_1^2)$ is obtained by taking the first-order partial derivative of $p_{x,t}(T, \kappa_0, \sigma_1^2)$ with respect to σ_1^2 :

$$\begin{aligned} V_{x,t}(T) &:= \frac{\partial p_{x,t}(T, \kappa_0, \sigma_1^2)}{\partial \sigma_1^2} = E\left[\frac{\partial S_{x,t}(T)}{\partial \sigma_1^2} \middle| \mathcal{F}_0\right] \\ &= E\left[\exp(-W_{x,t}(T)) \left(-\sum_{s=1}^T \exp(Y_{x,t}(s)) \left(b_{x+s-1} \sum_{u=1}^{t+s} \frac{\partial \sigma_u \eta_u}{\partial \sigma_1^2}\right)\right) \middle| \mathcal{F}_0\right] \\ &= -\sum_{s=1}^T b_{x+s-1} E\left[\exp(Y_{x,t}(s) - W_{x,t}(T)) \left(\sum_{u=1}^{t+s} \frac{\eta_u}{2\sigma_u} \frac{\partial \sigma_u^2}{\partial \sigma_1^2}\right) \middle| \mathcal{F}_0\right], \end{aligned} \quad (4.21)$$

where $\frac{\partial \sigma_u^2}{\partial \sigma_1^2} = 1$ for $u = 1$, and $\frac{\partial \sigma_u^2}{\partial \sigma_1^2}$ for $u \geq 2$ depends on the chosen GARCH-type model.

For the GARCH, GJR-GARCH and N-GARCH models, the expression of $\frac{\partial \sigma_u^2}{\partial \sigma_1^2}$ for $u \geq 2$ can be easily derived from the corresponding expressions of σ_u^2 for $u \geq 2$ in Table 4.6. For the E-GARCH model, we use the chain rule to get

$$\frac{\partial \sigma_u^2}{\partial \sigma_1^2} = \frac{\partial \sigma_u^2}{\partial \ln(\sigma_u^2)} \frac{\partial \ln(\sigma_u^2)}{\partial \ln(\sigma_1^2)} \frac{\partial \ln(\sigma_1^2)}{\partial \sigma_1^2} = \frac{\sigma_u^2}{\sigma_1^2} \frac{\partial \ln(\sigma_u^2)}{\partial \ln(\sigma_1^2)},$$

where $\frac{\partial \ln(\sigma_u^2)}{\partial \ln(\sigma_1^2)} = \beta^{u-1}$ for $u \geq 2$ can be obtained straightforwardly from the expression of σ_u^2 for $u \geq 2$ for the E-GARCH model as shown in Table 4.6. Lastly, for the T-GARCH model, the chain rule is used to get

$$\frac{\partial \sigma_u^2}{\partial \sigma_1^2} = \frac{\partial \sigma_u^2}{\partial \sigma_u} \frac{\partial \sigma_u}{\partial \sigma_1} \frac{\partial \sigma_1}{\partial \sigma_1^2} = \frac{\sigma_u}{\sigma_1} \frac{\partial \sigma_u}{\partial \sigma_1},$$

where $\frac{\partial \sigma_u}{\partial \sigma_1} = \prod_{v=1}^{u-1} (\alpha(|\eta_{u-v}| - \gamma \eta_{u-v}) + \beta)$ for $u \geq 2$ can be derived from the expression of σ_u^2 for $u \geq 2$ for the T-GARCH model as shown in Table 4.6. The resulting expressions of $\frac{\partial \sigma_u^2}{\partial \sigma_1^2}$ for $u \geq 2$ for all GARCH-type models under consideration are presented in Table 4.7.

The expressions of both $Y_{x,t}(s)$ and $W_{x,t}(T)$ in equation (4.21) also depend on the chosen GARCH-type model. In particular, they depend on σ_u^2 for $u \geq 2$ (which in turn depends on the GARCH-type model chosen) through equations (4.11), (4.12) and (4.13). The calculation of $Y_{x,t}(s)$ and $W_{x,t}(T)$ is enabled by the expressions provided in Table 4.6.

Let us revisit the longevity vega under the GARCH model assumption. From Table 4.7 and equation (4.21), we observe that in the improved framework the longevity vega under the GARCH model assumption is non-zero unless *both* α and β are zero (which happens only when σ_t^2 is indeed a constant), suggesting that the spurious zero vega problem found in Chapter 2's longevity Greeks framework is mitigated. This desirable property also applies to all other GARCH-type models under consideration except the E-GARCH, for which the longevity vega must be zero if $\beta = 0$ regardless of whether or not α is zero.

4.4.4 Longevity Delta and Gamma for $p_{x,t}(T, \kappa_0, \sigma_1^2)$

As the partial derivatives of $p_{x,t}(T, \kappa_0, \sigma_1^2)$ and $p_{x,t}(T, \kappa_0, \sigma_0^2)$ with respect to κ_0 are identical, longevity delta and gamma in the improved framework remain the same as those in the previous framework. They are reported below for completeness.

The longevity delta for $p_{x,t}(T, \kappa_0, \sigma_1^2)$ is

$$\Delta_{x,t}(T) := \frac{\partial p_{x,t}(T, \kappa_0, \sigma_1^2)}{\partial \kappa_0} = - \sum_{s=1}^T b_{x+s-1} \mathbb{E}[\exp(Y_{x,t}(s) - W_{x,t}(T)) \mid \mathcal{F}_0], \quad (4.22)$$

and the longevity gamma for $p_{x,t}(T, \kappa_0, \sigma_1^2)$ is

$$\Gamma_{x,t}(T) \quad (4.23)$$

$$\begin{aligned} &:= \frac{\partial^2 p_{x,t}(T, \kappa_0, \sigma_1^2)}{\partial \kappa_0^2} \\ &= \mathbb{E} \left[\exp(-W_{x,t}(T)) \left(\left(\sum_{s=1}^T b_{x+s-1} \exp(Y_{x,t}(s)) \right)^2 - \sum_{s=1}^T b_{x+s-1}^2 \exp(Y_{x,t}(s)) \right) \middle| \mathcal{F}_0 \right]. \end{aligned} \quad (4.24)$$

As discussed in the previous sub-section, $Y_{x,t}(s)$ and $W_{x,t}(T)$ in the above expressions depend on the chosen GARCH-type model.

4.4.5 Additional Remarks

We compute the values of $\Delta_{x,t}(T)$, $\Gamma_{x,t}(T)$ and $V_{x,t}(T)$ with simulations. In particular, using N simulated paths of $\{\eta_s; s = 1, \dots, t+T\}$, we calculate N realizations of $Y_{x,t}(s)|\mathcal{F}_0$, $W_{x,t}(T)|\mathcal{F}_0$ and $\frac{\partial \sigma_u^2}{\partial \sigma_1^2}|_{\mathcal{F}_0}$ for $u \geq 2$, with which the expectations in equations (4.21), (4.22) and (4.24) can be evaluated.

The values of annuity/pension liabilities and typical mortality-linked instruments can be expressed as linear combinations of $p_{x,t}(T, \kappa_0, \sigma_1^2)$ for different values of x , t and T . As such, their longevity Greeks can be expressed as linear combinations of $\Delta_{x,t}(T)$, $\Gamma_{x,t}(T)$ or $V_{x,t}(T)$ for different values of x , t and T . The calculation of longevity Greeks for the values of liabilities and instruments is illustrated in Sections 4.6.2 and 4.6.3.

4.5 A New Longevity Greek: Dynamic Delta

When a GARCH-type model is used, a shock to κ_0 has both direct and indirect impacts on $p_{x,t}(T, \kappa_0, \sigma_1^2)$:

1. Direct impact

It is clear from equation (4.14) that a shock to κ_0 directly affects the distribution of $S_{x,t}(T)$, and hence the value of $p_{x,t}(T, \kappa_0, \sigma_1^2)$.

2. Indirect impact

A shock to κ_0 (represented by the time-0 innovation ϵ_0) alters the value of σ_1^2 through the conditional variance dynamics, thereby leading to changes in the values of σ_u^2 for all $u \geq 2$. These changes affect the distribution of $S_{x,t}(T)$ through equation (4.14), and thus the value of $p_{x,t}(T, \kappa_0, \sigma_1^2)$.

Longevity delta captures only the direct impact but not the indirect impact, because it is defined as a *partial* derivative which is taken with respect to κ_0 while σ_1^2 is held constant. This limitation makes longevity delta an inadequate measure of the sensitivity to changes in κ_0 .

To mitigate this limitation, we propose a new longevity Greek known as ‘dynamic delta’. This new longevity Greek is derived on the basis of a *total* derivative, in which the interrelationship between κ_0 and σ_1^2 is captured through the chain rule. More specifically, the dynamic delta for $p_{x,t}(T, \kappa_0, \sigma_1^2)$ is defined as the first-order *total* derivative of $p_{x,t}(T, \kappa_0, \sigma_1^2)$ with respect to κ_0 :

$$\begin{aligned}\Lambda_{x,t}(T) &:= \frac{dp_{x,t}(T, \kappa_0, \sigma_1^2)}{d\kappa_0} \\ &= \frac{d\kappa_0}{d\kappa_0} \frac{\partial p_{x,t}(T, \kappa_0, \sigma_1^2)}{\partial \kappa_0} + \frac{d\sigma_1^2}{d\kappa_0} \frac{\partial p_{x,t}(T, \kappa_0, \sigma_1^2)}{\partial \sigma_1^2} \\ &= \Delta_{x,t}(T) + \frac{d\sigma_1^2}{d\kappa_0} V_{x,t}(T).\end{aligned}\tag{4.25}$$

Equation (4.25) says that dynamic delta is the sum of (i) longevity delta and (ii) longevity vega with an adjusting term, $\frac{d\sigma_1^2}{d\kappa_0}$, which represents the sensitivity of σ_1^2 to changes in κ_0 . The direct impact of a shock to κ_0 is captured by (i), while the indirect impact is captured by (ii).

To calculate dynamic delta, we need the values of $\Delta_{x,t}(T)$, $V_{x,t}(T)$ and $\frac{d\sigma_1^2}{d\kappa_0}$. The calculation of $\Delta_{x,t}(T)$ and $V_{x,t}(T)$ is detailed in the previous section. The expression for $\frac{d\sigma_1^2}{d\kappa_0}$ is derived below.

First, we use the chain rule to obtain

$$\frac{d\sigma_1^2}{d\kappa_0} = \frac{d\sigma_1^2}{d\epsilon_0} \frac{d\epsilon_0}{d\kappa_0} = \frac{d\sigma_1^2}{d\epsilon_0},$$

where $\frac{d\epsilon_0}{d\kappa_0} = 1$ according to equation (4.2). We then derive $\frac{d\sigma_1^2}{d\epsilon_0}$ for each GARCH-type model under consideration:

• GARCH

For the GARCH(1,1) model, we have

$$\begin{aligned} \frac{d\sigma_1^2}{d\epsilon_0} &= \frac{d}{d\epsilon_0} (\omega + \alpha\epsilon_0^2 + \beta\sigma_0^2) \\ &= 2\alpha\epsilon_0. \end{aligned}$$

• E-GARCH

For the E-GARCH(1,1) model, we use the chain rule to get

$$\begin{aligned} \frac{d\sigma_1^2}{d\epsilon_0} &= \frac{d\eta_0}{d\epsilon_0} \frac{d\sigma_1^2}{d\eta_0} \\ &= \frac{1}{\sigma_0} \frac{d}{d\eta_0} \exp \left(\omega + \gamma\eta_0 + \alpha \left(|\eta_0| - \sqrt{\frac{2}{\pi}} \right) + \beta \ln \sigma_0^2 \right) \\ &= \frac{\sigma_1^2}{\sigma_0} \left(\gamma + \alpha \frac{|\eta_0|}{\eta_0} \right), \end{aligned}$$

where $\frac{d\eta_0}{d\epsilon_0} = \frac{1}{\sigma_0}$ according to equation (4.3).

• GJR-GARCH

If the chosen model is the GJR-GARCH(1,1) model, then we have

$$\begin{aligned} \frac{d\sigma_1^2}{d\epsilon_0} &= \frac{d}{d\epsilon_0} (\omega + \alpha\epsilon_0^2 + \gamma\epsilon_0^2 \mathcal{I}_{\{\epsilon_0 < 0\}} + \beta\sigma_0^2) \\ &= 2\alpha\epsilon_0 + 2\gamma\epsilon_0 \mathcal{I}_{\{\epsilon_0 < 0\}}. \end{aligned}$$

- **N-GARCH**

For the N-GARCH(1,1) model, we use the chain rule to get

$$\begin{aligned}\frac{d\sigma_1^2}{d\epsilon_0} &= \frac{d\eta_0}{d\epsilon_0} \frac{d\sigma_1^2}{d\eta_0} \\ &= \frac{1}{\sigma_0} \frac{d}{d\eta_0} (\omega + \alpha\sigma_0^2(\eta_0 - \gamma)^2 + \beta\sigma_0^2) \\ &= 2\alpha\sigma_0(\eta_0 - \gamma).\end{aligned}$$

- **T-GARCH**

If the T-GARCH(1,1) model is used, we have

$$\begin{aligned}\frac{d\sigma_1^2}{d\epsilon_0} &= \frac{d}{d\epsilon_0} (\omega + \alpha(|\epsilon_0| - \gamma\epsilon_0) + \beta\sigma_0)^2 \\ &= 2\alpha\sigma_1 \left(\frac{|\epsilon_0|}{\epsilon_0} - \gamma \right).\end{aligned}$$

Given \mathcal{F}_0 , $\frac{d\sigma_1^2}{d\kappa_0}$ is non-random and can be analytically calculated. Thus, once the values of $\Delta_{x,t}(T)$ and $V_{x,t}(T)$ are calculated, dynamic delta can be computed easily without any additional simulations.

4.6 Illustrations

In this section, we provide two real-data illustrations to demonstrate the impact of asymmetry in mortality volatility on index-based longevity hedging. We begin with a list of assumptions, followed by the derivations of the longevity Greeks for the liability being hedged and the hedging instrument. Hedge calibration is then discussed. Finally, numerical results are presented.

4.6.1 General Assumptions

The following assumptions are used in both illustrations.

- The liability being hedged is a pension plan for pensioners who are all aged 60 at time 0. The plan pays each pensioner \$1 at the end of each year until death or age 90, whichever is the earliest. The mortality experience of the pensioners is identical to that of the Italian female population. The plan contains an infinitely large number of pensioners, so diversifiable risk can be ignored.
- The hedger establishes a Greek longevity hedge for the pension plan using a S-forward at time 0. No adjustment is made to the hedge after time 0.
- At time 0, freshly launched S-forwards with a reference age 60 and times-to-maturity from 1 to 20 years are available. The hedger uses S-forwards of which the reference population is Italian female, so there is no population basis risk. Further information about S-forwards is given in Section 4.6.3.
- The evaluation of hedge effectiveness is based on the E-GARCH(1,1) model, which, as shown in Section 4.2, is found to be the best fitting model for the Italian female population. Parameter estimates of the E-GARCH(1,1) model fitted to the data from the Italian female population (over ages 40 to 89 and years 1900 to 2014) are reported in Table 4.8.
- Time 0 is defined as the end of year 2014 (i.e., the end point of the calibration window).
- When discounting future cash flows, an interest rate of $r = 3\%$ per annum for all durations is used.

4.6.2 Longevity Greeks for the Liability being Hedged

We now derive the longevity Greeks of the value of the pension plan. As per the assumptions made, we have

$$\mathcal{L} = \sum_{s=1}^{30} (1+r)^{-s} S_{60,0}(s)$$

as the sum of all future cash flows (per pensioner), discounted to time 0. Given \mathcal{F}_0 , \mathcal{L} is a random variable which depends on the evolution of mortality between time 1 and time 30. It follows that on a per pensioner basis, the time-0 value of the plan is

$$L(\kappa_0, \sigma_1^2) := \mathbb{E}[\mathcal{L}|\mathcal{F}_0] = \sum_{s=1}^{30} (1+r)^{-s} p_{60,0}(s, \kappa_0, \sigma_1^2).$$

As $L(\kappa_0, \sigma_1^2)$ is a linear combination of $p_{60,0}(s, \kappa_0, \sigma_1^2)$ for different values of s , the longevity Greeks of $L(\kappa_0, \sigma_1^2)$ can be calculated straightforwardly using the results in Sections 4.4 and 4.5. The longevity delta, longevity gamma, longevity vega, and dynamic delta of $L(\kappa_0, \sigma_1^2)$ are given by

$$\begin{aligned}\Delta^{(L)} &:= \frac{\partial L(\kappa_0, \sigma_1^2)}{\partial \kappa_0} = \sum_{s=1}^{30} (1+r)^{-s} \Delta_{60,0}(s), \\ \Gamma^{(L)} &:= \frac{\partial^2 L(\kappa_0, \sigma_1^2)}{\partial \kappa_0^2} = \sum_{s=1}^{30} (1+r)^{-s} \Gamma_{60,0}(s), \\ V^{(L)} &:= \frac{\partial L(\kappa_0, \sigma_1^2)}{\partial \sigma_1^2} = \sum_{s=1}^{30} (1+r)^{-s} V_{60,0}(s),\end{aligned}$$

and

$$\Lambda^{(L)} := \frac{dL(\kappa_0, \sigma_1^2)}{d\kappa_0} = \sum_{s=1}^{30} (1+r)^{-s} \Lambda_{60,0}(s),$$

respectively.

4.6.3 Longevity Greeks for the Hedging Instrument

Here we derive the longevity Greeks of the value of a S-forward. A S-forward is a zero-coupon swap with a fixed leg proportional to a forward survival rate S^f that is pre-determined at inception, and a floating leg proportional to a (random) realized survival rate. For a S-forward with a time-to-maturity of t^f and a reference age of x^f , the realized survival rate is the one for individuals aged x^f when the S-forward is launched over a period of t^f years. To mitigate longevity risk, a hedger can participate in a S-forward as a

fixed-rate payer, so that when future mortality turns out to be lighter than expected (i.e., the realized survival rate turns out to be lower than expected), the hedger will receive from the counterparty a positive net payment, which can be used to offset the correspondingly higher pension/annuity liability.

From the fixed-rate payer's perspective, the payoff of a S-forward (with a reference age of $x^f = 60$ and an issue date of $t = 0$) discounted to time 0 is

$$\mathcal{H} = (1 + r)^{-t^f} (S_{60,0}(t^f) - S^f)$$

per \$1 notional. Given \mathcal{F}_0 , \mathcal{H} is a random variable which depends on the evolution of mortality between time 1 and time t^f . It follows that the time-0 value of the S-forward is

$$H(\kappa_0, \sigma_1^2) := \mathbb{E}[\mathcal{H} | \mathcal{F}_0] = (1 + r)^{-t^f} (p_{60,0}(t^f, \kappa_0, \sigma_1^2) - S^f).$$

per \$1 notional.

As $H(\kappa_0, \sigma_1^2)$ is linearly related to $p_{60,0}(t^f, \kappa_0, \sigma_1^2)$, the longevity Greeks of $H(\kappa_0, \sigma_1^2)$ can be obtained easily using the results in Section 4.4 and 4.5. The longevity delta, longevity gamma, longevity vega, and dynamic delta of $H(\kappa_0, \sigma_1^2)$ are given by

$$\begin{aligned}\Delta^{(H)} &:= \frac{\partial H(\kappa_0, \sigma_1^2)}{\partial \kappa_0} = (1 + r)^{-t^f} \Delta_{60,0}(t^f), \\ \Gamma^{(H)} &:= \frac{\partial^2 H(\kappa_0, \sigma_1^2)}{\partial \kappa_0^2} = (1 + r)^{-t^f} \Gamma_{60,0}(t^f), \\ V^{(H)} &:= \frac{\partial H(\kappa_0, \sigma_1^2)}{\partial \sigma_1^2} = (1 + r)^{-t^f} V_{60,0}(t^f),\end{aligned}$$

and

$$\Lambda^{(H)} := \frac{dH(\kappa_0, \sigma_1^2)}{d\kappa_0} = (1 + r)^{-t^f} \Lambda_{60,0}(t^f),$$

respectively.

The longevity Greeks of a S-forward do not depend on its forward survival rate S^f , because S^f is pre-determined at time 0 and is thus treated as a constant. We set S^f to $\mathbb{E}[S_{60,0}(t^f) | \mathcal{F}_0]$, a forward survival rate which implies that no payment exchanges hands at time 0 (i.e., $\mathbb{E}[\mathcal{H} | \mathcal{F}_0] = 0$).

4.6.4 Hedge Calibration

A Greek longevity hedge can be created by matching the longevity Greek(s) of the liability being hedged and the hedging instrument(s). The longevity hedges in both of our illustrations are calibrated by matching dynamic delta, the new longevity Greek proposed in this chapter.

Since we are matching one longevity Greek, only one S-forward is needed. When the dynamic deltas of the liability being hedged and the S-forward are matched, the notional amount of the S-forward is calculated at time 0 as

$$u = \frac{\Lambda^{(L)}}{\Lambda^{(H)}}.$$

To demonstrate the impact of asymmetry in mortality volatility on the longevity hedges, we calculate two sets of results which respectively represent the situations when asymmetry in mortality volatility is ignored and taken into account:

(I) Asymmetry in mortality volatility is ignored

For this set of results, the longevity Greeks (and hence the notional amount u) are derived from a GARCH(1,1) model, which does not permit volatility to respond asymmetrically to positive and negative shocks. The GARCH(1,1) model is fitted to the Italian female data described in Section 4.6.1. The forward survival rate S^f is also calculated from the GARCH(1,1) model to mimic the situation when participants in the S-forward market ignore any asymmetry in mortality volatility. However, the mortality scenarios used to evaluate hedge effectiveness are generated from the E-GARCH(1,1) model as described in Section 4.6.1 to reflect the fact that asymmetry in mortality volatility exists.

(II) Asymmetry in mortality volatility is taken into account

In line with the model from which the mortality scenarios for evaluating hedge effectiveness are generated, the longevity Greeks (and hence the notional amount u) as well as the forward survival rate S^f for this set of results are calculated from the E-GARCH(1,1) model which permits asymmetry in mortality volatility.

4.6.5 Illustration 1: Value Hedge

The first illustration concerns a value hedge, which aims to reduce the variability of the values of the pension plan sponsor's position at time 1. We measure hedge effectiveness by the reduction in the 1-year ahead 99.5% Value-at-Risk over the time-0 value of the unhedged position:

$$1 - \frac{\text{VaR}_{99.5\%}(\mathbb{E}[\mathcal{L} - u\mathcal{H}|\mathcal{F}_1]|\mathcal{F}_0) - \mathbb{E}[\mathcal{L}|\mathcal{F}_0]}{\text{VaR}_{99.5\%}(\mathbb{E}[\mathcal{L}|\mathcal{F}_1]|\mathcal{F}_0) - \mathbb{E}[\mathcal{L}|\mathcal{F}_0]}.$$

The following comments concerning this metric of hedge effectiveness are made.

- In the expression, \mathcal{L} is the pension plan sponsor's position in the absence of a longevity hedge. Measured in time-0 dollars, the time-0 and time-1 values of the position are $\mathbb{E}[\mathcal{L}|\mathcal{F}_1]$ and $\mathbb{E}[\mathcal{L}|\mathcal{F}_0]$, respectively.
- In the numerator of the expression, $\mathcal{L} - u\mathcal{H}$ is the pension plan sponsor's position when the longevity hedge is in place. Measured in time-0 dollars, the time-1 value of the position is $\mathbb{E}[\mathcal{L} - u\mathcal{H}|\mathcal{F}_1]$.
- Given \mathcal{F}_0 , $\mathbb{E}[\mathcal{L}|\mathcal{F}_1]$ and $\mathbb{E}[\mathcal{L} - u\mathcal{H}|\mathcal{F}_1]$ are random variables depending on the unknown realization of \mathcal{F}_1 , but $\mathbb{E}[\mathcal{L}|\mathcal{F}_0]$ is a known constant.
- If the value hedge is effective, then the value of the metric should be close to one; if the opposite is true, then the value of the metric should be close to zero.

We use nested simulations to calculate the value of the metric. In more detail, we first use the fitted E-GARCH model to generate 10,000 mortality scenarios at time 1 (i.e., 10,000 realizations of \mathcal{F}_1). For each of these mortality scenarios, another 10,000 mortality scenarios are generated (also using the fitted E-GARCH model) to compute 10,000 realizations of $\mathbb{E}[\mathcal{L}|\mathcal{F}_1]$ and $\mathbb{E}[\mathcal{H}|\mathcal{F}_1]$, from which empirical distributions of $\mathbb{E}[\mathcal{L} - u\mathcal{H}|\mathcal{F}_1]$ and $\mathbb{E}[\mathcal{L}|\mathcal{F}_1]$ given \mathcal{F}_0 are obtained. The 99.5th percentiles of these two empirical distributions give the estimated 99.5% Values-at-Risk of $\mathbb{E}[\mathcal{L} - u\mathcal{H}|\mathcal{F}_1]$ and $\mathbb{E}[\mathcal{L}|\mathcal{F}_1]$, respectively. Lastly, $\mathbb{E}[\mathcal{L}|\mathcal{F}_0]$ is calculated with non-nested simulations.

Figure 4.3 compares the effectiveness of the value hedges that are calibrated when (I) asymmetry in mortality volatility is ignored and when (II) asymmetry in mortality volatility is taken into account. When asymmetry in mortality volatility is incorporated into the calibration of the value hedge, the hedge effectiveness ranges between 0.9 and 1, indicating that the hedge reduces at least 90 percent of the 99.5% Value-at-Risk over a horizon of one year. If the hedger ignores asymmetry in mortality volatility, then the hedge effectiveness is significantly reduced (by up to 70 percentage points depending on the time-to-maturity of the S-forward used).

4.6.6 Illustration 2: Cash Flow Hedge

The second illustration concerns a cash flow hedge, which aims to reduce the variability of all future cash flows of the pension plan sponsor. In this illustration, we measure hedge effectiveness by the reduction in the 99.5% Value-at-Risk of all future cash flows measured in time-0 dollars over the time-0 value of the liability being hedged:

$$1 - \frac{\text{VaR}_{99.5\%}(\mathcal{L} - u\mathcal{H}|\mathcal{F}_0) - \text{E}[\mathcal{L}|\mathcal{F}_0]}{\text{VaR}_{99.5\%}(\mathcal{L}|\mathcal{F}_0) - \text{E}[\mathcal{L}|\mathcal{F}_0]},$$

where $\mathcal{L} - u\mathcal{H}$ and \mathcal{L} represent the present (time-0) value of all cash flows arising from the hedged and unhedged positions, respectively. If the cash flow hedge is effective, then the value of the metric should be close to one; if the opposite is true, then the value of the metric should be close to zero.

To compute the value of the metric defined above, we use the fitted E-GARCH model to generate 10,000 realizations of \mathcal{L} and \mathcal{H} , from which empirical distributions of $\mathcal{L} - u\mathcal{H}$ and \mathcal{L} given \mathcal{F}_0 are obtained. The 99.5th percentiles of these two empirical distributions give the estimated 99.5% Values-at-Risk of $\text{E}[\mathcal{L} - u\mathcal{H}|\mathcal{F}_0]$ and $\text{E}[\mathcal{L}|\mathcal{F}_0]$, respectively. As in the first illustration, $\text{E}[\mathcal{L}|\mathcal{F}_0]$ is also calculated with non-nested simulations.

Figure 4.4 compares the effectiveness of the cash flow hedges that are calibrated when (I) asymmetry in mortality volatility is ignored and when (II) asymmetry in mortality volatility is taken into account. For all S-forward times-to-maturity considered, the effectiveness of the hedge that takes asymmetry in mortality volatility into account is higher compared

to the hedge that ignores asymmetry in mortality volatility. The difference in hedge effectiveness ranges from 10 to 40 percentage points, depending on the time-to-maturity of the S-forward used.

4.7 Concluding Remarks

We have investigated the existence of asymmetry in mortality volatility by using a range of GARCH-type models that permit volatility to respond asymmetrically to positive and negative shocks. It is found that for six out of the nine populations under consideration, asymmetry in mortality volatility is significant and needs to be modeled.

We have also studied the impact of asymmetry in mortality volatility on index-based longevity hedging, through three technical contributions that are made in this chapter.

First, we have improved the framework introduced in Chapter 2 by redefining the building block on which longevity Greeks are built. The longevity vega defined in the improved framework works with a wider range of α and β parameters in various GARCH-type models.

Second, we have derived, under the improved framework, semi-analytic expressions for the longevity vega under different GARCH model assumptions. These expressions enable us to calibrate longevity hedges when the assumed model is one that incorporates asymmetry in mortality volatility.

Third, we have introduced a new longevity Greek called dynamic delta. Derived on the basis of total derivative with respect to κ_0 , dynamic delta incorporates both the direct and indirect impacts of a shock to the period effect. We have also shown that dynamic delta is a linear combination of longevity delta and longevity vega with an adjusting term that is known at time 0, so that the value of dynamic delta can be obtained easily from the calculated values of longevity delta and longevity vega without any additional simulations.

We have provided two real-data illustrations to demonstrate the impact of asymmetry in mortality volatility on index-based longevity hedging. The results of both illustrations point to the conclusion that if mortality volatility is in fact asymmetric but the asymmetry

in mortality volatility is not taken into account when a longevity hedge is calibrated, then the resulting hedge effectiveness could be significantly impaired.

In financial markets, two types of volatility (realized and implied) are considered. In this chapter, we have focused on realized volatility, which is estimated from historical data. Implied volatility on the other hand is assembled from market expectation and obtained by back-solving the volatility parameter of a pricing model using observed market prices. The study of implied mortality volatility is impeded by the lack of market price data in today's infantile market for longevity risk transfers. However, it would be interesting to investigate implied mortality volatility when the market becomes more mature.

Finally, we remark that along the lines of dynamic delta, we can define 'dynamic gamma' as the second-order total derivative with respect to the time-0 period effect. The derivation of dynamic gamma can be initiated as follows:

$$\begin{aligned} \frac{d^2 p_{x,t}(T, \kappa_0, \sigma_1^2)}{d\kappa_0^2} &= \frac{d}{d\kappa_0} \left(\frac{dp_{x,t}(T, \kappa_0, \sigma_1^2)}{d\kappa_0} \right) = \frac{d}{d\kappa_0} \Lambda_{x,t}(T) \\ &= \frac{d}{d\kappa_0} \left(\Delta_{x,t}(T) + \frac{d\sigma_1^2}{d\kappa_0} V_{x,t}(T) \right) \\ &= \Gamma_{x,t}(T) + \frac{d^2 \sigma_1^2}{d\kappa_0^2} (V_{x,t}(T)) + \frac{d\sigma_1^2}{d\kappa_0} \left(\frac{d}{d\kappa_0} V_{x,t}(T) \right). \end{aligned}$$

Applications of this new longevity Greek are left as a topic for further research.

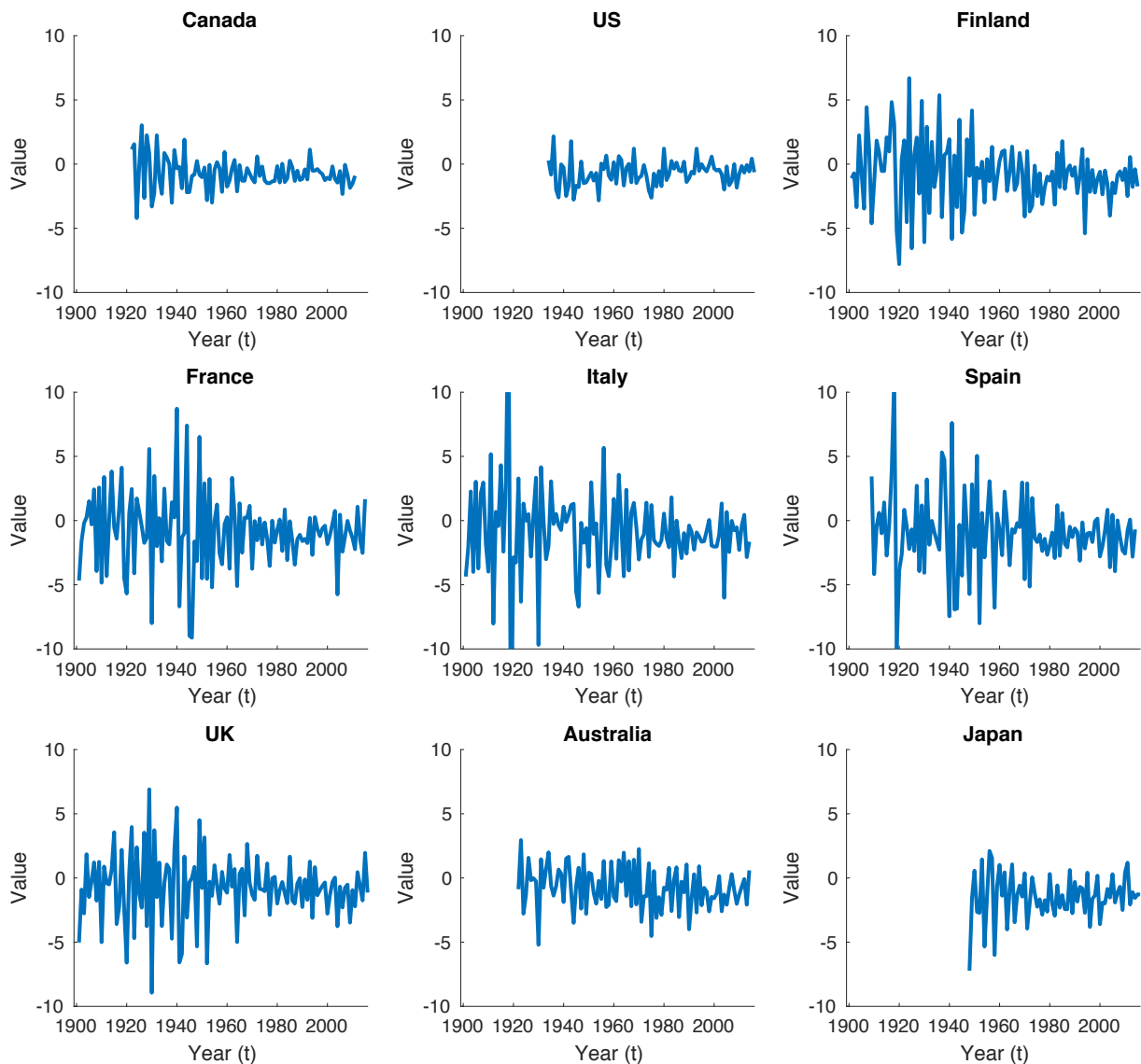


Figure 4.1: The estimated series of $(\kappa_t - \kappa_{t-1})$ for each of the nine populations under consideration.

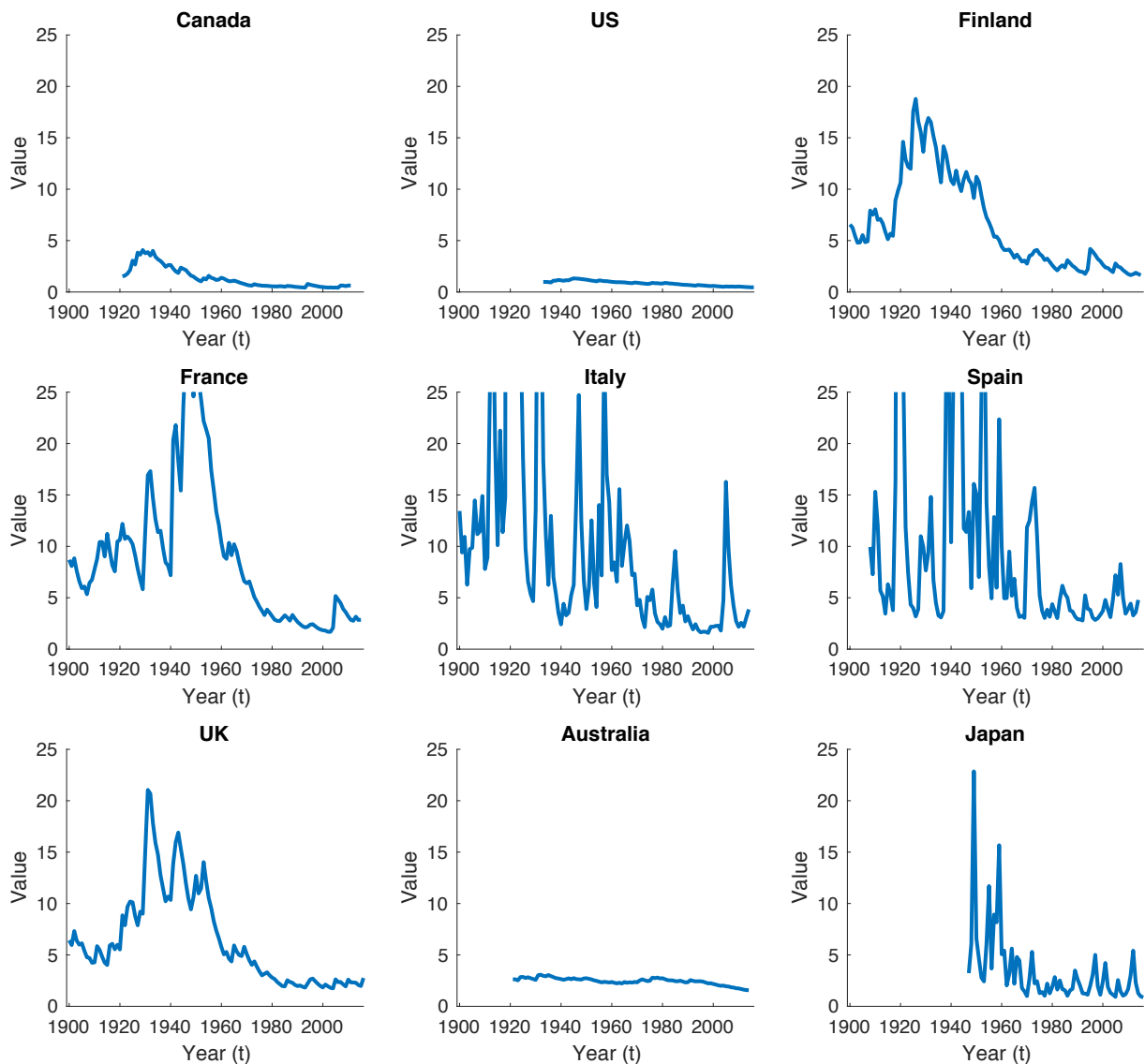


Figure 4.2: The inferred values of σ_t^2 derived from the estimated GARCH(1,1) models for the nine populations under consideration.

Lag	1	2	3	4	5
Canada	0.3250 (0.5686)	1.9275 (0.3815)	2.0685 (0.5583)	2.7649 (0.5979)	2.6145 (0.7592)
US	0.0613 (0.2597)	0.1474 (0.2280)	0.4116 (0.2778)	3.5730 (0.3262)	8.4085 (0.3748)
Finland	0.4489 (0.5029)	0.6515 (0.7220)	0.6034 (0.8956)	1.1397 (0.8879)	1.0648 (0.9572)
France	1.1372 (0.2863)	1.8028 (0.4060)	3.4347 (0.3293)	4.1475 (0.3864)	4.0885 (0.5367)
Italy	0.1206 (0.7284)	0.6007 (0.7406)	0.6155 (0.8929)	1.2811 (0.8646)	1.3904 (0.9254)
Spain	1.2405 (0.2654)	2.1881 (0.3349)	2.9848 (0.3940)	2.9233 (0.5707)	3.3817 (0.6414)
UK	0.2054 (0.6504)	0.2797 (0.8695)	0.9665 (0.8094)	1.6838 (0.7937)	1.8774 (0.8658)
Australia	0.3451 (0.5569)	1.1161 (0.5723)	1.1881 (0.7558)	5.9202 (0.2052)	5.8099 (0.3252)
Japan	0.0000 (0.9949)	0.7354 (0.6923)	2.4198 (0.4900)	4.4147 (0.3528)	6.1261 (0.2941)

Table 4.3: The test statistic and p-value (in parentheses) of the Engle's ARCH test (at lag 1 to 5) applied to the squared standardized residuals from the GARCH(1,1) for each of the nine populations under consideration.

	Constant	GARCH	E-GARCH	GJR-GARCH	N-GARCH	T-GARCH
Canada	3.3762	3.1447	3.2016	3.1925	3.1939	3.2452
US	2.9238	2.9668	3.0231	3.0193	3.0199	3.0731
Finland	4.8028	4.6416	4.6211	4.6277	4.6179	4.6461
France	5.0807	4.9103	4.8223	4.8099	4.8088	4.8470
Italy	38.3286	5.0997	5.0547	5.1396	5.0597	5.0550
Spain	5.2163	4.9746	4.8374	4.8123	4.8189	4.9095
UK	5.3489	5.2041	5.1991	5.1961	5.2085	5.1967
Australia	3.9126	3.9971	3.9588	3.9478	3.9693	4.0167
Japan	4.0182	4.0084	3.9396	3.9624	4.0642	4.2027

Table 4.4: The BIC values resulting from the constant volatility assumption, the GARCH model, and four GARCH-type models that incorporate asymmetry in volatility, fitted to the mean-corrected series of $(\kappa_t - \kappa_{t-1})$ for the nine populations under consideration. The lowest BIC value for each population is highlighted in red.

Country	Estimate	Standard error	t-Value
Finland	-3.86888	1.80264	-2.1462
France	-1.96910	0.75138	-2.6206
Italy	0.42944	0.10635	4.0380
Spain	-0.39775	0.00841	-47.3160
UK	-0.41025	0.20227	-2.0282
Japan	0.50631	0.10614	4.7703

Table 4.5: Estimates (and their standard errors and t-values) of parameter γ in the best performing models for Finland, France, Italy, Spain, UK and Japan.

Model	Expression of σ_u^2 , $u = 2, 3, \dots$, in terms of σ_1^2
GARCH	$\sigma_u^2 = \begin{cases} \omega \left(1 + \sum_{v=1}^{u-2} \prod_{v=1}^u (\alpha \eta_{u-v}^2 + \beta) \right) + \sigma_1^2 \prod_{v=1}^{u-1} (\alpha \eta_{u-v}^2 + \beta) & \text{if } u \geq 3 \\ \omega + \sigma_1^2 (\alpha \eta_1^2 + \beta) & \text{if } u = 2 \end{cases}$
E-GARCH	$\ln(\sigma_u^2) = \sum_{v=1}^{u-1} \beta^{u-1} \left(\omega + \gamma \eta_{u-v} + \alpha \left(\eta_{u-v} - \sqrt{\frac{2}{\pi}} \right) \right) + \beta^{u-1} \ln(\sigma_1^2)$
GJR-GARCH	$\sigma_u^2 = \begin{cases} \omega \left(1 + \sum_{v=1}^{u-2} \prod_{v=1}^u (\alpha \eta_{u-v}^2 + \gamma \eta_{u-v}^2 \mathcal{I}_{\{\eta_{u-v}<0\}} + \beta) \right) \\ + \sigma_1^2 \prod_{v=1}^{u-1} (\alpha \eta_{u-v}^2 + \gamma \eta_{u-v}^2 \mathcal{I}_{\{\eta_{u-v}<0\}} + \beta) & \text{if } u \geq 3 \\ \omega + \sigma_1^2 (\alpha \eta_1^2 + \gamma \eta_1^2 \mathcal{I}_{\{\eta_1<0\}} + \beta) & \text{if } u = 2 \end{cases}$
N-GARCH	$\sigma_u^2 = \begin{cases} \omega \left(1 + \sum_{v=1}^{u-2} \prod_{v=1}^u (\alpha (\eta_{u-v} - \gamma)^2 + \beta) \right) \\ + \sigma_1^2 \prod_{v=1}^{u-1} (\alpha (\eta_{u-v} - \gamma)^2 + \beta) & \text{if } u \geq 3 \\ \omega + \sigma_1^2 (\alpha (\eta_1 - \gamma)^2 + \beta) & \text{if } u = 2 \end{cases}$
T-GARCH	$\sigma_u = \begin{cases} \omega \left(1 + \sum_{v=1}^{u-2} \prod_{v=1}^u (\alpha (\eta_{u-v} - \gamma \eta_{u-v}) + \beta) \right) \\ + \sigma_1 \prod_{v=1}^{u-1} (\alpha (\eta_{u-v} - \gamma \eta_{u-v}) + \beta) & \text{if } u \geq 3 \\ \omega + \sigma_1 (\alpha (\eta_1 - \gamma \eta_1) + \beta) & \text{if } u = 2 \end{cases}$

Table 4.6: Expression of σ_u^2 , $u = 2, 3, \dots$, in terms of σ_1^2 for all GARCH-type models under consideration.

Model	Expression of $\frac{\partial \sigma_u^2}{\partial \sigma_1^2}$, $u = 2, 3, \dots$
GARCH	$\frac{\partial \sigma_u^2}{\partial \sigma_1^2} = \prod_{v=1}^{u-1} (\alpha \eta_{u-v}^2 + \beta)$
E-GARCH	$\frac{\partial \sigma_u^2}{\partial \sigma_1^2} = \beta^{u-1} \frac{\sigma_u^2}{\sigma_1^2}$
GJR-GARCH	$\frac{\partial \sigma_u^2}{\partial \sigma_1^2} = \prod_{v=1}^{u-1} (\alpha \eta_{u-v}^2 + \gamma \eta_{u-v}^2 \mathcal{I}_{\{\eta_{u-v}<0\}} + \beta)$
N-GARCH	$\frac{\partial \sigma_u^2}{\partial \sigma_1^2} = \prod_{v=1}^{u-1} (\alpha (\eta_{u-v} - \gamma)^2 + \beta)$
T-GARCH	$\frac{\partial \sigma_u^2}{\partial \sigma_1^2} = \frac{\sigma_u}{\sigma_1} \left(\prod_{v=1}^{u-1} (\alpha (\eta_{u-v} - \gamma \eta_{u-v}) + \beta) \right)$

Table 4.7: Expressions of $\frac{\partial \sigma_u^2}{\partial \sigma_1^2}$, $u = 2, 3, \dots$, for all GARCH-type models under consideration.

Parameter	Estimate	Standard error	t-Value
μ	-0.78690	0.22012	-3.57489
ω	0.25478	0.11267	2.26134
α	0.34416	0.23105	1.48955
β	0.87076	0.05254	16.5736
γ	0.42944	0.10635	4.03803

Table 4.8: Parameter estimates (and their standard errors and t-values) of the fitted E-GARCH model for the Italian female population.

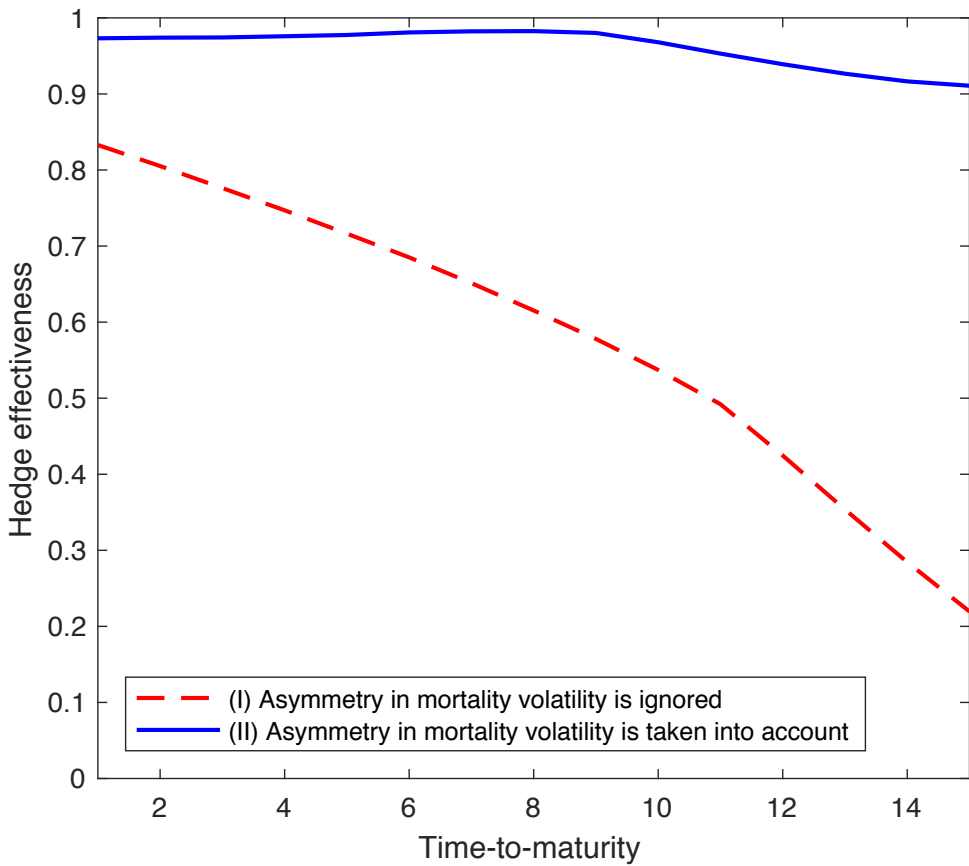


Figure 4.3: Effectiveness of the value hedges that are calibrated when (I) asymmetry in mortality volatility is ignored (dashed red line) and when (II) asymmetry in mortality volatility is taken into account (solid blue line), for S-forward with times-to-maturity ranging from 1 to 15 years.

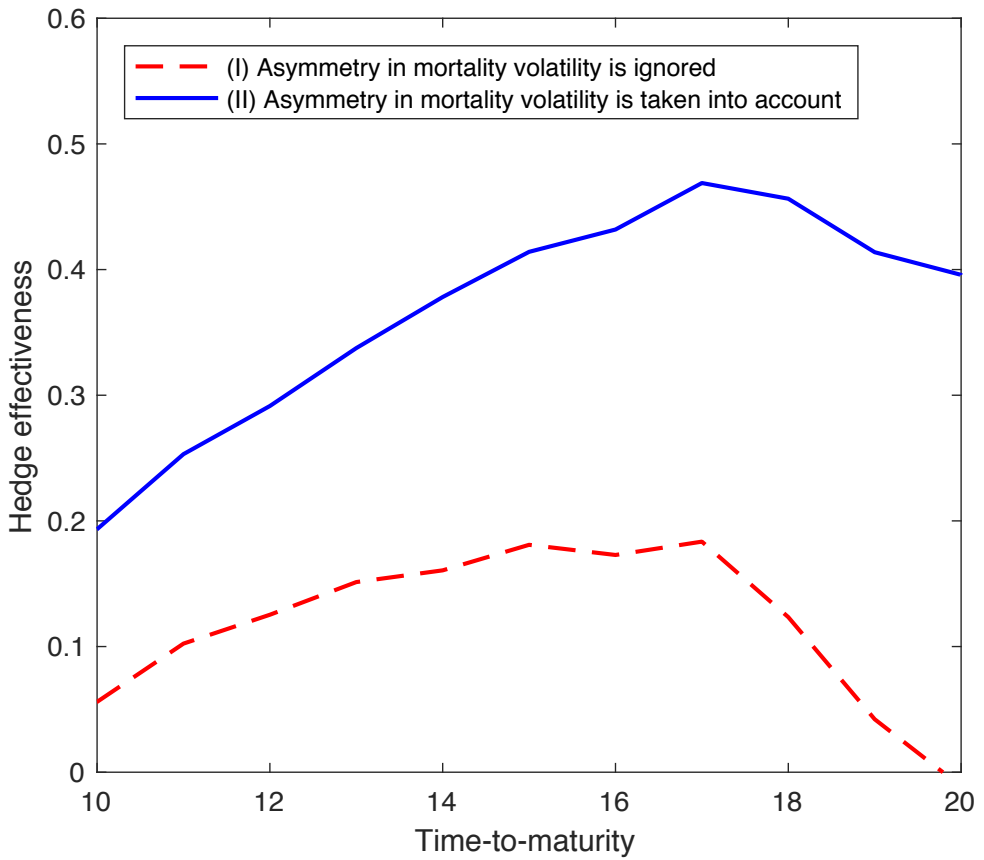


Figure 4.4: Effectiveness of the cash flow hedges that are calibrated when (I) asymmetry in mortality volatility is ignored (dashed red line) and when (II) asymmetry in mortality volatility is taken into account (solid blue line), for S-forward with times-to-maturity ranging from 10 to 20 years.

Chapter 5

Conclusion and Future Research

This thesis focused on (1) obtaining a deeper understanding of mortality modeling with specific attention on the volatility of mortality, and (2) investigating the implementation and implications of index-based longevity hedging via longevity Greeks. On the modeling front, we incorporated conditional heteroskedasticity and asymmetry in the volatility of mortality into the Lee-Carter model by applying various GARCH-type models to its period effect. We also utilized the M7-M5 model, a two-population model that is capable of capturing the period, cohort and population basis effects of mortality. On the hedging front, we pursued the sensitivity-matching approach of index-based longevity hedging, and worked along the lines of longevity Greeks. We studied the properties of longevity Greeks, proposed several Greek hedging strategies for longevity risk, and used real mortality data to demonstrate the implications of the proposed hedging strategies.

In Chapter 2, we first derived three important longevity Greeks—delta, gamma and vega—on the basis of an extended version of the Lee-Carter model that incorporates conditional heteroskedasticity. Semi-analytical expressions for the longevity Greeks of a q-forward and a stylized pension plan are provided. We then studied the properties of the three longevity Greeks for q-forwards. It is found that, for example, while the magnitudes of the longevity delta and gamma reduce with the time-to-maturity, the magnitude of the longevity vega increases and then decreases with the time-to-maturity. Lastly, we constructed static hedges by matching one or two longevity Greeks, and examined how the

performance of the Greek hedges may vary with the reference age and time-to-maturity of the q-forward(s) used. Our findings could help hedgers to decide which longevity Greek to use when a q-forward with a certain specification is available to them.

In Chapter 3, we contributed a discrete-time delta hedging strategy under both static and dynamic settings for use with the M7-M5 model. The proposed hedging strategy takes into account of both cohort effect uncertainty and population basis risk. Several metrics are defined for quantifying the effectiveness of the cash flow and value hedges considered. To overcome the technical problems of the ‘approximation of survival function’ method due to the structure of the M7-M5 model, we systematically divided all possibly encountered survival functions into five cases, and tailored a specific approximation method for each case. We also provided three real data illustrations to supplement our theoretical work, and discovered several interesting facts concerning index-based longevity hedging. For example, we found that if the liability being hedged is subject to cohort effect uncertainty, a delta hedge that matches the sensitivity to changes in cohort effect significantly outperforms one that does not.

In Chapter 4, we first investigated the existence of asymmetry in mortality volatility by using a range of GARCH-type models that permit volatility to respond asymmetrically to positive and negative shocks. Our empirical results suggested that six out of the nine populations considered exhibit asymmetry in mortality volatility. We then studied the impact of asymmetry in mortality volatility on index-based longevity hedging. To this end, we contributed an improved framework for deriving longevity vega, a set of semi-analytical expressions for longevity Greeks under different GARCH-type models, and a new longevity Greek (called dynamic delta) derived on the basis of total derivative. Lastly, we provided two real data illustrations to demonstrate the impact of asymmetry in mortality volatility on index-based longevity hedging. The results of both illustrations pointed to the conclusion that if mortality volatility is in fact asymmetric but the asymmetry is not taken into account when a longevity hedge is calibrated, then the resulting hedge effectiveness could be significantly impaired.

Our analyses on mortality volatility have been focused on the Lee-Carter model, which has only one period effect. It would be interesting to conduct a similar analysis on a wider range of stochastic mortality models, especially on those that have multiple period effects

and/or a cohort effect (e.g., the M7-M5 model). In such a case, a multivariate GARCH model may be needed to fully explain the interdependence in volatility changes between period and/or cohort effects.

Admittedly, there are numerous alternative methods that can incorporate conditional heteroskedasticity in the volatility of mortality. One promising approach is to use a regime-switching model (Hamilton, 1989; Hamilton and Susmel, 1994; Hardy, 2001) to govern the dynamics of mortality volatility. Assuming that there are only two regimes, one may correspond to a temporary period of high volatility in mortality (for example, during wars and pandemics), while the other one may represent the common low volatility periods. Milidonis et al. (2011) have considered applying a log-normal regime-switching model to the U.S. population mortality index, and also to the period effect of the Lee-Carter model fitted to the U.S. population.

We also acknowledge that the longevity Greeks defined in this thesis are model dependent. In other words, the expressions for longevity Greeks will be different if the mortality model assumed is changed. In this thesis, we have derived longevity Greeks under two main categories of stochastic mortality models: the Lee-Carter model (in Chapters 2 and 4) and the M7-M5 model, an extension of the Cairns-Blake-Dowd model (in Chapter 3). In Chapter 2, we have also attempted to address the problem by validating the proposed longevity hedges with a non-parametric simulation approach that does not depend on any model. Although the hedge effectiveness estimated using the model-free approach is not as good as the one estimated using the model from which the longevity Greeks are derived, many of our findings concerning the relationship between hedge effectiveness and q-forward specifications are still observed even when the mortality realizations are generated by a model-free approach.

Another important risk that is often encountered by small pension plans and insurance companies is small sample risk, which we have disregarded in this thesis. Small sample risk has no impact on the calculation of longevity Greeks, and can be easily taken into account by using a death count process (see, e.g., Zhou and Li, 2017). Future research warrants a study that analyses the impact of small sample risk on the effectiveness of various Greek longevity hedges.

References

- Ahmadi, S. S. and Li, J. S.-H. (2014). Coherent mortality forecasting with generalized linear models: A modified time-transformation approach. *Insurance: Mathematics and Economics*, 59:194–221.
- Badescu, A., Elliott, R. J., and Ortega, J.-P. (2014). Quadratic hedging schemes for non-Gaussian GARCH models. *Journal of Economic Dynamics and Control*, 42:13–32.
- Bekaert, G. and Wu, G. (2000). Asymmetric volatility and risk in equity markets. *Review of Financial Studies*, 13(1):1–42.
- Biffis, E. and Blake, D. (2014). Keeping some skin in the game: How to start a capital market in longevity risk transfers. *North American Actuarial Journal*, 18(1):14–21.
- Blake, D., Cairns, A., Coughlan, G., Dowd, K., and Macminn, R. (2013). The new life market. *Journal of Risk and Insurance*, 80(3):501–557.
- Blake, D., Cairns, A. J., and Dowd, K. (2006). Living with mortality: Longevity bonds and other mortality-linked securities. *British Actuarial Journal*, 12(1):153–197.
- Blake, D., El Karoui, N., Loisel, S., and MacMinn, R. (2018). Longevity risk and capital markets: The 201516 update. *Insurance: Mathematics and Economics*, 78:157–173.
- Brouhns, N., Denuit, M., and Van Keilegom, I. (2005). Bootstrapping the Poisson log-bilinear model for mortality forecasting. *Scandinavian Actuarial Journal*, 1238(3):212–224.

- Brouhns, N., Denuit, M., and Vermunt, J. K. (2002). A Poisson log-bilinear regression approach to the construction of projected lifetables. *Insurance: Mathematics and Economics*, 31(3):373–393.
- Cairns, A. J. (2011). Modelling and management of longevity risk: Approximations to survivor functions and dynamic hedging. *Insurance: Mathematics and Economics*, 49(3):438–453.
- Cairns, A. J. (2013). Robust hedging of longevity risk. *Journal of Risk and Insurance*, 80(3):621–648.
- Cairns, A. J., Blake, D., and Dowd, K. (2006). A two-factor model for stochastic mortality with parameter uncertainty: Theory and calibration. *Journal of Risk and Insurance*, 73(4):687–718.
- Cairns, A. J., Blake, D., and Dowd, K. (2008). Modelling and management of mortality risk: A review. *Scandinavian Actuarial Journal*, 2008(2-3):79–113.
- Cairns, A. J., Blake, D., Dowd, K., Coughlan, G. D., Epstein, D., Ong, A., and Balevich, I. (2009). A quantitative comparison of stochastic mortality models using data from England & Wales and the United States. *North American Actuarial Journal*, 13(1):1–35.
- Cairns, A. J., Blake, D., Dowd, K., Coughlan, G. D., and Khalaf-Allah, M. (2011). Bayesian stochastic mortality modelling for two populations. *ASTIN Bulletin*, 41(1):29–59.
- Cairns, A. J., Dowd, K., Blake, D., and Coughlan, G. D. (2014). Longevity hedge effectiveness: A decomposition. *Quantitative Finance*, 14(2):217–235.
- Campbell, J. Y. and Hentschel, L. (1992). No news is good news: An asymmetric model of changing volatility in stock returns. *Journal of Financial Economics*, 31(3):281–318.
- Chai, C. M. H., Siu, T. K., Zhou, X., Hui, M., Chai, C. M. H., Kuen, T., and Xian, S. (2013). A double-exponential GARCH model for stochastic mortality. *European Actuarial Journal*, 3(2):385–406.

- Chen, H., MacMinn, R., and Sun, T. (2015). Multi-population mortality models: A factor copula approach. *Insurance: Mathematics and Economics*, 63:135–146.
- Coughlan, G., Epstein, D., Sinha, A., and Honig, P. (2007). q-Forwards: Derivatives for transferring longevity and mortality risk. Technical report.
- Coughlan, G. D. (2009). Longevity risk transfer: Indices and capital market solutions. *The Handbook of Insurance-Linked Securities*, pages 261–281.
- Coughlan, G. D., Khalaf-Allah, M., Ye, Y., Kumar, S., Cairns, A. J., Blake, D., and Dowd, K. (2011). Longevity hedging 101. *North American Actuarial Journal*, 15(2):150–176.
- Crépey, S. (2004). Delta-hedging vega risk? *Quantitative Finance*, 4(5):559–579.
- Currie, I. D., Durban, M., and Eilers, P. H. (2004). Smoothing and forecasting mortality rates. *Statistical modelling*, 4(4):279–298.
- Czado, C., Delwarde, A., and Denuit, M. (2005). Bayesian Poisson log-bilinear mortality projections. *Insurance: Mathematics and Economics*, 36(3):260–284.
- Dahl, M., Glar, S., and Møller, T. (2011). Mixed dynamic and static risk-minimization with an application to survivor swaps. *European Actuarial Journal*, 1(S2):233–260.
- Dahl, M., Melchior, M., and Møller, T. (2008). On systematic mortality risk and risk-minimization with survivor swaps. *Scandinavian Actuarial Journal*, 2008(2-3):114–146.
- Dahl, M. and Møller, T. (2006). Valuation and hedging of life insurance liabilities with systematic mortality risk. *Insurance: Mathematics and Economics*, 39(2):193–217.
- De Rosa, C., Luciano, E., and Regis, L. (2017). Basis risk in static versus dynamic longevity-risk hedging. *Scandinavian Actuarial Journal*, 2017(4):343–365.
- Duan, J.-C. (2009). The garch option pricing model theory, numerical methods, evidence and applications. *Risk Management Institute and Department of Finance National University of Singapore*.

- Engle, R. F. and Ng, V. K. (1993). Measuring and testing the impact of news on volatility. *The Journal of Finance*, 48(5):1749.
- Engle, R. F. and Rosenberg, J. V. (1995). GARCH gamma. *Journal of Derivatives*, 2(4):47–59.
- Engle, R. F. and Rosenberg, J. V. (2000). Testing the volatility term structure using option hedging criteria. *Journal of Derivatives*, 8(1):10–28.
- Fung, M. C., Peters, G. W., and Shevchenko, P. V. (2017). A unified approach to mortality modelling using state-space framework: characterisation, identification, estimation and forecasting. *Annals of Actuarial Science*, 11(02):343–389.
- Gao, Q. and Hu, C. (2009). Dynamic mortality factor model with conditional heteroskedasticity. *Insurance: Mathematics and Economics*, 45(3):410–423.
- Giacometti, R., Bertocchi, M., Rachev, S. T., and Fabozzi, F. J. (2012). A comparison of the Lee-Carter model and AR-ARCH model for forecasting mortality rates. *Insurance: Mathematics and Economics*, 50(1):85–93.
- Glosten, L. R., Jagannathan, R., and Runkle, D. E. (1993). On the Relation between the Expected Value and the Volatility of the Nominal Excess Return on Stocks. *The Journal of Finance*, 48(5):1779–1801.
- Graziani, G. (2014). Longevity risk - A fine balance. *Institutional Investor Journals: Special Issue on Pension and Longevity Risk Transfer for Institutional Investors*, pages 35–37.
- Haberman, S., Kaishev, V., Millossovich, P., Villegas, A. M., Baxter, S., Gaches, A., Gunnlaugsson, S., and Sison, M. (2014). Longevity basis risk. A methodology for assessing basis risk. Technical report.
- Hamilton, J. D. (1989). A new approach to the economic analysis of nonstationary time series and the business cycle. *Econometrica*, 57(2):357–384.

- Hamilton, J. D. and Susmel, R. (1994). Autoregressive conditional heteroskedasticity and changes in regime. *Journal of Econometrics*, 64(1-2):307–333.
- Hardy, M. R. (2001). A regime-switching model of long-term stock returns. *North American Actuarial Journal*, 5(2):41–53.
- Hatzopoulos, P. and Haberman, S. (2013). Common mortality modeling and coherent forecasts. an empirical analysis of worldwide mortality data. *Insurance: Mathematics and Economics*, 52(2):320–337.
- Jarner, S. F. and Kryger, E. (2011). Modelling adult mortality in small populations: The SAINT model. *ASTIN Bulletin*, (August 2013):377–418.
- Javaheri, A., Wilmott, P., and Haug, E. G. (2004). GARCH and volatility swaps. *Quantitative Finance*, 4(5):589–595.
- Kleinow, T. (2015). A common age effect model for the mortality of multiple populations. *Insurance: Mathematics and Economics*, 63:147–152.
- Koissi, M. C., Shapiro, A. F., and Hognas, G. (2006). Evaluating and extending the Lee-Carter model for mortality forecasting: Bootstrap confidence interval. *Insurance: Mathematics and Economics*, 38(1):1–20.
- Koutmos, G. and Booth, G. (1995). Asymmetric volatility transmission in international stock markets. *Journal of International Money and Finance*, 14(6):747–762.
- Lee, R. and Miller, T. (2001). Evaluating the performance of the Lee-Carter method for forecasting mortality. *Demography*, 38(4):537–549.
- Lee, R. D. and Carter, L. R. (1992). Modeling and forecasting U.S. mortality. *Journal of the American Statistical Association*, 87(419):659–671.
- Lehar, A., Scheicher, M., and Schittenkopf, C. (2002). GARCH vs stochastic volatility: Option pricing and risk management. *Journal of Banking & Finance*, 26:323–345.
- Li, J. (2014). A quantitative comparison of simulation strategies for mortality projection. *Annals of Actuarial Science*, 8(02):281–297.

- Li, J. S.-H. and Hardy, M. R. (2011). Measuring Basis Risk in Longevity Hedges. *North American Actuarial Journal*, 15(2):177–200.
- Li, J. S.-H., Hardy, M. R., and Tan, K. S. (2009). Uncertainty in Mortality Forecasting: An Extension to the Classical Lee-Carter Approach. *ASTIN Bulletin*, 39(01):137–164.
- Li, J. S.-H. and Luo, A. (2012). Key Q-duration: A framework for hedging longevity risk. *ASTIN Bulletin*, 42(2):413–452.
- Li, J. S.-H. and Ng, A. C.-Y. (2011). Canonical valuation of mortality-linked securities. *Journal of Risk and Insurance*, 78(4):853–884.
- Li, J. S.-H., Zhou, R., and Hardy, M. (2015). A step-by-step guide to building two-population stochastic mortality models. *Insurance: Mathematics and Economics*, 63:121–134.
- Li, N. and Lee, R. (2005). Coherent mortality forecasts for a group of populations: An extension of the Lee-Carter method. *Demography*, 42(3):575–594.
- Lin, T. and Tsai, C. C.-L. (2013). On the mortality/longevity risk hedging with mortality immunization. *Insurance: Mathematics and Economics*, 53(3):580–596.
- Lin, T. and Tsai, C. C.-L. (2014). Applications of mortality durations and convexities in natural hedges. *North American Actuarial Journal*, 18(3):417–442.
- Lin, T., Wang, C. W., and Tsai, C. C.-L. (2015). Age-specific copula-AR-GARCH mortality models. *Insurance: Mathematics and Economics*, 61:110–124.
- Liu, X. and Braun, W. J. (2010). Investigating Mortality Uncertainty Using the Block Bootstrap. *Journal of Probability and Statistics*, 2010:1–15.
- Liu, Y. and Li, J. S.-H. (2016). It's all in the hidden states: A longevity hedging strategy with an explicit measure of population basis risk. *Insurance: Mathematics and Economics*, 70:301–319.
- Liu, Y. and Li, J. S.-H. (2017). The locally linear Cairns-Blake-Dowd model: A note on delta-nuga hedging of longevity risk. *ASTIN Bulletin*, 47(1):79–151.

- Luciano, E. and Regis, L. (2014). Efficient versus inefficient hedging strategies in the presence of financial and longevity (value at) risk. *Insurance: Mathematics and Economics*, 55(1):68–77.
- Luciano, E., Regis, L., and Vigna, E. (2012). Delta-gamma hedging of mortality and interest rate risk. *Insurance: Mathematics and Economics*, 50(3):402–412.
- Luciano, E., Regis, L., and Vigna, E. (2017). Single- and Cross-Generation Natural Hedging of Longevity and Financial Risk. *Journal of Risk and Insurance*, 84(3):961–986.
- McDonald, R. L. (2012). *Derivatives Markets*. Pearson Boston.
- Michaelson, A. and Mulholland, J. (2014). Strategy for increasing the global capacity for longevity risk transfer: Developing transactions that attract capital markets investors. *The Journal of Alternative Investments*, pages 18–28.
- Milidonis, A., Lin, Y., and Cox, S. H. (2011). Mortality regimes and pricing. *North American Actuarial Journal*, 15(2):266–289.
- Nelson, D. B. (1991). Conditional Heteroskedasticity in Asset Returns: A New Approach. *Econometrica*, 59(2):347.
- Ngai, A. and Sherris, M. (2011). Longevity risk management for life and variable annuities: The effectiveness of static hedging using longevity bonds and derivatives. *Insurance: Mathematics and Economics*, 49(1):100–114.
- Pedroza, C. (2006). A Bayesian forecasting model: Predicting U.S. male mortality. *Biostatistics*, 7(4):530–550.
- Plat, R. (2011). One-year Value-at-Risk for longevity and mortality. *Insurance: Mathematics and Economics*, 49(3):462–470.
- Renshaw, A. E. and Haberman, S. (2006). A cohort-based extension to the Lee-Carter model for mortality reduction factors. *Insurance: Mathematics and Economics*, 38(3):556–570.

- Renshaw, A. E. and Haberman, S. (2008). On simulation-based approaches to risk measurement in mortality with specific reference to Poisson Lee-Carter modelling. *Insurance: Mathematics and Economics*, 42(2):797–816.
- Ribeiro, R. and Di Pietro, V. (2009). Longevity risk and portfolio allocation. *Investment Strategies*, 57.
- Statistics Canada (2018). Life tables, Canada, provinces and territories 1980/1982 to 2014/2016. Catalogue no. 84-537.
- Tsai, C. C.-L. and Chung, S. L. (2013). Actuarial applications of the linear hazard transform in mortality immunization. *Insurance: Mathematics and Economics*, 53(1):48–63.
- Tsai, C. C.-L. and Jiang, L. (2011). Actuarial applications of the linear hazard transform in life contingencies. *Insurance: Mathematics and Economics*, 1(49):7–80.
- Tsai, C. C.-L. and Yang, S. (2015). A linear regression approach to modeling mortality rates of different forms. *North American Actuarial Journal*, 19(1):1–23.
- Tsai, J. T., Wang, J. L., and Tzeng, L. Y. (2010). On the optimal product mix in life insurance companies using conditional value at risk. *Insurance: Mathematics and Economics*, 46(1):235–241.
- Tsay, R. S. (2005). *Analysis of financial time series*. John Wiley & Sons.
- Villegas, A. M. and Haberman, S. (2014). On the modeling and forecasting of socioeconomic mortality differentials: An application to deprivation and mortality in england. *North American Actuarial Journal*, 18(1):168–193.
- Villegas, A. M., Haberman, S., Kaishev, V. K., and Millossovich, P. (2017). A comparative study of two-population models for the assessment of basis risk in longevity hedges. *ASTIN Bulletin*, 47(3):631–679.
- Villegas, A. M., Millossovich, P., and Kaishev, V. (2016). StMoMo: An R package for stochastic mortality modelling.

- Wang, J. L., Huang, H., Yang, S. S., and Tsai, J. T. (2010). An optimal product mix for hedging longevity risk in life insurance companies: The immunization theory approach. *Journal of Risk and Insurance*, 77(2):473–497.
- Wang, Z. and Li, J. S.-H. (2016). A DCC-GARCH multi-population mortality model and its applications to pricing catastrophic mortality bonds. *Finance Research Letters*, 16:103–111.
- Wong, T. W., Chiu, M. C., and Wong, H. Y. (2014). Time-consistent mean-variance hedging of longevity risk: Effect of cointegration. *Insurance: Mathematics and Economics*, 56(1):56–67.
- Yang, B., Li, J., and Balasooriya, U. (2015). Using bootstrapping to incorporate model error for risk-neutral pricing of longevity risk. *Insurance: Mathematics and Economics*, 62:16–27.
- Yang, S. S., Yue, J. C., and Huang, H.-C. (2010). Modeling longevity risks using a principal component approach: A comparison with existing stochastic mortality models. *Insurance: Mathematics and Economics*, 46(1):254–270.
- Zakoian, J.-M. (1994). Threshold heteroskedastic models. *Journal of Economic Dynamics and Control*, 18(5):931–955.
- Zhou, K. Q. and Li, J. S.-H. (2017). Dynamic longevity hedging in the presence of population basis risk: A feasibility analysis from technical and economic perspectives. *The Journal of Risk and Insurance*, 84(S1):417–437.
- Zhou, R., Wang, Y., Kaufhold, K., Li, J. S.-H., and Tan, K. S. (2014). Modeling period effects in multi-population mortality models: Applications to Solvency II. *North American Actuarial Journal*, 18(1):150–167.

APPENDICES

Appendix A

Derivation of the Longevity Greeks

This appendix presents the derivations of the three longevity Greeks for $p_{x,t}(T, \kappa_0, \sigma_0^2)$. In all derivations, it is assumed that the expectation and differential operator are interchangeable.

- The longevity delta for $p_{x,t}(T, \kappa_0, \sigma_0^2)$:

$$\begin{aligned}
\Delta_{x,t}(T) &= \frac{\partial p_{x,t}(T, \kappa_0, \sigma_0^2)}{\partial \kappa_0} \\
&= \frac{\partial}{\partial \kappa_0} \mathbb{E}[e^{-W_{x,t}(T)} \mid \mathcal{F}_0] \\
&= \mathbb{E}\left[e^{-W_{x,t}(T)} \left(-\frac{\partial}{\partial \kappa_0} W_{x,t}(T)\right) \mid \mathcal{F}_0\right] \\
&= \mathbb{E}\left[e^{-W_{x,t}(T)} \left(-\sum_{s=1}^T e^{Y_{x,t}(s)} \left(\frac{\partial}{\partial \kappa_0} Y_{x,t}(s)\right)\right) \mid \mathcal{F}_0\right] \\
&= -\sum_{s=1}^T b_{x+s-1} \mathbb{E}[e^{Y_{x,t}(s)-W_{x,t}(T)} \mid \mathcal{F}_0].
\end{aligned}$$

- The longevity gamma for $p_{x,t}(T, \kappa_0, \sigma_0^2)$:

$$\begin{aligned}
\Gamma_{x,t}(T) &= \frac{\partial^2 p_{x,t}(T, \kappa_0, \sigma_0^2)}{\partial \kappa_0^2} \\
&= \frac{\partial}{\partial \kappa_0} \left(\frac{\partial p_{x,t}(T, \kappa_0, \sigma_0^2)}{\partial \kappa_0} \right) \\
&= \frac{\partial}{\partial \kappa_0} \left(\mathbb{E} \left[- \sum_{s=1}^T b_{x+s-1} e^{Y_{x,t}(s) - W_{x,t}(T)} \mid \mathcal{F}_0 \right] \right) \\
&= \mathbb{E} \left[- \sum_{s=1}^T b_{x+s-1} e^{Y_{x,t}(s) - W_{x,t}(T)} \frac{\partial}{\partial \kappa_0} (Y_{x,t}(s) - W_{x,t}(T)) \mid \mathcal{F}_0 \right] \\
&= \mathbb{E} \left[- \sum_{s=1}^T b_{x+s-1} e^{Y_{x,t}(s) - W_{x,t}(T)} \left(b_{x+s-1} - \sum_{u=1}^T b_{x+u-1} e^{Y_{x,t}(u)} \right) \mid \mathcal{F}_0 \right] \\
&= \mathbb{E} \left[e^{-W_{x,t}(T)} \left(\left(\sum_{s=1}^T b_{x+s-1} e^{Y_{x,t}(s)} \right)^2 - \sum_{s=1}^T b_{x+s-1}^2 e^{2Y_{x,t}(s)} \right) \mid \mathcal{F}_0 \right].
\end{aligned}$$

- The longevity vega for $p_{x,t}(T, \kappa_0, \sigma_0^2)$:

$$\begin{aligned}
V_{x,t}(T) &= \frac{\partial p_{x,t}(T, \kappa_0, \sigma_0^2)}{\partial \sigma_0^2} \\
&= \mathbb{E} \left[e^{-W_{x,t}(T)} \left(- \sum_{s=1}^T e^{Y_{x,t}(s)} \left(\frac{\partial}{\partial \sigma_0^2} Y_{x,t}(s) \right) \right) \mid \mathcal{F}_0 \right] \\
&= \mathbb{E} \left[e^{-W_{x,t}(T)} \left(- \sum_{s=1}^T e^{Y_{x,t}(s)} \left(b_{x+s-1} \frac{\partial \kappa_{t+s}}{\partial \sigma_0^2} \right) \right) \mid \mathcal{F}_0 \right] \\
&= - \sum_{s=1}^T b_{x+s-1} \mathbb{E} \left[e^{Y_{x,t}(s) - W_{x,t}(T)} \left(\frac{\partial \kappa_{t+s}}{\partial \sigma_0^2} \right) \mid \mathcal{F}_0 \right],
\end{aligned}$$

where

$$\frac{\partial \kappa_{t+s}}{\partial \sigma_0^2} = \sum_{u=1}^{t+s} \frac{\eta_u}{2\sigma_u} \frac{\partial \sigma_u^2}{\partial \sigma_0^2}$$

and

$$\frac{\partial \sigma_u^2}{\partial \sigma_0^2} = \begin{cases} \beta \prod_{v=1}^{u-1} (\alpha \eta_{u-v}^2 + \beta) & \text{if } u \geq 2 \\ \beta & \text{if } u = 1 \end{cases}.$$

Appendix B

Proof of Theorem 1

For convenience, we let $E_t[\cdot] := E_t[\cdot | \mathcal{F}_t]$. Because $\eta_t \stackrel{i.i.d.}{\sim} N(0, 1)$, we have $E_{t-1}[\eta_t] = 0$, $E_{t-1}[\eta_t^2] = 1$, $E_{t-1}[\eta_t^3] = 0$, and $E_{t-1}[\eta_t^4] = 3$ for $t \geq 1$. These results are used in this and the following two appendices.

Proof of Theorem 1. For $t^f = 1$,

$$E_0[(\sigma_1 \eta_1)^2] = \omega + \alpha \epsilon_0 + \beta \sigma_0^2 = z_{1,0} + z_{1,1} \sigma_0^2,$$

where $z_{1,0} = \omega + \alpha \epsilon_0$ and $z_{1,1} = \beta$ do not depend on σ_0^2 . Thus, equation (2.13) holds for $t^f = 1$. Let $t > 1$ be given and suppose that equation (2.13) holds for $t^f = t - 1$. Then,

for $t^f = t$,

$$\begin{aligned}
E_0 \left[\left(\sum_{s=1}^t \sigma_s \eta_s \right)^2 \right] &= E_0 \left[\left(\sum_{s=1}^{t-1} \sigma_s \eta_s + \sigma_t \eta_t \right)^2 \right] \\
&= E_0 \left[\left(\sum_{s=1}^{t-1} \sigma_s \eta_s \right)^2 \right] + E_0 [\sigma_t^2] \\
&= z_{t-1,0} + z_{t-1,1} \sigma_0^2 + \left(\frac{\omega - \omega(\alpha + \beta)^t}{1 - \alpha - \beta} \right) + (\alpha + \beta)^{t-1} (\alpha \epsilon_0^2 + \beta \sigma_0^2) \\
&= z_{t-1,0} + \left(\frac{\omega - \omega(\alpha + \beta)^t}{1 - \alpha - \beta} + \alpha(\alpha + \beta)^{t-1} \epsilon_0^2 \right) \\
&\quad + (z_{t-1,1} + \beta(\alpha + \beta)^{t-1}) \sigma_0^2 \\
&= z_{t,0} + z_{t,1} \sigma_0^2,
\end{aligned}$$

where $z_{t,0}$ and $z_{t,1}$ do not depend on σ_0^2 . Hence, equation (2.13) also holds for $t^f = t$. By the principle of induction, equation (2.13) holds for $t^f \geq 1$. \square

Appendix C

Proof of Theorem 2

To prove Theorem 2, we need the following lemma.

Lemma 4. For $t^f \geq 2$,

$$E_0 \left[\left(\sum_{s=1}^{t^f-1} \sigma_s \eta_s \right) \sigma_{t^f}^2 \right] = 0. \quad (\text{C.1})$$

Proof of Lemma 4. For $t^f = 2$,

$$E_0 [\sigma_1 \eta_1 \sigma_2^2] = \sigma_1 E_0 [\eta_1] \sigma_2^2 = 0.$$

Thus, equation (C.1) holds for $t^f = 2$. Let $t > 2$ be given and suppose equation (C.1) holds for $t^f = t - 1$. Then, for $t^f = t$,

$$\begin{aligned} E_0 \left[\left(\sum_{s=1}^{t-1} \sigma_s \eta_s \right) h_t \right] &= E_0 \left[\left(\sum_{s=1}^{t-2} \sigma_s \eta_s + \sigma_{t-1} \eta_{t-1} \right) (\omega + (\alpha \eta_{t-1}^2 + \beta) \sigma_{t-1}^2) \right] \\ &= E_0 \left[\left(\sum_{s=1}^{t-2} \sigma_s \eta_s \right) \sigma_{t-1}^2 \right] (\alpha + \beta) \\ &= 0. \end{aligned}$$

So, equation (C.1) also holds for $t^f = t$. By the principle of induction, equation (C.1) holds for $t^f \geq 2$. \square

Proof of Theorem 2. For $t^f = 1$,

$$E_0 [(\sigma_1 \eta_1)^3] = \sigma_1^3 E_0 [\eta_1^3] = 0.$$

Thus, equation (2.14) holds for $t^f = 1$. Let $t > 1$ be given and suppose equation (2.14) holds for $t^f = t - 1$. Then, for $t^f = t$,

$$\begin{aligned} E_0 \left[\left(\sum_{s=1}^t \sigma_s \eta_s \right)^3 \right] &= E_0 \left[\left(\sum_{s=1}^{t-1} \sigma_s \eta_s + \sigma_t \eta_t \right)^3 \right] \\ &= E_0 \left[\left(\sum_{s=1}^{t-1} \sigma_s \eta_s \right)^3 \right] + 3E_0 \left[\left(\sum_{s=1}^{t-1} \sigma_s \eta_s \right) \sigma_t^2 \right] \\ &= 0, \end{aligned}$$

since $E_0 \left[\left(\sum_{s=1}^{t-1} \sigma_s \eta_s \right) \sigma_t^2 \right] = 0$ by Lemma 4. Hence, equation (2.14) also holds for $t^f = t$. By the principle of induction, equation (2.14) holds for $t^f \geq 1$. \square

Appendix D

Proof of Theorem 3

To prove Theorem 3, we need the following two lemmas.

Lemma 5. *For $t^f \geq 1$,*

$$E_0 [\sigma_{tf}^4] = \phi_{tf,0} + \phi_{tf,1}\sigma_0^2 + \phi_{tf,2}\sigma_0^4, \quad (\text{D.1})$$

where $\phi_{tf,0}$, $\phi_{tf,1}$ and $\phi_{tf,2}$ do not depend on σ_0^2 .

Proof of Lemma 5. For $t^f = 1$,

$$E_0 [\sigma_1^4] = (\omega + \alpha\epsilon_0^2)^2 + 2\beta(\omega + \alpha\epsilon_0^2)\sigma_0^2 + \beta^2\sigma_0^4 = \phi_{1,0} + \phi_{1,1}\sigma_0^2 + \phi_{1,2}\sigma_0^4,$$

where $\phi_{1,0} = (\omega + \alpha\epsilon_0^2)^2$, $\phi_{1,1} = 2\beta(\omega + \alpha\epsilon_0^2)$ and $\phi_{1,2} = \beta^2$ do not depend on σ_0^2 . Hence, equation (D.1) holds for $t^f = 1$. Let $t > 1$ be given and suppose equation (D.1) holds for

$t^f = t - 1$. Then, for $t^f = t$,

$$\begin{aligned}
& \mathbb{E}_0 [\sigma_t^4] \\
&= \mathbb{E}_0 [(\omega + (\alpha\eta_{t-1}^2 + \beta)\sigma_{t-1}^2)^2] \\
&= \mathbb{E}_0 [\omega^2 + 2\omega(\alpha + \beta)\sigma_{t-1}^2 + (3\alpha^2 + 2\alpha\beta + \beta^2)\sigma_{t-1}^4] \\
&= \omega^2 + \pi_1 \left(\frac{\omega - \omega(\alpha + \beta)^{t-1}}{1 - \alpha - \beta} + (\alpha + \beta)^{t-2}(\alpha\epsilon_0^2 + \beta\sigma_0^2) \right) + \pi_2 (\phi_{t-1,0} + \phi_{t-1,1}\sigma_0^2 + \phi_{t-1,2}\sigma_0^4) \\
&= \pi_2\phi_{t-1,0} + \omega^2 + \frac{\pi_1\omega(1 - (\alpha + \beta)^{t-1})}{1 - \alpha - \beta} + \pi_1\alpha(\alpha + \beta)^{t-2}\epsilon_0^2 \\
&\quad + (\pi_2\phi_{t-1,1} + \pi_1\beta(\alpha + \beta)^{t-2})\sigma_0^2 + \pi_2\phi_{t-1,2}\sigma_0^4 \\
&= \phi_{t,0} + \phi_{t,1}\sigma_0^2 + \phi_{t,2}\sigma_0^4,
\end{aligned}$$

where $\phi_{t,0}$, $\phi_{t,1}$ and $\phi_{t,2}$ do not depend on σ_0^2 , and $\pi_1 = 2\omega(\alpha + \beta)$ and $\pi_2 = 3\alpha^2 + 2\alpha\beta + \beta^2$. Thus, equation (D.1) also holds for $t^f = t$. By the principle of induction, equation (D.1) holds for $t^f \geq 1$.

□

Lemma 6. For $t^f \geq 2$,

$$\mathbb{E}_0 \left[\left(\sum_{s=1}^{t^f-1} \sigma_s \eta_s \right)^2 \sigma_{t^f}^2 \right] = \psi_{t^f,0} + \psi_{t^f,1}\sigma_0^2 + \psi_{t^f,2}\sigma_0^4, \quad (\text{D.2})$$

where $\psi_{t^f,0}$, $\psi_{t^f,1}$ and $\psi_{t^f,2}$ do not depend on σ_0^2 .

Proof of Lemma 6. For $t^f = 2$,

$$\begin{aligned}
\mathbb{E}_0 [(\sigma_1\eta_1)^2 \sigma_2^2] &= \omega\sigma_1^2 + (3\alpha + \beta)\sigma_1^4 \\
&= (\omega^2 + \omega\alpha\epsilon_0^2 + (3\alpha + \beta)(\omega + \alpha\epsilon_0^2)^2) + (\beta\omega + 2\beta(3\alpha + \beta)(\omega + \alpha\epsilon_0^2))\sigma_0^2 \\
&\quad + \beta^2(3\alpha + \beta)\sigma_0^4 \\
&= \psi_{2,0} + \psi_{2,1}\sigma_0^2 + \psi_{2,2}\sigma_0^4,
\end{aligned}$$

where $\psi_{2,0} = \omega^2 + \omega\alpha\epsilon_0^2 + (3\alpha + \beta)(\omega + \alpha\epsilon_0^2)^2$, $\psi_{2,1} = \beta\omega + 2\beta(3\alpha + \beta)(\omega + \alpha\epsilon_0^2)$ and $\psi_{2,2} = \beta^2(3\alpha + \beta)$ do not depend on σ_0^2 . Thus, equation (D.2) holds for $t^f = 2$. Let $t > 2$

be given and suppose equation (D.2) holds for $t^f = t - 1$. Then, for $t^f = t$,

$$\begin{aligned}
& \mathbb{E}_0 \left[\left(\sum_{s=1}^{t-1} \sigma_s \eta_s \right)^2 \sigma_t^2 \right] \\
&= \mathbb{E}_0 \left[\left(\sum_{s=1}^{t-2} \sigma_s \eta_s + \sigma_{t-1} \eta_{t-1} \right)^2 (\omega + (\alpha \eta_{t-1}^2 + \beta) \sigma_{t-1}^2) \right] \\
&= (\alpha + \beta) \mathbb{E}_0 \left[\left(\sum_{s=1}^{t-2} \sigma_s \eta_s \right)^2 \sigma_{t-1}^2 \right] + \omega \mathbb{E}_0 \left[\left(\sum_{s=1}^{t-1} \sigma_s \eta_s \right)^2 \right] + (3\alpha + \beta) \mathbb{E}_0 [\sigma_{t-1}^4] \\
&= ((\alpha + \beta) \psi_{t-1,0} + (3\alpha + \beta) \phi_{t-1,0} + \omega z_{t-1,0}) \\
&\quad + ((\alpha + \beta) \psi_{t-1,1} + (3\alpha + \beta) \phi_{t-1,1} + \omega z_{t-1,1}) \sigma_0^2 + ((\alpha + \beta) \psi_{t-1,2} + (3\alpha + \beta) \phi_{t-1,2}) \sigma_0^4 \\
&= \psi_{t,0} + \psi_{t,1} \sigma_0^2 + \psi_{t,2} \sigma_0^4,
\end{aligned}$$

where $\psi_{t,0}$, $\psi_{t,1}$ and $\psi_{t,2}$ do not depend on σ_0^2 . Hence, equation (D.2) also holds for $t^f = t$. By the principle of induction, equation (D.2) holds for $t^f \geq 2$. \square

Proof of Theorem 3. For $t^f = 1$,

$$\begin{aligned}
\mathbb{E}_0 [(\sigma_1 \eta_1)^4] &= 3(\omega + \alpha \epsilon_0^2)^2 + 6\beta(\omega + \alpha \epsilon_0^2) \sigma_0^2 + 3\beta^2 \sigma_0^4 \\
&= c_{1,0} + c_{1,1} \sigma_0^2 + c_{1,2} \sigma_0^4,
\end{aligned}$$

where $c_{1,0} = 3(\omega + \alpha \epsilon_0^2)^2$, $c_{1,1} = 6\beta(\omega + \alpha \epsilon_0^2)$ and $c_{1,2} = 3\beta^2$ do not depend on σ_0^2 . Thus, equation (2.15) holds for $t^f = 1$. Let $t > 1$ be given and suppose equation (2.15) holds for $t^f = t - 1$. Then, for $t^f = t$,

$$\begin{aligned}
\mathbb{E}_0 \left[\left(\sum_{s=1}^t \sigma_s \eta_s \right)^4 \right] &= \mathbb{E}_0 \left[\left(\sum_{s=1}^{t-1} \sigma_s \eta_s + \sigma_t \eta_t \right)^4 \right] \\
&= \mathbb{E}_0 \left[\left(\sum_{s=1}^{t-1} \sigma_s \eta_s \right)^4 \right] + 6\mathbb{E}_0 \left[\left(\sum_{s=1}^{t-1} \sigma_s \eta_s \right)^2 \sigma_t^2 \right] + 3\mathbb{E}_0 [\sigma_t^4] \\
&= (c_{t-1,0} + 6\psi_{t,0} + 3\phi_{t,0}) + (c_{t-1,1} + 6\psi_{t,1} + 3\phi_{t,1}) \sigma_0^2 \\
&\quad + (c_{t-1,2} + 6\psi_{t,2} + 3\phi_{t,2}) \sigma_0^4 \\
&= c_{t,0} + c_{t,1} \sigma_0^2 + c_{t,2} \sigma_0^4,
\end{aligned}$$

where $c_{t,0}$, $c_{t,1}$ and $c_{t,2}$ do not depend on σ_0^2 . Therefore, equation (2.15) also holds for $t^f = t$. By the principle of induction, equation (2.15) holds for $t^f \geq 1$. Furthermore, $z_{t^f,1}$ in equation (2.13), $\phi_{t^f,1}$ and $\phi_{t^f,2}$ in equation (D.1), and $\psi_{t^f,1}$ and $\psi_{t^f,2}$ in equation (D.2) can be solved as follows:

$$\begin{aligned} z_{t^f,1} &= \frac{\beta - \beta(\alpha + \beta)^{t^f}}{1 - \alpha - \beta}, \\ \phi_{t^f,1} &= \left(\frac{\beta\pi_1}{\alpha + \beta - \pi_2} \right) (\alpha + \beta)^{t^f-1} + \left(2\beta(\omega + \alpha\epsilon_0^2) - \frac{\beta\pi_1}{\alpha + \beta - \pi_2} \right) \pi_2^{t^f-1} \\ &= \pi_3(\alpha + \beta)^{t^f-1} + \pi_4\pi_2^{t^f-1}, \\ \phi_{t^f,2} &= \beta^2\pi_2^{t^f-1}, \\ \psi_{t^f,1} &= \frac{\pi_4(3\alpha + \beta)}{\alpha + \beta - \pi_2} \left((\alpha + \beta)^{t^f-1} - \pi_2^{t^f-1} \right) + \frac{\beta\omega}{(1 - \alpha - \beta)^2} \left(1 - (\alpha + \beta)^{t^f-1} \right) \\ &\quad + \left(\frac{2\beta\omega(3\alpha + \beta)}{\alpha + \beta - \pi_2} - \frac{\beta\omega}{1 - \alpha - \beta} \right) (\alpha + \beta)^{t^f-1}(t^f - 1), \\ \psi_{t^f,2} &= \frac{\beta^2(3\alpha + \beta)}{\alpha + \beta - \pi_2} \left((\alpha + \beta)^{t^f-1} - \pi_2^{t^f-1} \right), \end{aligned}$$

where $\pi_3 = \frac{\beta\pi_1}{\alpha + \beta - \pi_2}$ and $\pi_4 = 2\beta(\omega + \alpha\epsilon_0^2) - \pi_3$. Substituting the expressions above into $c_{t^f,1}$ and $c_{t^f,2}$, we obtain

$$\begin{aligned} c_{t^f,1} &= 6\beta(\omega + \alpha\epsilon_0^2) + \left(\frac{6\pi_4(3\alpha + \beta)}{\alpha + \beta - \pi_2} - \frac{6\beta\omega}{(1 - \alpha - \beta)^2} + 3\pi_3 \right) \left(\frac{\alpha + \beta - (\alpha + \beta)^{t^f}}{1 - \alpha - \beta} \right) \\ &\quad + 6 \left(\frac{2\beta\omega(3\alpha + \beta)}{\alpha + \beta - \pi_2} - \frac{\beta\omega}{1 - \alpha - \beta} \right) \left(\frac{(\alpha + \beta) - t^f(\alpha + \beta)^{t^f} + (t^f - 1)(\alpha + \beta)^{t^f+1}}{(1 - \alpha - \beta)^2} \right) \\ &\quad + \left(3\pi_4 - \frac{6\pi_4(3\alpha + \beta)}{\alpha + \beta - \pi_2} \right) \left(\frac{\pi_2 - \pi_2^{t^f}}{1 - \pi_2} \right) + \frac{6\beta\omega}{(1 - \alpha - \beta)^2}(t^f - 1), \\ c_{t^f,2} &= 3\beta^2 + \left(\frac{6\beta^2(3\alpha + \beta)}{\alpha + \beta - \pi_2} \right) \left(\frac{\alpha + \beta - (\alpha + \beta)^{t^f}}{1 - \alpha - \beta} \right) \\ &\quad + \left(3\beta^2 - \frac{6\beta^2(3\alpha + \beta)}{\alpha + \beta - \pi_2} \right) \left(\frac{\pi_2 - \pi_2^{t^f}}{1 - \pi_2} \right). \end{aligned}$$

It is clear that $c_{t^f,1}$ tends to ∞ as $t^f \rightarrow \infty$, and if $\pi_2 = 3\alpha^2 + 2\alpha\beta + \beta^2 < 1$ then $c_{t^f,2}$ tends a constant as $t^f \rightarrow \infty$. \square

Appendix E

Deriving the Approximation Formula for Case B

Here we derive the approximation formula for $E[S_{x,u}^{(i)}(T) | \boldsymbol{\kappa}_u^{(i)}, \gamma_{u-x_a \wedge u-x+1}^{(R)}]$ when $t < u$. Let Z be a standard normal random variable that is independent of the period and cohort effects. Using the approximation formula derived in Section 3.4.2, we get

$$\begin{aligned}
& E[S_{x,u}^{(i)}(T) | \boldsymbol{\kappa}_u^{(i)}, \gamma_{u-x_a \wedge u-x+1}] \\
& \approx \Phi(d_{x,u,0}^{(i)}(T) + \mathbf{d}_{x,u}^{(i)}(T)'(\boldsymbol{\kappa}_u^{(i)} - \hat{\boldsymbol{\kappa}}_u^{(i)}) + d_{x,u,\gamma}^{(i)}(T)(\gamma_{u-x_a \wedge u-x+1} - \hat{\gamma}_{u-x_a \wedge u-x+1})) \\
& = \Pr(Z \leq d_{x,u,0}^{(i)}(T) + \mathbf{d}_{x,u}^{(i)}(T)'(\boldsymbol{\kappa}_u^{(i)} - \hat{\boldsymbol{\kappa}}_u^{(i)}) \\
& \quad + d_{x,u,\gamma}^{(i)}(T)(\gamma_{u-x_a \wedge u-x+1} - \hat{\gamma}_{u-x_a \wedge u-x+1}) | \boldsymbol{\kappa}_u^{(i)}, \gamma_{u-x_a \wedge u-x+1}) \\
& = E[I_{Z \leq d_{x,u,0}^{(i)}(T) + \mathbf{d}_{x,u}^{(i)}(T)'(\boldsymbol{\kappa}_u^{(i)} - \hat{\boldsymbol{\kappa}}_u^{(i)}) + d_{x,u,\gamma}^{(i)}(T)(\gamma_{u-x_a \wedge u-x+1} - \hat{\gamma}_{u-x_a \wedge u-x+1})} | \boldsymbol{\kappa}_u^{(i)}, \gamma_{u-x_a \wedge u-x+1}] \\
& = E[I_{Z \leq d_{x,u,0}^{(i)}(T) + \mathbf{d}_{x,u}^{(i)}(T)'(\boldsymbol{\kappa}_u^{(i)} - \hat{\boldsymbol{\kappa}}_u^{(i)}) + d_{x,u,\gamma}^{(i)}(T)(\gamma_{u-x_a \wedge u-x+1} - \hat{\gamma}_{u-x_a \wedge u-x+1})} | \mathcal{F}_u],
\end{aligned}$$

where I_A is an indicator function which equals to one if event A holds and 0 otherwise. The last step in the above follows from the Markov property of the assumed processes for

the period and cohort effects. Using this result, we obtain

$$\begin{aligned}
& \mathbb{E}[S_{x,u}^{(i)}(T) | \boldsymbol{\kappa}_t^{(i)}, \gamma_{t-x_a \wedge u-x+1}] \\
&= \mathbb{E}[\mathbb{E}[S_{x,u}^{(i)}(T) | \boldsymbol{\kappa}_u^{(i)}, \gamma_{u-x_a \wedge u-x+1}] | \mathcal{F}_t] \\
&\approx \mathbb{E}\left[\mathbb{E}\left[I_{Z \leq d_{x,u,0}^{(i)}(T) + \mathbf{d}_{x,u}^{(i)}(T)'(\boldsymbol{\kappa}_u^{(i)} - \hat{\boldsymbol{\kappa}}_u^{(i)}) + d_{x,u,\gamma}^{(i)}(T)(\gamma_{u-x_a \wedge u-x+1} - \hat{\gamma}_{u-x_a \wedge u-x+1})} \mid \mathcal{F}_u\right] \mid \mathcal{F}_t\right] \\
&= \mathbb{E}\left[I_{Z \leq d_{x,u,0}^{(i)}(T) + \mathbf{d}_{x,u}^{(i)}(T)'(\boldsymbol{\kappa}_u^{(i)} - \hat{\boldsymbol{\kappa}}_u^{(i)}) + d_{x,u,\gamma}^{(i)}(T)(\gamma_{u-x_a \wedge u-x+1} - \hat{\gamma}_{u-x_a \wedge u-x+1})} \mid \mathcal{F}_t\right] \\
&= \Pr(Z \leq d_{x,u,0}^{(i)}(T) + \mathbf{d}_{x,u}^{(i)}(T)'(\boldsymbol{\kappa}_u^{(i)} - \hat{\boldsymbol{\kappa}}_u^{(i)}) + d_{x,u,\gamma}^{(i)}(T)(\gamma_{u-x_a \wedge u-x+1} - \hat{\gamma}_{u-x_a \wedge u-x+1}) | \mathcal{F}_t) \\
&= \Pr(Z - d_{x,u,0}^{(i)}(T) - \mathbf{d}_{x,u}^{(i)}(T)'(\boldsymbol{\kappa}_u^{(i)} - \hat{\boldsymbol{\kappa}}_u^{(i)}) - d_{x,u,\gamma}^{(i)}(T)(\gamma_{u-x_a \wedge u-x+1} - \hat{\gamma}_{u-x_a \wedge u-x+1}) \leq 0 | \mathcal{F}_t).
\end{aligned}$$

Again, the first step in the above is a consequence of the Markov property of the assumed processes. Let

$$V_u^{(i)} = Z - d_{x,u,0}^{(i)}(T) - \mathbf{d}_{x,u}^{(i)}(T)'(\boldsymbol{\kappa}_u^{(i)} - \hat{\boldsymbol{\kappa}}_u^{(i)}) - d_{x,u,\gamma}^{(i)}(T)(\gamma_{u-x_a \wedge u-x+1} - \hat{\gamma}_{u-x_a \wedge u-x+1}).$$

It is not hard to see that $V_u^{(i)} | \mathcal{F}_t$ follows a normal distribution, and that

$$\mathbb{E}[S_{x,u}^{(i)}(T) | \boldsymbol{\kappa}_t^{(i)}, \gamma_{t-x_a \wedge u-x+1}] \approx \Phi\left(\frac{-\mathbb{E}[V_u^{(i)} | \mathcal{F}_t]}{\sqrt{\text{Var}[V_u^{(i)} | \mathcal{F}_t]}}\right),$$

where

$$\begin{aligned}
\mathbb{E}[V_u^{(i)} | \mathcal{F}_t] &= -d_{x,u,0}^{(i)}(T) - \mathbf{d}_{x,u}^{(i)}(T)'(\mathbb{E}[\boldsymbol{\kappa}_u^{(i)} | \mathcal{F}_t] - \hat{\boldsymbol{\kappa}}_u^{(i)}) \\
&\quad - d_{x,u,\gamma}^{(i)}(T)(\mathbb{E}[\gamma_{u-x_a \wedge u-x+1} | \mathcal{F}_t] - \hat{\gamma}_{u-x_a \wedge u-x+1})
\end{aligned}$$

and

$$\text{Var}[V_u^{(i)} | \mathcal{F}_t] = 1 + \mathbf{d}_{x,u}^{(i)}(T)' \text{Var}[\boldsymbol{\kappa}_u^{(i)} | \mathcal{F}_t] \mathbf{d}_{x,u}^{(i)}(T) + (d_{x,u,\gamma}^{(i)}(T))^2 \text{Var}[\gamma_{u-x_a \wedge u-x+1} | \mathcal{F}_t].$$

Appendix F

Evaluating the Accuracy of the Approximation Methods

In this appendix, we evaluate the accuracy of the methods for approximating $\mathbb{E}[S_{x,u}^{(i)}(T)|\mathcal{F}_t]$ when $t = u$ (Section 3.4.2; Case A) and when $t < u$ (Section 3.4.2; Case B).

Case A: $\mathbb{E}[S_{x,u}^{(i)}(T)|\mathcal{F}_t]$ for $t = u$

The method presented in Case A approximates the value of $\mathbb{E}[S_{x,u}^{(i)}(T)|\mathcal{F}_u]$ for a given realization of \mathcal{F}_u . For the sake of space, we only present the evaluation result for $\mathbb{E}[S_{65,2010}^{(i)}(10)|\mathcal{F}_{2010}]$, which is involved in the $(2005, \mathcal{F}_{2010})$ -value of the liability being hedged for Illustrations 2 and 3. The evaluation results for other combinations of i , x , u and T are similar.

It follows from equation (3.16) that the approximation formula for $\mathbb{E}[S_{65,2010}^{(R)}(10)|\mathcal{F}_{2010}]$ is a function of $\kappa_{2010}^{(1)}$, $\kappa_{2010}^{(2)}$, $\kappa_{2010}^{(3)}$ and $\gamma_{1946}^{(R)}$, all of which are random as of $t_b = 2005$ when the hedges in Illustrations 2 and 3 are evaluated. The contour lines in Figure F.1 indicate the percentage errors (percentage deviations from the ‘actual’ values that are calculated using full nested simulations) of the approximation when it is applied to different combinations of the four variables. The dots in the figure represent 1,000 simulated values of the four variables given \mathcal{F}_{2005} , so that the clouds of dots can be interpreted as the possible ranges

of the four variables. It can be observed that within the boundary of each cloud, the maximum percentage error is only approximately 0.1%. We thereby conclude that the approximation method for Case A is reasonably accurate over the possible ranges of the four variables.

Case B: $\mathbf{E}[S_{x,u}^{(i)}(T)|\mathcal{F}_t]$ for $t < u$

The method presented in Case B approximates the value of $\mathbf{E}[S_{x,u}^{(i)}(T)|\mathcal{F}_t]$ for a realization of \mathcal{F}_t with $t < u$. Again, for the sake of space, we only show the evaluation results for $\mathbf{E}[S_{70,2019}^{(i)}(1)|\mathcal{F}_{2010}]$, which is involved in the $(2010, \mathcal{F}_{2010})$ -value of the q-forward that has a reference age of 70 and matures at the end of year 2020 (one of the q-forwards used in Illustration 2). For other combinations of i , x , u , T and t , the evaluation results are similar.

It follows from equation (3.20) that the approximation formula for $\mathbf{E}[S_{70,2019}^{(R)}(1)|\mathcal{F}_{2010}]$ is a function of $\kappa_{2010}^{(1)}$, $\kappa_{2010}^{(2)}$, $\kappa_{2010}^{(3)}$ and $\gamma_{1950}^{(R)}$, all of which are random as of $t_b = 2005$ when the hedge in Illustration 2 is evaluated. With a layout similar to Figure F.1, Figure F.2 shows the percentage errors of the approximation when it is applied to different combinations of the four variables. It can be observed that within the possible ranges of the four variables, the percentage errors are smaller than 0.01%, suggesting that the approximation method for Case B is highly accurate.

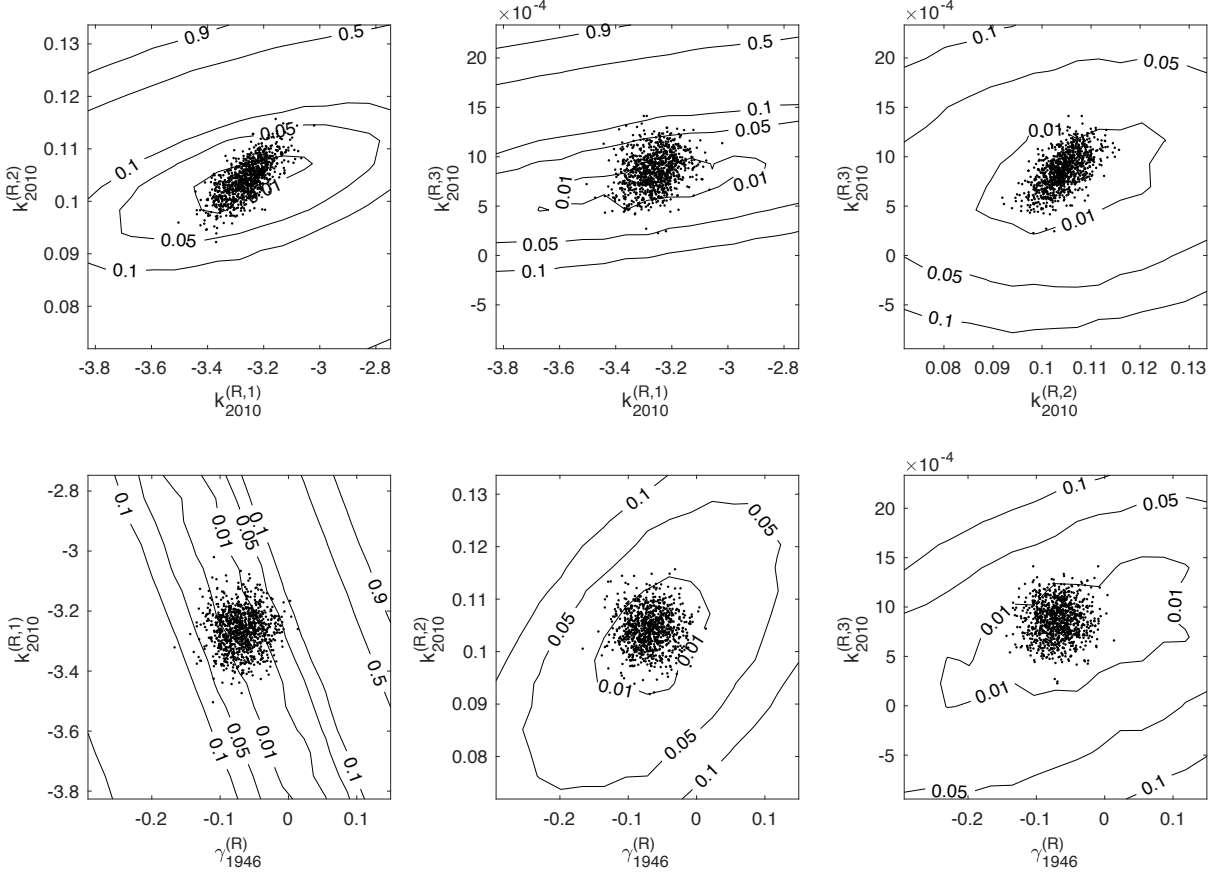


Figure F.1: Contour plots showing the percentage errors in approximating $E[S_{65,2010}^{(R)}(10)|\mathcal{F}_{2010}]$. The dots in the figure represent simulated values of $\kappa_{2010}^{(1)}$, $\kappa_{2010}^{(2)}$, $\kappa_{2010}^{(3)}$ and $\gamma_{1946}^{(R)}$ given \mathcal{F}_{2005} .

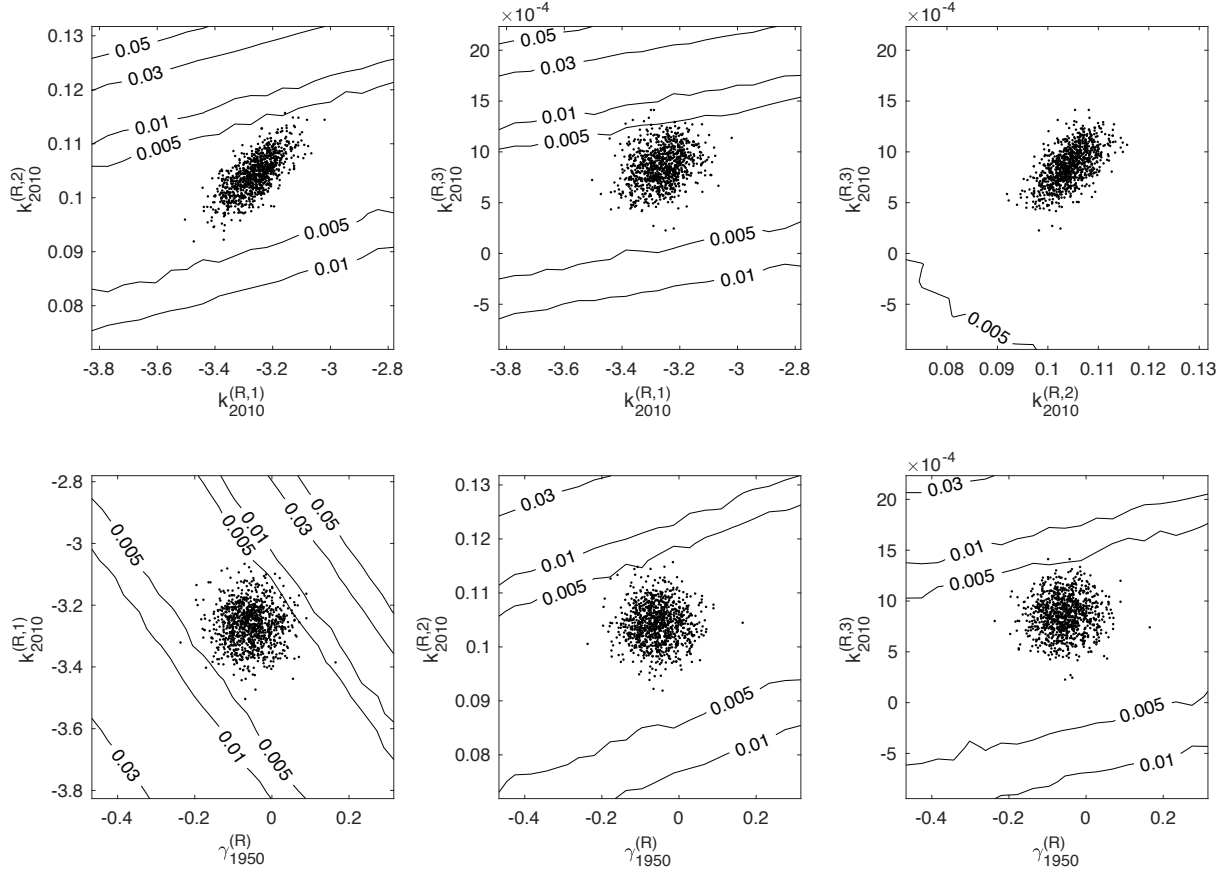


Figure F.2: Contour plots showing the percentage errors in approximating $E[S_{70,2019}^{(i)}(1)|\mathcal{F}_{2010}]$. The dots in the figure represent simulated values of $\kappa_{2010}^{(1)}$, $\kappa_{2010}^{(2)}$, $\kappa_{2010}^{(3)}$ and $\gamma_{1950}^{(R)}$ given \mathcal{F}_{2005} .

Appendix G

Deriving the Sensitivities of $\mathbf{E}[S_{x,u}^{(i)}(T)|\mathcal{F}_t]$ for $t = t_b$

Here we derive the first-order partial derivatives of $\mathbf{E}[S_{x,u}^{(i)}(T)|\mathcal{F}_t]$ with respect to $\kappa_t^{(1)}, \kappa_t^{(2)}$ and $\kappa_t^{(3)}$ for $t = t_b, u \geq t_b$ and any possible values of i, x and T , and that with respect to $\gamma_{t_b-x_a}$ for $t_b - x_a < u - x + 1$.

The partial derivatives of $\mathbf{E}[S_{x,u}^{(i)}(T)|\mathcal{F}_t]$ with respect to $\kappa_t^{(j)}$ for $j = 1, 2, 3$ are given by

$$\begin{aligned}\frac{\partial}{\partial \kappa_{t_b}^{(j)}} \mathbf{E}[S_{x,u}^{(i)}(T)|\mathcal{F}_t] &= \frac{\partial}{\partial \kappa_{t_b}^{(j)}} \mathbf{E}\left[\prod_{s=1}^T \left(1 + \exp(y_{x+s-1,u+s}^{(i)})\right)^{-1} \middle| \mathcal{F}_{t_b}\right] \\ &= -\mathbf{E}\left[\left(S_{x,u}^{(i)}(T)\right)^2 \frac{\partial}{\partial \kappa_{t_b}^{(j)}} \prod_{s=1}^T \left(1 + \exp(y_{x+s-1,u+s}^{(i)})\right) \middle| \mathcal{F}_{t_b}\right].\end{aligned}$$

In the above, $\frac{\partial}{\partial \kappa_{t_b}^{(j)}} \prod_{s=1}^T \left(1 + \exp(y_{x+s-1, u+s}^{(i)})\right)$ can be calculated recursively as

$$\begin{aligned} & \frac{\partial}{\partial \kappa_{t_b}^{(j)}} \prod_{s=1}^T \left(1 + \exp(y_{x+s-1, u+s}^{(i)})\right) \\ &= \begin{cases} \frac{\partial y_{x, u+1}^{(i)}}{\partial \kappa_{t_b}^{(j)}} \exp(y_{x, u+1}^{(i)}) & \text{if } T = 1 \\ \frac{\partial y_{x+T-1, u+T}^{(i)}}{\partial \kappa_{t_b}^{(j)}} \exp(y_{x+T-1, u+T}^{(i)}) \prod_{s=1}^{T-1} \left(1 + \exp(y_{x+s-1, u+s}^{(i)})\right) \\ + \left(1 + \exp(y_{x+T-1, u+T}^{(i)})\right) \frac{\partial}{\partial \kappa_{t_b}^{(j)}} \prod_{s=1}^{T-1} \left(1 + \exp(y_{x+s-1, u+s}^{(i)})\right) & \text{if } T > 1 \end{cases}, \end{aligned}$$

where

$$\frac{\partial y_{x+T-1, u+T}^{(i)}}{\partial \kappa_{t_b}^{(j)}} = \begin{cases} \frac{\partial y_{x+T-1, u+T}^{(i)}}{\partial \kappa_{u+T}^{(1)}} \frac{\partial \kappa_{u+T}^{(1)}}{\partial \kappa_{t_b}^{(1)}} = 1 & \text{if } j = 1 \\ \frac{\partial y_{x+T-1, u+T}^{(i)}}{\partial \kappa_{u+T}^{(2)}} \frac{\partial \kappa_{u+T}^{(2)}}{\partial \kappa_{t_b}^{(2)}} = x + T - 1 - \bar{x} & \text{if } j = 2 \\ \frac{\partial y_{x+T-1, u+T}^{(i)}}{\partial \kappa_{u+T}^{(3)}} \frac{\partial \kappa_{u+T}^{(3)}}{\partial \kappa_{t_b}^{(3)}} = (x + T - 1 - \bar{x})^2 - \sigma_x^2 & \text{if } j = 3 \end{cases}$$

for $T \geq 1$ are obtained using the chain rule and equations (3.3) and (3.4).

The partial derivatives of $E[S_{x,u}^{(i)}(T)|\mathcal{F}_t]$ with respect to $\gamma_{t_b-x_a}$ for $t_b - x_a < u - x + 1$ can be obtained by replacing $\kappa_{t_b}^{(j)}$ with $\gamma_{t_b-x_a}$ and using the fact that

$$\frac{\partial y_{x+T-1, u+T}^{(i)}}{\partial \gamma_{t_b-x_a}} = \frac{\partial y_{x+T-1, u+T}^{(i)}}{\partial \gamma_{u-x+1}} \frac{\partial \gamma_{u-x+1}}{\partial \gamma_{t_b-x_a}} = \psi_1^{u-x+1-t_b+x_a},$$

which can be derived easily with the chain rule and equations (3.3) and (3.6).

Appendix H

Deriving the Sensitivities of $\mathbf{E}[S_{x,u}^{(i)}(T)|\mathcal{F}_t]$ for $t > t_b$

Here we derive the first-order partial derivatives of $\mathbf{E}[S_{x,u}^{(i)}(T)|\mathcal{F}_t]$ with respect to $\kappa_t^{(1)}, \kappa_t^{(2)}, \kappa_t^{(3)}$ for $t > t_b$, $u \geq t$ and any possible values of i, x and T , and that with respect to γ_{t-x_a} for $t - x_a < u - x + 1$.

First, because of the Markov property of the assumed period and cohort effect processes, we have

$$\mathbf{E}[S_{x,u}^{(i)}(T)|\mathcal{F}_t] = \mathbf{E}[S_{x,u}^{(i)}(T)|\boldsymbol{\kappa}_t^{(i)}, \gamma_{t-x_a \wedge u-x+1}].$$

When $u = t$, we use approximation formula (3.16) to obtain

$$\begin{aligned} & \frac{\partial}{\partial \kappa_t^{(j)}} \mathbf{E}[S_{x,u}^{(i)}(T)|\boldsymbol{\kappa}_t^{(i)}, \gamma_{t-x_a \wedge u-x+1}] \\ & \approx \frac{\partial}{\partial \kappa_t^{(j)}} \Phi \left(d_{x,t,0}^{(i)}(T) + \mathbf{d}_{x,t}^{(i)}(T)'(\boldsymbol{\kappa}_t^{(i)} - \hat{\boldsymbol{\kappa}}_t^{(i)}) + d_{x,t,\gamma}^{(i)}(T)(\gamma_{t-x_a \wedge t-x+1} - \hat{\gamma}_{t-x_a \wedge t-x+1}) \right) \\ & = \phi \left(d_{x,t,0}^{(i)}(T) + \mathbf{d}_{x,t}^{(i)}(T)'(\boldsymbol{\kappa}_t^{(i)} - \hat{\boldsymbol{\kappa}}_t^{(i)}) + d_{x,t,\gamma}^{(i)}(T)(\gamma_{t-x_a \wedge t-x+1}^{(R)} - \hat{\gamma}_{t-x_a \wedge t-x+1}^{(R)}) \right) d_{x,t,j}^{(i)}(T) \end{aligned}$$

for $j = 1, 2, 3$, and

$$\begin{aligned} & \frac{\partial}{\partial \gamma_{t-x_a}^{(R)}} \mathbb{E}[S_{x,u}^{(i)}(T) | \boldsymbol{\kappa}_t^{(i)}, \gamma_{t-x_a \wedge u-x+1}^{(R)}] \\ & \approx \phi \left(d_{x,t,0}^{(i)}(T) + \mathbf{d}_{x,t}^{(i)}(T)' (\boldsymbol{\kappa}_t^{(i)} - \hat{\boldsymbol{\kappa}}_t^{(i)}) + d_{x,t,\gamma}^{(i)}(T) (\gamma_{t-x_a}^{(R)} - \hat{\gamma}_{t-x_a}^{(R)}) \right) d_{x,t,\gamma}^{(i)}(T) \end{aligned}$$

when $t - x_a < u - x + 1$. When $u > t$, we use approximation formula (3.20) to get

$$\begin{aligned} & \frac{\partial}{\partial \kappa_t^{(j)}} \mathbb{E}[S_{x,u}^{(i)}(T) | \boldsymbol{\kappa}_t^{(i)}, \gamma_{t-x_a \wedge u-x+1}] \approx \frac{\partial}{\partial \kappa_t^{(j)}} \Phi \left(\frac{-\mathbb{E}[V_u^{(i)} | \mathcal{F}_t]}{\sqrt{\text{Var}[V_u^{(i)} | \mathcal{F}_t]}} \right) \\ & = \phi \left(\frac{-\mathbb{E}[V_u^{(i)} | \mathcal{F}_t]}{\sqrt{\text{Var}[V_u^{(i)} | \mathcal{F}_t]}} \right) \frac{d_{x,u,j}^{(i)}(T)}{\sqrt{\text{Var}[V_u^{(i)} | \mathcal{F}_t]}} \end{aligned}$$

for $j = 1, 2, 3$, and

$$\frac{\partial}{\partial \gamma_{t-x_a}^{(R)}} \mathbb{E}[S_{x,u}^{(i)}(T) | \boldsymbol{\kappa}_t^{(i)}, \gamma_{t-x_a \wedge u-x+1}^{(R)}] \approx \phi \left(\frac{-\mathbb{E}[V_u^{(i)} | \mathcal{F}_t]}{\sqrt{\text{Var}[V_u^{(i)} | \mathcal{F}_t]}} \right) \frac{d_{x,u,\gamma}^{(i)}(T)}{\sqrt{\text{Var}[V_u^{(i)} | \mathcal{F}_t]}}$$

when $t - x_a < u - x + 1$.